IRRIGATION SCHEDULING OF MAIZE GROWN ON A VERTISOL SOIL UNDER CHANGING CLIMATE OF SOFIA'S FIELD

Maria IVANOVA*, Zornitsa POPOVA

Institute of Soil Science, Agrotechnology and Plant Protection "N. Poushkarov", Sofia, Bulgaria

The purpose of this study is to evaluate the impact of climate uncertainties on maize irrigation requirements, grown on a Vertisol soil, Sofia's field, Bulgaria. Through the validated WinIsareg model, four irrigation scheduling alternatives are simulated for the years of "very high", "high" and "average" irrigation demands of past (1952–1984) and present (1970–2004) climate. Adaptation of irrigation scheduling to the present climate conditions during the "very dry" years ($P_I \leq 12\%$) consists of an extension of the irrigation season by 15–20 days and a need of additional irrigation relative to alternative 1 and two irrigation events at alternatives 2 and 3. During the past climate alternatives 2 and 3 led to savings of 30 mm of water, while up to the current climate conditions the three irrigations alternatives should provide 360 mm of irrigation water. To obtain maximum yields in "dry" ($P_I = 12–30\%$) years, irrigation season should end by 05/09, as in the present climate, irrigation season has shifted about a week earlier for the three alternatives. In the "average" ($P_I = 30–60\%$) years the adaptation consist in accurately determination of the last allowed date for irrigation.

Keywords: irrigation scheduling, maize, climate change, water management, yield

Irrigation scheduling is crucial for the efficient management of water resources consumption and for optimizing the yield of irrigated areas. Net Irrigation Requirements (NIRs) of the crops are mainly characterized by climatic conditions in an agricultural area.

Sofia's field is characterized by moderate continental climate and is one of the wettest and coolest agricultural regions of Bulgaria. However, there has been found a trend of decreasing precipitation by 2.7 mm per year and increasing reference evapotranspiration (ETo) by 1.0 mm per year during the growing (May – September) season of the present climate conditions 1970–2004 (Figure 1a and 1b).

Regarding the irrigation season, similar trends of decrease in precipitation by 2.61 mm per year and increase the ETo by 0.86 mm per year have been identified under the present climatic conditions (1970–2004) (Popova, Ivanova,
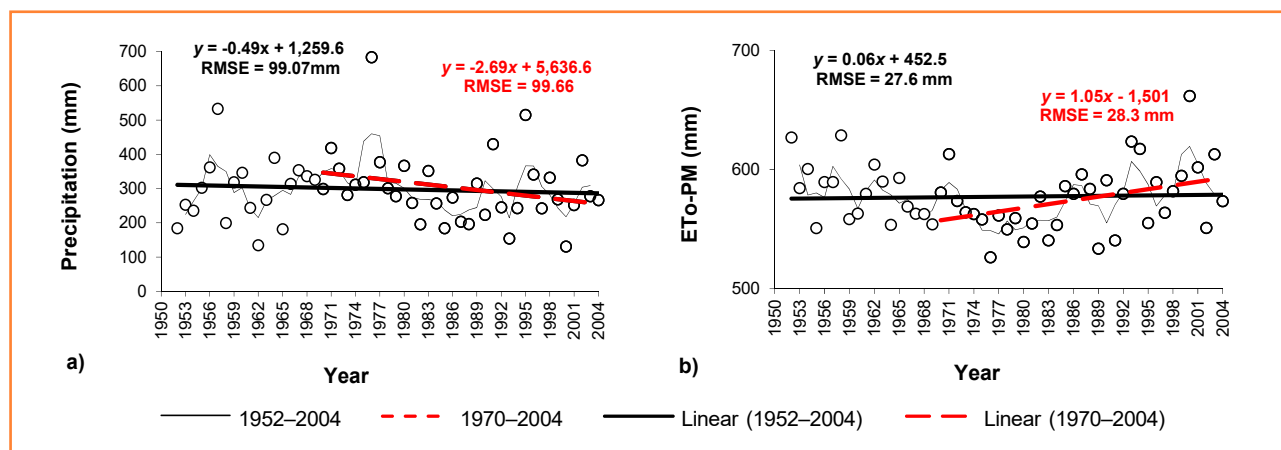
Figure 1   a) Precipitation and b) reference evapotranspiration by Penman-Monteith equation (ETo – PM) during the growing (1/05–30/09) period of maize, Sofia, 1952–2004
——— average for 3years; ━━━ trend for 1952–2004; ━ ━ trend for 1970–2004

Contact address: Maria Ivanova, Institute of Soil Science, Agrotechnology and Plant Protection "N. Poushkarov", Department of Physics, Erosion, Soil Biota; 7, Shosse Bankya str., Sofia 1331, Bulgaria, ☏ +35 98 78 90 95 76, e-mail: mulykostova@abv.bg
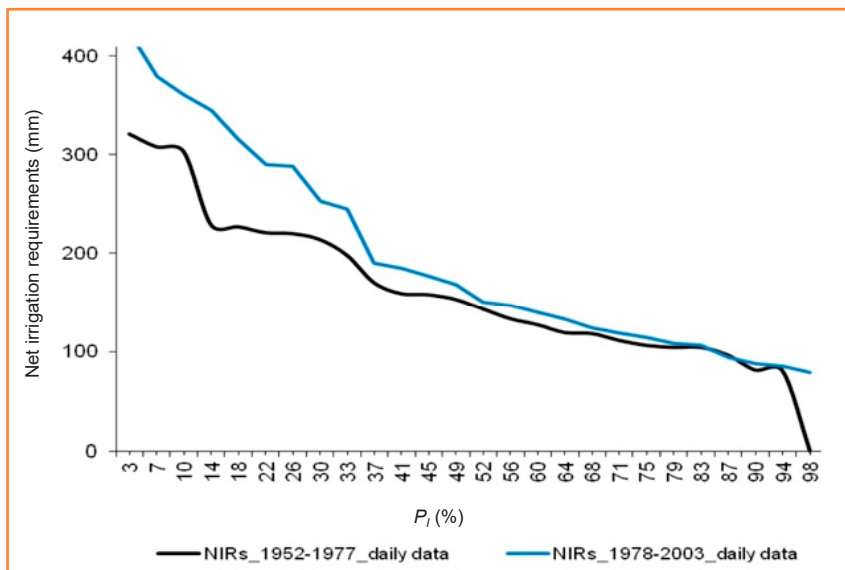
Figure 2 Comparison of probability of occurrence curves of a Net Irrigation Requirements, NIR (mm) of maize, computed with all required daily climate data during the past 1952–1977 and present 1978–2003 climate conditions, Sofia's field

Alexandrov, Doneva, 2014a; Popova, Ivanova, Martins, Pereira, Doneva, Alexandrov, Kercheva, 2014b; Popova, Ivanova, Pereira, Alexandrov, Kercheva, Doneva, Martins, 2015). The identical percentages of rainfall decreases and ETo increases during the growing and the irrigation season show that the trend is mainly due to the changes in climatic conditions during the irrigation season "June – August".

The defined trends inevitably lead to changes in NIRs. Figure 2 compares the NIRs, mm, for the past (1952–1977) and present (1978–2003) climate conditions. The impact of climate change is seen to be greatest during the very high irrigation demand years with a protbability of occurrence P_I ≤12% and the high irrigation demand (P_I =

12–30%) years, when NIRs increased by 60–115 mm and 40–100 mm, respectively. During the average years (P_I = 30–65%) NIRs increased by 10 to 40 mm.

Under the changes in climatic conditions established by us and other authors (Alexandrov, 2011; Slavov, Koleva, Alexandrov, 2003; Koleva, Alexandrov, 2008; Popova et al., 2014a, b), the published irrigation scheduling (Zahariev, Lazarov, Koleva, Gaidarova, Koichev, 1986) should be reviewed and updated, as well as include scheduling with different irrigation rate and with different degree of water depletion in soil.

The purpose of this study is to develop irrigation scheduling for the rational irrigation of Vertisol soil

grown maize, appropriate for the present climatic conditions in Sofia's field and to determine the effects of drought on irrigation rates and yields of semi-early and late maize hybrids for past (1952–1984) and present (1952–2004/1970–2004) weather. For this purpose, a validated simulation model of soil water balance, irrigation scheduling and the effects of water stress on yields WinISAREG (Teixeira, Pereira, 1992; Pereira, Teodoro, Rodrigues, Teixeira, 2003) was used, with soil and crop parameters adapted to the local conditions (Ivanova, Popova, 2012).

Material and method

For the calculation of evapotranspiration (ET) and NIRs of maize, a simulation model of irrigation scheduling and soil water balance WinISAREG (Pereira et al., 2003) was applied. ETo was calculated using the updated methodology proposed by Allen, Pereira, Raes, Smith (1998).

Data on soil texture and hydraulics are used to define the Total Available Water in the root zone of 1 m of TAW = 180 mm.m^{-1} (Table 1).

The previously validated crop parameters, as described by Ivanova, Popova (2012) have been presently used after respective adaptation to local climate and soil conditions (Table 2).

The WinISAREG model was also applied to compare simulated irrigation scheduling alternatives under different levels of soil moisture before irrigation and irrigation rates and for assessment of their impact on yields. The research aims to develop environment friendly

Table 1 Main soil physical and hydraulic properties of a Vertisol soil at Bojourishte experimental field of Sofia's field

Experimental field	Horizon	Depth (cm)	Soil particles in mm (%) (FAO system classification)			Ksat (cm day^{-1})
			clay <0.002 mm	silt 0.002–0.05 mm	sand 0.05–2.00 mm	
Bojurishte	A$_1$	0–45	54	33	13	0.63
	A$_2$B$_1$	45–100	63	27	10	0.63

Table 2 Dates limiting crop development stages and modeling parameters: crop coefficients *Kc* and depletion fraction for no stress *p*, Vertisol soil, Bojurishte experimental field, Sofia, 2004

Growth phases/Dates	Initial period/05/05 to 06/06	Mid-season/01/08 to 01/09	End-season/20/10
Kc	0.40	1.28	0.6
p	0.46–0.75	0.6	0.78

and water savings oriented alternatives to prevent soil cracking maintaining soil moisture levels above 80% FC, irregularity in water distribution, and water and yield losses. The Alternative 1 assumes a degree of Management Allowed soil water Depletion MAD = 0.50, i.e. up to 82% of Field Capacity (FC), and an irrigation rate of 90 mm, measured experimentally in continuous furrow irrigation (Figure 4a); the Alternative 2 deals with the case of replenishment of the soil reservoir to 88% of FC corresponding to MAD = 0.33, and irrigation rates of 60 mm, applied for impulse irrigation in order to reduce the lacking uniformity of water distribution and irrigation rate (Figure 4b); the Alternative 3 aims to better retain and use rainfall and irrigation water with a sprinkler irrigation. It consists of replenishing the soil reservoir up to 82% of TAW,

adopting MAD = 0.50 and irrigation rates of 60 mm. About 30 mm from the soil reservoir remain unfilled in order to accumulate any precipitation after the irrigation has been applied (Figure 4c); the Alternative 4 is the option "crop without irrigation". According to the regional irrigation practice published by Zahariev et al. (1986), the last allowed irrigation date is 21/08 for an average and a high irrigation demand years, having probability of exceedance of irrigation rate $P_I = 50\%$ and $P_I = 25\%$ and 31/08 for the year of very high irrigation demand ($P_I = 10\%$).

Irrigation simulations are performed with a complete set of daily data including maximum and minimum air temperature T_{max} and T_{min}, average daily relative humidity RH, wind speed WS at 2 m altitude and precipitation P for the period 1952–2007 (data from Meteorological Years

journals 1952–1980, Meteorological Months journals 1981–1984 and National Institute of Meteorology and Hydrology 1984–2007). The total solar radiation RS is calculated by the temperature difference method, which is based on the fact that the difference between the maximum and minimum temperatures gives the closest estimate of the actual RS in the area (Ivanova, Popova, 2011). The coefficient of proportionality Krs = 0.16 was found to be the most suitable for the Sofia's field (Ivanova, Popova, 2011).

Results and discussion

Yields and irrigation requirements in changing climate

Monthly precipitation and ETo series (1952–2004), computed as described by Ivanova, Popova (2011), have been used to build probability curves of occurrence of NIRs and corresponding Relative Yield Decrease RYD related to rainfed maize semi-early and late hybrids (Figure 3).

Comparing the years with different probability of exceedance of the hole studied 1952–2004 and the present 1970–2004 periods it can be seen that very high irrigation demand years (2001, 1993, 1994, 2000, 1988, 1985) with the probability of NIRs P_I <16%, high irrigation demand (1987, 1990, 1992, 1974, 2003) with $P_I = 20$–40%, the average (1973, 2004, 1998) with $P_I = 40$–60%, the medium-wet with $P_I = 60$–75% and the wet ($P_I \geq 80\%$) years have identical supply of NIRs in the two periods (Figs 3a and 3b). Therefore, the irrigation rates required and the relative losses of rainfed maize yield are practically the same over the two periods.

However, comparing the period of the past climate 1952–1984 and the long series of 53 years (1952–2004), it can be seen that the probability of exceedance of NIRs decreased from 9% to 2% in the extremely dry 1962 year, from 30% to 20% in the average dry 1974, from 46% to 35% in the average 1973 (Figs 3a and 3c). These changes reflect present climatic conditions, which show that the onset of drought leads to an increase in the required

Figure 3 Probability curves of Net Irrigation Requirements, NIR, mm (—) and Relative Yield Decrease of rainfed maize, RYD,%, comparing the semi-early P37-37 (∆), Ky = 1.2, and late H708 (▲), Ky = 1.6, maize hybrids, computed with all required daily data relative to three periods: a) 1952–2004; b) 1970–2004 and c) 1952–1984

NIRs and yield losses of rainfed maize (Figs 3b and 3c).

Figs 3b and 3c also show the simulated net irrigation rates and the corresponding relative losses of non-irrigated maize yield, calculated with a complete set of required meteorological data for the years 1952–1984 and 1970–2001. It can be seen that only during the wettest year (P_I = 98%) there is no need for irrigation and consequently loss of yield. During the current climate 1970–2004, the NIRs is higher by about: 20–30 mm in wet years (P_I = 65–95%), 20–35 mm in average (P_I = 30–65%), 45–100 mm in the dry (P_I = 12–30%) and 100–120 mm during the driest (P_I <8%) years.

Due to the water stress, RYD, in the present climate are raised by about 10% of both rainfed maize hybrids. It can be seen that when growing the late hybrid H708 rainfed maize, in both periods the yield losses are higher than those of the more resistant to drought, semi-early hybrid Kn-2L-611 by about 10% in the wet, up to 15% in the average and up to 20% in the high and very high irrigation demand years (Figs 3b and 3c). It is therefore advisable to grow drought-resistant semi-early maize hybrids in Sofia's field.

Evaluation of irrigation scheduling alternatives in the past (1952–1984) and present (1970–2004) climate

Figs 4a, 4b and 4c compare the simulated Available Soil Water (ASW, mm) under irrigation alternatives 1, 2 and 3 to the very high irrigation demand year 1963 (P_I = 11%, Figure 3c) of the past climate (1952–1984). Irrigation up to 02/09 (solid line) with irrigation rates of 270, 240 and 240 mm can be seen to provide soil moisture during the most intensive development phase, with the greatest need of water, without any loss of yield. Suspension of the irrigation season to 20/08 (dotted line) leads to a reduction in the number of irrigations with one for all three alternatives 1, 2 and 3 and yield losses of 8.7, 9.0, 8.7% respectively. In this case, the last date of irrigation (20/08) is close to the one established (11/08) by Zahariev et al. (1986), but irrigation rates are lower than those published (300 mm) in 1986.

In comparison to the past climate, the very high irrigation demand year 1988 (P_I = 13%) of the present climate, irrigation season starts about 20 days earlier for all three alternatives and ends at about the same time. During the dry years of the past climate, irrigation begins around 01/08, while in present climate conditions the start date is around 10/07. Number of irrigations increases by one for alternative 1 and by two for alternatives 2 and 3. When the last irrigation is submitted until 20/08, the optimum moisture supply decreases at the end of the growing season, at harvest, and results in yield losses of 8.8, 5.7, 3.8% respectively for alternatives 1, 2 and 3. For precise irrigation, without loss of yield, irrigation should end later on 03/09 (solid line) with one/two more irrigations.

During the high irrigation demand years 1954 and 1992 (P_I = 25%), respectively, from the past and present climate, aiming at maximum yields irrigation should be until 05/09 (solid line, Figure 5). The numbers of irrigations of the three alternatives are identical for the two periods considered, with water saving alternatives 2 and 3 having irrigation rates of 240 mm, unlike alternative 1, which requires 270 mm of irrigation water.
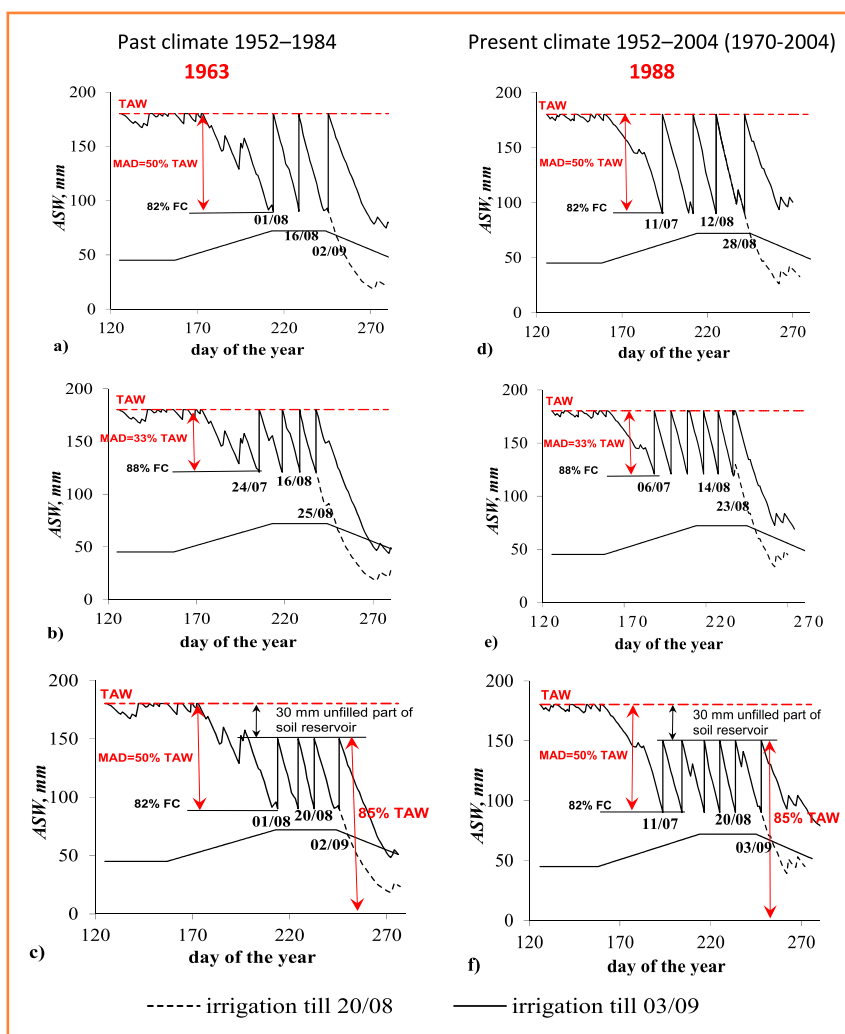
Figure 4   Simulation of the available soil water (ASW, mm) for the three irrigation scheduling alternatives in the very high irrigation demand 1963 and 1988 (P_I = 11–13%) relative to past (1952–1984) and present (1970–2004) weather: a) and d) alternative 1; b) and e) alternative 2; c) and f) alternative 3, with identification of the date of the last irrigation. The horizontal dashed line above corresponds to TAW and the broken line below to the non-stress threshold
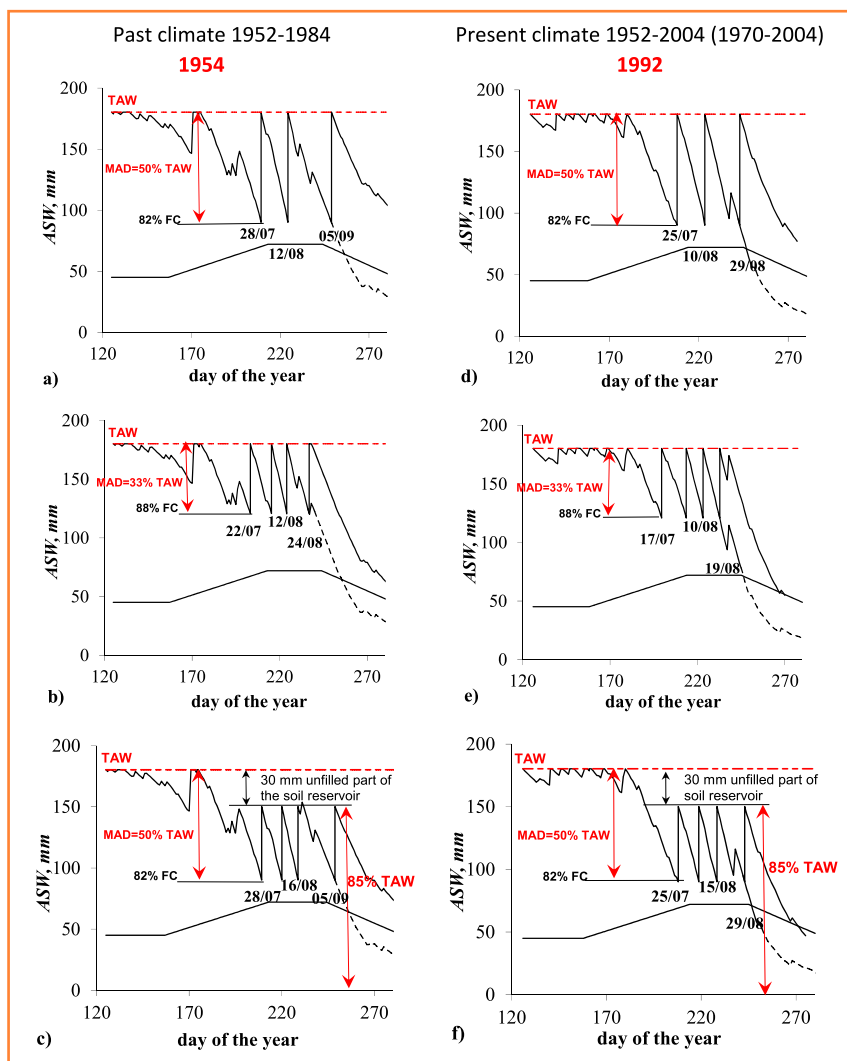
Figure 5 Available soil water (ASW, mm) for the three irrigation scheduling alternatives in the high irrigation demand 1954 and 1992 (P_I = 25%) relative to past (1952–1984) and present 1952–2004/ 1970–2004 weather conditions: a) and d) alternative 1; b) and e) alternative 2; and c) and f) alternative 3, with identification of the date of the first and last irrigation; The horizontal dashed line above corresponds to TAW and the broken line below to the non-stress threshold

Unlike the high irrigation demand year 1954 for the past climate, in 1992 from the present climate, irrigation began one week earlier. If one irrigation is cancelled, irrigation will end by 20/08 with yield losses of up to 5% in 1954 and up to 13% in 1992 for all three irrigation alternatives. During the 1992 to the present climate, irrigation seasons starts and ends several days earlier (Figure 5, Table 3). Also, under the present climate, ASW at harvest is lowering i.e. the usability of water reserves is increasing (Figure 5, Table 3).

A comparison on Figure 6a shows that the Irrigation Demands, IDs, i.e. the simulated applications of annual amount of irrigation water, of alternatives 1, 2 and 3 are close to NIRs for the past (1952–1984) climate, when very high demand years (P_I <12%) were irrigated till 05/09 and the rest years (P_I <98%) with up to 25/08. Irrigation rates of alternative 3, which allows greater degree of soil water depletion (MAD = 0.50) and better accumulation of rainfall in the maize root zone compared to alternatives 1 and 2, are closest to the NIR, leading to a 60 mm saving of water in the high irrigation demand (P_I = 12–30%) and average (P_I = 50–70%) years (Figure 6a). Alternative 2 has the highest irrigation rates in comparison with the other two alternatives, and for the most part of the probability of exceedance curve (P_I = 10–90%), they are above the NIRs. Alternative 1 saves 30 to 60 mm in the years having high irrigation demand (P_I = 10–30%). During the very high irrigation demand and average years, the irrigation rates under the three
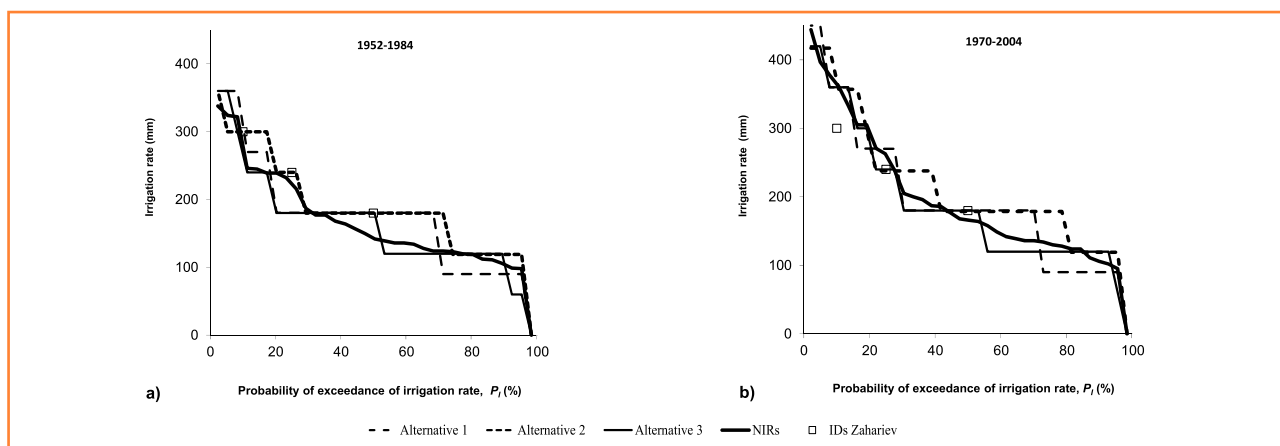
Figure 6 Irrigation Demands, IDs, mm, relative to irrigation scheduling alternative 1, 2 and 3 sorted according to the probability curve of Net Irrigation Requirements computed for each year of (a) 1952–1984 and (b) 1970–2004 using all required climate data on a daily basis

Table 3   Summary of water balance and relative yield decrease, RYD, results of irrigation scheduling alternatives 1, 2, 3 and rainfed alternative 4 for the very high and high irrigation demand years, 1952–1984* and 1952–2004/1970–2004. Last allowed irrigation date 03/09

Climate conditions	Very high irrigation demand								High irrigation demand							
	Past				Present				Past				Present			
	1952–1984				1952–2004				1952–1984				1952–2004			
Year	1963*				1988				1954*				1992			
P_I **(%) 1952–2004**	24%				9%				33%				22%			
P_I **(%) 1952–1984***	11%				8%				26%				25%			
Precipit. May–Sept (mm)	267				197				236				311			
Precipit. Jul–Aug (mm)	90				18				87				64			
Net irrigation requirements (mm)	246				334				216				239			
Irrigation alternatives	1	2	3	4	1	2	3	4	1	2	3	4	1	2	3	4
Annual amount of irrigation water (mm)	270	240		0	360		300	0	0	270		240	270	240		0
№ Irrigation events	3	4	4	0	4	6	6	0	3	4		0	3	4		0
Crop evapotranspiration (ETa) (mm)	577			353	593		586	309	548			368	553	545		324
Non-used precipitation (mm)	79				55	73	55	55	48	57	48		67			
ASW harvest (mm)	81	50		24	69	47	68	18	142	105		52	59	35		17
RYD (%) Ky = 1.21	0	0	0	46	0	0	0	58	0	0	0	40	0	0	0	50
RYD (%) Ky = 1.0				38				48				33				41
RYD (%) Ky = 1.6				60				77				53				6

alternatives are close to those previously published in the book of Zahariev et al. (1986) and used, whereas in the high irrigation demand seasons this refers only to traditional alternative 2, while alternatives 1 and 3 save irrigation rates of 60 mm (Figure 6a).

During the present climate (1970–2004), NIRs are significantly higher. Irrigation rates of alternative 3 are closest to NIRs, saving from 30 to 60 mm of water during the high irrigation demand and average years (Figure 6b). During the very high irrigation demand years, the irrigation rates for the three alternatives were by 60 to 100 higher than the published depths in the book of Zahariev et al. (1986), while in the high irrigation demand and average seasons they fluctuate around the NIRs and are close to those proposed in Zahariev et al. (1986). It is seen in the comparison between Figure 6a and 6b that NIRs and IDs became greater especially in very high and high demand years, as in the past IDs were lower than the ones published by Zahariev et al. (1986) but in the present they are higher. For the past climate (1952–1984) the NIRs and IDs are closer to those published in Zahariev et al. (1986) in the very high and high irrigation demand years, while in the present climate they are closer to the high and average irrigation demand years (Figs 6a and 6b).

Conclusions

The results are related to adapting irrigation scheduling to higher net irrigation requirements (NIRs, mm) of present climate conditions. The approach is applicable not only to other territory of Bulgaria, but everywhere in the world. The use of simulation models for irrigation management makes it possible to develop precise irrigation regimes that minimize water and yield losses.

From the simulated irrigation scheduling alternatives of maize grown on Vertisol soil at Sofia's field for the period 1952–2004 the following can be concluded:

1. Under the present climate conditions, NIRs have increased by 60–120 mm during the very high irrigation demand years (P_I <20%). In the remaining high and average irrigation demand years they raised with 40–100 mm and 10–40 mm respectively (Figure 2).

2. Losses of rainfed yields of late maize hybrids during the high irrigation demand years are in the range of 35–55% and about 70% during the very high irrigation demand years, whereas in the case of dry-resistant semi-early hybrids the impact of drought is mitigated and the yield losses do not exceed 55% during the very high irrigation demand years (P_I <8%). Due to the water stress, RYD in the present climate are raised by about 10% of both rainfed maize hybrids (Figure 3).

3. Adaptation of irrigation scheduling alternatives to the present climate during very high irrigation demand years (P_I ≤12%) consists of extending the irrigation season by 15–20 days and the need for additional irrigation at alternative 1 and two irrigations at alternatives 2 and 3 (Figure 4). In other years, adaptation to drought consists in precisely choosing the start and end dates for irrigation and extending or shifting the irrigation season.

4. During high irrigation demand years (P_I = 15–30%) irrigation without loss of yield should end by 05/09, as it begins and ends about a week earlier with the present climate. Alternatives 2 and 3 with IDs = 240 mm, compared

to 1 with IDs = 270 mm, save 30 mm of irrigation water over the two study periods (Figure 5).

5. In average irrigation demand years (P_I = 30–65%) irrigation for maximum yield results in the same irrigation rates of 180 mm in all three alternatives with the last allowed irrigation date of 15/08 for alternatives 1 and 2 and 22/08 for alternative 3 in both studied periods.

6. Simulations of the water saving and environmentally friendly, traditional alternative 2 for the conditions of the past climate lead to the same results as those published in thte book of Zahariev et al. (1986) for the average and high irrigation demand years. Alternative 2 also best describes the fluctuations in NIRs under the conditions of the "past" climate (Figure 6a). For the present climate conditions, this is valid for alternatives 2 and 3 for the high and average irrigation demand years, while in very high irrigation demand years all the three alternatives shows higher IDs (Figure 6b).

References

Alexandrov, V. (ed). (2011). In: *Methods for monitoring and estimation of drought vulnerability in Bulgaria*. Sofia: National Institute of Meteorology & Hydrology, Bulgarian Academy of Science (p. 216) (in Bulgarian).

Allen, R. G., Pereira, L.S., Raes, D., Smith, M. (1998). *Crop Evapotranspiration – Guidelines for Computing Crop Water Requirements.* Irrigation & Drainage Paper 56. Roma: FAO.

Ivanova, M., Popova, Z. (2011). Validation of FAO-56 Methodology for computing ETo with missing climate data. Application to Sofia's field. *Agricultural science*, *64*(2), 3–13 (in Bulgarian).

Ivanova, M., Popova, Z. (2012). Model validation and crop coefficients for maize irrigation scheduling based on field experiments in Sofia. In Popova (Ed.). *Risk assessment of drought in agriculture and irrigation management through simulation models (*pp. 29–39) (in Bulgarian).

Koleva, E., Alexandrov, V. (2008). Drought in the Bulgarian low regions during the 20th century. *Theor. Appl. Climatol., 92,* 113–120.

Pereira, L.S., Teododro, P. R., Rodriges, P. N., Teixeira, J. L. (2003). Irrigation scheduling simulation: the model ISAREG. In Rossi, G., Pereira, L. S., Zairi, A. (Eds.). *Tools for Drought Mitigation in Mediterranean Regions*. Dordrecht: Kluwer (pp. 161–180).

Popova, Z. (Ed.). (2012). In: *Risk assessment of drought in agriculture and irrigation management through simulation models* (p. 244) (in Bulgarian).

Popova, Z., Ivanova, M., Alexandrov, V., Doneva, K. (2014a). Drought and reference evapotranspiration ETo-PM in Bulgarian plains-2 Trend analyses. *Proceedings of Second scientific international conference "Theory and practice in Agriculture"*, Undola (pp. 210–218) (in Bulgarian).

Popova, Z., Ivanova, M., Martins, D., Pereira, L.S., Doneva, K., Alexandrov, V., Kercheva, M. (2014b). Vulnerability of Bulgarian agriculture to drought and climate variability with focus on rainfed maize systems. *Natural Hazards*, *74*(2) 865–886.

Popova, Z., Ivanova, M., Pereira, L.S., Alexandrov, V., Kercheva, M., Doneva, K., Martins, D. (2015). Droughts and climate change in Bulgaria: assessing maize crop risk and irrigation requirements in relation to soil and climate region. *Bulgarian Journal of Agricultural Sciences*, *21*(1), 35–53.

Slavov, N.. Koleva, E., Alexandrov, V. (2003). The climate of drought in Bulgaria. In: Knight GG, Raev I, Staneva M (eds.) *Drought in Bulgaria: a contemporary analog for climate change.* Aldershot: Ashgate Publishing Limited (pp. 39–52) (in Bulgarian).

Teixeira, J. L., Pereira, L.S. (1992). ISAREG, an irrigation scheduling simulation model. *Crop Water Models*, *41*(2), 29–48.

Zahariev, T., Lazarov, R., Koleva, S., Gaidarova, S., Koichev, Z. (1986). *Regional irrigation scheduling of agricultural crops.* Publisher Zemizdat (p. 646) (in Bulgarian).

AN IRRIGATION HOMOGENITY ASSESSMENT OF A VARIABLE RATE SPRINKLER IRRIGATION

Andrea SZABÓ*, János TAMÁS, Attila NAGY

University of Debrecen, Hungary

Nowadays, the development of irrigation is increasingly recognized as a necessary factor in agriculture, primarily because of global warming. Depending on the field conditions, the most commonly used method is sprinkler irrigation. The spray uniformity of sprinklers installed on the field irrigation equipment can be characterized by the Christiansen-uniformity coefficient (CUc%) and the distribution uniformity coefficient (DU%). Our investigations were carried out on the lateral moving irrigation equipment of University of Debrecen, Institutes for Agricultural Research and Educational Farm and Nyírbátor's company in Hungary in 2019. Variable rate irrigation (VRI) is used in Nyírbátor. In contrast, the VRI has given positive results, making an irrigation equipment with the VRI a safer and more uniform method than a conventional linear irrigation equipment.

Keywords: irrigation, Christiansen-uniformity, distribution uniformity, crop

The Intergovernmental Panel on Climate Change concluded in its second assessment report that global climate change will increase the frequency of floods and droughts. In the future, the increase of water demand will be influenced by a number of factors, such as urbanization, the growth of irrigated areas and intensive agriculture (Iglesias et al., 2010; Kellis, Kalavrouziotis, Gikas, 2013). There are 324 million hectares of irrigated land in the world, covering 21% of the world's total production area, with 61% of the harvested crops coming only from various cereals (FAO, 2016). The average annual precipitation in Hungary is 0.5–0.7 m. However, the annual precipitation shows a decreasing trend (MET, 2019). The changing weather in recent years is also a problem for agriculture (Szalai, 2009; Jolánkai et al., 2018). That is why the irrigation is now considered an increasingly necessary factor. Nevertheless, due to lack of irrigation, the yield averages fluctuate every year. Based on the available water resources and water management options, approximately 400,000 hectares of land in Hungary could be irrigated instead of the current 100.00 ha (Nemzeti Vízstratégia, 2017). In order to ensure the stability of crop safety, it would be necessary to apply 0.1–0.2 m of irrigation water/year, which means 1.000–2.000 $m^3.ha^{-1}$ of water for the field. After assessing the needs of the plants, a decision must be made to use a proper irrigation method (Smith, Baillie, 2009). Depending on the field conditions, the most common methods of irrigation within rainwater irrigation are linear and winder drum irrigation. The precision irrigation is when a precise water application minimizes the adverse effects on the environment, while meeting the needs of the individual plants (Raine et al., 2007), which is now identified as a 'variable rate irrigation' (VRI). When using the VRI, some

important information can be integrated into the irrigation, for example soil parameters, topographic maps and data of the plant to be irrigated (Boluwade, Madramootoo, Yari, 2016; Colaizzi et al., 2017; Yari et al., 2017). In our research, we aimed to compare the irrigation homogeneity of a linear irrigation equipment with the VRI controlled linear irrigation equipment, revealing the ratio of underserved and over-irrigated areas. The surveys were conducted under field conditions on sweet corn.

Material and method

The field surveys were carried out at the University of Debrecen, Institutes for Agricultural Research and Educational Farm and in the arable areas of Nyírbátor's company in Hungary in July and August in 2019 on different types of linear irrigation equipment (Table 1).

In the course of the research, we evaluated the spray uniformity of the conventional and linear irrigation equipments with the VRI, as well as the proportion of under- and over-irrigated areas. Three field surveys were conducted in which the precipitation meters were placed under the irrigation equipment. The measuring vessels were placed in a 4 × 4 grid at every 5 m to 0.3 m and 1.5 m height in the maize row spacing at each measurement time. The first two measurements were used to examine the standard deviation of the utilized water by the conventional linear irrigation equipment and the third measurement was used to examine the uniformity of spraying and interception of the VRI. The corn was 0.5 m high for all three measurements. Conventional linear water was applied with a uniform linear

Table 1　　　　The surveyed irrigation equipments

Location	University of Debrecen, Institutes for Agricultural Research and Educational Farm	Bátortrade Kft in Nyírbátor
Irrigation equipments	Linear irrigation equipment	Precision linear irrigation equipment with VRI
Type of the irrigation equipments	Valley 8120 universal irrigation equipment with underground induction control	Reinke E2060PL reversible linear
Type of the nozzles	Seninger	Rotator® Pivot Sprinkler (Nelson Irrigation Corporation)

velocity of 20 m.h^{-1} at the same water pressure and in the case of the VRI, with $10 \cdot 10^{-3}$ m irrigation water application. There was complete wind silence at the time of the measurements. The spray uniformity was calculated from the data of the amount of irrigation water ($1 \cdot 10^{-3}$) applied to the rain meters. To determine the uniformity values of the nozzles, we used the Christiansen-uniformity coefficient (CUc %) (1) calculated on the basis of the water volumes of the collecting vessels placed at a height of 1.5 m (Karmeli, 1978; Topak et al., 2005) (1). The other really important factor is the distribution uniformity (DU%) (2), which is particularly sensitive to underwatering, was calculated to determine the uniformity of a water application (Kruse, 1978):

$$CU_c = 100 \left[1 - \frac{\sum\limits_{i=1}^{n} \left| V_i - \overline{V} \right|}{\sum\limits_{i=1}^{n} V_i} \right] \qquad (1)$$

where:

$\sum \left| V_i - \overline{V} \right|$ – sum of the absolute deviations of the individual measurements in relation to the mean

$\overline{V}$ – average of all measurements

V_i – individual measurement data

n – number of measuring points

$$DU\% = 100 \left(\frac{\overline{X_{i25\%}}}{\overline{X_i}} \right) \qquad (2)$$

where:

$X_{i25\%}$ – the average of the water covering of the driest quarter

X_i – the average water covering of the whole area

In addition to the calculation of uniformity factors, the spatial distribution of the application was also examined in order to delimit the under- and over-irrigated areas. The limit value of underwatering was calculated as the median - (median–minimum) · CUc% (3) for the amount of the applied irrigation water. The limit value of over-irrigation was calculated as the median + (maximum – median) · CUc% (4) for the amount of the applied irrigation water. The distribution of an irrigation water application was analysed in a Surfer program.

We have also examined the gradual transition between the different irrigation sectors. During the measurements, 15 rain gauges per meter were placed at a height of 1.5 m. In the case of the conventional linear irrigation, its speed was reduced to 10 m.h^{-1} by increasing the amount of the applied irrigation water. Concerning the VRI, the water application

was increased to $20 \cdot 10^{-3}$. The development of the amount of interception was calculated on the basis of the linear and conventional results with the VRI at 0.5 m high maize stands with the water volumes of the measuring vessels placed at a height of 0.3 m.

Results and discussion

Christiansen's uniformity factor and the distribution uniformity results

The average amount of irrigation water collected in the rain gauges placed at a height of 1.5 m was 14.5 ±4.44 · 10^{-3} in the case of the conventional linear irrigation system. The irrigation uniformity of the nozzles was CUc% 75.43% and DU% 74.14%. The CUc% value must reach a minimum of 84% and the deviation uniformity in practice and the minimum value of homogeneity is 80% DU% (Irmak et al., 2011). Since the results do not reach the minimum values for homogenous irrigation, the application of linear water is not uniform. The use of the nozzles resulting from the older equipment can be the reason for the poor uniformity. The average amount of irrigation water collected in the rain gauges placed at a height of 1.5 m was 10.03 ±0.64 · 10^{-3} in the case of the VRI. The CUc% calculated from the data of the applied water was 95.25% high and the DU% showed 90.97% for the VRI, which means that the irrigation is homogenous. In addition, the VRI had smaller standard deviation than the conventional one without the VRI, which also suggests that the water application is more homogeneous and uniform in the case of the VRI. The spatial distribution study also reveals a significant difference in irrigation uniformity between two different linear technologies (Figure 1).

When we used the conventional linear irrigation equipment, the under-irrigated area was 46.15 m^2 which is 20.5% of the total irrigated area. The over-irrigated part is 7.45 m^2 which is 3.3% of the total area. In contrast, when the VRI was used, the under-irrigated area was 8.55 m^2 which is 3.8% of the total irrigated area, while the over-irrigated area was 0.007 m^2 which is 0.03% of the total area.

Evaluation of the gradualness of transition between the irrigation sectors

As a pilot study for the conversion of the water applications between the sectors, we set up 15 water collector dishes in one line in one meter distances. It is important that the result represents the increasing water application values of a single nozzle. In the case of the conventional linear system, we changed the speed of the irrigation equipment without changing the water pressure. Thus, the rate of a specific

Conventional linear irrigation system irrigation water application values

VRI system irrigation water application values
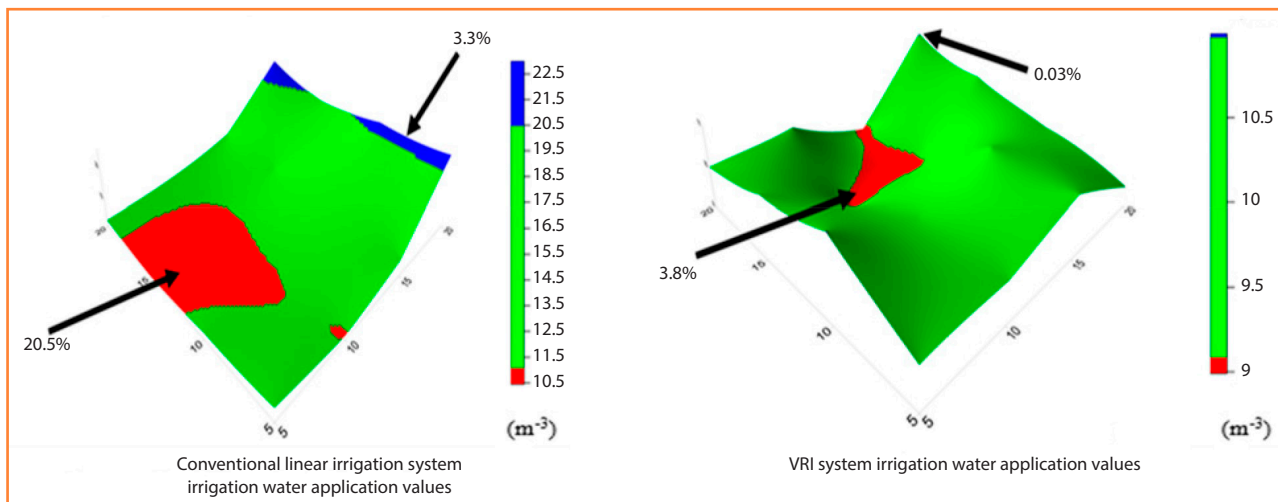
Figure 1　Spatial distribution of the irrigation water application
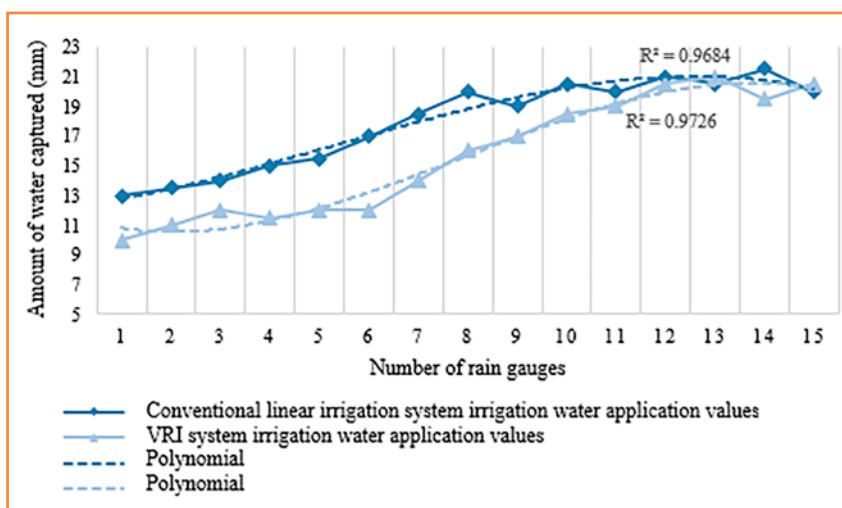
Figure 2　Irrigation water application between sectors

water application was modified. The amount of the applied irrigation water was regulated at the nozzle level in the VRI. In the case of the conventional linear system, the speed of the irrigation equipment was reduced from 20 m.h^{-1} to 10 m.h^{-1}. We increased the rate of the water application from $10 \cdot 10^{-3}$ to $20 \cdot 10^{-3}$ in the case of the VRI. The uniformity and gradualness of the switching between the sectors was evaluated with a polynomial function. Based on the deterministic coefficients, both the conventional and the VRI have a sufficiently smooth transition between the sectors ($R^2 = 0.968$ and $R^2 = 0.973$) (Figure 2).

Evaluation of the effect of interception of the irrigation distribution uniformity

The interception of the 0.5m high maize was calculated on the basis of the water collector dishes placed at a height of 0.3 m. We did not find a significant difference in the interception between the different linear technologies: the degree of interception ranged from 2.5 to $4.69 \cdot 10^{-3}$ in the area, with an average value of $3.42 \cdot 10^{-3}$. There is no significant change in the irrigation uniformity based on Christiansen-uniformity coefficient between the uniformity with and without an interception. In the case of the conventional linear system, the Christiansen uniformity coefficient (ICUc% 74.93%) is just 0.66% smaller than the interception-

free values, while for the VRI, the Christiansen-uniformity coefficient is ICUc% 93.64%, which is 1.69% below the coefficient calculated under the interception-free circumstances. In contrast, more differences were found between the conventional and the VRI in the case of changes in the DU values. The DU value with an interception is 58.05%, which is 21.7% smaller than the DU without an interception, while for the VRI, the decrease is only 4.06%. The DU is a more sensitive indicator of under-irrigation than the CU, because it compares the driest quarter water application to the average application. Though the distribution of interception is considered to be homogeneous, the effect of interception is more significant on the under-irrigated sites (20.5% of the studied area) with $9-11.5 \cdot 10^{-3}$ water utilization compared to the areas with an average $14.5 \cdot 10^{-3}$ water application. The $3.42 \cdot 10^{-3}$ interception represents 30-36% of the applied irrigation water in the driest area and in those sites where the water application was average ($14.5 \cdot 10^{-3}$), the interception is only 24% of the applied water amount. Therefore, besides the fact that less irrigation water was applied on the under-irrigated areas, the rate of the net irrigation water was smaller as well.

Conclusion

The lack of natural precipitation can be compensated primarily with irrigation to reduce yield fluctuations, increase yields and improve crop quality. The application of homogeneous and

adequate irrigation water in a field area is important in several aspects. Improper application of water can lead to the deterioration of the production area, pesticides can leach out of the soil as well as deterioration of the soil structure and the formation of salinisation can occur. For this reason, it is important to use an irrigation system that is suitable for applying safe and stable homogeneous irrigation water. Our research results, the application uniformity of the VRI, are homogeneous, while in the case of the conventional linear system, a significant heterogeneity can be observed. Use of the VRI in a long-term horizon ensures a good quality of field conditions and provides a solid basis for the design and development of precise agriculture as well as precise irrigation technologies. Moreover, the use of the VRI reduces the phenomenon of under- and over-irrigated areas.

Acknowledgements

References

Boluwade, A., Madramootoo, C., Yari, A. (2016). Application of unsupervised clustering techniques for management zone delineation: Case study of variable rate irrigation in Southern Alberta, Canada. *Journal of Irrigation and Drainage Engineering*, *142*(1), 1–8.

Colaizzi, P. D., O'Shaughnessy, S. A., Evett, S. R., Mounce, R. B. (2017). Crop evapotranspiration calculation using infrared thermometers aboard center pivots. *Agricultural Water Management,* (187), 173–189.

FAO (2016). *AQUASTAT website.* http://www.fao.org/nr/water/aquastat/didyouknow/index3.stm Query date: 2018.12.

Iglesias, R., Ortega, E., Batanero, G., Quintas, L. (2010). Water reuse in Spain: data overview and costs estimation of suitable treatment trains. *Desalination 263*, 1–10.

Irmak, S., Odhiambo, O. L., Kranz, L. W., Eisenhauer, E. D. (2011). Irrigation Efficiency and Uniformity, and Crop Water Use Efficiency. *Biological Systems Engineering: Papers and Publications,* (451) 8.

Jolánkai, M., Kassai, M. K., Tarnawa, Á., Pósa, B., Birkás, M. (2018). Impact of precipitation and temperature on the grain and protein yield of wheat (*Triticum aestivum* L) varieties. *Időjárás, 122*(1), 31–40.

Karmeli, D. (1978). Estimating sprinkler distribution pattern using linear regression. *Transactions of the ASAE*, (21), 682–686.

Kellis, M., Kalavrouziotis, I. K., Gikas, P. (2013). Review of wastewater reuse in the Mediterranean countries, focusing on regulations and policies for municipal and industrial applications. *Glob. Nest J., 15*, 333–350.

Kruse, E. G. (1978). Describing Irrigation Efficiency and Uniformity. *Journal of the Irrigation and Drainage Division, 104*(1), 35–41.

MET (2019). website. https://www.met.hu/eghajlat/magyarorszag_eghajlata/altalanos_eghajlati_jellemzes/csapadek/ Query date: 2019. 07.

Nemzeti Vízstratégia (2017). Nemzeti Vízstratégia (Kvassay Jenő Terv). In eng.: *National Water Strategy* (Jenő Kvassay Plan) (140 p.).

Raine, S. R., Meyer, W. S., Rassam, D. W., Hutson, J. L., Cook, J. F. (2007). Soil-water and solute movement under precision irrigation: Knowledge gaps for managing sustainable root zones. *Irrigation Science, 26*(1), 91–100.

Smith, R. J., Baillie, J. N. (2009). *Defining precision irrigation: A new approach to irrigation management.* National Centre for Engineering in Agriculture and Cooperative Research Centre for Irrigation Futures (pp. 18–21).

Szalai, S. (2009). Drought Tendencies in Hungary and its Impacts on the Agricultural Production. *Cereal Research Communications*, (37), 501–504.

Topak, R., Suheri, S., Ciftci, N., Acar, B. (2005). Performance evaluation of sprinkler irrigation in a semi-arid area. *Pakistan Journal of Biological Sciences*, (8), 97–103.

Yari, A., Madramootoo, A. C., Woods, A., Shelley-Adamchuk, I. V. (2017). Performance Evaluation of Constant Versus Variable Rate Irrigation. *Irrigation and Drainage*, *66*(4), 501– 509.

ASSESSMENT OF A YIELD PREDICTION METHOD BASED ON TIME SERIES LANDSAT 8 DATA

Andrea SZABÓ*, Odunayo David ADENIYI, János TAMÁS, Attila NAGY

University of Debrecen, Hungary

The active biomass of cultivated plants and average yield decreases as a result of biotic and abiotic stress effect. The extent of the reduction can be quantified on the basis of remotely sensed data. The aim of this research is to evaluate the suitability of Landsat 8 data for a wheat yield estimation. We processed Landsat 8 recordings for the period 2013–2019 and generated NDVI data. Time series NDVI data were calibrated and validated with observed wheat yield averages. The agricultural plots around Karcag, Hungary, were our research area. The relation between Landsat NDVI data and yield was strongest and highest in the total biomass period ($R^2 = 0.53$–0.54) and the estimation error based on RMSE is between 0.48–0.7 t.ha^{-1}.

Keywords: Landsat 8, crop, yield prediction

There has been an increase in the concern about food security and sustainable agricultural development in the world today, of which the actual estimation of supply and demand of major crops such as wheat is the main component. Wheat is the third most grown cereal after maize and rice with a production of 3.78 t.ha^{-1} globally (FAOSTAT, 2018). In Hungary, the temperature keeps increasing and this can be characterized by a decrease in precipitation and an increasing frequency of droughts (Szász, 2005). For this reason, monitoring the agricultural areas is essential. Remote sensing-based agricultural monitoring systems are able to provide timely information on the status, phases and expected yields of crop production (Bolton, Friedl, 2013; Tewkesbury et al. 2015; Vicente-Serrano et al., 2015), complementing the traditional methodology (Atzberger, 2013; Tamás, Nagy, Fehér, 2015; Nagy, Fehér, Tamás, 2018). This is important because the farmers can easily identify areas where changes in crop yields are expected (Clement et al., 2013). We aim to analyse and apply a yield estimation monitoring system based on Normalized Difference Vegetation Index (NDVI) data derived from Landsat 8 satellite imagery. The interest in using satellite remote sensed data for crop monitoring and crop production forecasting today has tremendously increased due to its potential to produce data synoptically, with much spatial coverage, potentially at global scale. Moreover, remote sensing is capable of providing timely (and potentially real-time) and objective data on crop growth at relatively small cost. We have calculated the NDVI and developed a model to monitor a crop yield. The NDVI as an indicator of photo synthetically active vegetation provides important information for farmers, as the value obtained correlates with the specific chlorophyll content and biomass content of the vegetation covering in the area (Bolton, Friedl, 2013; Panda, Ames, Panigrahi, 2010; Dempewolf et al., 2014; Mkhabela et al., 2011; De la Casa et al., 2018).

Material and method

We have processed satellite images prepared by Landsat 8 OLI, from which we have calculated the time series NDVI data of the area and compared to the real yield averages for the period 2013–2019, for our research. The Landsat 8 satellites orbit the Earth in a 16-day repetition cycle. Landsat captures approximately 740 scenes every 8 days on the Worldwide Reference System-2 (WRS-2) sequence system with a scene size of 185 × 180 km. Landsat 8 OLI/TIRS C1 Level-1 images with a cloud covering less than 50% were downloaded from https://earthexplorer.usgs.gov/. The downloaded files contain a total of 11 spectral bands at different wavelengths of visible, near-infrared and shortwave infrared, of which the data of B4 (red) and B5 (NIR) bands with 30 m spatial resolution were used for further processing in this study. The first calculation of the NDVI index (1) was performed in ArcGIS software with Raster Calculator according to the following formula.

$$NDVI = (NIR - RED)/(NIR + RED) \tag{1}$$

The average yield data (t.ha^{-1}) required for the research were provided by the Karcag Research Institute of Agriculture in Hungary. Wheat yield data from 16 arable lands (Figure 1) for the period 2013–2019 were used to calibrate the time

Contact address: Andrea Szabó, University of Debrecen, Faculty of Agricultural and Food Sciences and Environmental Management, Institute of Water and Environmental Management, ☏ +36 50 50 84 44/880 12; e-mail: szabo.andrea@agr.unideb.hu,
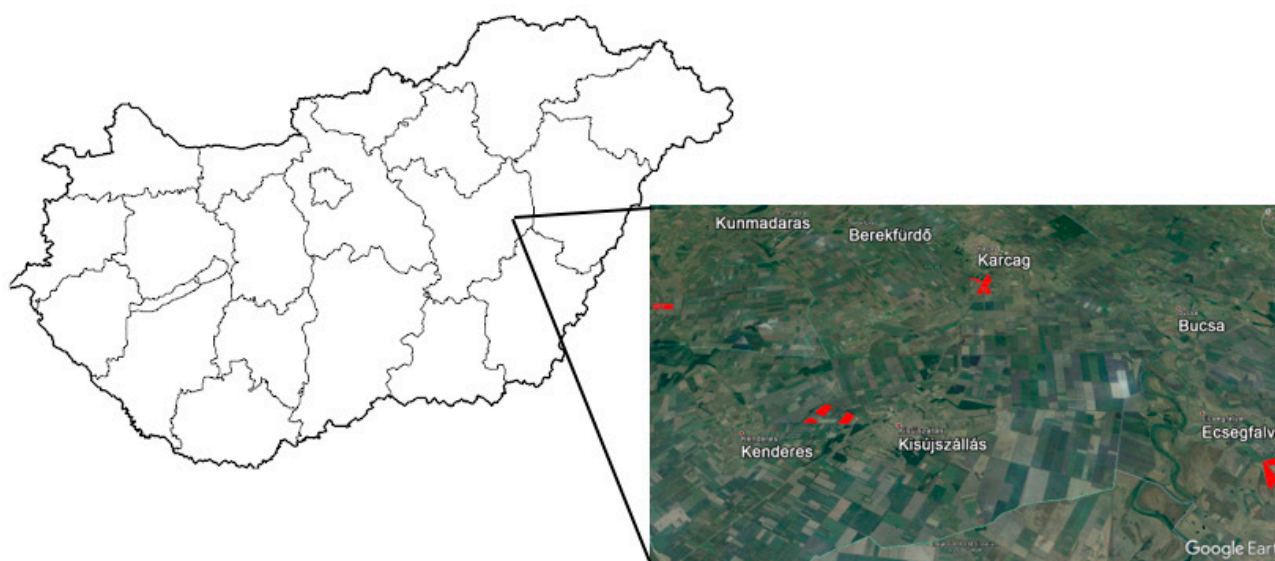
Figure 1 Location of the examined plots
Source: Google Earth

series NDVI data derived from Landsat 8 OLI and to validate the prepared model.

The research institute has provided us with the average yields of real wheat harvested/plot and a vector database of an arable land. We have performed the additional necessary calculations in the ArcGIS software environment. In the first step, we selected the mean NDVI values for each plot between March and August. The resulting average NDVI values/plot were calibrated with the actual yield average data. The calibration was performed by a linear regression (2) and we calculated the deterministic coefficient and estimation equations, the RMSE (Root Mean Square Error) (3) and NRMSE (Normalized Root Mean Square Error) (4) values were calculated to analyse the reliability of the regression and to validate the estimation equations. The calibration was based on data from the first 6 years (2013–2018), while the validation was based on data from 2018–2019, similarly to the research of Dempewolf et al. (2014) and Nagy, Fehér, Tamás (2018), where a minimum of 6-year remotely sensed time series were used for the yield analysis. In addition, we calculated the relative (5) and absolute (6) deviations of the estimated value from the actual harvested value.

$$R^2 = 1 - \frac{\sum_{i=1}^{n}(y_i - y_i')^2}{\sum_{i=1}^{n}(y_i - \overline{y})^2} \qquad (2)$$

$$RMSE = \sqrt{\frac{\sum_{i=1}^{n}(y_i - y_i')^2}{n}} \qquad (3)$$

$$NRMSE = \sqrt{\frac{\sum_{i=1}^{n}(y_i - y_i')^2}{n}} \Big/ \big(\max(y_i) - \min(y_i)\big) \qquad (4)$$

$$Relative\ deviation = \frac{y_i' - y_i}{\overline{y}} \cdot 100 \qquad (5)$$

$$Absolute\ deviation = \left| \frac{y_i' - y_i}{\overline{y}} \cdot 100 \right| \qquad (6)$$

where:
y_i – data measured on the sample (t.ha⁻¹)
y_i' – estimated yield of the sample (t.ha⁻¹)
        – average yield (t.ha⁻¹)
n – number of samples (t.ha⁻¹)

Results and discussion

Based on the results of the linear regression, the deterministic coefficient values calculated on the basis of the NDVI values at the end of May and the first half of June period have a stronger correlation (Figure 2) with the yield averages (on days 150, 154,160 and 163). It is noteworthy that the NDVI data on days 154 and 160 showed the strongest relation with the yield averages ($R^2 = 0.542$ and $R^2 = 0.536$) (Figure 2).

After calculating the estimation models, we validated the models based on the relative deviation, absolute deviation, RMSE and NRMSE% values based on the NDVI and yield data of period 2018–2019. The RMSE and NRMSE% values for the years are shown in the Table 1. The validated 2-year mean RMSE was 0.713 t.ha⁻¹ on day 150, 0.547 t.ha⁻¹ on day 154, 0.489 t.ha⁻¹ on day 160, and 0.491 t.ha⁻¹ on day 163. The mean NRMSE (%) values based on 2 validated years were 13.09% on day 150, 10.04% on day 154, 8.99% on day 160, and 9.01% on day 163.

The relative deviation of the forecast value from fair values was -6.87% on day 150, on day 154 it was -5.05%, on day 160 it was -5.06%, and on day 163 it was -5.31%. Concerning the absolute differences, the difference on day 150 was 8.37%, on day 154 it was 7.51%, on day 160 it was 6.35% and on day 163 it was 6.14% (Figure 3).
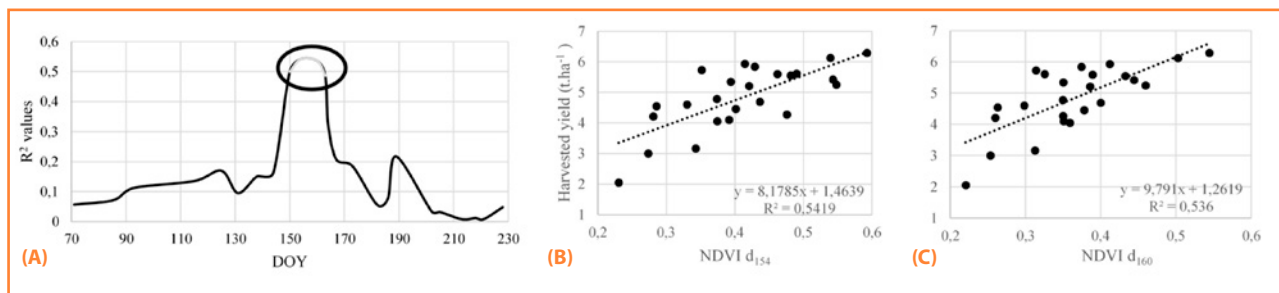
Figure 2   Determination coefficients of NDVI versus yield (A) and linear regression of NDVI and yield on days 154 (B) and 160 (C)

Table 1   Yield estimation models from 2018 to 2019

Day	Equation	Year	RMSE	NRMSE (%)
150.	$y = 9.5592 \cdot NDVI_{150} + 0.792$	2018	0.865	15.87
		2019	0.519	9.54
154.	$y = 8.1785 \cdot NDVI_{154} + 1.4639$	2018	0.455	8.35
		2019	0.626	11.49
160.	$y = 9.791 \cdot NDVI_{160} + 1.2619$	2018	0.439	8.07
		2019	0.535	9.82
163.	$y = 9.1427 \cdot NDVI_{163} + 1.7047$	2018	0.401	7.36
		2019	0.566	10.39

Based on the relative differences, it can be stated that the predicted yield values are just slightly smaller that the measured yield values. The values of the absolute deviation were not much higher than the 5% threshold accepted in the literature (Ferencz et al., 2004). The closest to the 5% threshold was the 160th day with the highest R^2, which differed barely by 1%.

Figure 3   Relative and absolute deviations of the predicted value from the actual values

Conclusions

In this study, the Landsat derived vegetation indices during the flowering stage of the wheat development was found to be siginificantly correlated with the wheat yield in whole study site. In agreement with previous studies, the current study has demostrated correlations between NDVIs during the flowering/ fruiting spike period and crop yields (Marti et al., 2007; Labus et al., 2002; Mkhabela et al., 2011; Tiecheng et al., 2019), which has been admited as the most critical period for most crops yield forecasting. The NDVI of 160th day of the year was verified to fit for the wheat yield prediction with the highest R^2 the best. Our study concludes that the Landsat 8-OLI time series data are suitable for forecasting the crop yield. The analysis of satellite images will help farmers to forecast the crop yield, as the NDVI can be used to estimate the expected yield before harvest. Climate change models predict that Hungary will experience more serious drought events. Therefore, timely information on potential yield losses helps farmers or decision makers to minimize the impacts of droughts and take appropriate mitigation measures.

References

Atzberger, C. (2013). Advances in remote sensing of agriculture: context description, existing operational monitoring systems and major information needs. *Remote Sens., 5*, 949–981.

Bolton, D. K., Friedl, M. A. (2013). Forecasting crop yield using remotely sensed vegetation indices and crop phenologymetrics. *Agric. For. Meteorol., 173*, 74–84.

Clement, S., Lassman, F., Barley, E., Evans-Lacko, S., Williams, P., Yamaguchi, S., Slade, M., Rüsch, N., Thornicroft, G. (2013). Mass media interventions for reducing mental health-related stigma (Review). *The Cochrane Library,* (7).

De la Casa, A., Ovando, G., Bressanini, L., Martínez, J., Díaz, G., Miranda, C. (2018). Soybean crop coverage estimation from NDVI images with different spatial resolution evaluate yield variability in a plot. *ISPRS J. Photogramm. Remote Sens., 146*, 531–547.

Dempewolf, J., Adusei, B., Becker-Reshef, I., Hansen, M., Potapov, P., Khan, A., Barker, B. (2014). WheatyieldforecastingforPunjabProvincefromvegetation index time series and historic crop statistics. *Remote Sens., 6*, 9653–9675.

FAOSTAT (2018). website. http://www.fao.org/faostat/en/#data/QC/ Query date: 2020. 05.

Ferencz, Cs., Bognár, P., Lichtenberge, J., Hamar, D., Tarcsai, GY., Timár, G., Molnár, G., Pásztor, Sz., Steinbach, P., Székely, B., Ferencz, O. E., Ferencz-Árkos, I. (2004). Crop yield estimation by satellite remote sensing. *Int. J. Remote Sens., 25*(20), 4113–4149.

Labus, M. P., Nielsen, G. A., Lawrence, R. L., Engel, R., Long, D. S. (2002). Wheat yield estimates using multi-temporal NDVI satellite imagery. *International Journal of Remote sensing*, *23*(20), 4169-4180.

Marti, J., Bort, J., Slafer, G. A., Araus, J. L. (2007). Can wheat yield be assessed by early measurements of normalized difference vegetation index? *Annals of Applied Biology*, *150*, 253–257.

Mkhabela, M. S., Bullock, P., Raj, S., Wang, S., Yang, Y. (2011). Crop yield forecasting on the Canadian Prairies using MODIS NDVI data. *Agric. For. Meteorol., 151*, 385–393.

Nagy, A., Fehér, J., Tamás, J. (2018).Wheat and maize yield forecasting for the Tisza river catchment using MODIS NDVI time series and reported crop statistics. *Computers and Electronics in Agriculture, 151*, 41–49.

Panda, S. S., Ames, D. P., Panigrahi, S. (2010). Application of vegetation indices for agricultural crop yield prediction using neural network techniques. *Remote Sens., 2*, 673–696.

Szász, G. (2005). Termésingadozást kiváltó éghajlati változékonyság a Kárpát-medencében. "*Agro-21" füzetek,* (40) 33–69.

Tamás, J., Nagy, A., Fehér, J. (2015). Agricultural biomass monitoring on water sheds based on remotely sensed data. *Water Science and Technology, 72*(12), 2212–2220.

Tewkesbury, A. P., Comber, A. J., Tate, N. J., Lamb, A., Fisher, P. F. (2015). A critical synthesis of remotely sensed optical image changed detection techniques. *Remote Sensing of Environment, 160,* 1–14.

Tiecheng, B., Nannan, Z., Benoit, M., Youqi, C. (2019). Jujube yield prediction method combining Landsat 8 Vegetation Index and the phenological length. *Computers and Electronics in Agriculture*, *162*, 1011–1027.

Vicente-Serrano, S. M., Cabello, D., Tomás-Burguera, M., Martín-Hernández, N., Beguería, S., Azorin-Molina, C., Kenawy, A. E. (2015). Droughtvariability and land degradation in semiarid regions: assessment using remote sensing data and drought indices (1982–2011). *Remote Sens., 7*, 4391–4423.

WATER MANAGEMENT WITHIN THE SOIL-PLANT SYSTEM – A CHALLENGE FOR THE 21ST CENTURY

Márta BIRKÁS[1], Danijel JUG[2], Ivica KISIĆ[3], Katalin M. KASSAI[1], Ákos TARNAWA[1], Márton JOLÁNKAI*[1]

[1]Szent Istvan University, Gödöllő, Hungary
[2]Josip Juraj Strossmayer University of Osijek, Osijek, Croatia
[3]University of Zagreb, Zagreb, Croatia

Water is the most essential substance regarding the physiological processes of any living system. Agricultural activities and global food security are highly influenced by water availability. The value of water and water resources already exceeds that of energy sources today. The water-related concepts are very diverse in agricultural relations. The aim of this paper was to revive some terms related to water and discuss their importance in soil-plant systems. In this paper, eight phrases were selected paying attention to the importance of water management, namely soil water management, soil moisture range for workability, rain stress, water logging, water shortage, irrigation, water intake and water loss, avoiding water loss and reply to climate change phenomena. Findings of water management research point to a relationship between soil quality and improvement of water intake capacity, parallel with climate stress mitigation.

Keywords: soil moisture, rain stress, water shortage, irrigation, climate prognoses

The Pannonian Basin covers the whole or parts of the territory of as many as nine countries. The basin is dominated by the combined effects of Atlantic, Mediterranean and continental climates and fairly exposed to climate extremes (Szalai, Lakatos, 2013). Soil as the largest potential natural water reservoir in the basin has increasing importance under conditions of predicted climate change resulting in an increase of probability of extreme hydrological events (Farkas, Birkás, Várallyay, 2009). The distribution of the amount of precipitation, the number of precipitation events, and longer dry periods show upward tendencies and may have serious effects on the available water amount and the surface water balance (Jolánkai, Nyárai, Kassai, 2013; Jug et al., 2017). A great part of the atmospheric precipitation can be stored in the 0–100 cm layer of the soil; however, this water storage may be reduced by hydrological stresses (Várallyay, 2010). Findings of the water management research point to a relationship between soil quality and improvement of water intake capacity, parallel with climate stress mitigation (Birkás et al., 2018, 2019).

This study highlights various manifestations of the water forms and the discussion of certain consequences of the lack and surplus of water in soils that can be measured and a description of the possible remedies that should be applied to soils so damaged.

Material and method

This paper is based on works and scientific communications reviewing the subjects of water management and on stating in long term experiments underway in the countries as well as on the conclusions drawn from them (Birkás et al., 2015, 2017a,b; Bogunović, Kisić (2017). The water management problem referred to in this paper was also studied in the long term Soil quality – climate experiment that has been underway since 2002 at Hatvan-Józsefmajor (47 41' 31.7" N 19 36' 36.1" E, 110 m a.s.l), in the year 2002 with a soil of a clay-loam texture, Endocalcic Chernozems, Loamic (IUSS Working Group WRB, 2015). The experiment was of the single-factor type, in random stripe arrangement in four replications, in which six treatments were applied, that are direct drilling (DD), shallow disking (12–15 cm), shallow and medium deep cultivator (18–20 cm and 22–25 cm) ploughing followed by surface forming (30–34 cm, P) and loosening (40–45 cm). This long-term experiment has given useful information to understand the change in water content in soils that are in different physical conditions (Farkas, Birkás, Várallyay, 2009). On the one hand, the long-term experiments provided important data on the fact that water conservation is actually a reduction of water loss and, on the other hand, confirmed that, despite the difficulties of the climate, there are tillage methods suitable for alleviation of the natural induced damages.

Contact address: Márton Jolánkai, Szent István University, 1. Páter Károly utca, 2100 Gödöllő, Hungary, ☏ +362 04 17 43 63, https//:www.szie.hu; e-mail: jolankai.marton@mkk.szie.hu

Results and discussion

Water has a profound impact on our lives and on all agricultural management activities. Nowadays, water in agriculture will continue to play a critical role in global food security. The value of water and water sources already exceeds the value of energy sources today. The water-related concepts are very diverse in agricultural relation. In this paper, eight phrases were selected, relevant to the importance of the soil water management.

Soil water management

There are some new terms often cited by authors in relation to water, such as e.g. the green, the blue and the brown water. The first term can apply to our case, because the water that is stored in unsaturated soil layer forms the green water resource (Velpun, Senay, 2017). Soil water management comprises the amount of water in the soil, its state, form and movement and changes in these factors in time and in space, affected by soil water intake, its water permeability, its capacity to retain and store water and the conditions of its desiccation. Dexter, Bird (2001) noted that loose soil takes water in quickly (infiltration, percolation), later, the process slows down and its rate becomes constant. The amount of water retained by soil against gravitation is referred to as water capacity.

Water availability for plants depends on soil moisture tension that ranges from field capacity to wilting regime and may vary by the soil physical type as it can be seen in Figure 1. Plant species abilities in water uptake range between 1 to 12 at osmotic pressure in general.

Soil moisture range of workability

Soil workability is defined as the ease of working with well-drained soil to produce desirable conditions for sowing that is not consisting of structures that are either too fine or too coarse for crop establishment. Soil is workable within a range of water content and soil tillage operations produce the desirable state for crop production. The various types of soils have their own specific workable moisture range, just like the way they differ from each other in terms of

Figure 1   Water retention curves for three different texture classes

their specific particle compositions and clay ratios. A soil workable moisture range is determined by the quantity and quality of its clay fraction, organic matter content, structure and compactness. The tillage of any type of soil takes less energy in the moisture range that is favourable from the aspect of workability and tool effectiveness (Birkás et al., 2018). Moreover, soil organic matter plays a crucial role in soil health and represents one of the key functions for determining soil suitability for crop production.

Rain stress

Due to the amount or intensity of rainfall, rain stress can cause damage to the upper layer of soil, either temporary or long-term. Climate change-induced precipitation phenomena tend to have adverse impacts on soils. Intensive spring showers following the dry early spring period wash chemicals distributed on the soil surface into the cracks in the soil, making double damage, as the applied chemicals failed to have exerted their action during the dry period and then when the rains come and soak the soil through they are washed away (Birkás et al., 2017b). On sloping fields, severe damages are caused by heavy downpours washing soil off (Kisić, Bogunović, Bilandžija, 2017).

Water logging

The Carpathian basin, considering the geological formation, geographic location and climate threats, is continuously exposed to water-related phenomena that are water surplus and deficit. Damages and hazards associated with water surplus appearing in the soils or on the surface are expressed with various phrases e.g. excess water inundation, inland excess water, flooding, water-logging, water pond, water saturation and over-moistening. Water-logging may be regarded as naturally induced when the water table of the groundwater is too high and the excess water may appear on the surface and stagnate there for longer time (Pálfai, 2010). A long period of water-logging deteriorates soil workability and fertility and it also reduces the site's economic value. Moreover, the stagnant water saturates the soil, silts the fertile layer, destroys the crops and increases nitrogen leaching which seeping into the groundwater and then finally moving into live bodies of water.

Water shortage

Water output is affected by the type of the land use, soil tillage (water wasting or conserving) and water utilization of plants. A drought-induced loss cannot be avoided in soils where water wasting tillage has been applied for multiple years (Birkás et al., 2018). Soils dry out through evaporation and transpiration. Moisture is lost from the topmost soil layers in the form of water vapour to the near-surface atmosphere, and this process continues until the relative humidity matching. The near surface air layer is permanently replaced by the movement of the air and therefore it takes continuous evaporation to re-establish the equilibrium. Avoiding the water loss from arable soils requires new moisture conservation solutions including optimised soil disturbance and surface protection (Jug et al., 2017).
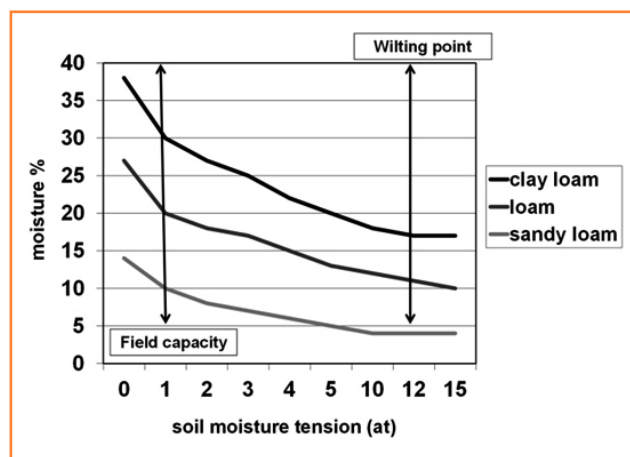
Irrigation

Irrigation is aimed at supplementing the crop's natural water supply under the prevailing weather conditions that prevent water shortage for yield safety, increasing or maintaining the yield quality and biomass and improving crop conditions.

Besides its benefits, irrigation has some negative impacts on soil e.g. regular soaking of soil makes a stress factor, frequent soaking may result in inadequate aeration in soil, water transports colloids, dust and silt into deeper layers which, settling down in a compact layer, aggravate its compaction (Table 1).

There are solutions to prevent soil deterioration in the irrigated soils. The most important factors are as follows: water intake capacity and the water saturation capacity; optimal water infiltration; depth of water table level of soil; regular soil condition tests; preventing anaerobic conditions; organic matter and water conserving; mitigating drought and heat stress; irrigation out of the growing season e.g. covering the surface, growing green manure crops; irrigation in a rotation – in which cropping is practised without irrigation – enables the soil to recover (Liu et al., 2016).

Water intake and water loss

Soil natural water transport characteristics can be altered by means of hydro-melioration procedures (Farkas, Birkás, Várallyay, 2009). Tillage affects the ratio of water intake and water loss that is of the soil moisture transport. The importance of the soil state lies in its impacts on the ratio of the water taken and stored in the soil, relative to utilised and wasted water (Várallyay, 2010). Intake is the part of precipitation that ends up in soil, most often some 65–70%, rarely exceeding 80%. Water infiltration and storage depend on the depth of the loosened layer and on the water permeability of the soil underneath the disturbed layer. The extent of water loss is affected outside the growing season by the shape of the tilled surface, surface cover and the depth of disturbance (Birkás et al., 2018). The role of the soil condition and that of tillage is illustrated in Table 2.

Soil moisture loss is alleviated by Birkás et al. (2018): loosening any compact layer that impedes water intake; covering the soil with chopped/crushed stubble residues and by reducing the soil surface area by creating water conservation surface; applying organic matter conservation tillage; avoiding the clod formation during dry periods, thus, loosening + crumbling + pressing is recommended; producing crops of different growing seasons with different times of sowing as well as harvesting,; adapting crop density to season controlling weed infestation in the field. Soil moisture should be managed reasonably.

Avoiding the water loss in relation with climate change

According to long-term prognoses milder winters with more precipitation, warm and dry summers, extreme fluctuations in the annual distribution of the total precipitation and increased numbers of windy and stormy days should be expected in the Pannonian region from the second decade of the 21st century (Bartholy et al., 2004). After heavy rains water stagnates in the soil surface, suffocating the plants. If there is no impervious layer in soil, water does not stagnate on the soil surface for a long period even after a very heavy rain. Water is lost through the large surface of dry, cloddy soil and it even takes in water less efficiently. The large clumps should be broken down first with heavy slicer rolls, pressing them at the same time into the disturbed soil to create conditions under which they soak through more

Table 1   Important factors affecting the results of irrigation

Unfavourable	Favourable
– higher than soil intake capacity – partly utilization for crops or harmful – water surplus or absence	**Amount:** – crop refreshing – soil saturation in 8–10 hours
– >10 mm.h^{-1}, when water waste is unavoidable	**Intensity:** – 4–10 mm.h^{-1}
– crumb degrading, causing harmful leaching (N, dust)	**Form:** – soil structure conservation method
– quick soaking with crumb deterioration – harmful transformation in soil surface: crumb desintegration, siltation	**Impact on soil:** – slow soaking – no surface siltation or minimal – crumbling may slightly decrease

Table 2   The role of the soil condition and that of tillage in controlling the loss of water

Factor	Basic requirement	Avoiding
– water intake	– loosened structure	– compact structure
– reducing the loss of water	– covered and minimised surface area	– overconsolidation of soil
– increasing the loss of water	– moderate soil disturbance	– large and bare surface area
– tillage	– any depth, as long as the surface area is minimised	– deep disturbance leaving large exposed surface area on hot and/or windy days

effectively (Birkás et al., 2017b). In disturbed soils, levelling and/or consolidating (with rolls) should be carried out in the summer and in the spring, while in the autumn, levelling should be applied before wintering. The levelled soil will take rainwater and water from melting snow and at the same time, it will lose less water on mild and windy days. Any compact layer impeding the intake of water and the flow of the moisture into the root zone must be eliminated and the soil harmonious water transport processes must be restored. Extreme climate conditions require maintenance of the continuity of water storage capability in the soil along with increasing water infiltration and minimising water loss.

Conclusion

The main postulate from our investigation is that under identical ecological conditions, the uniform and over-standardized adaptation of tillage methods for soil moisture conservation poses a risk. Such applications need special care, and the future belongs likely to site-specific precision technologies. It can be concluded that quantification of the soil water balance components (including plant water uptake and transpiration) and water use efficiency calculations would be beneficial concerning the studied soil management systems with respect to moisture conservation.

Acknowledgements

References

Bartholy, J., Pongrácz, R., Matyasovszky, I., Schalenger, V. (2004). Trends of climate having taken place in the 20th century and expected in the 21st century on the territory of Hungary. *"Agro-21" Füzetek*, *33*, 3–18.

Birkás, M., Đekemati, I., Kende, Z., Kisić, I. (2015). Excess water phenomena – long-lasting remediation. In: Baban, M., Rasić, S. (eds.). Proceedings and abstracts. *8th International Scientific Professional Conference. Agriculture in nature and environmental protection*. Osijek: Glas Slavonije (pp. 34–44).

Birkás, M., Dekemati, I., Kende Z., Pósa, B. (2017a). Review of soil tillage history and new challenges in Hungary. *Hungarian Geographical Bulletin*, *66*(1), 55–64.

Birkás, M., Đekemati, I., Kende, Z., Kisić, I., Pósa, B. (2017b). Results of the soil quality preservation in the extreme seasons. In: Mijić P, Ranogajeć L. (eds.) Proceedings and abstracts. *10th International Scientific/Professional Conference Agriculture in the Nature and Environment Protection*. Osijek: Glas Slavonije (pp. 10–19).

Birkás, M., Jug, D., Kende Z., Kisić, I., Szemők, A. (2018). Soil tillage response to the climate threats – Revaluation of the classic theories. *Agriculturae Conspectus Scientificus*, *83*(1), 1–9.

Birkás, M., Jug, D., Kisić, I., Đekemati, I., Kovács, G.P. (2019). Challenge in the 21st century – water management is soils. In: Jug, D, Brozović, B. (eds.). Proceedings and abstracts. *12th International Scientific/ Professional Conference Agriculture in the Nature and Environment Protection*. Osijek, Croatia: Glas Slavonije (pp. 10–19).

Bogunović, I., Kisić, I. (2017). Compaction of clay loam soil in Pannonian region of Croatia under different tillage systems. *J. Agr. Science and Techn.*, *19*(2), 475–486.

Dexter, A. R., Bird, N. R. A. (2001). Methods for predicting the optimum and the range of soil water contents for tillage based on the water retention curve. *Soil and Tillage Research.*, 57, 203–212.

Farkas, C., Birkás, M., Várallyay, G. (2009). Soil tillage systems to reduce the harmful effect of extreme weather and hydrological situations. *Biologia*, *64*(3), 624–628.

Jolánkai, M., Nyárai, H. F., Kassai, M. K. (2013). A water stress assessment survey based on the evaportranspiration balance of major field crop species. *Növénytermelés*, *62*(Suppl), 351–354.

Jug, D., Jug, I., Vukadinović, V., Đurđević, B., Stipešević, B., Brozović, B. (2017). *Conservation soil tillage as a measure for climate change mitigation*. Osijek, Croatian: Croatian Soil Tillage Research Organization.

Kisić, I., Bogunović, I., Bilandžija, D. (2017). The influence of tillage and crops on particle size distribution of water-eroded soil sediment on Stagnosol. *Soil and Water Research*, *12*(3), 170–176.

Liu, X., Feike, T., Shao, L., Sun, H., Chen, S., Zhang, X. (2016). Effects of different irrigation regimes on soil compaction in a winter wheat–summer maize cropping system in the North China Plain. *Catena*, *137*, 70–76.

Pálfai, I. (2010). Evaluation of the hydrology aspects of groundwater floods in 2010. Clima-21 Brochures. *Climate change – Impacts – Responses*, (61), 43–51.

Szalai, S., Lakatos, M. (2013). Precipitation climatology of the Carpathian Region and its effects on the agriculture. *Növény-termelés*, 62(Suppl.), 315–318.

Várallyay, G. (2010). Increasing importance of the water storage function of soils under climate change. *Agrokémia és Talajtan*, *59*(1), 7–18.

Velpun, M. N., Senay, G. B. (2017). *Partitioning evapotranspiration into green and blue water sources in the Conterminous United States*. Sci. Rep. 7, 6191. www.ncbi.nlm.nih.gov Articles/PMC5522464

IMPACT OF CLIMATE CHANGE ON SOME AGRICULTURAL CROPS DISTRIBUTION AND PRODUCTIVITY IN GEORGIA

Lia MEGRELIDZE[1]*, Nato KUTALADZE[1], Gizo GOGICHAISHVILI[1], Marina SHVANGIRADZE[2]

[1]National Environmental Agency of Ministry of Environment Protection and Agriculture of Georgia, Tbilisi, Georgia
[2]Sustainable Development Centre – Remission, Tbilisi, Georgia

Under the increase of the concern for food security in the world, mainly caused by water resources shortages, the forecast and determination of crop yield at regional scale has been considered as a strategic topic. This study has been conducted to assess the possible impacts of the climate change on cereal crops productivity and irrigation requirement for two main producing regions of Georgia, according to the current crop pattern, and for the 2050s periods. With this aim, water-driven FAO-AquaCrop model has been used. Furthermore, ongoing and forecasted changes, up to the end of the century, in agro-climatic zones relevant for cereals production have been assessed. The climate change data was generated for RCP4.5 scenario through the global circulation model ECHAM4.1, dynamically downscaled on the region via regional climate model (RegCM4.1). Results show overall increase in cereal crop yields, but also enhancement in water shortages even considering optimum management practices under rainfed conditions. Based on the results obtained, recommendations have been developed for adaptation measures to the climate change for the Georgia Agriculture sector.

Keywords: climate change, impact modeling, agro-climatic zoning

The Cclimate change already revealed occuring on the territory of Georgia significantly influences on one of the priority sectors of economy – agriculture due to increase in water demand, decrease in harvest productiveness and limitation in water accessibility particularly in those regions, where irrigation is essential or an advantageous necessity (NALAG, 2016). Besides, changes in agro-climatic zones against the background of the temperature increase and changing precipitation patterns is one of the highest risks caused by the climate change for the agriculture sector (Cola et al., 2017). Reduction, growth or shifting of agro-climatic zones requires implementation of significant changes in this sector.

The aim of the paper is to assess the impact of the current and the future climate change on the territorial distribution (agro-climatic zoning) of grain crops (winter wheat, maize), as well as on the crop productivity and irrigation water requirement in the main regions producing these crops (Kakheti, Samegrelo-Zemo Svaneti).

Material and method

Crop productivity and irrigation water requirement

For assessment of the climate change impact on the agricultural crop productivity and irrigation water demand it there was selected the quantitative model – Aquacrop,

developed by the FAO (Food and Agriculture organization) Land and Water Department (Steduto et al., 2012). The model is already calibrated and validated for the number of crops of worldwide global and local food security importance; it particularly goes well with the conditions, where the water limitation factor is the main determinant in harvest productivity.

The following information should be provided to the Aquacrop model for crop simulation:

– Characteristics of environmental conditions – climate parameters (ETo, temperature, precipitation, CO_2).
– Agricultural crop type and parameters of (sowing method, phenological phases, canopy cover, root depth, degree of response to various soil stresses).
– Agricultural management – irrigation (method, schedule) and field measures (mulching, soil tillage…).
– Soil profile characteristics: soil type and parameters (physical parameters, soil granulometric composition, organic matter content (humus), number of horizons, water content, pedotransfer functions).
– Groundwater table (depth and salinity).

The model has the ability to change the starting date of the growing season, simulation period, the initial (soil water content and salinity) and off-season (description of irrigation and field management practices carried out outside the growing season) conditions. In addition, in the presence of relevant

Contact address: Lia Megrelidze, National Environmental Agency of Ministry of Environment Protection and Agriculture of Georgia, 150, David Agmashenebeli Ave., 0112, Tbilisi, Georgia; ☏ +995 591 404 139; e-mail: l_megrelidze@hotmail.com

observational data at different stages of crop development, through model utilization, it is possible to test the validity of the results obtained using known statistical means.

Current climate data (air temperature, atmospheric precipitation, wind speed, relative humidity, water vapour pressure, etc.), as well as agriculture crop (phenological calendar, root depth) and soil parameters was were taken from the database of the Georgian meteorology and agrometeorology observation network.

Reference evapotranspiration was calculated using FAO ETo calculator (Allen et al., 1998).

For simulation of the future climate change, IPCC climate change For simulation of future climate change, IPCC climate change Representative Concentration Pathways (RCPs) scenario 4.5 was used (IPCC, 2014), that is intermediate stabilisation pathway in which radiative forcing is stabilised at approximately 4.5 W.m^{-2} after 2100 without ever exceeding that value (the corresponding Extended Concentration Pathways (ECPs) assuming constant concentrations after 2150). Simulated with the Global Change Assessment Model (GCAM), RCP4.5 includes long-term, global emissions of greenhouse gases, short-lived species, and land-use-land-cover in a global economic framework..

Climatic parameters were obtained from the Global Circulation Model (ECHAM4.1) dynamically downscaled on the region utilizing the Regional Climate Model (RegCM4.1).

For the assessment of current changes, according to the selected locations for the specific agricultural crops, tendencies of changes of crop yield related parameters (growing season rainfall, reference evapotranspiration, growing degree days, carbon dioxide concentration, Infiltrated water, drained water, surface runoff, soil evaporation, crop transpiration, growing cycle, soil salinity and fertility stress, temperature stress, leaf expansion stress, stomatal stress, total biomass, relative biomass, harvest index, yield, water productivity) and irrigation water requirement were evaluated in the period 1966–2015, also, average indicators of the two 25-year sub-periods were compared (1966–1990 and 1991–2015). With the aim of assessment of future changes, the same indicators for the period 2021–2050 were calculated in accordance with locations and crops and compared with the second reporting period (1991–2015). According to studies (Ahouissoussi et al., 2014a; Ahouissoussi et al., 2014b), the stimulation of plant photosynthesis due to elevated CO_2 concentrations, leading led to either enhanced productivity and/or efficiency of primary production. To account the "fertilization" effect of increasing atmospheric CO_2 on crop yield, modeling was conducted twice, once with an annually adapted CO_2 concentration according to the RCP-4.5 scenario and once with a fixed concentration of 400 ppm to separate the influence of CO_2 from that of the other input variables.

Impact of the climate change on winter wheat productivity and water demand was assessed for the Kakheti region based on observations of the Dedoplistskaro meteorological station, and for maize – for the Samegrelo-Zemo Svaneti region based on the Zugdidi meteorological station.

The model simulation was performed at the research territory in correspondence with the widespread main soil types. One modifications of soil parameters of three

different soil types (Vertisols, natric Vertisols, black alkalized and natric) in the Dedoplistskaro municipality and one type (plinting and stagnic acri soils) – in the Zugdidi municipality were selected, with regard of to soil horizons depths. These soils with granulometric composition correspond to the types of sandy loam and clay soils in Kakheti and silt loam, loam and sandy loam soils in Samegrelo.

In case of wheat, soil water initial content and salinity were taken as an initial condition: Total Available Water (TAW) for Vertisols were taken as 70% of Field Capacity (FC), 50% for Natric Vertisols and 30% for black alcalized and natric (saline) soils. However, another initial condition was added for the black alcalized and natric soil: soil salinity.

The initial conditions for maize were not considered in the model, as the Total Available Water (TAW) was taken to be equal to Field Capacity (FC).

In order to assess Net Irrigation Requirement and irrigation effect on crop productivity, water deficit was calculated for all soil types according to two scenarios of Readily Available Water (RAW) in the root expansion zone, when the soil water depletion of the root zone is 50% and 30% of RAW (RAW50, RAW30) for winter wheat and 50% and 70% of RAW (RAW50, RAW70) – for maize.

When simulating maize yield, the presence of groundwater table was also taken into account – on average at a depth of 3 m and with no salinity.

Agro-climatic zones

The main factors of agriculture crop productivity are heat and moisture supply conditions. To characterize these conditions, areal changes of the agro-climatic zones of selected crops was were evaluated regarding changes of the following agro-climatic parameters: growing degree-days, growing season rainfall and average of absolute minimum temperature (these are the parameters used for agro-climatic zoning of Georgia for the first time in 1970s (Turmanidze, 1978)).

As in the modeling case, climate data of the period 1966–2015 was were used from the database of the Georgia meteorological observation network and based on these data, favourable areas for the spread of research crops were compared in two 25-years sub-periods (1966–1990 & 1991–2015). Forecasted changes of agro-climatic zones was were performed for the end of century (2070–2099), as changes in the distribution or shifting of zones are likely to be more apparent in the relatively long run.

The allocation of favourable areas for the cultivation of selected agricultural crops was carried out based on the following agro-climatic parameters:
- in order to produce winter wheat, growing degree-days in the interval 2,100–2,200 °C and 600 mm precipitation in total are required. Vegetation period of this crop commences from September, it halts from late November, up to the end of March and further continues development up to the harvesting (late June);
- to produce maize, for the early and late species, growing degree-days required is 1,700–2,800, °C and for the averagely ripened maize – 2,200 °C. Required total precipitation for both, early and late species, is 800 mm. Agro-climatic zoning was performed for the averagely ripened maize (Meladze, Meladze, Trapaidze, 2018)

By this approach, the following three zones were identified as a result of agro-climatic zoning:
1. There areis not enough heat supply to produce wheat/maize.
2. There are additional water supply requirements to produce wheat/maize.
3. There are favourable climatic conditions to produce wheat/maize.

Results and discussion

Climate change – current trends and future scenarios

During the last half-a-century (1966–2015), mean annual air temperature in Georgia has demonstrated solely growing tendency (Keggenhoff, Elizbarashvili, King, 2015; Elizbarashvili et al., 2017). The average increment of temperature between two periods of time (1966–1990 and 1991–2015) at the most parts of the territory made about 0.5 °C, thereto it should be noted that the warming process is the most intense in the municipalities selected for the modeling (Zugdidi, Dedoplistskaro), where the annual temperature increase reaches 0.8-1.0 °C. Warming is taking place in most areas, mainly due to increase in air temperatures in June – October period. The sharpest increase took place in August, varying in the range of 1.2–1.6 °C. In April-May, the change in the average temperature is insignificant and relatively unstable.

According to the projection (UNFCCC, 2015), to 2050s the growth of temperature over the entire territory will be more even and limited in the interval 1.0–1.5 °C. However, at the territory of Samegrelo (Zugdidi), the temperature increment will be smaller and vary between 0.5 and 1.0 °C.

For the period 2070–2099, warming is expected on the whole territory of the country, within 3–4 °C

For the past half-a-century, the variation of annual amount of precipitation has exhibited a mosaic character and the apparent trends did not take place, but there are is noticeable a certain regularity (Elizbarashvili et al., 2014; Elizbarashvili et al., 2016). In particular, the annual rainfall in western Georgia has mainly increased (within 5–15%), while in some regions of eastern Georgia – reduced. In the annual pattern, changes in seasonal sums of precipitation is are in the range of 15–25%. Precipitation increase in western Georgia is relatively intense in autumn and in the east – in spring. In the most parts of the territory, especially in Kakheti, reliable negative tendencies in summer precipitation (within 20–25%) were observed (Meladze, 2017).

According to the projection, by 2050s, precipitation increase is expected to be prevailinged throughout Georgia. Rainfall increase, as in the recent period, is still more intense in western country and precipitation growth tendencies in eastern Georgia is are relatively insignificant (on average 3–5%).

By 2100, significant decrease of precipitation is expected on the whole territory with the largest reduction in Samegrelo and Kakheti (20–25%).

Model validation

For the main agricultural crops, the crop characteristics have been calibrated by FAO, which are offered in the model as so called default values. The specific crop yield is dependent on the sowing date, on the utilization of fertilizers, pesticides and herbicides and other field management measures and is different from year to year. The influence of this variation was considered during the model validation.

The model was tested for the period 1999–2015 when statistical information on the average yield of wheat and maize in the study regions are available. According to statistical analysis, the acceptable consistency of the simulated harvest compared to the measured one is noted. However, the correlation dependence on a number of factors, such as: amount of precipitation during the growing season, irrigation, soil salinity was find found out.

Modeling results

Based on the modeling results, Tables 1–3 present the values of winter wheat and maize yield and net irrigation water requirement and its changes between two recent 25-years sub-periods and the 30-years forecast period for investigated sites using the above described input data and initial conditions and according to two scenarios of readily available water (RAW).

Crop productivity

According to modeling results, average yield of winter wheat in the Dedoplistskaro district during the current period has increased by 10–20%, depending on irrigation and initial conditions. From the three types of soil discussed here (not shown in the tables), yield of winter wheat harvested on Vertisols and Natric Vertisols shows an increase. Exceptions are saline (black alkalized and natric) soils with an area of about 25% in the municipality (although the share of arable land in such soils does not exceed 5% ($\approx$2.2 thousand ha)), where a significant decrease in yield (25–30%) was revealed. As for maize, according to Table 2, maize yield in the Zugdidi district decreases slightly between the two recent sub-periods (-2%), although the trend for the whole investigated period (1966–2015) is positive.

According to the projection, it is likely that the trend of yield changes occurred occurring in the current period (1966–2015) will continue until the middle of the century. Growth for winter wheat is significant both in terms of CO_2 fertilization or without it, and in rainfed farming in the forecast period it is in the range of 70–100% compared to the second 25-years period (1991–2015), which corresponds to 4–5 t.ha^{-1}, in on average. It should be noted that increase in yield was revealed for all three types of soil. In the case of maize, as in the current period, the changes are insignificant and in the forecast period with regard to the period 1991–2015 are in the range of ±4%, which does not exceed 0.1 t.ha^{-1} on average.

The climate change will decrease the variability of winter wheat from year to year, on maize yield, this impact is again negligible. It could be seen from the crop variation coefficient (CV). In the investigated periods, it varies slightly from 0.1 to 0.3 for maize, and in case of wheat in the two current sub-periods it ranges from 0.6 to 0.8, but in 2021–2050 it is twice as small (0.3). Therefore, under the current rainfed farming conditions, less stable wheat yields are expected. The forecast is the most optimal for the forecast period, which implies a higher and more stable harvest of winter wheat.

Figure 1 shows the exceedance probability curves of simulated crops for the baseline (1966–2015) and forecast (2021–2050) periods for study regions and confirms future changes in crop productivity compared to the baseline period. However, for example, if in the forecast period in Dedoplistskaro once in 100 years (1% probability) it is probable that the yield will be at least 4 t.ha^{-1}, in the current period (1966–2015), crop yield of the same probability (1%) drops to 0. The yield of 2% probability (expected once in 50 years) is 2 t.ha^{-1} in the current period, and increases to 4–5 t.ha^{-1} in the future (2021–2050).

Table 1   Values and changes of growing season climate characteristics and winter wheat productivity between the periods: 1991–2015 (2) vs 1966–1990 (1) and 2021–2050 (3) vs 1991–2015 (2)

Period	Rainfall (mm)	Reference evapotranspiration (mm)	Growing Degree Days (°C)	Atmospheric CO_2 concentration (ppm)	Yield (t.ha^{-1})					
					rainfed	irrigated, RAW50	rainfed, RAW30	rainfed	irrigated, RAW50	rainfed, RAW30
					assuming CO_2 fertilization			assuming no CO_2 fertilization		
1966–1990 (1)	467	494	2185	336	2.4	6.2	6.2	2.4	6.2	6.2
1991–2015 (2)	441	505	2329	376	2.7	7.5	7.5	2.6	7.3	7.3
2021–2050 (3)	449	385	2544	449	5.4	8.5	8.3	4.6	7.5	7.3
Abs. change_21	-25	11	144	40	0.2	1.2	1.2	0.2	1.1	1.1
Abs. change_32	8	-120	215	73	2.7	1.0	0.9	1.9	0.2	0.0
Rel. change_21	-5%	2%	7%	12%	9%	20%	20%	7%	17%	17%
Rel. change_32	2%	-24%	9%	19%	102%	14%	12%	75%	3%	0%

Table 2   Values and changes of growing season climate characteristics and winter wheat productivity between the periods: 1991–2015 (2) vs 1966–1990 (1) and 2021–2050 (3) vs 1991–2015(2) (Samegrelo-Zemo svaneti, Zugdidi)

Period	Rainfall (mm)	Reference evapotranspiration (mm)	Growing degree days (°C)	Atmospheric CO_2 concentration (ppm)	Yield (t.ha^{-1})		
					rainfed	irrigated, RAW50	rainfed, RAW70
1966–1990 (1)	742	470	1740	336	2.03	2.10	2.09
1991–2015 (2)	677	492	1891	376	1.99	2.16	2.14
2021–2050 (3)	910	506	1912	449	1.94	2.21	2.17
Abs. change_21	-65	22	152	40	-0.04	0.06	0.05
Abs. change _32	233	14	21	73	-0.05	0.05	0.03
Rel. change_21	-9%	5%	9%	12%	-2%	3%	3%
Rel. change _32	34%	3%	1%	19%	-3%	2%	1%

Table 3   Values and changes of winter wheat and maize net irrigation requirements between the periods: 1991–2015 (2) vs 1966–1990 (1) and 2021–2050 (3) vs 1991–2015 (2). RAW30, RAW50, RAW70 refers to readily available water in the root expansion zone, when the soil water depletion of the root zone is 30%, 50%, 70%, respectively

Period	Kaheti, Dedoplistskaro		Samegrelo-Zemo Svaneti, Zugdidi	
	RAW50	RAW30	RAW50	RAW70
1966–1990 (1)	126	140	17	6
1991–2015 (2)	154	168	30	16
2021–2050 (3)	60	73	41	18
Abs. change_21	28	28	14	9
Abs. change _32	-93	-95	11	2
Rel. change_21	22%	20%	82%	148%
Rel. change _32	-61%	-57%	37%	14%
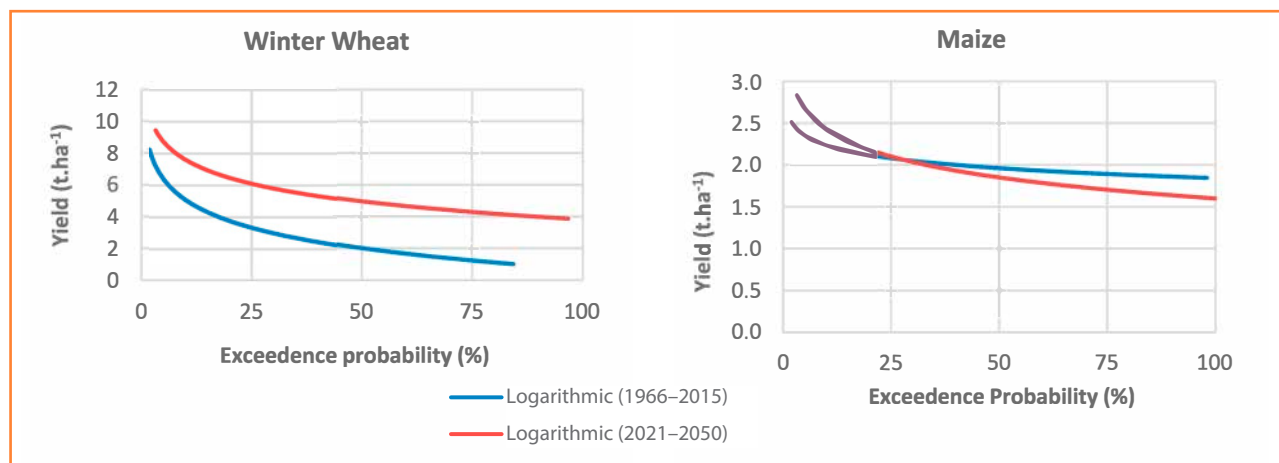
Figure 1   Exceedance probability (%) of wheat and maize yields for the recent and forecast periods

Irrigation water requirement

During the recent period, the study area has shown a tendency to increase the water shortage of grain crops, which is obvious against the background of declining rainfall during the growing season (Table 3). The demand for winter wheat irrigation water between the two recent sub-periods has increased by 20–25%, while that of maize – by about 2–2.5 times. However, as the water deficit for maize is negligible, the quantitative increase is only 10–30 mm.

Against the background of climate change, according to both scenarios of soil waterlogging in the future, to maintain maximum yields of winter wheat, in the forecast period compared to the current situation, whilst maintaining almost the same amount of precipitation in the growing season, irrigation water demand decreases by 55–60%, which should be due to a significant reduction in evapotranspiration (-24%). The irrigation demand for maize is growing (40% -60%), but quantitatively remains insignificant in the future and does not exceed 20–50 mm. In other words, it can be said that the problem of water shortage for maize in the study area is not revealed and according to the modeling results, such a problem is not expected with in athe future scenario.

To ensure maximum yield of winter wheat, the largest amount of water is still needed for sown areas on saline soils, and the least water will be lacking in Vertisols, where the average irrigation demand during the recent period (1966–2015) is 100–150 mm, and in the future decreases to 50–100 mm (not shown in the tables). About 5–15% more water is needed on Natric Vertisols, and 30–60% more on saline soils, which is currently 150–200 mm, and in the future it will be in the range of 80–120 mm. However, it should be noted that these are averaged indicators, and future climate change scenarios suggest an increase in the probability of certain dry, hot years, with severe droughts, which will significantly increase the irrigation water demand of any area during such periods.

The results also indicate that under proper irrigation it is possible to significantly increase the average yield of wheat. In particular, as a result of sufficient irrigation in the study region, winter wheat yields may increase by 2–3 times. During the recent period, such an increase will result in an average yield of 6–8 t.ha^{-1}, and by the middle of the century the yield will reach 9 t.ha^{-1}. Growth of yields are approximately equal between rainfed and irrigated farming conditions in the whole investigated period. Irrigation will have relatively less effect in the forecast period when the plant's water deficit is the smallest. As for maize irrigation, modeling confirms that due to the high moisture content of study area, use of irrigation will not have any significant impact on crop yield and as a result of irrigation, increase in maize productivity will not exceed 10–15%, which is in averages 2–2.5 t.ha^{-1} for both rainfed and irrigated agriculture in the forecast period.

Changes in water demand for considered agricultural crops have been assessed under the constant fertility level and other boundary conditions.

It is important to mention that irrigation technology will also have an effect on water demand, which will be used on certain location, due to the fact that different irrigation systems are characterized by different levels of water provision effectiveness. The model relies on the so-called sprinkler irrigation technology for net irrigation requirement calculation.

Ongoing and forecasted changes in agro-climatic zones relevant for cereals production

Figures 2 and 3 show the zoning of Georgia territory according to the investigated periods (1966–1990, 1991–2015, 2070–2099) for winter wheat and corn, and in the Table 4 the areas of zones where cultivation of these crops is favourable is are presented.

Areas of the zones favourable for growing of winter wheat where this crop can be grown in rainfed conditions are currently increased by about 5% and will increase by up to 40% in the future and this will occur basically due to temperature growth, when growing degree-days achieve 2,100–2,200 °C at 1,200–1,500 m altitudes above sea level. This is the medium-sized mountainous zone distinguished with complex orography, extensively fragmented and represented with small land plots. The soil is favourable for wheat growing. The most part of the territory is currently covered with the forests and pastures.

According to Figure 3 and Table 4, in the recent period (1966–2015), the areas favourable for maize growing
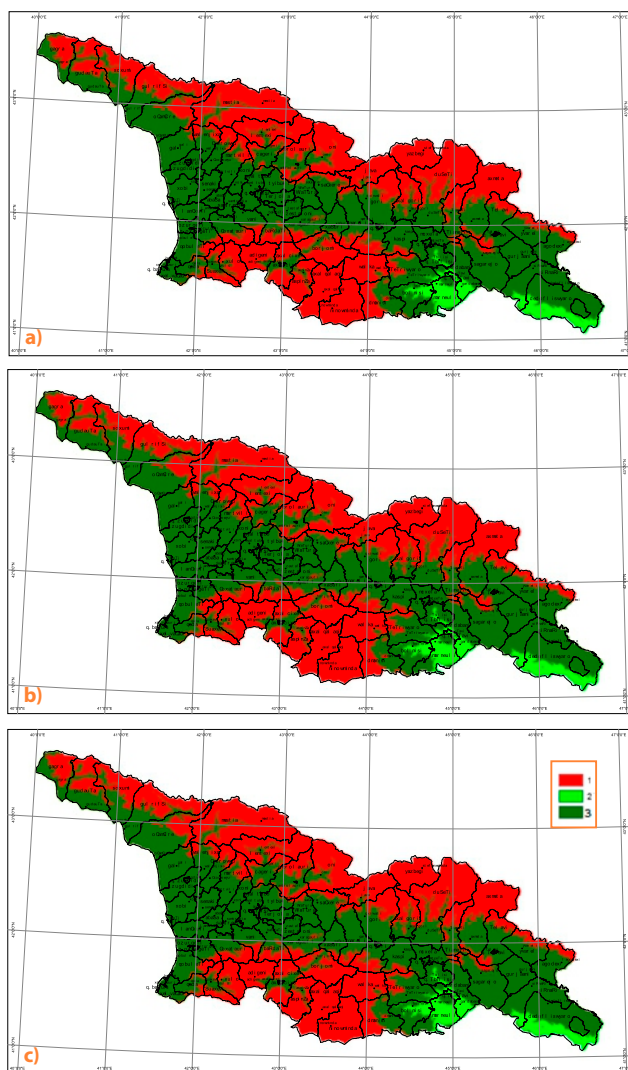
Figure 2   Changes in wheat agro-climatic zoning: a) 1966–
1990, b) 1991–2015 and c) 2070–2099
1 – zone with insufficient heat supply to produce crop;
2 – zone require additional water supply; 3 – zone with
favourable climate conditions
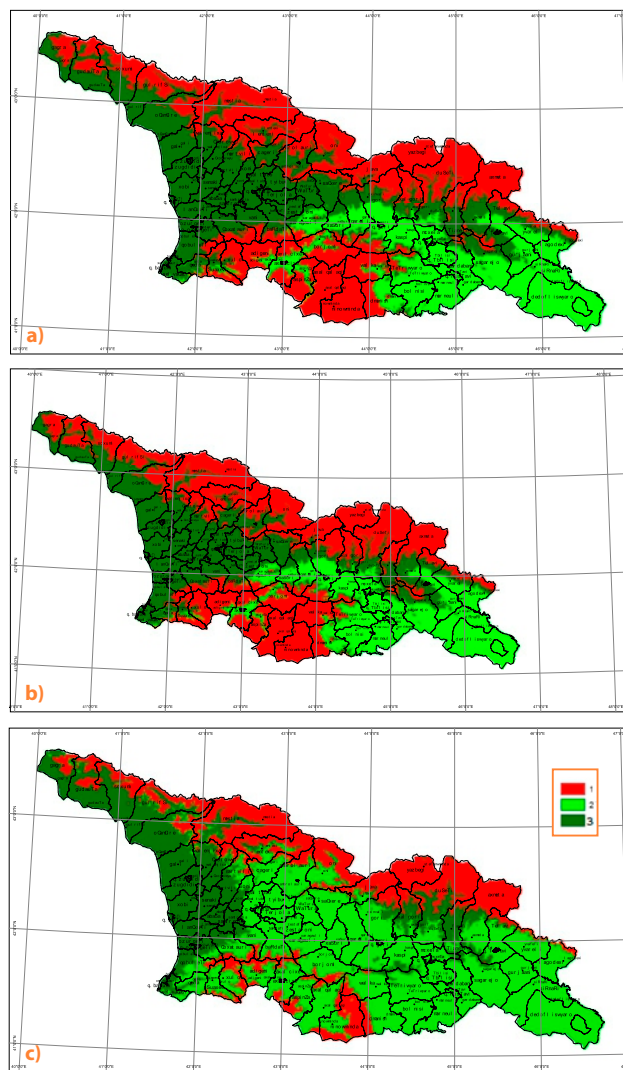
Figure 3   Changes in maize agro-climatic zoning: a) 1966–
1990, b) 1991–2015 and c) 2070–2099
1 – zone with insufficient heat supply to produce crop; 2 –
zone require additional water supply; 3 – zone with
favourable climate conditions

are increasing. In the future, suitable areas will increase significantly in case of irrigated crops while the areas with rainfed farming will reduce. Part of the territories warm enough to grow maize is mostly the highlands where, supposedly, the precipitation will be sufficient for maize growing without irrigation. Thus, in these areas, maize growing might be more reasonable in economic respect.

Although, it should be noted that even in the current period, the sown areas of wheat and maize are much smaller

compared to the area with favourable climatic conditions for growing these cereals. This is due to the advantage of other economically more profitable crops, historical-cultural or other circumstances.

Conclusions

According to the climate change selected scenario (that stabilizes radiative forcing at 4.5 W.m^{-2} in the year 2100), potential yield of winter wheat will grow, both with and without irrigation. Irrigation effect is particularly significant for the cultivated areas on saline (black alkalized and natric) soils in the recent time while in the prognosis period the effect is relatively lower. Whilst the climate change has smaller effect on maize productivity, in particular: potential yields of the maize will remain quite stable from year to year, both for rainfed and irrigated agriculture and changes between the investigated periods is are insignificant (+4%), amounting, in average, to 2–2.5 t.ha^{-1}. Also, by the end of the century, the areas favourable for growing cereals will increase significantly.

Table 4   Areas of the zones (ha) favourable for wheat and maize growing in different periods

Crop	Period	1966–1990	1991–2015	2070–2099
Wheat	Zone 2	844,200	846,900	954,600
	Zone 3	3,171,800	3,365,300	4,675,600
Maize	Zone 2	1,601,500	1,643,400	3,528,000
	Zone 3	2,414,600	2,568,800	1,742,200

For winter wheat cultivation by about 40%will extend zones with suitable climate conditions will extend by about 40%, but for maize, growth is expected to increase by almost 2 times areas requiring additional water supply.

Irrigation effect is particularly significant for winter wheat cultivated on saline (black alkalized and natric) soils in the current period while in the prognosis period the effect is relatively lower.

For winter wheat that belongs to the crops moderately sensitive to soil water stress, effect of precipitation reduction is apparent only for the plantations on saline (black alkalized and natric) soils. On the rest of territory, water deficiency caused by reduction of precipitation is compensated by reduction of evapotranspiration and improvement of crop water productivity. According to the future projection, this trend will be maintained at least up to the middle of the century and in the Dedoplistskaro district, even in case of rainfed cultivation, growth of the yields could be expected. Hence, during prognosis period, to maintain maximal yields, water requirement will be 40–60% lower, compared with the current period. At the same time, it should be considered that by the end of the century, against the background of a significant decrease in precipitation overall country territory would increase areas, where additional water will be needed to grow cereals.

For the maize that belongs to the crops sensitive to soil water stress, effect of precipitation reduction was not apparent due to high moisture content in the studied territory. Due to this, no any significant effect of irrigation on yields was identified.

Increases in air temperature and CO_2 are considered as being one of the main components of changing climate, thatclimate that would have significant impact on agriculture crop productivity by the means of increased crop water effectiveness and through the biomass production. The modeling results indicate that the increased concentration of the CO_2 will have a positive effect on biomass production of winter wheat, however, CO_2 fertilization effect in some cases overlaps with the unfavourable changes of climatic parameters during growing season and is specific depending on the soil type common in the study area. For maize, the above effect and yield increase are relatively small, which is explained by the high ability of carbon fixation by maize.

By default, the AquaCrop model discusses agro-technical measures taken against agricultural crops (such as pest and disease control, weed control, etc.) at the optimal level, which is largely inconsistent with the real situation. Such influences are involved in the model through soil fertility stress. Such stress was not taken into account when simulating the model, as accurate information about the above measures was not available. Thus, the real decline in wheat yields should not only be due to changes in climatic conditions and is likely to be the result of improper exploitation of land and agro-technical measures and inconsistent management. As for maize, it seems that in the studied region, conditions favourable for maize growing exist now, will exist in the future and low average yields (compared with the global figures) are supposedly caused by the crop varieties or some other reasons (vermin, diseases, ineffective management).

One should also bear in mind that nor neither model not nor agro-climatic zoning approach does do not take into consideration impact of such significant factors as extreme phenomena, like floods, hail, strong winds etc. on agricultural crop spatial distribution and productivity. In addition, raised temperature and more frequent heat waves results in increase of the fire risks, vermin propagation and frequency of diseases.

References

Ahouissoussi, N., Neumann J. E., Srivastava, J. P., Okan, C., Droogers, P. (2014a). *Reducing the vulnerability of Georgia's agricultural systems to climate change.* World Bank. https://doi.org/10.1596/978-1-4648-0148-8

Ahouissoussi, N., Neumann, J. E., Srivastava, J. P. (2014b). *Building resilience to climate change in south caucasus agriculture.* World Bank. http://dx.doi.org/10.1596/978-1-4648-0214-0

Allen, R. G., Pereira, L. S., Raes, D., Smith, M. (1998). *Crop evapotranspiration: guidelines for computing crop water requirements.* FAO. http://www.fao.org/3/X0490E/X0490E00.htm.

Cola, G., Failla, O., Maghradze, D., Megrelidze, L., Mariani, L. (2017). Grapevine Phenology and Climate Change in Georgia. International *Journal of Biometeorology*, (61), 761–773.

Elizbarashvili, E., Kutaladze, N., Keggenhoff, I., Elizbarashvili, M., Kikvadze, B., Gogia, N. (2014). Climate Indices for the Moistening Regimen in the Territory of Georgia amidst Global Warming. *European Researcher*, (66), 102–107.

Elizbarashvili, E., Elizbarashvili, M., Kutaladze, N., Keggenhoff, I., Elizbarashvili, Sh, Kikvadze, B., Gogia, N. (2016). Spatiotemporal Variations in Climate Moisture Indices in Georgia under Global Warming. *Russian Meteorology and Hydrology*, (41), 261–267.

Elizbarashvili, M., Elizbarashvili, E., Tatishvili, M., Elizbarashvili, Sh., Meskhia, R., Kutaladze, N., King, L., Keggenhoff, I., Khardziani, T. (2017). Georgian climate change under global warming conditions. *Annals of Agrarian Science,* (15), 17–25.

Keggenhoff, I., Elizbarashvili, M., King, L. (2015). Recent changes in Georgia's temperature means and extremes: Annual and seasonal trends between 1961 and 2010. *Weather and Climate Extremes*, (8), 34–45.

IPCC (2014). AR5 *Climate change 2014: impacts, adaptation, and vulnerability*. IPCC. https://www.ipcc.ch/report/ar5/wg2/

Meladze, M. (2017). Climate change: A trend of increasingly frequent droughts in Kakheti Region (East Georgia). *Annals of Agrarian Science*, (15), 96–102.

Meladze, M., Meladze, G., Trapaidze, V. (2018). Evaluation of the Agro-Ecological Potential of Racha-Lechkhumi-Kvemo Svaneti region (Georgia) and Zoning of Crops. *SGEM, Ecology and Environment Protection,* (18), 361–367.

NALAG (2016). *The Georgian Road Map on Climate Change Adaptation*. USAID. http://nala.ge/climatechange/uploads/RoadMap/TheRoadMapEngPre-design_reference191_Final.pdf

Steduto, P, Hsiao, T. C., Fereres, E., Raes, D. (2012). *Crop yield response to water*. FAO. http://www.fao.org/3/i2800e/i2800e.pdf

Turmanidze, T. (1978). *Agroklimaticheskie Resursi Gruzinskoi SSR*. Leningrad: Gidrometeoizdat.

UNFCCC (2015). *Georgia's Third National Communication to the UNFCCC*. GEF. https://unfccc.int/resource/docs/natc/geonc3.pdf

CLIMATE CHANGE IMPACT ON THE GLACIERS OF THE RIONI RIVER BASIN (GEORGIA)

George KORDZAKHIA[1]*, Larisa SHENGELIA[1], Genadi TVAURI[2], Murman DZADZAMIA[3]

[1]Georgian Technical University, Tbilisi, Georgia
[2]Ivane Javakhishvili Tbilisi State University, Tbilisi, Georgia
[3]National Environmental Agency, Tbilisi, Georgia

Since the beginning of the 21st century, studies of glaciers in Georgia have become more important, because the degradation of glaciers causes an increase in the intensity and frequency of natural disasters of a glacial and hydrological nature, an increase in water levels in the Black Sea, and a changes in river water regime. Studying the current state of the ice sheet in Georgia is an important national economic task, and to obtainobtaining a scientifically sound answer on modern conditions of the glaciers, due to the impact of current climate change is an urgent task. To solve this task, high-resolution satellite remote sensing (SRS) is used. The r. Rioni basin (West Georgia) is one of the most important glacier basins in Georgia, where the powerful glaciers are spread and their change is of great interest. In this work there are presented the results of the study of r. Rioni glasiers glaciers degradation due to the influence of current climate change including the expected time of their full melting.

Keywords: Georgian glaciers, degradation, climate change, satellite remote sensing

The cryosphere (including, snow, glaciers, permafrost, lake and river ice) is an integral element of high mountain regions, which are home for about 10% of the global population. Widespread cryosphere changes affect physical, biological and human systems in the mountains and surrounding lowlands, with impacts evident even in the ocean/sea (IPCC Special Report on the Ocean and Cryosphere in a Changing Climate, 2018). Observations show general decline of glaciers due to the climate change in recent decades with high confidence and likely this is most negative in the southern Andes, Caucasus and the European Alps/Pyrenees.

The World Meteorological Organization (WMO) held High Mountain Summit in Geneva (Switzerland) at the end of 2019. At the summit work, the priority importance was assigned to cryosphere problems.

Scientific studies of glaciers in the Caucasus, namely in Georgia began in the second half of the 19th century. Several scientists of different generations participated in field works, which began in 1860 in the former Russian Empire and continued throughout the 70sn in the Soviet Union (Abikh, 1870; Khatisyan, 1864; Tsomaia and Drobishev, 1970). The outputs of these studies were summarized and presented in several issues of the glacier catalog (hereinafter – the catalog) of the former Soviet Union (Maruashvili et. al., 1975; Tsomaia, 1975; Panov, Borovik, 1977; Tsomaia, Drobishev, 1977).

The Georgian glaciers in this catalog were not presented independently and were systematized as a part of the Caucasian system of glaciers. Due to the importance of this catalog, it was later included in the World Glacier Inventory (WGI).

Under the conditions of global warming (approximately from the second half of the 20th century), the glaciers of Georgia are have been retreating and degrading (Kordzakhia et al., 2016; Kordzakhia et al., 2019). At present, glaciers research is stipulated to indicate climate change impact on glaciers at regional and global scales, surface water level rise in oceans/seas, landscape changes due to melting glaciers, and increasing occurrence of natural disasters related to glaciers.

The aim of this study is to determine changes of glaciers of r. Rioni basin (Western Georgia) due to the global climate change.

Material and method

The study region is the glacial basin of the r. Rioni basin (Western Georgia). This glacial basin is located in a high mountain region on the watershed ridge of the Central Caucasus from Mount Namkwami to Mount Kozihokh, where mountain ranges are more than 4,000 m high.

To give a scientifically based answer to the glaciers degradation under the impact of modern climate change and determine the corresponding risks of glacier related disasters, it is necessary to use high-resolution satellite remote sensing (SRS), since it allows studying glaciers in the large regions with the necessary resolution and accuracy within limited material and human resources and time.

Contact address: George Kordzakhia, Georgian Technical University, Tbilisi, Georgia; ☏ +995 599 14 56 56;
e-mail: giakordzakhia@gmail.com

Technological and methodological approaches based on SRS were tested both by foreign researchers, for example (Pellika and Gareth Rees, 2010) and by the authors of this work (Kordzakhia et al., 2016; Kordzakhia et al., 2019), shows showing that it is possible to determine all glaciers main characteristics, i.e. maximum length, area, minimum and maximum heights, firn line-height, accumulation, and ablation areas. The basis of methodology used by authors' is application of historical data (Maruashvili et. al., 1975; Tsomaia, 1975; Panov, Borovik, 1977; Tsomaia and Drobishev, 1977), glacier schemes from the catalog, existing field works outputs along with SRS data and the use of expert knowledge. The methodology includes the implementation of necessary procedures for the quality assessment and quality control (QA/QC) of SRS data (Kordzakhia et al., 2016).

The influence of the current climate change on Georgia's glaciers is revealed in the statistics of melting of small glaciers (area in the range from 0.1 to 0.5 km^2); it can be characterized by changes in both integral and detailed characteristics of glaciers: the area and number of glaciers in glacial basins and retreat dynamics of large glaciers (area of more than 2 km^2). In the work, the glacial basin of the r. Rioni, which is one of the most powerful and important basins of Georgia, was analysed. For this purpose, SRS images, namely, Landsat data (resolution 15–30 m) and the data of "Global measurements of land ice from space" (GLIMS) were used. Google Earth is an effective program that offers satellite images with a high spatial resolution (0.5–0.8 m), which makes it possible to more accurately determine the contours of the glacier.

Results and discussion

To determine the impact of the climate change on the present glacial basin, the glaciers data derived from the SRS are compared with the corresponding data from the catalog. A 50-year difference between the catalog and SRS data (2015) creates the prerequisite for determining changes in basins glacialisation.

The schematic diagrams of glaciers (Figure 1a) from the catalog and GLIMS data were used to identify all glaciers from the r. Rioni basin i.e. determine the locations and quantities of glaciers in the images of SRS. In Figure 1a, as an example, the identification of the Boko glacier in the r. Rioni basin is given. The next step is to determine the area of the studied glaciers in the SRS images and compare them with the data of the same glaciers from the catalog and topographic maps of the 60s of the last century (Figure 1b). Comparing the contours of glaciers obtained from SRS data with the contours on topographic maps, it was found that the areas of all glaciers in Georgia have declined over the past 50 years.

Data on the area of some glaciers in the catalog were less lower than those accessed from SRS and topographic maps, giving the impression that the area of such glaciers increased in comparison with the 60s. Using the outlines of glaciers shown on a topographic map of the same period, the inaccurate catalog were was corrected.

Table 1 shows the main characteristics of the glaciers of the Rioni river basin (№ 388–400) according to the SRS (column (1)), catalog (column (2)) and corrected inaccurate
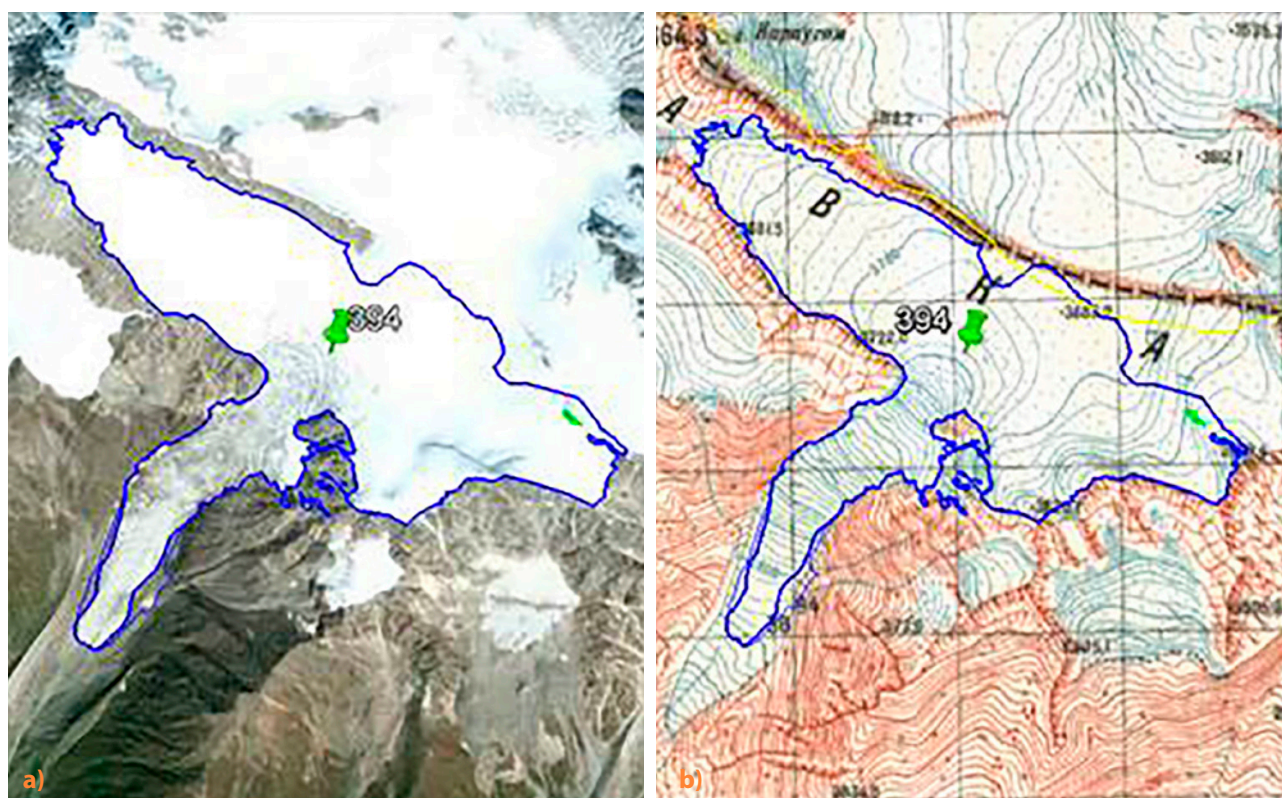
Figure 1 Boko Glacier – No. 394: a. in a) – satellite image; and b) – on a topographic map of the 60s of the last century. The contours of the glacier are shown in blue, both on a satellite image and on a topographic map

Table 1   The main characteristics of the glaciers (№388-400) of the Rioni river basin according to SRS (1), catalog (2) and corrected inaccurate data catalog (3)

№	Glacier Name and № from WGI catalog	Identification №, ID according to WGI	Glacier № on SRS image	Max. length (km)		Area (km²)			Min. elevation (m)		Max. elevation (m)	
				(1)	(2)	(1)	(2)	(3)	(1)	(2)	(1)	(2)
1	353	SU5T09106388	388	1.5	1.5	0.6	0.7		3,090	2,930	3,627	3,810
2	***	***	***			0.06						
3	Natsarula, 355a	SU5T09106389	389	2.3	2.0	1.0	1.3		3,052	2,700	3,923	3,750
4	355b	SU5T09106390	390	0.6	0.9	0.1	0.2		3,494	3,050	3,875	3,650
5	355c	SU5T09106391	391	2.6	3.2	1.0	1.2		3,032	2,550	4,315	3,820
6	356	SU5T09106392	392	0.8	0.7	0.3	0.3	0.3	3,170	3,130	3,491	3,520
7	Kotsan-sara	SU5T09106393	393	1.2	1.6	1.0	1.2		3,246	3,060	3,864	3,750
8	Boko	SU5T09106394	394	4.2	4.5	3.7	4.6		2,616	2,450	3,996	3,900
9	***	***	***			0.2						
10	361	SU5T09106395	395	0.7	0.8	0.4	0.5		3,202	3,150	3,532	3,460
11	Tbilisa,362	SU5T09106396	396	3.3	3.3	3.6	3.1	3.8	2,940	2,750	4,422	3,920
12	Buba,363	SU5T09106397	397	3.0	2.7	2.3	1.6	2.9	2,943	2,760	3,950	4,050
13	364	SU5T09106398	398	0.7	0.6	0.2	0.1	0.4	3,201	3,160	3,500	3,450
14	Chanc-hakhi, 365a	SU5T09106399	399a	2.3	2.9	0.8	1.4		3,042	2,850	4,297	4,020
			399b	0.9		0.3			3,273		4,115	
15	365b	SU5T09106400	400	0.3	0.7	0.1	0.2		3,281	3,180	3,599	3,490

Table 2   The area and number of glaciers of the r. Rioni basin

Rioni river basin							
Glaciers №		area			quantity		
	size	(1)	(2)	Δ	(1)	(2)	Δ
	small	9.2	11.3	-2.1	36	47	-11
296, 335–409	**medium**	28.2	14.6	13.6	29	13	16
	large	36	25.9	10.1	11	8	3
	total	73.4	51.8	21.6	76	68	8

catalog data (column (3)). In Table 1, the *** sign indicates snowfields[1] that are not listed in the catalog.

Table 2 presents the integrated data of glaciers (the total area and number) for the corresponding sizes of glaciers in the r. Rioni basin. Data from the catalog is are placed in column (1), and SRS data is in column (2). Δ – indicates differences in areas and quantities between the catalog and SRS data.

The Aanalysis of Table 2 shows that in the glacial basin of the r. Rioni in the past (catalog data), the total area of glaciers was 73.4 km². At present, the area of glaciation has decreased by 21.6 km², and its value makes 70.6% of the catalog data; in the past, the number of glaciers was

76. There were 11 large, 29 medium and 36 small glaciers. Currently, according to SRS data, due to the impact of the current climate change, there exist 8 large, 13 medium and 47 small glaciers, a total of 68 glaciers. Thus, the total number of glaciers decreased by 8. The number of remaining glaciers amounted to 89.5% of the one existing in the catalog.

It is important to determine the possible complete melting time of the glaciers in r. Rioni basin. For that, the largest glacier Boko from the basin r. Rioni basin is chosen. It is natural that when this glacier melts completely, it means that all other glaciers will be fully melted. The methodology for determining the retreat rate of the glacier tongue is given in Kordzakhia et al. (2019). To determine the average retreat rate of the Boko glacier and analysis of retreat trends, the dynamics of the glacier retreat was created based on the SRS images for the time range 1977–2015 (Figure 2).

In different years, the location of the glacier tongue is shown by different color contours. The retreat locations

---

1   Snowfields – motionless natural accumulation of snow, snow cover, snow cover season (seasonal snow cover) or not melting throughout the year (permanent snow cover, overflow). During the degradation of glaciers, snowfields act as their remnants.
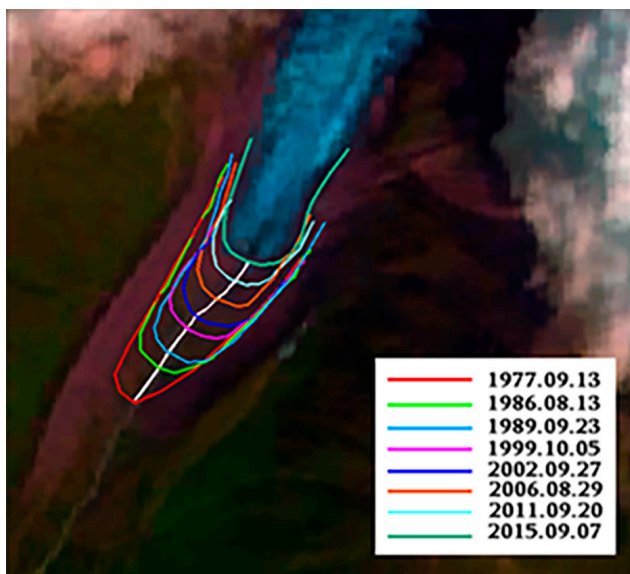
Figure 2   The schematic picture of glacier Boko retreat

and lengths are calculated using the white zigzag line that crosses the contours of the glacier.

Based on Figure 2 the retreat distances were calculated. It was determined that the retreat of the Boko glacier with a high probability can be described by a parabola (Figure 3). For the Boko glacier, the parabola equation is: $y = 0.0542t^2 + 13.717t$.

To determine the expected time of the complete melting of the Boko glacier, a climate change scenario so-called business as usual (BaU) was used.

Calculating the period when the length of glacier Boko (7,856 m) will be decreased and be equal to zero, we achieve that the time for the Boko glacier full melting is 197 years.

It means that the Boko glacier and hence, all the glaciers from r. Rioni basin will disappear in 2,175.
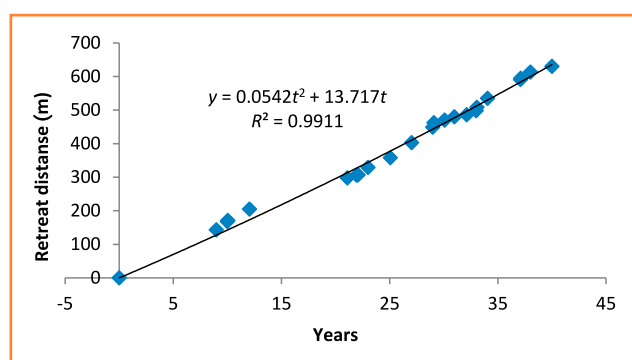
Figure 3   Boko Glacier Retreat

Conclusion

The impact of the current climate change on the degradation of glaciers of the r. Rioni basin can be summarized as follows:

1. The area of glaciation of the glacial basin of the r. Rioni and the number of glaciers have declined significantly over the past 50 years.

2. The area of glaciation of the r. Rioni basin has decreased by 21.6 km^2, i.e. to 70.6% of the original area according the; the number of glaciers has decreased by 8 units, which is 89.5% of the existing in the catalog.

3. Boko glasier glacier estimated complete melting time is 197, assuming the BAU scenario of the current climate change.

References

Abikh, G.V. (1870). *Iccledovanie nastoiacshchikh i drevnikh lednikov Kavkaza*. Otdel 1. Opisanie nine sushchectvuiuchego Devdorakskogo lednika i sledov deistvia prerhnikh lednikov v doline Tereka. Otdel 2. O sledakh prerhnikh lednikov v dolinakh rek Assi, Narti-dona i Shasni. G. Abikh; Per. F. Fon-Koshkul. Tiflis (42 p.) (in Russian).

IPCC Special Report on the Ocean and Cryosphere in a Changing Climate (2018).

Khatisyan, G.S. (1864). Kratkii ocherk deistvii dvukh komissii dlia issledovaniia Kazbekskikh lednikov v 1862 i 1863 gg. *Tiflis: Zap. KORGO*, *6*(2), 220–230 (in Russian).

Kordzakhia, G. I., Shengelia, L.D., Tvauri, G. A., Dzadzamia, M. SH. (2016). Impact of modern climate change on glaciers in East Georgia. *Bull. Georg. Nat. Acad. Sci.*, *10*(4), 56–63.

Kordzakhia, G. I., Shengelia, L.D., Tvauri, G. A., Dzadzamia, M. SH. (2019). The climate change impact on the glaciers of Georgia. *Journal World Science*, *1*(4(44)), 29–34. DOI: https://doi.org/10.31435/rsglobal_ws.

Maruashvili, L.S., Kurdgelaidze, G.M., Lashkhi, T.A., Inashvili, SH.V. (1975). *Katalog Lednikov SSSR (*T. 9, vip 1. ch. 2–6). Zakavkazie i Dagestan, L.: Gidrometeoizdat (in Russian).

Panov, V.D., Borovik, E.S. (1977). *Katalog Lednikov SSSR* (T. 8, ch. 13. 1977). Severni Kavkaz: Gidrometeoizdat (in Russian).

Pellika, P., Gareth Rees, W. (2010). *Remote sensing of glaciers: techniques for topographic, spatial and thematic mapping of glaciers* (pp. 330).

Tsomaia, V.Sh. (1975). *Katalog Lednikov SSSR* (T. 9, vip. 3, ch. 1). Zakavkazie i Dagestan, L.: Gidrometeoizdat (in Russian).

Tsomaia, V.Sh., Drobishev, O.A. (1970). Resultati glatsiologicheskikh nabliudenii na lednikakh Kavkaza. *Trudy ZakNIGMI*, *45*(51), 141–146. (in Russian).

Tsomaia, V.Sh., Drobishev, O.A. (1977). *Katalog Lednikov SSSR* (T. 8, ch. 11). Severni Kavkaz, L.: Gidrometeoizdat (in Russian).

ESTIMATING RAINFALL EROSIVITY FACTOR USING FUTURE CLIMATE PROJECTION IN THE MYJAVA REGION (SLOVAKIA)

Peter VALENT[1, 2]*, Roman VÝLETA[2]

[1]Vienna University of Technology, Vienna, Austria
[2]Slovak University of Technology in Bratislava, Bratislava, Slovakia

Rainfall erosivity factor (R) of the USLE model is one of the most popular indicators of areas potentially susceptible to soil erosion. Its value is influenced by the number and intensity of extreme rainfall events. Since the regional climate models expect that the intensity of heavy rainfall events will increase in the future, the currently used R-factor values are expected to change as well. This study investigates possible changes in the values of R-factor due to climate change in the Myjava region in Slovakia that is severely affected by soil erosion. Two rain gauge stations with high-resolution 1-minute data were used to build a multiple linear regression model (r^2 = 0.98) between monthly EI_{30} values and other monthly rainfall characteristics derived from low-resolution daily data. The model was used to estimate at-site R-values in 13 additional rain gauge stations homogeneously dispersed over the whole region for four periods (1981–2010, 2011–2040, 2041–2070, 2071–2100). The at-site estimates were used to create R-factor maps using a geostatistical approach. The results showed that the mean R-factor values in the region might change from 429 to as much as 520 MJ.mm.ha^{-1}.h^{-1}.yr^{-1} in the second half of the 21st century representing a 20.5% increase.

Keywords: R-factor, soil erosion, climate change, ordinary kriging

Soil erosion by water has become one of the greatest environmental threats worldwide. It negatively affects soil quality and fertility by reducing its infiltration rates, water-holding capacity or the nutrient and organic matter contents. The implications are associated not only with reduced agricultural productivity but also with compromised biodiversity, ecosystem services, water quality and quantity and recreational activities (Korbeľová, Kohnová, 2017; Stolte et al., 2016). In Europe, the most dominant cause of soil loss is induced by water erosion in the form of heavy rainfall episodes (Boardman, Poesen, 2006).

As soil erosion by water is difficult to measure in a regional scale, it is often estimated using empirical models such as the universal soil loss equation (USLE) model (Wischmeier, Smith, 1978). The model estimates mean annual soil loss resulting from the erosive effect of raindrops by multiplying six empirically derived factors from which rainfall erosivity factor (*R*) has the highest impact (Loureiro, Coutinho, 2001; Panagos et al., 2015). The *R*-factor is a multi-annual average index representing kinetic energy and intensity of high-intensity rainfall events with a potential to cause soil erosion. Its accurate estimation relies on high-temporal-resolution of precipitation records that should be available for 10–20 years at least (Brychta, Janeček, 2019). Since such data is often not available everywhere, several studies emerged to map the spatial distribution of *R*-factor values to promote regional soil erosion assessments and its easy application

to land management or soil conservation practices (Angulo-Martínez et al., 2009; Goovaerts, 1999).

In the last years, there were some efforts trying to update *R*-factor values in the Central European region based on the extended datasets in terms of both longer records and denser network of rain gauge stations (Brychta, Janeček, 2019). Studies from Slovakia and the Czech Republic showed that the historically used values were significantly underestimated (Hanel et al., 2016; Onderka, Pecho, 2019) with the updated values twice as large as those historically used.

Despite these updates, several studies have already shown that soil erosion rates might significantly increase in the near future as a result of the expected climate change (Panagos et al., 2017). In Europe, the simulations using regional climate models revealed that the total number of rainfall events will decrease while rainfall intensities will increase especially for extreme rainfall events (Westra et al., 2014). Panagos et al. (2017) predict that these changes might increase the rainfall erosivity factor in Europe by as much as 18% by the end of 2050, with Central Europe being one of the most affected regions in Europe.

The objective of this study is to estimate the expected change in *R*-factor due to climate change in one of the regions that are most severely affected by soil erosion in Slovakia. Within the study, high-resolution 1-minute rainfall data was used to build a regression model enabling to extend the dataset of rainfall erosive events in the region by
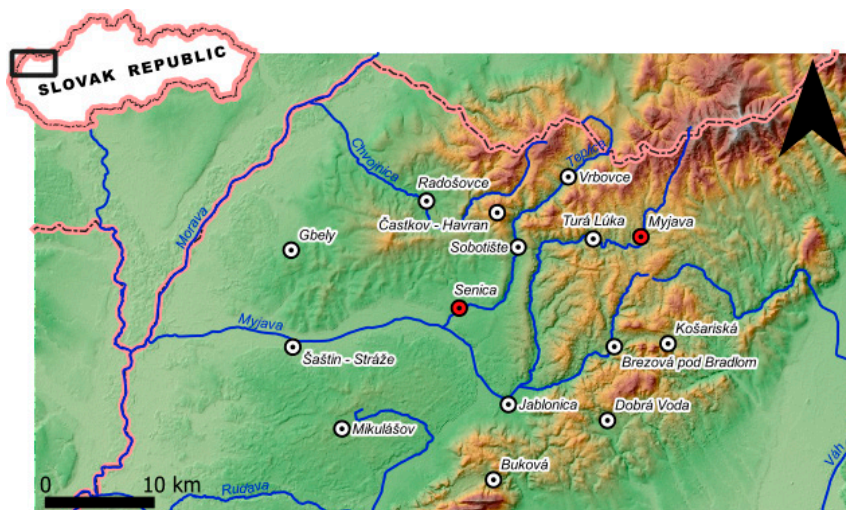
Figure 1   Location of the study area and the position of 15 rain gauge stations used in the analysis. White circles represent stations with low-resolution daily data and red circles with high-resolution 1-minute data

stations for which only low-resolution daily rainfall data were available. The estimated at-site *R*-factor values were spatially interpolated to create rainfall erosivity maps of the region for the current and the three future periods.

Material and method

Study area

The area of interest is situated in the western part of Slovakia. It encompasses the geomorphological units of the Myjava Hill Land, Chvojnica Hill Land and the northern part of the Bor Lowlands (Figure 1). The altitude in the area ranges between 160 m a.s.l. (the western part near the rivers) and 580 m a.s.l. (northern part in the hills). A large part of the area lies in the Myjava River catchment, which has historically been significantly influenced by anthropogenic processes represented

mainly by massive deforestation and subsequent large-scale agriculture. Many of these changes took place in the second half of the 20th century, since when the region has been a subject to increased occurrence of flash floods and significantly intensified erosion processes (Stankoviansky, 2001). The mean annual rainfall in the area varies between 550 and 700 mm, with the mean annual air temperature of 9 °C (Figure 2). During the winter months, the elevated parts of the area are partially covered with snow that usually melts away with the first spring months.

Observed data

The rainfall data used in this study were taken from the national meteorological and climatological databases administered by the Slovak Hydrometeorological Institute. The data available come from 15 rain gauges that are evenly distributed over the study

area (see Figure 1). The elevation of the stations is diverse and represents all elevation zones in the investigated area (see Table 1). For all stations, daily rainfall heights are available for a 30-year period between January 1st, 1981 and December 31st, 2010. In addition to the daily data, high-resolution tipping-bucket rain gauge data in a 1-minute time step was available at Myjava and Senica stations. The high-resolution data covers only the "warm" period of the year when it is ensured that the precipitation occurs exclusively in its liquid state. For this study, this assumption was taken as the rainfall erosivity factor analysed here does not account for the erosive forces of thaw and snowmelt processes (Onderka, Pecho, 2019; Wischmeier, Smith, 1978). The high-resolution data then covers the months from April to October and a 15-year period between April 1st, 1995 and October 31st, 2009.

Climate change scenarios

In order to assess the possible changes in the *R*-factor values due to the expected changes in climate, projections of daily precipitation totals for each station were included in the analysis. Scenarios of changes in daily precipitation totals in Slovakia have been prepared using model outputs from the Canadian Global General Circulation Model (GCM) called CGCM3.1 and the ICCP SRES-A1B (moderate) emission scenario, issued in 2011. The results were regionally downscaled using the KNMI (Dutch) Regional Circulation Model (RCM), which is based on the German ECHAM5 GCM boundary conditions (Hlavčová et al., 2015; Lapin et al., 2012). The models were used to prepare projections of daily precipitation totals for a period between 2011 and 2100. The data was split into three 30-year periods.

Estimation of *R*-factor from high-resolution data

Rainfall erosivity factor (*R*) is usually determined as the sum of erosive storm index values EI_{30} occurring during a mean year. EI_{30} of each storm is defined as a product of a total storm kinetic energy (*E*) and the maximum 30-minute rainfall intensity (I_{30}), where *E* is in MJ.ha^{-1} and I_{30} in mm.h^{-1}. As not all of the observed rainfall events have a potential to cause
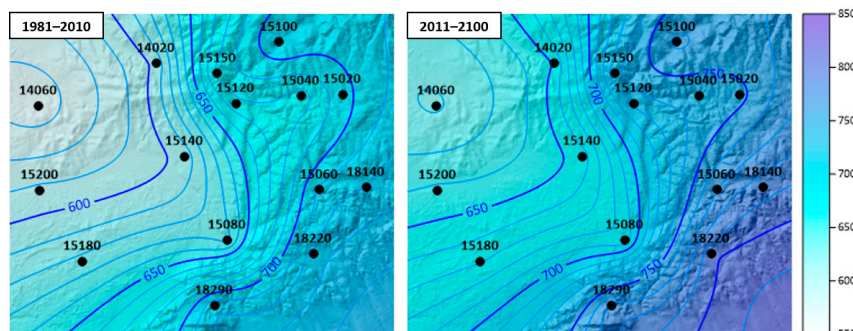
Figure 2   Maps of mean annual precipitation in mm for the current (1980–2010) and the future periods (2011–2100)

Table 1   List of rain gauge stations with the estimated values of mean annual *R*-factors

ID	Location	Elevation (m a.s.l)	*R*-factor (MJ.mm.ha^{-1}.h^{-1}.yr^{-1})			
			1981–2010	2011–2040	2041–2070	2071–2100
15060	Brezová pod Bradlom	290.0	455	526	535	522
18290	Buková	336.0	519	592	623	621
15150	Častkov – Havran	475.0	452	548	548	531
18220	Dobrá Voda	257.0	475	590	607	602
14060	Gbely	204.0	343	440	460	439
15080	Jablonica	204.0	450	513	523	526
18140	Košariská	319.0	453	522	547	522
15180	Mikulášov	236.0	402	497	479	502
15020	Myjava	349.0	435	484	503	484
14020	Radošovce	225.0	400	487	488	470
15200	Šaštín – Stráže	172.0	353	452	465	453
15140	Senica	195.0	372	447	451	437
15120	Sobotište	240.0	438	527	529	508
15040	Turá Lúka	295.0	421	511	518	502
15100	Vrbovce	310.0	467	547	559	542

significant soil erosion, various authors have defined sets of rules to select only those events that can trigger soil erosion (Brychta, Janeček, 2017; Wischmeier, Smith, 1978). Although multiple authors tried to optimize the rules for a particular region, in this study, we decided to stick to the widely used selection criteria for comparative reasons as suggested by Onderka and Pecho (2019). In this study, a rainfall event to be considered as potentially erosive had to match the following criteria:

1. individual rainfall events are separated from each other by at least 6 hours during which no rainfall occurs;
2. a minimum rainfall depth of such event is greater than 12.5 mm;
3. a maximum 15-minute rainfall intensity is greater than 6.25 mm.

After identifying the possible erosive rainfall events in the "warm" period of the year, the calculation of the *R*-factor was conducted using the metric version of the empirical equation that was originally developed by Wischmeier, Smith (1978). The high-resolution 1-minute rainfall data was available only in Myjava and Senica rain gauge stations. The *R*-factor was then computed using the following formula:

$$R = \frac{1}{n}\sum_{j=1}^{n} R \sum_{k=1}^{mj} (EI_{30})_k \qquad (1)$$

where:
R   –   an average annual rainfall erosivity (MJ.mm.ha^{-1}.h^{-1}.yr^{-1})
n   –   the number of years covered by the data records
mj   –   the number of erosive events of a given year *j*
EI_{30} –   the rainfall erosivity index (MJ.mm.ha^{-1}.h^{-1}) of a single event *k*

The event erosivity EI_{30} (MJ.mm.ha^{-1}.h^{-1}) is defined as:

$$EI_{30} = \left(\sum_{r=1}^{0} e_r v_r\right) I_{30} \qquad (2)$$

where:
e_r –   the unit rainfall energy (MJ.ha^{-1}.mm^{-1})
v_r –   the rainfall volume (mm) during each interval *r* of rainfall event (in this case 1-minute)

I_{30} is the maximum rainfall intensity during a 30-minute period of the rainfall event (mm.h^{-1}). The unit rainfall energy (e_r) is calculated for each 1-minute interval as follows:

$$e_r = 0.29\left(1 - 0.72e^{-0.05i_r}\right) \qquad (3)$$

where:
i_r –   the rainfall intensity during the interval (mm.h^{-1})

Estimation of *R*-factor from low-resolution data

In the case only low-resolution data is available, the *R*-factor can also be estimated from daily or monthly values of precipitation. In this study, we used the high-resolution rainfall data from stations Myjava and Senica to build a relationship between the monthly storm erosivity index ($EI_{30,\ month}$) and two independent variables represented by i) the monthly rainfall height for days where precipitation exceeds 10 mm ($rain_{10}$) and ii) the monthly number of days where precipitation exceeds 10 mm ($days_{10}$). All the three rainfall parameters were calculated from the high-resolution rainfall data in the two stations for the "warm" months only. The $EI_{30,\ month}$ values were computed as the sum of EI_{30} for each erosive storm during the month. The rainfall parameters were then used to build a multiple linear

regression model with $EI_{30, month}$ being the dependent and $rain_{10}$ and $days_{10}$ the independent variables. Such a model has already been successfully used by several authors (Ferreira, Panagopoulos, 2014; Goovaerts, 1999; Loureiro, Coutinho, 2001).

As the two stations with high-resolution rainfall data represent both higher and lower elevation zones in the area of interest, it was reasonable to merge the three rainfall parameters from both stations into one dataset (Goovaerts, 1999; Loureiro, Coutinho, 2001). This should secure that the estimated model parameters could then be used to compute the $EI_{30, month}$ values for all stations with low-resolution rainfall data in the region. To estimate the *R*-factor for the stations with only low-resolution data available the rainfall parameters $rain_{10}$ and $days_{10}$ were computed from the daily data. In the next step, equation (4) was used to compute $EI_{30, month}$ values for each month available. As the parameters of the regression model were estimated using data from the "warm" part of the year only, the resulting *R*-factor is a sum of the positive monthly $EI_{30, month}$ values for months from April to October (Goovaerts, 1999).

Spatial mapping of *R*-factor

Different authors have already emphasized the need to extend the traditional at-site analysis of *R*-factor to account for its high spatial variability (Angulo-Martínez et al., 2009; Hanel et al., 2016). This is of large importance as a better understanding of the spatial variability and its relation to environmental variables (Ballabio et al., 2017; Hanel et al., 2016; Meusburger et al., 2012; Panagos et al., 2015) would help to prepare better land management strategies and to identify preferential areas where action against soil erosion is needed. With the advent of Geographic Information Systems (GIS), various interpolation techniques have become available to produce high-quality maps of many different environmental characteristics. From among a large number of methods, many authors have reported that satisfactory results could be obtained using geostatistical methods such as ordinary or universal kriging (Angulo--Martínez et al., 2009; Goovaerts, 1999).

In this study, ordinary kriging was used as the most common type of the kriging method. It relies on a correct estimation of the semivariogram model from the sample data. Since the estimation of the model parameters is based only on 15 observations, this type of model was preferred over the universal kriging or co-kriging, which require larger datasets to account for their increased complexities (Angulo-Martínez et al., 2009). The model uses a simple idea that the unknown erosivity value at the unsampled location is a linear combination of neighbouring observations. The unknown value can then be calculated using:

$$R^* = \sum_{i=1}^{n} \lambda_i R_i \qquad (4)$$

where:
R^* and R_i – unknown and observed values respectively
n – the total number of stations used in the interpolation
λ_i – a weight that is unique for each station

The kriging weights are determined such as to minimize the estimation variance, while ensuring the unbiasedness of the estimator. For more information, the reader is referred to a geostatistical textbook (Isaaks and Srivastava, 1989).

In the first step of the analysis, the high-resolution 1-minute rainfall data from stations Senica and Myjava were screened for possible erosive storms. During the "warm" part of the 15-year period, 131 and 140 such storms were identified for the two stations, respectively. This represents approximately 9 erosive storms per year, which complies with similar studies conducted in the region (Onderka, Pecho, 2019). For all the erosive storms identified, three monthly descriptive rainfall characteristics ($EI_{30, month}$, $rain_{10}$, $days_{10}$) were calculated. The data showed that despite larger mean annual rainfall height in Myjava (Figure 2), the erosive storms from the two stations are very similar in terms of their time of occurrence and characteristics. Because of this, multiple linear regression model between the three rainfall characteristics was fitted using the merged dataset (excluding months without any precipitation). The model was fitted in MATLAB R2019b using its Curve fitting tool. The coefficient of determination r^2 of the fit was 0.98 meaning that the model used was able to explain most of the variance in $EI_{30, month}$. The regression model that was fitted to the merged dataset was given by the following equation:

$$EI_{30, month} = 3.11 \, rain_{10} - 26.94 \, days_{10} \qquad (5)$$

where:
$EI_{30, month}$ – the monthly storm erosivity index
$rain_{10}$ – the monthly rainfall height for days where precipitation exceeds 10 mm (mm)
$days_{10}$ – the monthly number of days where precipitation exceeds 10 mm

Equation (4) shows that the estimated rainfall erosivity is larger in months in which more rainfall falls in lesser number of days.

In the next step, this relationship was used to calculate the values of $EI_{30, month}$ from the low-resolution daily data for all the stations in the region. The estimated monthly values for the "warm" months were aggregated for each year and averaged over the 30-year periods of observation and climate scenario projections to get the mean *R*-factor estimates. The estimated *R*-factor values that are given in Table 1 show a significant increase between the current and all the future periods. In average, the difference between the *R*-factor estimated for the current dataset and any of the three climate scenario projection datasets is +20.5%. This complies with the results presented in Panagos et al. (2017) for Central Europe but is in contrast with the mean annual rainfall totals, where the difference is also positive but only around +8% in average (Figure 2). This could be explained by the fact that apart from the slight increase in the rainfall totals, the climate scenario projections also expect the interannual distribution of rainfall will change (Gera et al.,
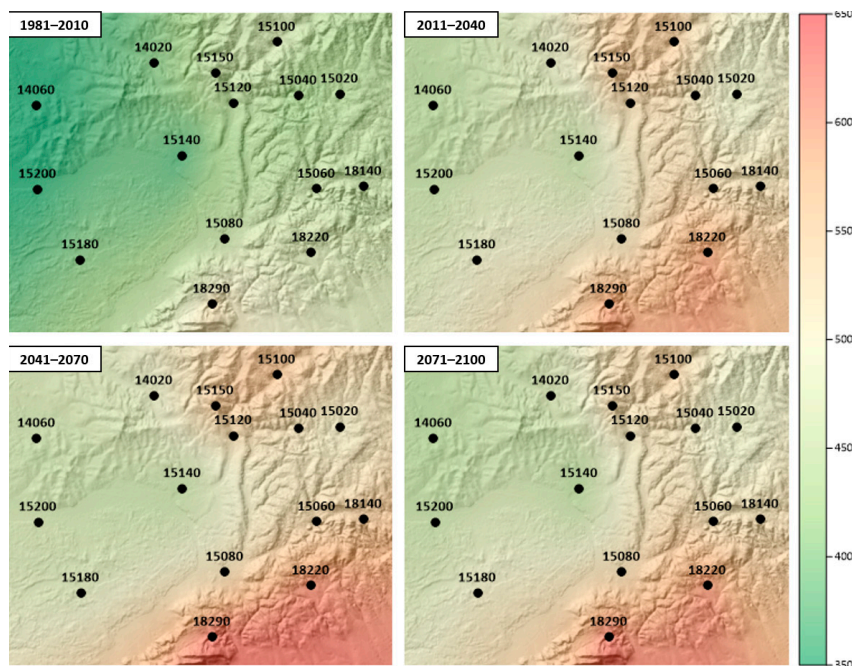
Figure 3 Annual rainfall erosivity maps in MJ.mm.ha^{-1}.h^{-1}.yr^{-1} produced by ordinary kriging and the estimates of *R*-factors from the low-resolution daily precipitation data

2019; Kohnová et al., 2018; Lapin et al., 2012). The results also indicate that the number and the severity of extreme rainfall events will increase, which will have large implications for not only land management or soil conservation practices, but also the operation of existing water management structures (Rončák et al., 2019). When comparing the three periods of the climate scenario projections, the estimated *R*-factors in the individual stations are very similar without any significant trend observed.

To better understand the spatial pattern of the *R*-factor in the region, ordinary kriging interpolation method was used to perform this task. Analysis of the empirical semivariograms showed that the best model of the semivariogram would be a simple linear model with no nugget effect. Despite the fact that *R*-factor values are very often associated with large spatial variability and temporal variability (Angulo-Martínez et al., 2009; Ballabio et al., 2017), the interpolated surfaces were rather smooth without any interpolation artifacts (see Figure 3). Figure 3 also shows that the *R*-factor follows the same pattern as mean annual rainfall (Figure 2) and gradually increases from west to east. The main reason for this is a strong orographic effect that is present in this region

due to the prevailing west-east winds. When looking into the future, the analysis shows that the *R*-factor estimates will increase especially in the mountainous part of the region. This might mainly be problematic for the northern part (around Sobotište, Turá Lúka and Vrbovce), which was subject to the largest anthropogenic changes, accompanied by soil erosion (Hlavčová et al., 2019). In this part of the region, the estimated *R*-factor values will increase from around 420 to as much as 520 MJ.mm.ha^{-1}.h^{-1}.yr^{-1}.

Conclusions

This study investigates the expected impact of climate change on mean annual rainfall erosivity factor (*R*) used in the USLE model. The analysis tried to compare the *R*-factor values estimated for four 30-year periods: one representing the current period (1981–2010) and three the future periods (2011–2040, 2041–2070, 2071–2100). *R*-factor values for the specific periods were estimated from daily precipitation data based on a relationship build between three monthly rainfall characteristics estimated directly from high-resolution 1-minute precipitation data. The biggest changes could be observed between the current and any of the three future periods, where the *R*-factor values increased by as

much as 20.5% in all stations. This might have severe consequences for the future development of the region as its northern part is already a subject to severe soil erosion. It is also a part of the region with multiple mid- to large-scale agricultural and forestry businesses, which might be threatened by the expected rise of soil erosion. This increase in *R*-factor for the future periods could be tracked down to the increased frequency of heavy precipitation days with higher rainfall intensities as projected by the regional climate model.

The information about the spatial distribution of the *R*-factor in this region is of great value as it is a very popular place for site, local or regional erosion studies (Németová et al., 2020; Nosko et al., 2019; Stankoviansky, 2003; Valent, Výleta and Danáčová, 2019). As many of these studies utilize a GIS implementation of the USLE model, the accuracy of the spatial distribution of the *R*-factor plays an important role in minimizing the uncertainties of soil loss estimates.

Further research should focus on finding additional independent variables that could be used to improve the reliability of $EI_{30, month}$ estimates from daily rainfall data. Moreover, additional spatial interpolation methods could be tested, including those utilizing secondary variables such as elevation or rainfall to further reduce the estimation variance.

References

Angulo-Martínez, M., López-Vicente, M., Vicente-Serrano, S. M., Beguería, S. (2009). Mapping rainfall erosivity at a regional scale: A comparison of interpolation methods in the Ebro Basin (NE Spain). *Hydrology and Earth System Sciences*, 13(10), 1907–1920. https://doi.org/10.5194/hess-13-1907-2009

Ballabio, C., Borrelli, P., Spinoni, J., Meusburger, K., Michaelides, S., Beguería, S., ... & Aalto, J. (2017). Mapping monthly rainfall erosivity in Europe. *Science of the Total*

Environment, 579. https://doi.org/10.1016/j.scitotenv.2016.11.123

Boardman, J., Poesen, J. (Eds.). (2006). *Soil Erosion in Europe.* Chichester: John Wiley and Sons, Ltd.

Brychta, J., Janeček, M. (2017). Evaluation of discrepancies in spatial distribution of rainfall erosivity in the Czech Republic caused by different approaches using GIS and geostatistical tools. *Soil and Water Research*, *12*(2), 117–127. https://doi.org/10.17221/176/2015-SWR

Brychta, J., Janeček, M. (2019). Determination of erosion rainfall criteria based on natural rainfall measurement and its impact on spatial distribution of rainfall erosivity in the Czech Republic. *Soil and Water Research*, *14*(3), 153–162. https://doi.org/10.17221/91/2018-SWR

Ferreira, V., Panagopoulos, T. (2014). Seasonality of Soil Erosion Under Mediterranean Conditions at the Alqueva Dam Watershed. *Environmental Management*, *54*(1), 67–83. https://doi.org/10.1007/s00267-014-0281-3

Gera, M., Damborská, I., Lapin, M., Melo, M. (2019). Climate Changes in Slovakia: Analysis of Past and Present Observations and Scenarios of Future Developments. In Negm, A. M. - Zeleňáková, M. (Eds.), *Water Resources in Slovakia: Part II: Climate Change, Drought and Floods* (pp. 21–47). https://doi.org/10.1007/698_2017_157

Goovaerts, P. (1999). Using elevation to aid the geostatistical mapping of rainfall erosivity. *CATENA*, *34*(3–4), 227–242. https://doi.org/10.1016/S0341-8162(98)00116-7

Hanel, M., Máca, P., Bašta, P., Vlnas, R., Pech, P. (2016). The rainfall erosivity factor in the Czech Republic and its uncertainty. *Hydrology and Earth System Sciences*, *20*(10), 4307–4322. https://doi.org/10.5194/hess-20-4307-2016

Hlavčová, K., Lapin, M., Valent, P., Szolgay, J., Kohnová, S., Rončák, P. (2015). Estimation of the impact of climate change-induced extreme precipitation events on floods. *Contributions to Geophysics and Geodesy*, *45*(3), 173–192. https://doi.org/10.1515/congeo-2015-0019

Hlavčová, K., Danáčová, M., Kohnová, S., Szolgay, J., Valent, P., Výleta, R. (2019). Estimating the effectiveness of crop management on reducing flood risk and sediment transport on hilly agricultural land – A Myjava case study, Slovakia. *CATENA*, *172*, 678–690. https://doi.org/10.1016/J.CATENA.2018.09.027

Isaaks, E. H., Srivastava, M. R. (1989). *Applied Geostatistics.* New York: Oxford University Press.

Kohnová, S., Vasilaki, M., Hanel, M., Szolgay, J., Hlavčová, K., Loukas, A., Földes, G. (2018). Detection of future changes in trends and scaling exponents in extreme short-term rainfall at selected stations in Slovakia. *Contributions to Geophysics and Geodesy*, *48*(3), 207–230. https://doi.org/10.2478/congeo-2018-0009

Korbeľová, L., Kohnová, S. (2017). Methods for Improvement of the Ecosystem Services of Soil by Sustainable Land Management in the Myjava River Basin. *Slovak Journal of Civil Engineering*, *25*(1), 29–36. https://doi.org/10.1515/sjce-2017-0005

Lapin, M., Bašták, I., Gera, M., Hrvoľ, J., Kremler, M., Melo, M. (2012). New climate change scenarios for Slovakia based on global and regional general circulation models. *Acta Meteorologica Universitatis Comenianae*, *37*, 25–73.

Loureiro, N. de S., Coutinho, M. de A. (2001). A new procedure to estimate the RUSLE EI30 index, based on monthly rainfall data and applied to the Algarve region, Portugal. *Journal of Hydrology*, *250*(1–4), 12–18. https://doi.org/10.1016/S0022-1694(01)00387-0

Meusburger, K., Steel, A., Panagos, P., Montanarella, L., Alewell, C. (2012). Spatial and temporal variability of rainfall erosivity factor for Switzerland. *Hydrology and Earth System Sciences*, *16*(1), 167–177. https://doi.org/10.5194/hess-16-167-2012

Németová, Z., Honek, D., Kohnová, S., Hlavčová, K., Šulc Michalková, M., Sočuvka, V., Velísková, Y. (2020). Validation of the EROSION-3D Model through Measured Bathymetric Sediments. *Water*, *12*(4), 1082. https://doi.org/10.3390/w12041082

Nosko, R., Maliariková, M., Brziak, A., Kubáň, M. (2019). Formation of Gully Erosion in the Myjava Region. *Slovak Journal of Civil Engineering*, *27*(3), 63–72. https://doi.org/10.2478/sjce-2019-0023

Onderka, M., Pecho, J. (2019). Update of the erosive rain factor in Slovakia using data from the period 1961–2009. *Contributions to Geophysics and Geodesy*, *49*(3), 355–371. https://doi.org/10.2478/congeo-2019-0018

Panagos, P., Ballabio, C., Borrelli, P., Meusburger, K., Klik, A., Rousseva, S., ... & Aalto, J. (2015). Rainfall erosivity in Europe. *Science of the Total Environment*, *511*, 801–814. https://doi.org/10.1016/j.scitotenv.2015.01.008

Panagos, P., Ballabio, C., Meusburger, K., Spinoni, J., Alewell, C., Borrelli, P. (2017). Towards estimates of future rainfall erosivity in Europe based on REDES and WorldClim datasets. *Journal of Hydrology*, *548*, 251–262. https://doi.org/10.1016/j.jhydrol.2017.03.006

Rončák, P., Hlavčová, K., Kohnová, S., Szolgay, J. (2019). Impacts of Future Climate Change on Runoff in Selected Catchments of Slovakia. In Leal Filho, W., Trbic, G., Filipovic, D. (Eds.). *Climate Change Adaptation in Eastern Europe*: *Managing Risks and Building Resilience to Climate Change* (pp. 279–292). https://doi.org/10.1007/978-3-030-03383-5_19

Stankoviansky, M. (2001). Erózia z orania a jej geomorfologický efekt s osobitým zreteľom na Myjavsko-Bielokarpatskú kopaničiarsku oblasť. *Geografický časopis*, *53*(2), 95–110.

Stankoviansky, M. (2003). Historical evolution of permanent gullies in the Myjava Hill Land, Slovakia. *CATENA*, *51*(3), 223–239. https://doi.org/10.1016/S0341-8162(02)00167-4

Stolte, J., Tesfai, M., Oygarden, L., Kvaerno, S., Keizer, J., Verheijen, F., ... & Hessel, R. (2016). Soil threats in Europe: status, methods, drivers and effects on ecosystem services: deliverable 2.1 RECARE project. European Commission DG Joint Research Centre.

Valent, P., Výleta, R., Danáčová, M. (2019). A Joint Sedimentation-Flood Retention Assessment of a Small Water Reservoir in Slovakia: A New Hope for Old Reservoirs? *Geosciences*, *9*(4), 158. https://doi.org/10.3390/geosciences9040158

Westra, S., Fowler, H. J., Evans, J. P., Alexander, L. V., Berg, P., Johnson, F., ... & Roberts, N. M. (2014). Future changes to the intensity and frequency of short-duration extreme rainfall. Reviews of *Geophysics*, *52*(3), 522–555. https://doi.org/10.1002/2014RG000464

Wischmeier, W. H., Smith, D. D. (1978). *Predicting Rainfall Erosion Losses: A Guide to Conservation Planning.* Washington, D.C.: USDA-SEA (p. 58).

LONG-TERM RUNOFF VARIABILITY ANALYSIS OF RIVERS IN THE DANUBE BASIN

Pavla PEKÁROVÁ[1]*, Jakub MÉSZÁROS[1], Pavol MIKLÁNEK[1],
Ján PEKÁR[2], Stevan PROHASKA[3], Aleksandra ILIĆ[4]

[1]Institute of Hydrology of the Slovak Academy of Sciences, Bratislava, Slovakia
[2]Comenius University in Bratislava, Slovakia
[3]Jaroslav Černi Institute for the Development of Water Resources, Beograd, Serbia
[4]University of Niš, Serbia

The long-term runoff variability is identified to consist of the selected large rivers with long-term data series in the Danube River Basin. The rivers were selected in different regions of the Danube River Basin and have a large basin area (Danube: Bratislava gauge with 131,338 km^2; Tisza: Senta with 141,715 km^2; and Sava: Sremska Mitrovica with 87,966 km^2). We worked with the station Danube: Reni in the delta as well. A spectral analysis was used to identify the long-term variability of three different types of time series: (1) Average annual discharge time series, (2) Minimum annual discharge time series and (3) Maximum annual discharge time series. The results of the study can be used in a long-term forecast of the runoff regime in the future.

Keywords: long-term discharge analysis, spectral analysis, Danube River Basin

The Danube River with a total length of 2,857 km and a long-term daily mean discharge of about 6,500 m^3.s^{-1} is listed as the second biggest river in Europe. In the terms of length, it is listed as the 21st biggest river in the world, in the terms of a drainage area, it is ranked as the 25th with a drainage area of 817,000 km^2. Nineteen countries share the Danube basin, though two thirds of the catchment lie within five countries (Romania, Hungary, Serbia, Austria and Germany). In the large international river basins – such as the Danube basin- it is necessary to synchronise the methodologies of the calculation of the hydrological characteristics and to prepare common procedures. In 1971, the hydrologists of eight Danube countries launched a regional hydrological cooperation on a voluntary basis, aiming to produce consistent hydrological information about the whole Danube basin. Since 1987, this cooperation has been carried out in the framework of the International Hydrological Programme (IHP) of UNESCO. The cooperation of the Danube countries within the framework of IHP of UNESCO is based on the project work on one hand and on the other, on the regular conferences. Several projects were finalised within the Danube collaboration. The topic of floods was observed by several of them in the last years:

– Project No. 4: Coincidence of flood flow of the Danube River and its tributaries (Prohaska et al., 1999; Prohaska, Ilić, 2010).
– Project No. 5.2: Flow regime of river Danube and its catchment (Belz et al., 2004).
– Project No. 7: Regional analysis of the annual peak discharges in the Danube catchment (Stănescu, Ungureanu, Mătreaţă, 2004).

– Project No. 9 Flood regime of rivers in the Danube River basin (Pekárová, Miklánek (eds), 2019).

Since the very inception of hydrology as a scientific discipline, hydrologists and climatologists around the world have been trying to make a science-based prediction of the future development in the hydrosphere. Generally, it is expected that the increase of temperature will increase evapotranspiration in summer and decrease the runoff.

There are two main approaches to stream the runoff prognosis in the next decades:

1. Statistical analysis of the long-term discharge series followed by a prognosis using stochastic auto-regressive models.
2. Application of the hydrological rainfall-runoff models based on the precipitation-temperature-stream runoff relations. The precipitation and temperature data are modified according to the selected climate scenarios for the future time horizons (most frequently 2050, 2075 or 2100).

In this study, the first method was used and changes in statistical characteristics of the discharge, using detailed statistical analysis of the daily, monthly and annual time series in the four selected sub-basins of the Danube River Basin were identified.

Material and method

A Danube discharge description

The Danube River originates in the Schwarzwald (Black Forest) mountains in Bavaria in Germany. It has its sources
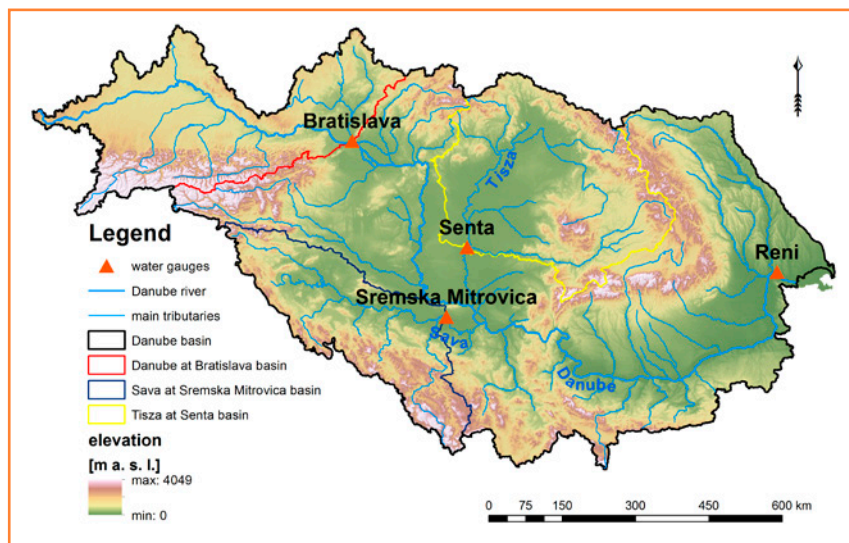
Figure 1 Scheme of the Danube River Basin. Water gauges were used

In the period 1931–1990, the mean annual discharge of the upper Danube (upstream the confluence with Tisa), and of the Tisza and Sava River was 2,943 $m^3.s^{-1}$, 791 $m^3.s^{-1}$, and 1,572 $m^3.s^{-1}$, respectively. The mean annual discharge downstream the confluence of the three major sub-basins was 5,374 $m^3.s^{-1}$, and the mean annual runoff was 6,846 $m^3.s^{-1}$ in the Danube delta.

The maximum runoff occurs in June in the upper Danube basin, but in April in the Sava and Tisza basins (Figure 2). After the confluence of these three major sub-basins, the maximum is shifted to April at the end of the middle river section. Concerning downstream, the maximum is shifted to May in the delta region due to the tributaries in the lower Danube section. The minimum monthly runoff occurs in autumn season in the major part of the Danube basin with an exception of the Sava River with minimum flows in August and September. The increase of the monthly runoff in November and December in the Sava basin is the reason for an increase of flows at the lower section of the Danube River (Miklánek and Pekárová, 2016).

outside the Alps in an old mountainous massif. From the hydrological point of view, the Danube is an important hydrologic and hydrographic system, which is formed by several significant tributaries. Over 120 major rivers directly confluence with the Danube and a majority of them has its own significant tributaries. Approximately, in the middle of the Danube length near the end of the middle section, the Danube receives its two main tributaries Tisza and Sava in a short distance (Figure 1).

The regime of precipitation differs in different parts of the Danube basin. This variability is also reflected in a runoff regime of the individual sub-basins and it corresponds to the position of the sub-basins within the whole basin.

To analyse the long-term runoff variability, the daily discharge series from four water gauge stations: Danube: Bratislava gauge with 131,338 km^2 (Slovakia – SK); Tisza: Senta with 141,715 km^2 (Serbia – SR); Sava: Sremska Mitrovica with 87,966 km^2 (Serbia – SR); and Danube: Reni with 805,700 km^2 (Ukraine – UA) (Table 1, Figure 3) were used. The Tisza basin is one of the driest sub-basins in the Danube basin according to the specific yield. The daily discharge series of the Danube River were obtained from the database of the UNESCO subproject No. 4.2.1 "Water temperature simulation during summer low flow conditions in the Danube basin".

Figure 2 Mean monthly discharges of the Danube basin and its sub-basins (1931–1990)

Table 1 Long-term mean annual and daily discharge characteristics of the Danube in Bratislava (SK), Tisza in Senta (SR), Sava in Sremska Mitrovica (SR), and Danube in Reni (UA)

	A (km^2)	Q (m^3.s^{-1})	q (l.s^{-1}.km^{-2})	R (mm)	$Q_{d,\ min}$	$Q_{d,\ max}$	Period	
Danube: Bratislava	131,338	2,052	15.6	492.8	580	10,810	1875	2017
Tisza: Senta	141,715	782	5.5	173.9	79	3,730	1921	2017
Sava: Sr. Mitrovica	87,966	1,552	17.6	556.5	194	6,420	1926	2017
Danube: Reni	805,700	6,551	8.1	256.4	1280	15,900	1921	2015

A – a basin area; $Q/q/R$ – long-term average annual discharge/specific yield/runoff depth; $Q_{d,\ min}/Q_{d,\ max}$ – minimal/maximal daily discharge (m^3.s^{-1})
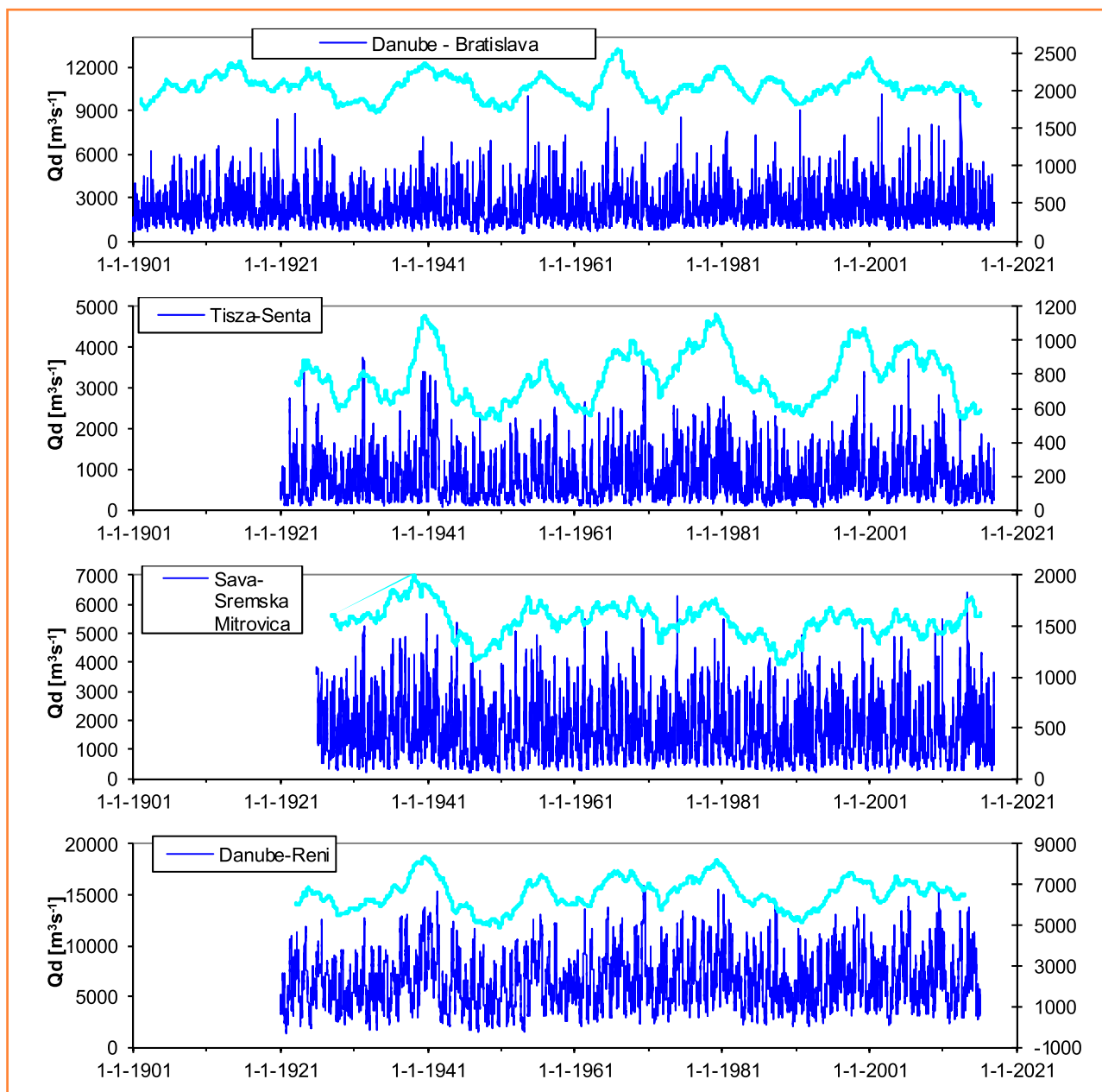
Figure 3   Daily discharge at selected stations of the Danube basin (dark blue lines) and 4-years moving averages (light blue lines) since 1901 or 1921

Identification of the long-term variability – autocorrelation, spectral and trend analysis

From Figure 3, it is evident that annual discharge series are marked by the multi-annual cycles of the dry and wet periods (data are not independent).

It is possible to identify the cyclicity in the time series by an auto-correlation and a spectral analysis. Both methods were used to look for the long-term cycles of runoff decrease and increase in the analysed runoff time series.

The estimation of both, the auto-covariance and the auto-correlation functions of given empirical series $\{x_{ij}\}_{i=1}^{n}$, is the base tool of a time series analysis.

The auto-covariance function $R(\tau)$ can be estimated by the formula:

$$R(\tau) = \frac{\sum_{i=1}^{n-\tau} (x_i - \overline{x}) \cdot (x_{i+\tau} - \overline{x}_{i+\tau})}{n - \tau} \qquad (1)$$

where:
$\overline{x}$ – mean of $\{x_{ij}\}$

The normalized auto-covariance function (with respect to the standard deviation s_x) provides an estimation of the auto-correlation function $r(\tau)$ of the form:

$$r(\tau) = \frac{R(\tau)}{s_x^2} \qquad (2)$$

where:

$\tau = 0, 1, 2...; m = n/2$

Function $r(\tau)$ reaches its values within the interval <-1, 1>.

The spectral analysis is used to examine the periodical properties of random processes $\{x_i\}_{i=1}^{n}$. The spectral analysis generalises a classical harmonic analysis by introducing the mean value in time of the periodogram obtained from the individual realizations. The fundamental statistical characteristic of the spectral analysis is its spectral density.

The basic tool in estimating the spectral density is a periodogram. The periodogram (a line spectrum) is a frequency plot with ordinate pairs for a specific time period. This graph breaks time series into a set of sine waves of various frequencies. It is used to construct a frequency spectrum. A periodogram can be helpful in identifying randomness and seasonality in the time series data and in recognizing the predominance of a negative or positive autocorrelation – the help you often need to identify an appropriate model for forecasting the given time series. If the periodogram contains one spike, the data may not be random. The spectral density is defined as a mean value of the set of periodogram for $n \to \infty$.

The periodogram is calculated according to the formula:

$$I(\lambda_j) = \frac{1}{2\pi n}\left|\sum_{\tau=1}^{n} x_\tau e^{-i\tau\lambda_j}\right|^2 =$$

$$= \frac{1}{2\pi n}\left\{\left(\sum_{\tau=1}^{n} x_\tau . \sin(\tau.\lambda_j)\right)^2 + \left(\sum_{\tau=1}^{n} x_\tau . \cos(\tau.\lambda_j)\right)^2\right\} \quad (3)$$

We compute the squared correlation between the series and the sine/cosine waves of frequency λ_j. By the symmetry $I(\lambda_j) = I(-\lambda_j)$ we need only to consider $I(\lambda_j)$ on $0 \le \lambda_j \le \pi$.

For real centred series, the periodogram $I(\lambda_j)$ can be estimated by an auto-covariance function as:

$$I(\lambda_j) = \frac{1}{2\pi}\left(R_0 + 2\sum_{\tau=1}^{n-1} R_\tau \cdot \cos(\tau \cdot \lambda_j)\right) \quad (4)$$
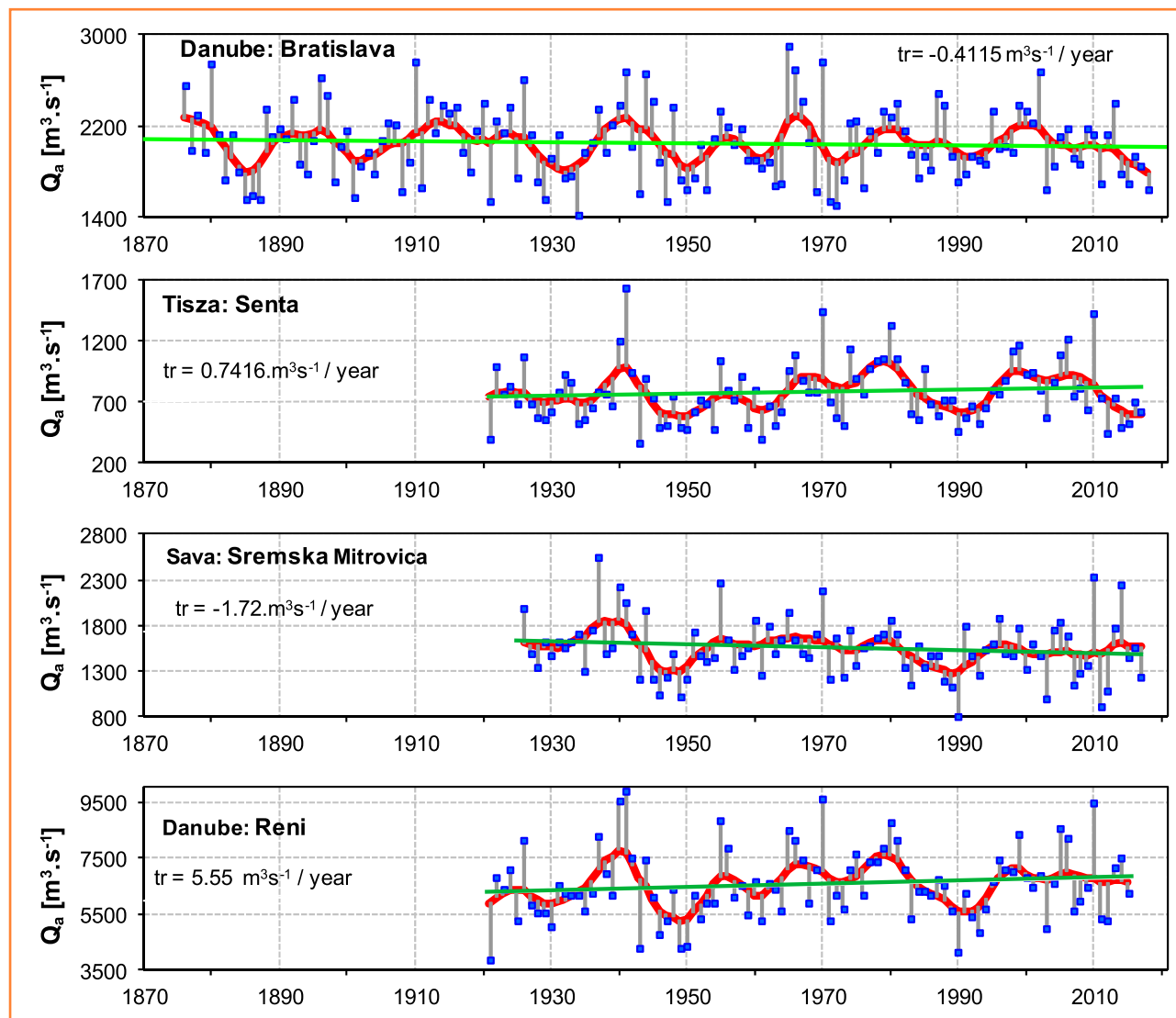
Figure 4   Average annual discharge at selected stations of the Danube basin (blue points), double 7-year moving averages (red line), long-term trend *tr* (green line)

for Fourier frequencies:

$$\lambda_{j'} = \frac{2\pi \cdot j}{n} \qquad (5)$$

where:

$$j = \left\langle 1, \frac{n}{2} \right\rangle$$

Due to the trend analysis of the time series, the parametric and non-parametric tests can be used. The parametric test considers the linear regression of the random variable x_i in time. The parameters of the trend line are calculated by using a standard method for an estimation of the parameters of a simple linear regression model, i.e. by using the least square method. Mann-Kendall nonparametric trend test was used to identify the long-term trends. The Mann-Kendall nonparametric test (M-K test) is one of the most widely used

non-parametric tests for a significant trends detection in time series. By M-K test, the null hypothesis H_0 of no trend was tested, i.e. the observations x_i are randomly ordered in time, against the alternative hypothesis H_1, where there is an increasing or decreasing monotonic trend.

Results and discussion

Multi-annual variability identification of the runoff

More than 60 years ago, by the studies of long-term storage requirements on the Nile River, Hurst (1951) discovered special behaviour of the hydrological and other geophysical time series, which has become known as the 'Hurst phenomenon'. This behaviour is essentially the tendency of the wet years to cluster into wet periods, or of the dry years to cluster into periods of drought (Lin and Lye, 1994). In this
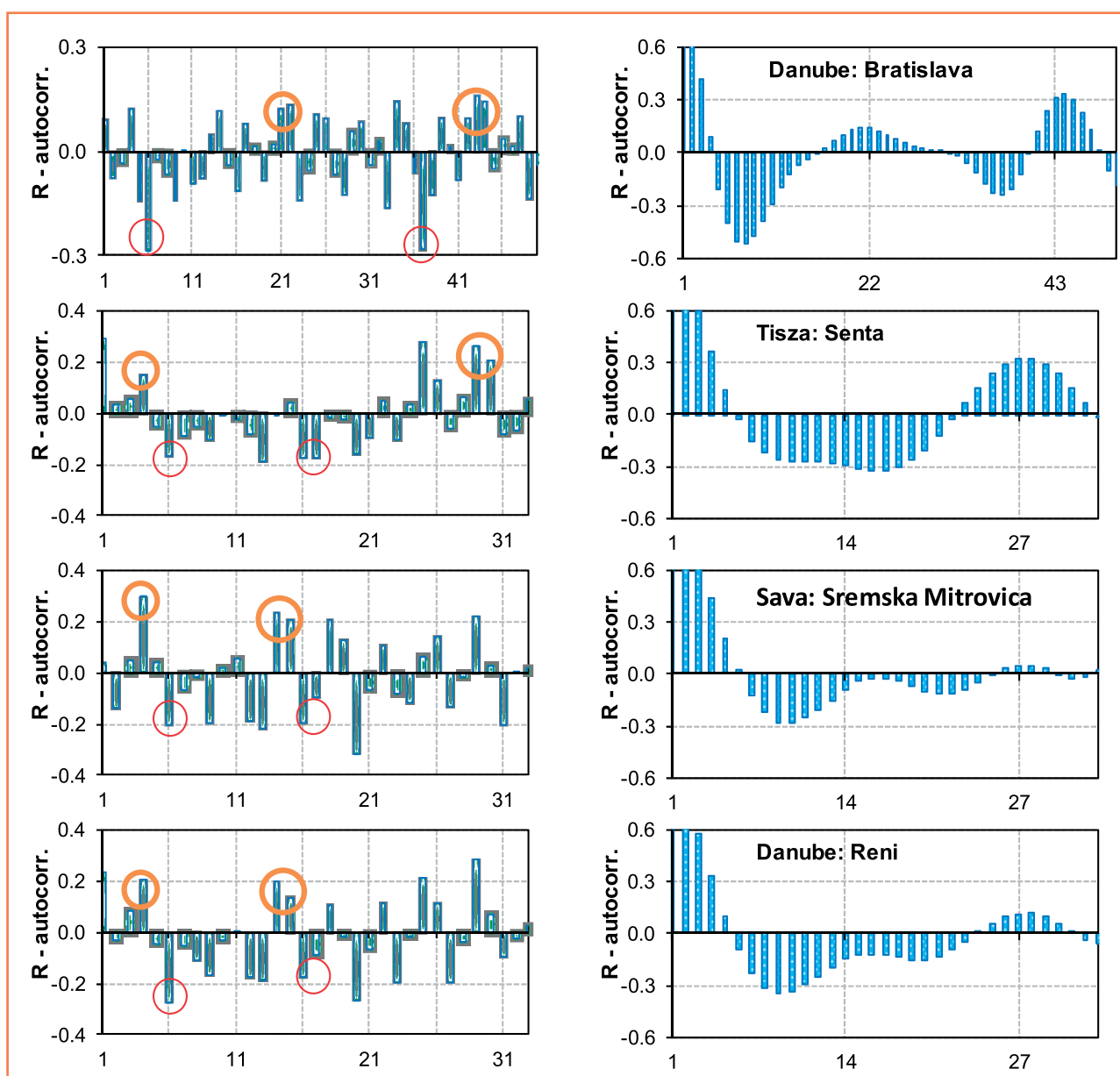
Figure 5   The auto-correlograms of the average annual discharges of the time series of the selected stations (time lag in years)
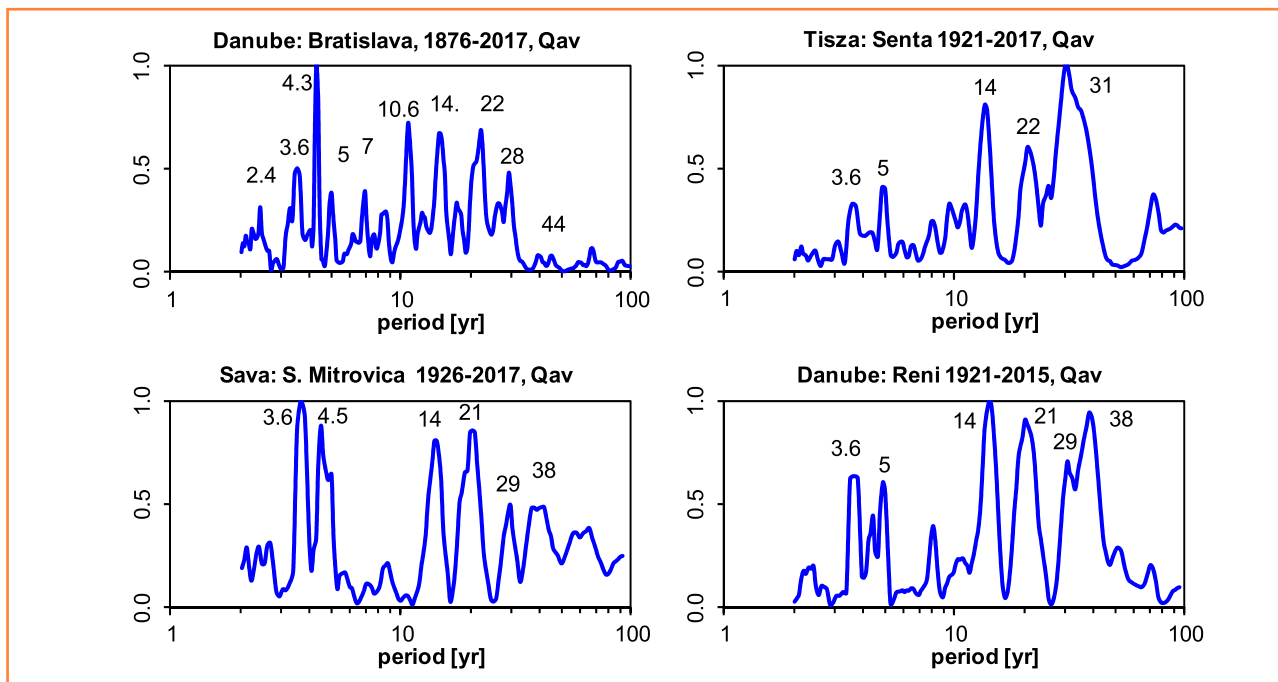
Figure 6　The combined periodograms of the average annual discharges of the selected stations

part of the study, we focused on a dry and wet multi-annual cycles identification in the annual discharge time series (Figure 4) for selected river stations.

The multi-annual cyclic component of the average annual discharges was identified by the auto-correlation analysis and also the spectral analysis. In the Figure 5, there are auto-correlograms of the average annual discharge (left), and the auto-correlograms of the 7-year moving average series of the annual discharge (right). The years of the most significant auto-correlations are marked by circles in the auto-correlogram plots. The negative dependency at minus 6 years is the most significant one. The positive dependency is at 21–22 years. It means that there exists app. 21–22 years cycle in the series.

Figure 6 depicts combined periodograms (Pekárová, Miklánek, Pekár, 2003) of average annual discharges. The spectral analysis confirmed that the occurrence of multi-annual cycles within dry and wet periods (in all basins) is of the following durations: 2.4; 3.6; 5–6; 7; 10–11; 14; 21–22; and 28–30 years.

The spectral and auto-correlation analyses show that the discharge series include cyclic components, which are to be removed from the time series before the analysis of the long-term trends is applied. The significant cycles are

3.6; 21–22 and 29 years. If we start to analyse the long-term trend during the wet period and finish during the dry period, we shall obtain a decreasing trend, of course. The long-term trend analysis has to start and finish in the same phase of the cycle.

Long-term trends identification of the runoff

In the previous part, we have shown that the annual discharge time series include cyclic components. This fact has to be included into the identification of the long-term trends.

With respect to the multiannual cycles of low and high discharges, we have to estimate the long-term trend of the Danube at Bratislava station:

1. from high discharge period to low period (e.g. since 1876 to 2018;
2. from low discharge period to low period (e.g. since 1881 to 2018; Table 2).

For cyclic functions, it is necessary to identify the trend in the whole cycles, starting at the minimum and ending at the minimum (or starting at the maximum and ending at the maximum), because data from an incomplete cycle can influence the trend.

Table 2　Results of annual discharge M-K trend tests for selected time periods, gauging station Danube: Bratislava
Equation of the lines: $f(\text{year}) = A(\text{year} - \text{first Data Year}) + B$

Time series	First year	Last year	n	Sen's slope estimate							
				test *Z*	signific.	*A*	*Amin 95*	*Amax 95*	*B*	*Bmin 95*	*Bmax 95*
Qa	1876	2018	143	-0.69	Non	-0.44	-1.75	0.85	2068	2145	1978
Qa	1882	2018	137	-0.10	Non	-0.06	-1.42	1.34	2033	2129	1927

** – level of significance α = 0.01; * – level of significance α = 0.05; +- level of significance α = 0.1, or Non – non significant trend; *A*min 95–95% confidence interval

Danube: Bratislava

Tisza: Senta

Sava: Sremska Mitrovica

Danube: Reni
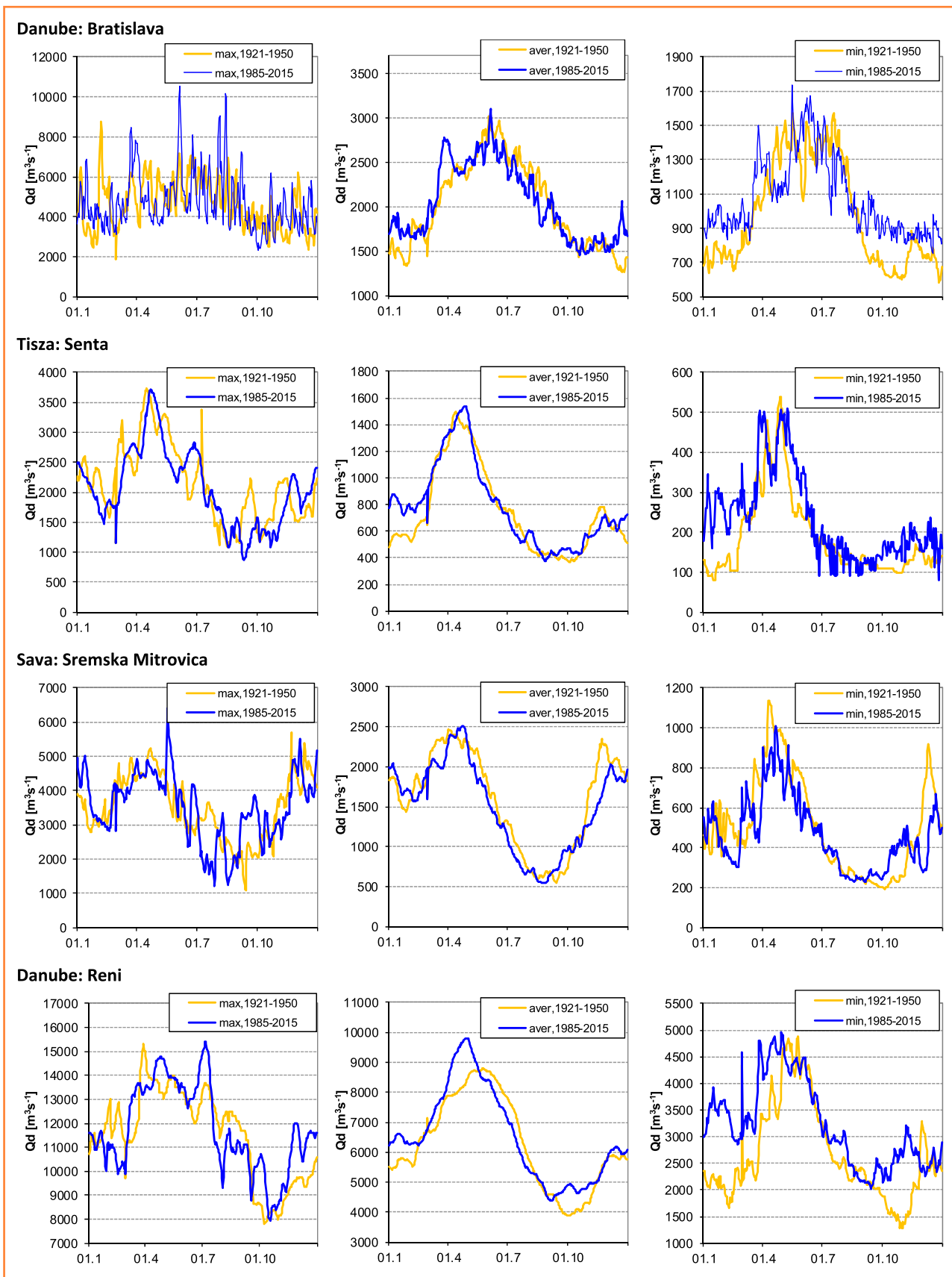
Figure 7 Comparison of the maximum (left), average (middle) and minimum (right) daily discharge regime in two different 30-year periods

Regime changes of the daily minimum, average and maximum discharge

In the last part, we focused on changes in the statistical characteristics of the minimum, average and maximum discharge of four studied rivers. In Figure 7, there are plotted the long-term daily discharges of the period 1921–1950 (yellow colour) and of the period 1985–2015 (blue colour).

We can observe an increase of discharge in the winter months in the case of the Danube in Bratislava and of the Tisza in Senta during the second period. The Danube in Reni has a higher discharge in winter-spring months, mainly in March.

Minimum long-term Danube discharges have increased, probably due to the reservoir construction and operation at the upper Danube in Germany and Austria.

Conclusions

The spectral and auto-correlation analyses show that the yearly discharge series include cyclic components, which are to be removed from the time series before the analysis of the long-term trends is applied. The significant cycles are 2.4; 3.6; 21–22 and 29 years. The length of the cycles of about 3.6 years, which was found in the flow rates, is probably related to the Southern Oscillation, expressed by the SO index. The length of cycles of about 2.47 years may be related to the QBO oscillation. The length of the cycles of about 14 years is related to the North Atlantic Oscillation, expressed by the NAO index. It follows that both the NAO and the SO phenomenon have an effect on the course of runoff fluctuations in the Danube basin.

If we start to analyse the long-term trend during the wet period and finish during the dry period, we shall obtain a decreasing trend, of course. The long-term trend analysis has to start and finish in the same phase of the cycle.

We used the statistical methods of the nonparametric Mann-Kendall test for testing the presence of the monotonic increasing or decreasing trend and the nonparametric Sen's method for estimating the slope of a linear trend.

The results show that the increasing/decreasing trends of the Danube, Sava and Tisza discharge are not significant yet. Changes can be observed in case of an increased minimum discharge at stations on the Danube River. A decrease did not occur as it could be expected due to higher air temperature and evapotranspiration.

These results have to be included into the long-term forecast of the runoff regime in the Danube River Basin.

Acknowledgements

References

Belz, J.-U., Goda, L., Buzás, Z., Domokos, M., Engel, H., Weber, J. (2004). *Flow regime of River Danube and its Catchment* (Follow-up volume no. VIII/2 to the Danube Monograph) (152 p.). Germany : Koblenz, Hungary: Baja.

Hurst, H.E. (1951). Long term storage capacity of reservoirs. *Trans. Am. Soc. Civ. Eng., 116*, 770–808.

Lin, Y., Lye, L. (1994). Modelling long-term dependence based on cumulative departures of annual flow series. *Journal of Hydrology*, *160*, 105–121.

Miklánek, P., Pekárová, P. (2016). *Danube River Basin*. Handbook of Applied Hydrology (2nd ed.) (5 p.). McGraw-Hill Education.

Pekárová, P., Miklánek, P., Pekár, J. (2003). Spatial and temporal runoff oscillation analysis of the main rivers of the world during the 19th–20th centuries. *Journal of Hydrology*, *274*, (1–4), 62–79.

Pekárová, P., Miklánek, P. (eds.). (2019). *Flood regime of rivers in the Danube River basin* (Follow-up volume no. IX to the Danube Monograph) (215 p. + 527 p. app.). Bratislava: IH SAS. DOI: https://doi.org/10.31577/2019.9788089139460

Prohaska, S., Isailović, D., SRNA, P., Marčetić, I. (1999). *Coincidence of flood flow of the Danube River and its tributaries* (Follow-up volume No. IV to the Danube Monograph). VÚVH, Bratislava, 187 pp. ISBN 80-968282-3-1.

Prohaska, S., Ilić, A. (2010). Coincidence of Flood Flow of the Danube River and Its Tributaries. In Mitja Brilly (Ed.). *Hydrological Processes of the Danube River Basin – Perspectives from the Danubian Countries*. Book Chapter 6. Springer (pp. 175–226). Doi: 10.1007/978-90-481-3423-6_6

Stănescu, V. A., Ungureanu, V., Mătreață, M. (2004). *Regional analysis of annual peak discharges in the Danube Catchment* (Follow-up volume no. VII to the Danube Monograph) (64 p.). București: INMH.

ANALYSIS OF AIR TEMPERATURE AND PRECIPITATION IN NITRA, SLOVAKIA IN 2005–2019

Vladimír KIŠŠ[1]*, Peter ŠURDA[2]

[1]Slovak University of Agriculture in Nitra, Slovak Republic
[2]Slovak Academy of Science, Bratislava, Slovak Republic

High air temperatures and low amount of precipitation occur more and more frequently in Slovakia. The aim of this work is to evaluate the temperature conditions and total precipitation during the period 2005–2019 and to compare it with the 50-year climatic normal 1951–2000. Also, there was calculated the probability of summer days, tropical days, super-tropical days, frost days and ice days occurrence. Annual temperature is higher by 0.9 °C (1.1 °C during vegetation period) than normal. Rainfall, especially in the last 5 years, has a decreasing character (-75 mm.year^{-1}) with frequent fluctuations. New phenomena – super-tropical days has occurrence of up to 20% between July and August. This study provides information based on which adaptation measures to the climate change need to be taken.

Keywords: precipitation, air temperature, drought, probability of occurrence

The average temperature of the Earth's surface has increased by almost 0.9 °C since the beginning of the 20th century, whereas since 1951, it has warmed by 0.72 °C. The annual air temperature trend for the period 1960–2012 reached 0.2 °C per decade in south-eastern Europe and up to 0.4 °C in northern and north-eastern Europe. Precipitation in some parts of southern Europe dropped by 70 mm in a decade (Horák, 2017). Agroclimatic analyses of the last decades confirm the increasing impact of weather on various areas of human activity. There will be a change in temperature and humidity security, a change in phenological conditions, a change in agroclimatic production potential, etc. (Čimo et al., 2014). The occurrence of very hot days and the duration of very low rainfall events are projected to increase by the end of the 21st century. The predicted higher incidence of extreme weather events will have an increasing influence on agricultural productivity (Al Jbawi, 2020). Droughts can arise from a range of hydrometeorological processes that supress precipitation or limit surface water or groundwater availability, creating conditions that are significantly drier than normal or limiting moisture availability to a potentially damaging extent (WMO and GWP, 2016).

Material and method

The aim of the work is to evaluate the air temperature and precipitation conditions for the Nitra locality during period 2005–2019 and to compare it with the climatic normal in 1951–2000. Agrometeorological Station of the Department of Biometeorology and Hydrology is at an altitude of 172.6 m a.s.l. (18° 07' longitude and 48° 19' latitude). The climate area according to Konček (1955) is warm, very dry with mild winter (Bochníček, Hrušková, 2015).

For the evaluation there were used mean monthly temperatures, total monthly precipitation and comparison according to 50-year climate normal and calculation of the Standardized Precipitation Index (SPI) and probability of occurrence of the phenomenon.

The SPI measures precipitation anomalies at a given location, based on a comparison of the observed total precipitation amounts for an accumulation period of interest, with the long-term historic rainfall record for that period. The average SPI value for the study area and the specific reference period is zero, leading to a straightforward identification of wet (positive values) and dry (negative values) periods (Tigkas, Vangelis, Tsakiris, 2018). For SPI calculation there was used the software SPI Generator by the National Drought Mitigation Centre, University of Nebraska (NDMC, 2018).

The determination of the period with the onset of characteristic days (mean daily temperatures ≤0 °C, ≥5 °C, ≥10 °C and ≥15 °C) according to the formulas (Čimo et al., 2012):

• onset of temperatures (days):

$$r_v = R \frac{T_n - T_2}{T_1 - T_2} \qquad (1)$$

- termination of temperatures (days)

$$r_p = R\frac{T_1 - T_u}{T_1 - T_2} \qquad (2)$$

where:

T_n – onset temperature (°C)
T_u – termination temperature (°C)
T_1 – the nearest average monthly temperature above the onset or termination of temp. (°C)
T_2 – the nearest average monthly temperature below the onset or termination of temp. (°C)
R – the difference in days between the middle of the months with the average temperature T_2 and the average temperature T_1, can be expressed as an average number $R = 30$
r_v – difference in days between the middle of the month with temperature T_2 and the date of onset of temperature T_n
r_p – difference in days between the middle of the month with temperature T_2 and the date of termination of temperature T_u

The probability of occurrence of the phenomenon was calculated by the formula (SHMÚ, 2020):

$$p(A) = \frac{m}{n} \cdot 100 \quad (\%) \qquad (3)$$

where:

$p(A)$ – probability of the phenomenon
m – the total frequency of the observed event over a period
n – length of observation period in years

Results and discussion

The monthly mean temperature (Figure 1) in most cases exceeds the values of the climatic normal. Especially in 2007, the mean temperature reached 4.4 °C in January and 5.0 °C in February, which is by 5.8 °C and 4.5 °C higher than normal, respectively. Negative extremes are also seen in the observed period. In January 2017, the temperature reached -9.1 °C (7.7 °C below normal), and in May 2019, it reached 9.3 °C (5.9 °C below normal).

The monthly total precipitation (Figure 2) exceeded the values of the climatic normal in certain months. Extreme values occurred in 2010 (April – June), 2011 (July – September) and 2013 (January – March). A significant decrease is visible in 2015–2019, when from April to August there occur dry, very dry and extremely dry months. The lack of precipitation was not compensated by extremely wet months (February, July 2016; September 2017; May 2019).

Monthly values should follow the trend of the long-term climate normal. This is the case in monthly temperatures, except in the winter months, where fluctuations are visible. Precipitation in recent years has shown a frequent occurrence of extremely wet and extremely dry months compared to normal.

The annual total precipitation (Figure 3), in 2010 reached 869 mm (321 mm more than the normal – very wet year). In the vegetation period (VP) precipitation reached by 322 mm more. Extremely wet were the months April, May and June. The year 2011 was also extreme – the total rainfall was by 198 mm more than the normal (extremely wet July, August and September). In recent years, however, the opposite trend is observed with a lack of precipitation. The biggest decline is in 2018 – the total amount was by 180 mm less than the normal (July and August – extremely dry, April, October and November – very dry, and May and June – dry). Over the past 5 years, rainfall decreased by an average of 75 mm.year^{-1} and by 62 mm per VP^{-1} compared to the normal.

We used the values of 3-month and 12-month SPI for the period 2005–2019. The SPI time scales between 3 and 6 months may be relevant for agricultural users. Hydrologists may be more interested in values between 12 and 24 months (Portela et al., 2015; Wu et al., 2005; Tigkas, Vangelis, Tsakiris, 2018). SPI-3 (Figure 4) shows the alternation of dry and wet periods. Extremely humid months occurred in 2010, 2011 and 2013. Nowadays, there are more frequent occurrences of dry months. SPI-12 (Figure 5) shows this trend when very dry and extremely dry periods have been observed in the last 5 years.
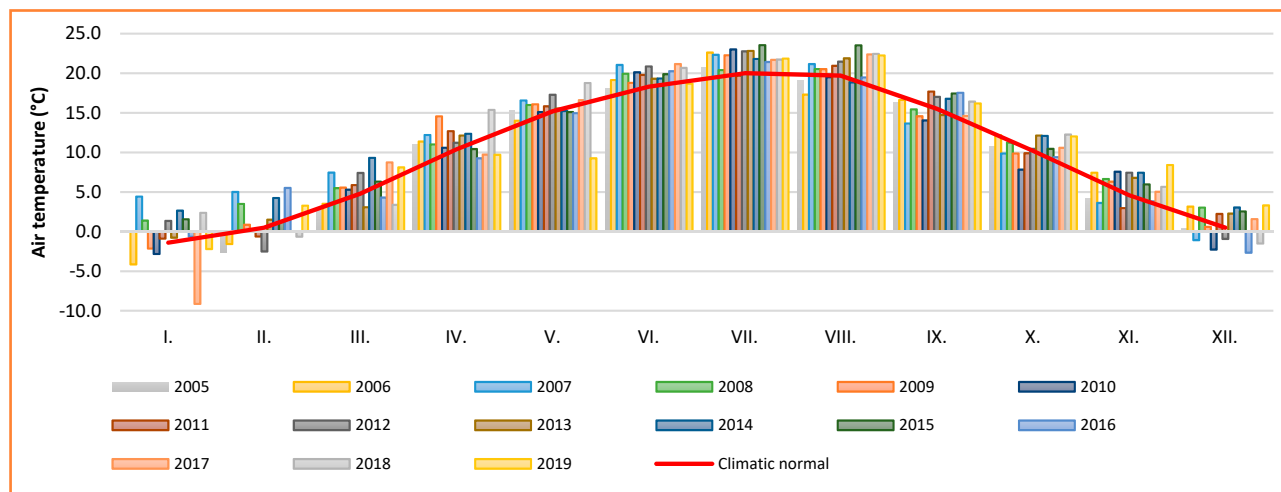
Figure 1 Mean monthly temperatures (2005–2019) compared to the climatic normal 1951–2000
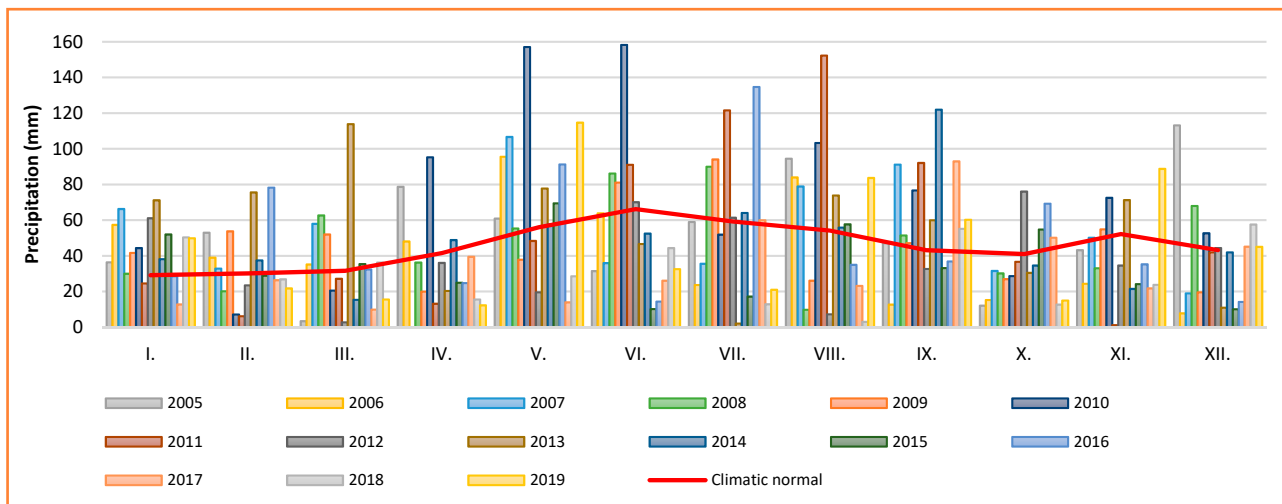
Figure 2   Total monthly precipitation (2005–2019) compared to the climatic normal (1951–2000)
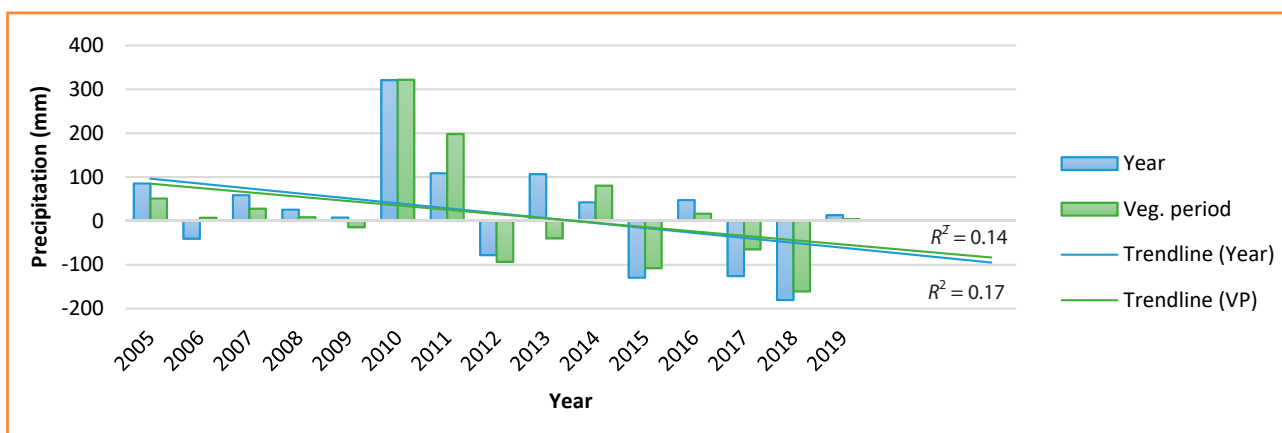
Figure 3   Evaluation of precipitation in 2005–2019 compared to the climatic normal 1951–2000
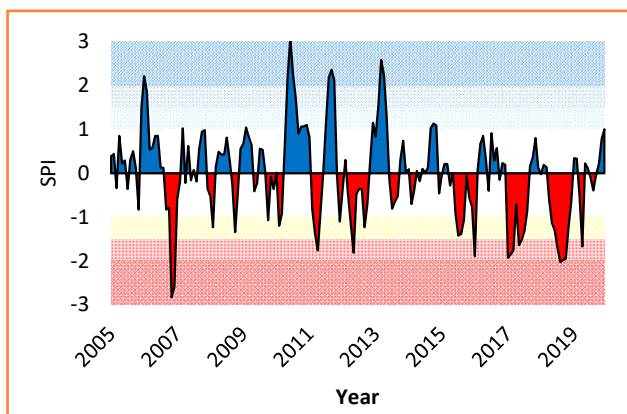
Figure 4   SPI-3 in 2005–2019
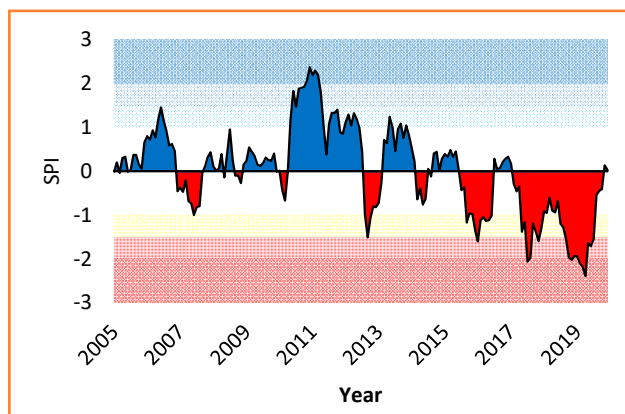
Figure 5   SPI-12 in 2005–2019

Figure 6 shows the probability of occurrence of atmospheric precipitation ≥0.1 mm and ≥10 mm during the year for the reference period from 2005 to 2019. On average, the annual probability is 40% and 4% respectively. During the growing season, this represents 37% and 6%, respectively.

The evaluation of mean temperatures (annual and VP) in comparison with the normal showed an increase in annual temperatures (Figure 7). The warmest year was 2014, when the mean temperature reached 11.9 °C (2.0 °C higher than the normal). The highest temperature during the VP was reached in 2018, when it exceeded the normal by 2.7 °C (April and May – extremely warm, June and August – very warm, and July and October – warm). However, 2019 is different during the VP, which caused cold weather in April and May (temperature was 9.7 °C and 9.3 °C, respectively). During the study period (2005–2019), there is an increase in the mean annual air temperature by 0.9 °C and in the growing season by 1.1 °C.

We calculated the probability of occurrence of characteristic days of the summer period (Figure 8) – summer days (T_{max} ≥25 °C), tropical days (T_{max} ≥30 °C) and super-tropical days (T_{max} ≥35 °C). Based on the reference period 2005–2019, the probability of occurrence of summer days from the beginning of June to the end of August is 60–80%, on some days up to 93%. The highest occurrence of tropical days (60%) is between July and August. In this time there also occur super-tropical days with the probability of up to 20%.

We also determined the probability of occurrence of frost days with Tmin <0 °C (Figure 9), which is above 40% and lasts from the end of November to the middle of March, except on 23.12., when it falls to 33%. Ice days with T_{max} <0 °C follow the trend of frost days, but their probability of occurrence from November 15 to March 15 is on average 17%. The highest probability of occurrence of a frost day (100%) and an ice day (53%) is on January 25.

The calculation of the onset, duration and termination of certain temperatures is related to physiological and biological processes. The onset and termination of T ≥5.0 °C limits the great vegetation period (GVP) – this temperature activates the physiological processes in the organs in the spring and ends in the autumn. The onset and termination of T ≥10.0 °C delimits the main vegetation period (MVP) and the onset and termination of T ≥15.0 °C delimits the vegetation summer (VS) (Čimo et al., 2012). During the years 2005–2019, the number of days of individual periods (GVP, MVP, VS) in comparison with the period 1951–2000 increased by 15 days (T ≥5 °C), by 9 days (T ≥10 °C) and by 6 days (T ≥15 °C) (Figure 10). These changes also affected the dates of onset and end of individual phenophases. The great vegetation
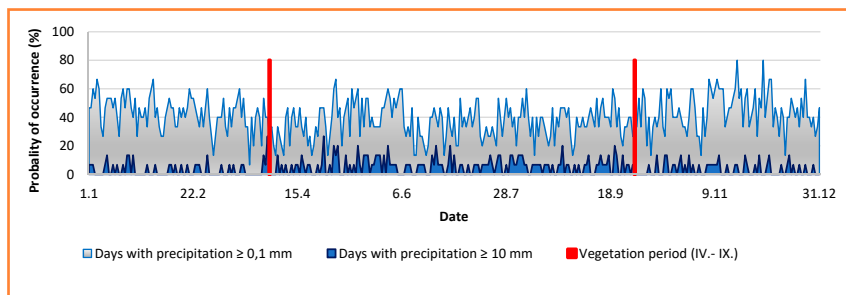
Figure 6   Probability of occurrence the precipitation during year
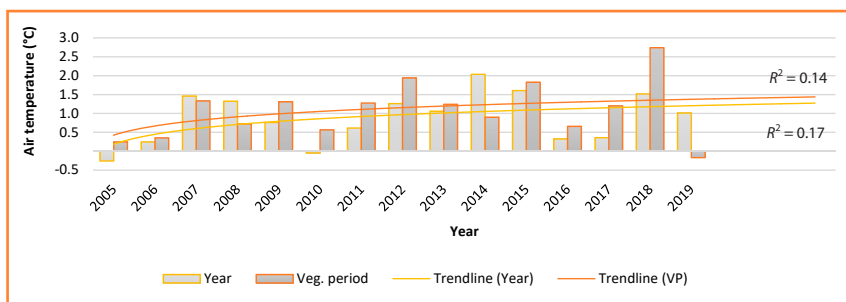
Figure 7   Evaluation of air temperature in 2005–2019 compared to climatic normal
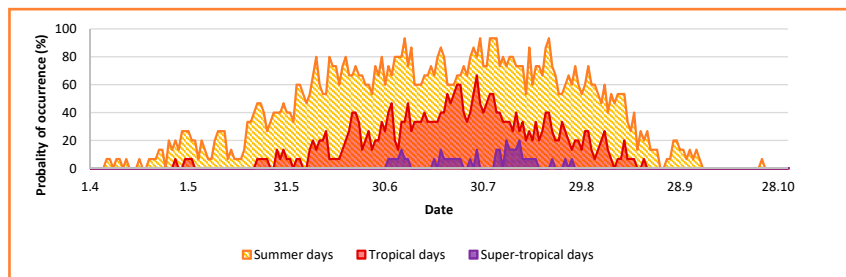
Figure 8   Probability of occurrence of summer days, tropical days and super-tropical days
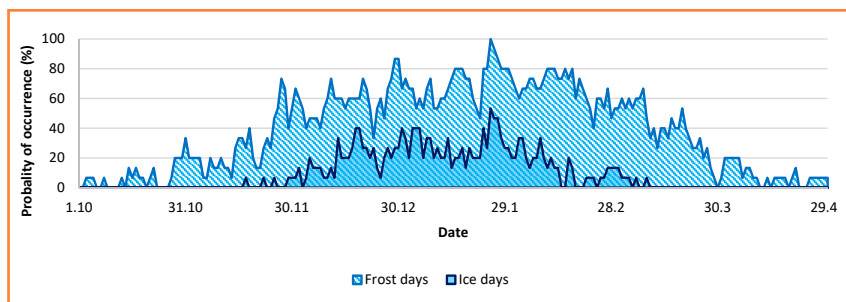
Figure 9   Probability of occurrence of frost days and ice days
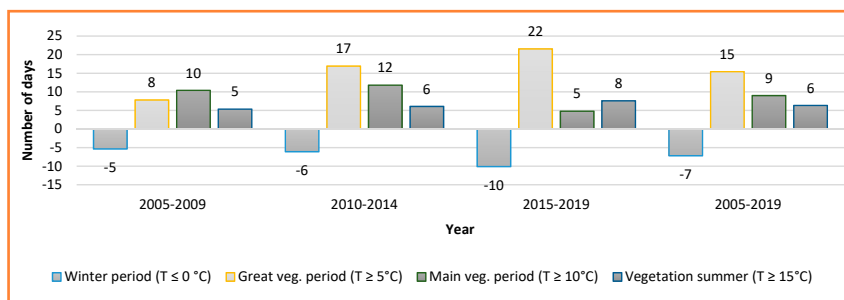
Figure 10 Evaluation of the number of days with temperature $T \leq 0$ °C, $T \geq 5$ °C, $T \geq 10$ °C and $T \geq 15$ °C compared to the climatic normal

period compared to the period 1951–2000 (March 17 – November 13) has a postponed date from March 9 to November 20, the main growing season April 8 – October 21 (normal April 13 – October 17) and vegetation summer May 10 – September 21 (normal May 13 – September 19). The opposite phenomena is the number of days with $T \leq 0$ °C, which decreased on average by 7 days.

Nowadays, scientific papers are focused on researching the impact of the climate change. Changes in the number of days with the occurrence of characteristic temperatures (Čimo, Malenčíkova and Szomorová, 2015), extreme precipitation values (Repel et al., 2020), alternating wet and dry extremities (Zeleňáková et al., 2018) as well as analysis of long-term air temperatures and precipitation (Faško, Lapin and Pecho, 2008; Labudová, Faško and Ivaňáková, 2015; Hlavatá, Tomková, 2015) confirm the change in climatic conditions in Slovakia, which we claim in this study. In this study we focused on the period 2005–2019, which can be the base for future prediction of temperature in agricultural areas in Slovakia.

Conclusion

The aim of this work was to evaluate the air temperature and precipitation conditions in the locality of Nitra, Slovakia for the period 2005–2019. The measured data show an increased mean monthly and annual temperatures. Also, the temperature during the VP is higher by 1.1 °C compared to the normal. Summer, tropical and subtropical days occur in late July and early August. The probability of their occurrence is up to 80% (SD), 60% (TD) and up to 20% (STD). The total precipitation is uneven

and alternates extremely humid months with extremely dry ones. In the last 5 years, the total precipitation has decreased by an average of 75 mm compared to the long-term normal. This review study provides information, which can be the base for prediction and with additional information (relative humidity, wind direction, soil moisture, etc.) can help agronomists to prepare for the ongoing climate change in Slovakia.

References

Al Jbawi, E. (2020). Effect of Climate Change on Agriculture. *International Journal of Environment*, *9*(1).

Bochníček, O., Hrušková, K. (2015). *Climate atlas of Slovakia*. Bratislava: Slovenský hydrometeorologický ústav (in Slovak),.

Čimo, J., Malenčíková, T., Szomorová, L. (2015). *Agroclimatic indicators review in Danubian lowland for period 1961–2000* (1st ed.). SGEM (pp. 433–440).

Čimo, J., Špánik, F., Antal, J., Tomlain, J. (2014). *Biometeorológia*. Nitra: SPU.

Čimo, J., Špánik, F., Šiška, B., Tomlain, J., Horák, J. (2012). *Praktická biometeorológia*. Nitra: SPU.

Faško, P., Lapin, M., Pecho, J. (2008). 20-year extraordinary climatic period in Slovakia. *Meteorologický časopis*, *11*, 99–105.

Hlavatá, H., Tomková, M. (2015). Analýza vývoja teploty vzduchu na stanici Michalovce v zimnom období počas rokov 1961 – 2014. *Acta Hydrologica Slovaca*, *16*(2), 153–158.

Horák, J. (2017). *Klimatológia (*1st ed.). Nitra: SPU (219 p.).

Konček, M. (1955). Index zavlaženia. *Meteorologické zprávy*, *8*(4), 96–99.

Labudová, L., Faško, P., Ivaňáková, G. (2015). Changes in climate and changing climate regions in Slovakia. *Moravian Geographical Reports, 23*(3). DOI: 10.1515/mgr-2015-0019.

National Drought Mitigation Center (NDMC). (2018). *SPI Program* [online] [cit.

2020-04-23]   https://drought.unl.edu/droughtmonitoring/SPI/SPIProgram.aspx

Portela, M. M., Zelenáková, M., Santos, J. F., Purcz, P., Silva, A. T., Hlavatá, H. (2015). Drought analysis in Slovakia: regionalization, frequency analysis and precipitation thresholds. *WIT Transactions on Ecology and The Environment*, *197*. DOI:10.2495/RM150211.

Repel, A., Zelenáková, M., Vranayová, Z., Kanaliková, A., Hlavatá, H. (2020). Analysis of trends in precipitation time series in selected precipitation stations in eastern Slovakia. In *IOP Conf. Series: Earth and Environmental Science*, *444,* 012048. DOI:10.1088/1755-1315/444/1/012048.

Slovenský Hydrometeorologický Ústav (SHMÚ). (2020). *Klimatická zabezpečenosť* [online], [cit. 2020-04-03]. Available at: http://www.shmu.sk/sk/?page =1072

Tigkas, D., Vangelis, H., Tsakiris, G. (2018). Drought characterisation based on an agriculture-oriented standardised precipitation index. *Theoretical and Applied Climatology*, (135), 1435–1447. DOI /10.1007/s00704-018-2451-3.

World Meteorological Organization (WMO) and Global Water Partnership (GWP). (2016). Handbook of Drought Indicators and Indices. In Svoboda, M., Fuchs, B.A. *Integrated Drought Management Programme (IDMP), Integrated Drought Management Tools and Guidelines, Series 2*. Geneva.

Wu, H., Hayes, M. J., Wilhite, D. A., Svoboda, M. (2005). The Effect of the Length of Record on the Standardized precipitation Index Calculation. *International Journal of Climatology*, (25), 505–520. DOI: 10.1002/joc.1142.

Zeleňáková, M., Purcz, P., Blišťan, P., Vranayová, Z., Hlavatá, H., Diaconu, D. C., Portela, M. M. (2018). Trends in Precipitation and Temperatures in Eastern Slovakia (1962–2014). *Water*, *10*, 727. DOI:10.3390/w10060727.

CLIMATE CHANGE AND ITS IMPACT ON AGRICULTURE

Adrián VARGA

Institute of Hydrology SAS, Bratislava, Slovak Republic

We live in the times of climate change when global temperatures are constantly rising. The impacts of climate change will also be felt in agriculture in Slovakia: increased productivity and yields in colder areas, reduced production in warmer areas due to temperature stress, risk of erosion as a result of more extreme weather conditions (stronger winds, more intense precipitation), the occurrence of new pests etc. Hence, we should be prepared for adaptation measures that would help mitigate it. The aim of this paper is to present the impacts of climate change on agriculture and land, and to offer adaptation measures, and show the prognosis of the climate indicator *Ts* >10 °C from now until 2100.

Keywords: climate change, impacts, adaptation, *Ts* >10 °C

Climate is, in simplified terms, a characteristic weather regime in a given area. For several meteorological elements (temperature, atmospheric precipitation, air pressure, air flow, wind direction and speed, snow cover, etc.), their statistical characteristics are evaluated (averages, extreme temperatures, daily and annual runs, variability, number of days, etc.) over a longer period, usually at least 30 years. Climate variability, i.e. long-term characteristics, is important just as weather variability (Metelka and Tolasz, 2009).

Climate change – this term has been used in the past for all climate-related changes , currently according to the UN

Intergovernmental Panel on Climate Change (IPCC, 1996), this is only a natural climate change, so it comprises altered solar activity and other astronomical factors, volcanic eruptions, changes in ocean circulation, etc. Climate change is only the part of all climate change caused by men by changing the greenhouse effect of the atmosphere (emissions of greenhouse gases and aerosols, changes in land use) (Lapin, 2014).

In recent years, our farmers have also been bothered by weather fluctuations during the growing season, heavy torrential rains, storms, and hail, or, conversely, the lack of rainfall, which reduces yields per hectare and the quality of crops. We know that climate change can have a major impact on human life, so it is particularly important to know its likely effect in terms of both quality and quantity. The subject of research is mainly climate change, i.e. only the part of all climate change that was conditioned by man's activities. Climate change, which is also expected to change the current nature of the flow in the atmosphere over the area, may significantly affect the typical nature of climatic conditions in our territory and subsequently significantly affect the agricultural sector. It was found that the onset of the growing season is accelerating, and the end is delayed compared to the last assessed climate standard 1961–1990 (Polák, 2018).

Material and method

Climate change scenarios

Although we know that global warming is happening today and is already affecting human society, its greatest consequences are in the future. Climate change is driven by several societal factors in the coming decades and centuries. The future development of most of these factors is deeply uncertain and will be influenced by our actions. It is therefore useless to ask, "What will happen?" and try to predict further climate change. The future, while inherently uncertain, is not entirely unknowable. Scenarios can be used to examine "What can happen?" and even "What should happen?", given the fact that we have been shaping our future. It is not about predicting the future, but about projecting what can happen by creating credible, coherent, and internally consistent descriptions of possible future climate change (Kriegler et al., 2020).

In general, seven different types of scenarios can be identified (Kriegler et al., 2020):

- Socio-economic scenarios that describe the development of social factors of human intervention in the climate system. Climate change and socio-economic development are deeply linked. Social and economic activities are major drivers of climate change. Climate change will have a serious impact on these activities, for example, by rising sea levels and exposing them to adverse weather events.
- Emission, concentration and climate scenarios resulting from these developments.
- Climate change scenarios resulting from human impact on the climate
- Climate impact scenarios due to these climate changes.

Contact address: Adrián Varga, Institute of Hydrology SAS, Dúbravská cesta č. 9, 841 04 Bratislava, Slovak Republic; e-mail: varga@uh.savba.sk
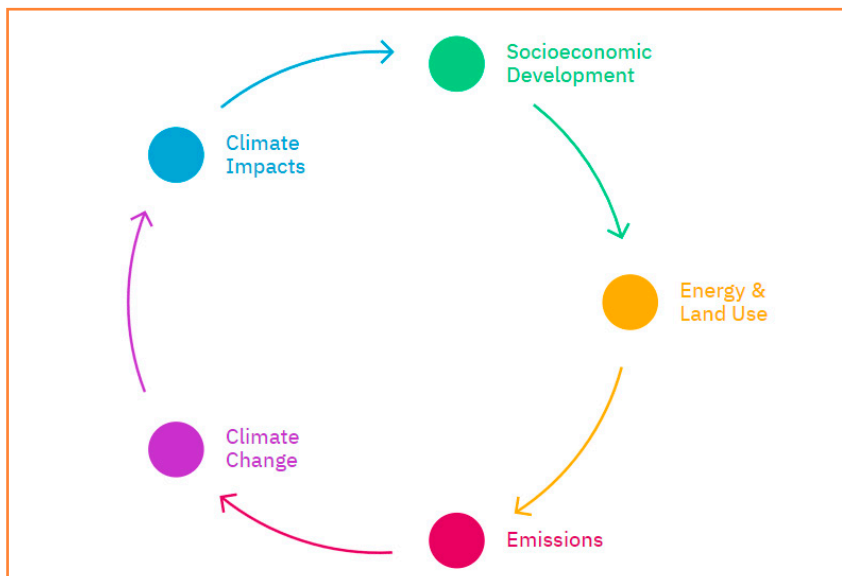
Figure 1 Mutual socio-economic and climate relations
Source: Kriegler et al., 2020

Figure 2 Greenhouse gases emissions projection by WOM, WEM and WAM scenarios
Source: Enviroportal, 2016

Figure 3 Global warming scenarios based on commitments and current policy
Source: Climateactiontracker.org, 2020

• Mitigating scenarios that limit man-made climate change.
• Adaptation scenarios that limit the impact of climate change on societies.
• Integrated scenarios that capture some of the above components of future climate change.

Take a closer look at the Figure 1. to understand the underlying relationships. Since it is us, humans, who drive climate change, we can also act to reduce the impact of our activities on the climate (mitigation) as well as the impact of climate change on us (adaptation) (Kriegler et al., 2020).

Greenhouse gases emissions projection in Slovakia

Emission projections were prepared based on the 2014 emission inventory, in three scenarios: a no-action scenario (WOM), an existing measures scenario (WEM) and an added measures scenario (WAM) (Figure 2). The effect of the monitored measures is manifested mainly until 2020, measures of a medium-term nature until 2030 are poorly quantified, which is also reflected in the results until 2030 (Enviroportal.sk, 2016).

In the absence of policies (Figure 3), global warming is expected to reach 4.1 °C to 4.8 °C by the end of the century. The emissions that cause this warming are often called baseline scenarios, in the A scenario of "optimistic policies", that considers other as well as planned but not yet implemented policies and the continuation of recent developments. Given the optimistic assumption that governments will continue to meet these expectations, the average warming estimate is 2.8 °C or likely below 3.0 °C. Scenario in line with current policy is 2.8 to 3.2 °C. Scenario in line with targets and commitments is 2.5 to 2.8 °C Consistent scenarios for rapid reduction of global CO_2 emissions, estimated warming from 1,3 °C to 2 °C by 2100 (Climateactiontracker.org, 2020).
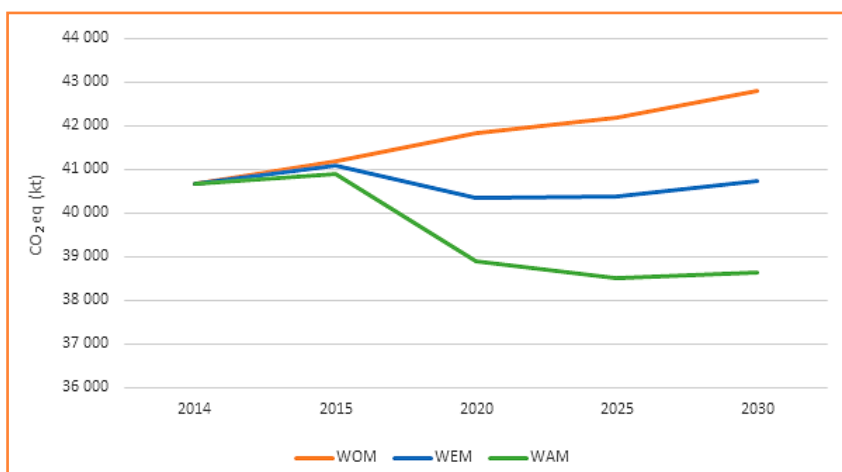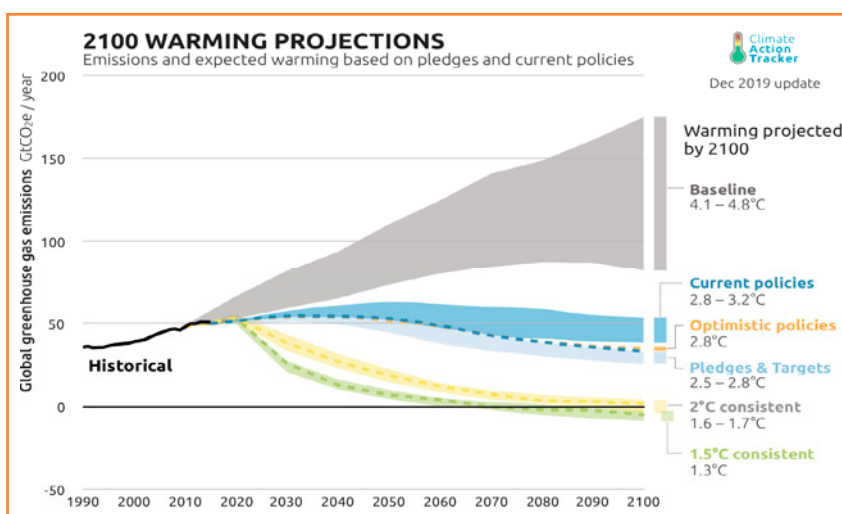
Greenhouse gases emissions

A. CO_2 – *Carbon dioxide*

Carbon dioxide (CO_2) is a colourless, tasteless, and odourless gas that is a common part of the Earth's atmosphere (0.04%). The most

important anthropogenic sources of carbon include any combustion of carbonaceous substances (from transport, industry, to domestic heating) and its leakage from the products in which it is contained. In the atmosphere, carbon dioxide absorbs infrared radiation and thus contributes to the so-called Greenhouse effect. Normal concentrations of carbon

dioxide are harmless, short-term exposure to higher doses can cause headaches, dizziness, breathing difficulties, tremors, confusion, and ringing in the ears. Higher exposure can then cause convulsions, coma, and death (Kleger, Válek, 2014).

CO_2 emissions for Slovakia (Figure 4) and major economies emissions (Figure 6).

Greenhouse gas emissions from agriculture have seen a declining trend since 1990, mainly due to a reduction in the number of livestock and the amount of industrial fertilizers used (Figure 5) (Enviroportal.sk, 2020).

B. Nitrous oxide (N_2O)

It is the third most important greenhouse gas according to the Kyoto Protocol. It is characterized by the production and use of mineral fertilizers, in the chemical industry, in agriculture, etc. It represents about 6% of global warming (Luna-anapa.ru, 2019).

The main source of nitrous oxide (N_2O) is crop production – excess mineral nitrogen in the soil (due to intensive fertilization) and the unfavourable air regime of soils (soil compaction). The production of nitrous oxide from agriculture has had a fluctuating course after 2005 (Figure 7). In 2017, 4.66 Gg of nitrous oxide was produced from agriculture (Enviroportal.sk, 2020).

C. CH_4 – methane

Of all the greenhouse gases, methane is one of the most efficient due to its ability to efficiently absorb heat in the Earth's atmosphere. Studies have shown that over a 20-year period, a kilogram of methane heats the planet up to 80 times more than a kilogram of carbon dioxide. Methane lasts for about ten years in the Earth's atmosphere until it begins to react with free radicals called hydroxyl and is converted to carbon dioxide. Therefore, most of the methane time in the atmosphere is spent as a molecule of CO_2. Methane is released much less into the air than carbon dioxide. Nevertheless, methane has lasting consequences. For example, one of these effects is a phenomenon called thermal expansion. Greenhouse gases such as methane heat the atmosphere and up to 90% of this excess heat is absorbed by the oceans. This heat causes the volume of seawater to expand. This effect, together with the melting of glaciers, causes an increase in sea levels (Leman, 2020).

The largest producers of methane (CH_4) include animal production-large cattle and pig farms. CH_4 is formed as a direct product of metabolism in herbivores (enteric fermentation) and
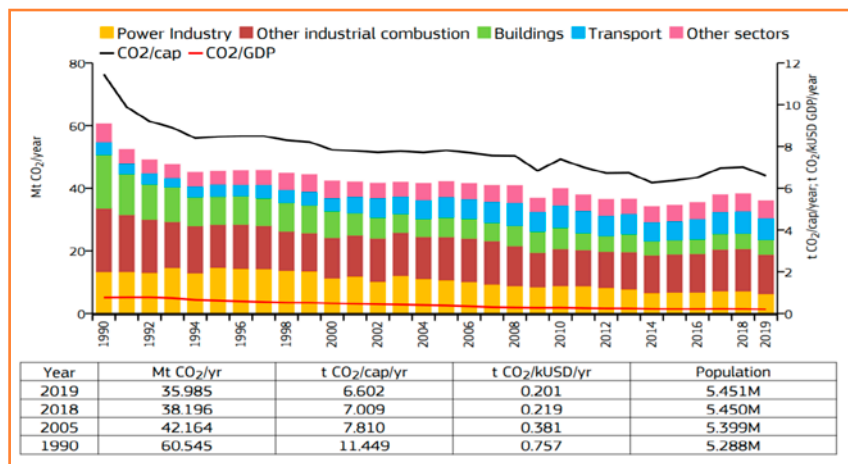
Figure 4 CO_2 emissions by sector for Slovakia
Source: Crippa et al., 2020
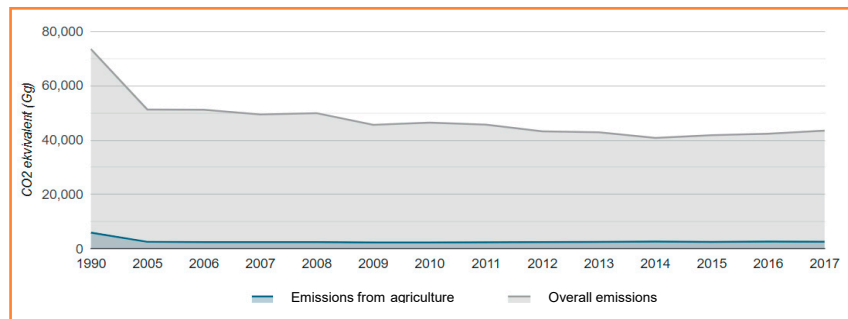
Figure 5 CO_2 emissions from agriculture and overall emissions in Slovakia
Source: Enviroportal.sk, 2020
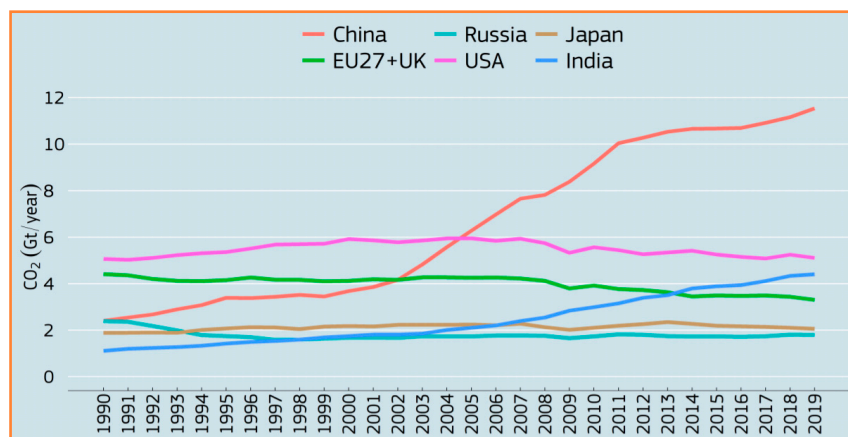
Figure 6 Fossil CO_2 emissions of the major emitting economies
Source: Crippa et al., 2020
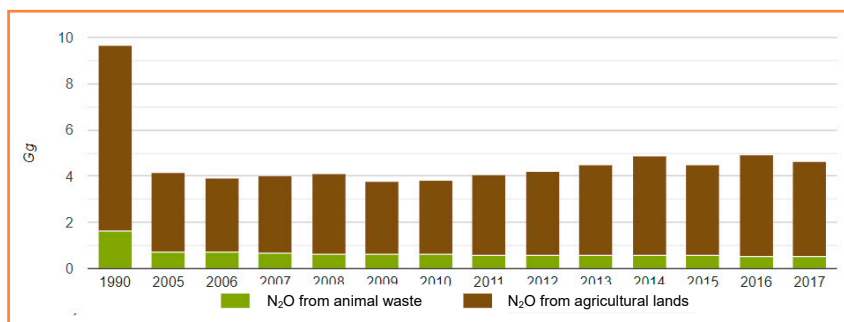
Figure 7　Nitrous oxide emissions agriculture in Slovakia
Source: Enviroportal.sk, 2020
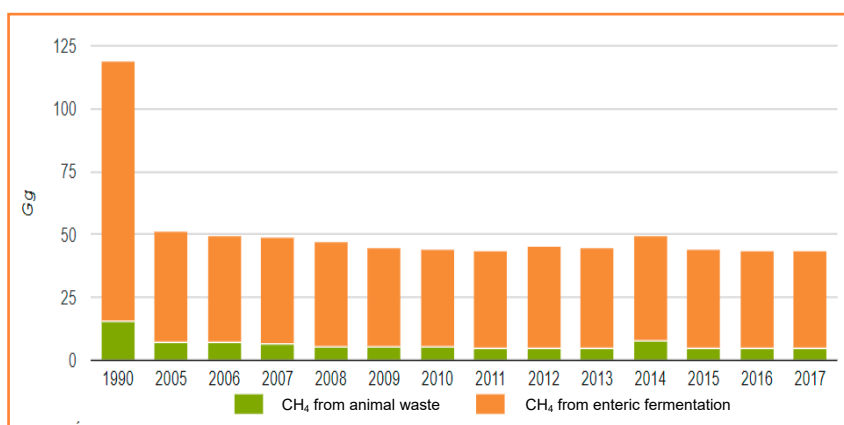
Figure 8　Methane emissions from agriculture in Slovakia
Source: Enviroportal.sk, 2020

as a product of degradation of animal excrement. The share of agriculture in total methane production has been mostly decreasing since 2005 (Figure 8). In 2017, 43.44 Gg (gigagram) of methane was produced from agriculture (Enviroportal.sk, 2020).

Climate change impacts

Climate change, in which the change in the current nature of the current in the atmosphere over a given area is to change, may also have a more significant effect on the typical nature of climatic conditions in our territory and consequently, significantly affect the agricultural sector. It was found that the onset of the growing season is accelerating and ends late compared to the last evaluated climatic standards 1961–1990. Long growing seasons significantly affect the possibilities of agriculture in growing more thermophilic crops, they also affect the total amount (input) of photosynthetically active radiation. It was found that in the case of climate conditions at $2 \times CO_2$ during the large growing season (VVO) in the Danube lowlands, VVO (with

daily average air temperatures of 5 °C and more) can persist throughout the winter, which may adversely affect the overwintering of some fruit trees. At the same time, the projected warming is expected to significantly affect the regions of current agricultural production and the zoning of the distribution of field and garden crops. It is expected that the cultivation of more temperature-intensive crops will shift from today's conditions of the Danube and East Slovak lowlands to the locations of the Liptov and Turiec basins. In recent years, heat waves, i.e. periods with extremely warm weather, often accompanied by high humidity, have become more frequent in our country. They last longer than e.g. in the 80s of the last century. Surely you have also registered episodes of very warm weather in the winter months, e.g. February 2016, when we had daily temperatures of up to 20 °C. Of course, if after such a heat the flow of cold air comes to us, the fruit trees are very sensitive and the frost "harvests" the crop at the beginning. This happened both in 2016 and in 2017. In the summer, there are more

frequent torrential rains and storms with intense hail in our territory, which can also damage the crops. Drought is becoming a big problem. The long rainless periods in our territory deplete the vegetation, but also the soil. Therefore, water needs to be brought to plants and their proper growth and development ensured, including by restoring irrigation systems in our fields, or focusing on growing plants that can withstand the stress of water scarcity more. Climate change can affect all spheres of society. Therefore, as stated in the final report on the Consequences of Climate Change and possible adaptation measures in individual sectors, it is necessary for society to prepare for the consequences of climate change not only in agriculture and forestry, and water management, but also in energy, transport, finance or health care as soon as possible (Polák, 2018).

Adaptation measures

Adaptation measures in plant production

The issue of coping with the consequences of climate change is one of the most serious global problems today. This is an issue that is not short-term or easy to solve. It requires the cooperation of experts from many scientific disciplines and sufficient funding. From a factual point of view, it will generally be primarily the solution and implementation of projects in agriculture aimed at (Takáč, Zuzula, 2000):

1. application of protective and conservation technologies of tillage,
2. changes in crop technology,
3. changes in agroclimatic zoning and structure of cultivated crops and varieties,
4. changes in breeding programs,
5. changes in integrated crop protection,
6. changes in the regulation of the soil water regime,
7. changes in plant nutrition,
8. reduction of greenhouse gas emissions, processing of excrement and waste in animal production,
9. changes in the management of agricultural production,
10. revitalization of existing and construction of new irrigation facilities.

Change of cultivated crops

Such a radical step will be possible in regions with higher altitudes, where thermal comfort is increased by growing crops, which are today different from the warmest regions of Slovakia. There is also a need to redesign crop technologies with an emphasis on sustainable farming systems, so that the natural fertility of the soil is maintained without degrading the environment (Takáč, Zuzula, 2000).

Crop variety change

Cultivated varieties should be adaptable to biotic and abiotic stresses. They should be less sensitive to temperature extremes, drought, and disease. The choice of a suitable variety will have to consider changing wintering conditions as well as ripening conditions. Better use of radiation power during the growing season can also be achieved by selecting varieties with a longer growing season (Takáč, Zuzula, 2000).

Shift of the seeding date

The onset of spring is likely to be very rapid compared to today's conditions. Maintaining current sowing dates could carry the risk of high temperatures during sensitive phenophases. The postponement of the sowing date to an earlier date is associated with the risk of reduced radiation energy input (Takáč, Zuzula, 2000).

Irrigation systems

The expected changes in the hydrological balance and in the hydrological cycle will result in an increased irrigation need. Supplemental irrigation is considered to be an effective way to alleviate or eliminate water stress of crops, and is still a necessary condition for optimizing the water regime of the soil for the needs of agricultural production in the southern regions of Slovakia (Takáč, Zuzula, 2000).

Soil adaptation measures

It is desirable to reduce interventions in the soil and optimize the dates of application of individual operations. To increase the content of soil organic matter, the effect of organic fertilization and incorporation of plant residues is considered to be a positive effect. It is recommended to increase the share of fodder on arable land and cover the vegetation in the winter months, which is an effective measure against erosion. Other protection measures include ploughing protection systems and crop rotation (Takáč, Zuzula, 2000).

Methodology

Data from meteorological stations were processed in spreadsheet software, the prognosis was calculated using the trend curve from previous known data (Figure 9). The formula used for calculation of the prognosis data:

$$f(x) = 11.6912779974x + 2{,}715.9628282828$$

Substitute column number for x. (1)

From these values, map outputs were created using the interpolation method Kriging (raster pixel resolution 50) in ArcGIS software. Theoretical knowledge was obtained by researching available resources.

Results and discussion

Data overview is based on the existing measurements (1970, 2000) and prognosis (2050, 2100) of the used meteorological stations (Table 1). The calculation method is specified in the methodology.
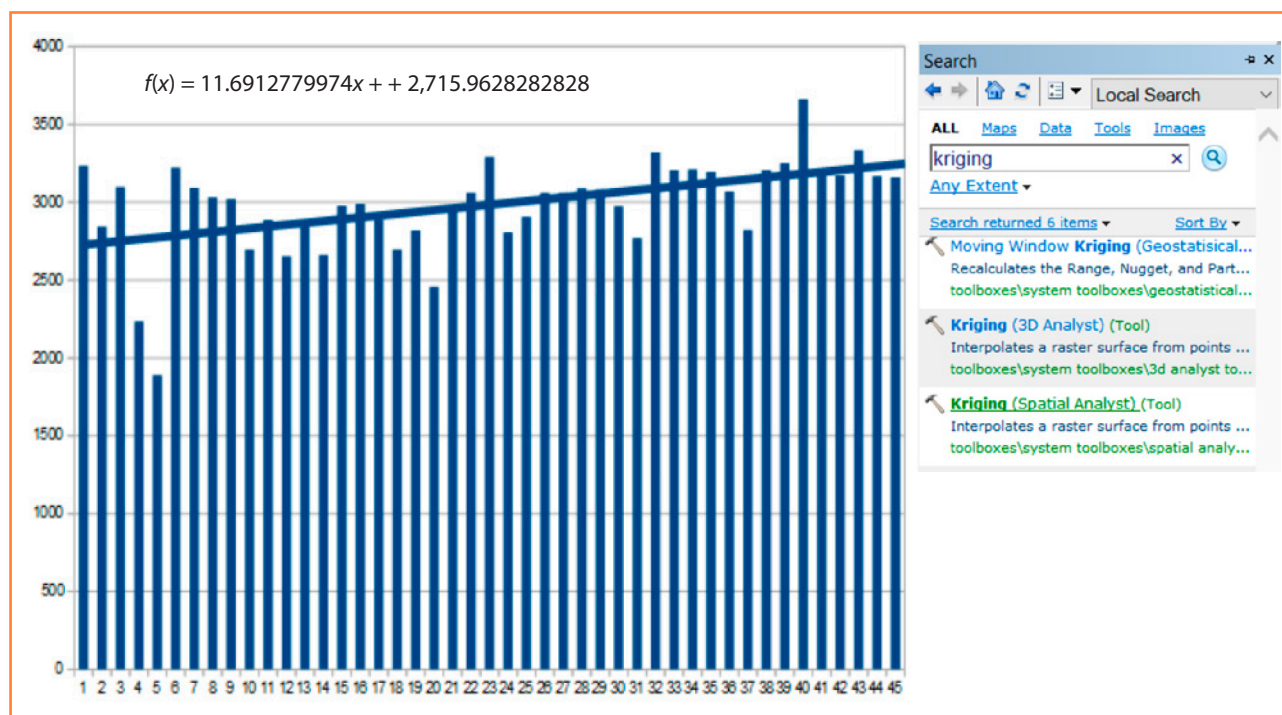
Figure 9   Prognosis metodology for Ts >10 °C
                 Source: Author

Table 1   *Ts* >10 °C sum values of used meteorological stations in Slovakia

↓ station/year →	1970	2000	2050	2100
Holíč	2,695.8	3,662.7	3,768.2	4,352.7
Kuchyňa, air base Malacky	2,706.4	3,640.4	3,571.1	3,989.2
Biskupice, at the airport Trenčín	2,564.5	3,554.7	3,360.0	3,701.1
Malacky	2,819.0	3,704.6	3,616.5	4,013.0
Senica	2,610.4	3,589.1	3,439.3	3,807.2
Myjava	2,319.6	3,239.9	3,322.2	3,880.0
Bratislava, Karlova Ves	2,848.5	3,711.9	3,621.9	4,018.2
Jurske jazero, Borinka pri BA	2,169.9	3,076.0	2,963.5	3,336.4
Bratislava, Koliba	2,646.9	3,564.0	3,512.8	3,934.6
Pezinok	2,887.6	3,722.4	3,631.4	4,021.9
Bratislava, airport	2,934.4	3,352.3	3,653.9	4,041.9
Kráľová pri Senci	2,925.4	3,785.1	3,622.5	3,981.5
Gabčíkovo	2,930.8	3,391.4	3,528.3	3,820.3
Jaslovské Bohunice, nuclear powerplant	2,680.8	3,599.7	3,430.4	3,758.9
Žihárec	2,906.5	3,366.5	3,531.4	3,837.6
Piešťany, airport	2,679.0	3,231.9	3,371.0	3,669.1
Trenčianske Teplice	2,397.2	3,359.2	3,151.5	3,478.8
Piesok	2,245.0	3,152.1	3,048.7	3,433.2
Dolný Hričov, airport Žilina	2,169.4	3,059.2	2,885.8	3,208.5
Veľké Ripňany	2,774.3	3,642.6	3,439.7	3,740.7
Krušovce	2,773.6	3,654.4	3,481.4	3,819.9
Lovce	2,587.5	3,514.3	3,325.9	3,648.6
Podhájska	2,888.5	3,772.9	3,547.9	3,872.2
Nitra – Janíkovce, airport	2,815.6	3,718.0	3,579.2	3,945.7
Hurbanovo	2,917.3	3,811.7	3,584.5	3,912.0
Beluša	2,323.6	3,310.8	3,117.5	3,464.9
Bystrička	2,037.7	2,932.8	2,870.0	3,271.4
Žilina	2,087.5	2,995.9	2,863.4	3,214.3
Čadca	2,120.4	2,839.8	2,701.2	3,001.1
Oravská Lesná	1,402.9	1,802.9	2,102.7	2,448.8
Rabča	1,622.4	2,740.2	2,329.3	2,636.2
Ružomberok	2,175.2	3,012.0	2,813.9	3,111.6
Liptovský Hrádok	1,876.5	2,677.6	2,406.6	2,614.5
Liptovský Mikuláš – Liptovská Ondrašová	1,976.7	2,767.6	2,524.8	2,751.9
Dudince	2,832.3	3,734.0	3,480.8	3,770.1
Želiezovce	2,888.0	3,781.7	3,591.6	3,940.9
Vieska nad Žitavou	2,786.3	3,702.4	3,481.4	3,801.0
Oravské Veselé	1,442.3	1,866.7	2,099.8	2,400.9
Oravský Podzámok	1,929.3	2,845.5	2,705.8	3,074.5
Martin – Záturčie	2,031.2	2,906.0	2,633.0	2,913.5
Turčianske Teplice	2,437.7	3,200.3	2,928.5	3,098.9
Žiar nad Hronom	1,940.3	2,376.3	2,377.3	2,617.8

Continuation of table 1

↓ station/year →	1970	2000	2050	2100
Bzovík	2,353.3	3,247.1	3,164.3	3,540.8
Sielnica	2,344.1	3,199.7	3,148.3	3,536.8
Vígľaš – Pstruša	2,325.0	3,221.3	3,156.9	3,565.9
Dolné Plachtince	2,711.4	3,500.5	3,321.5	3,605.0
Liptovské Revúce	1,933.4	2,744.5	2,660.0	3,029.0
Sihla – Drábsko	1,463.1	2,020.0	2,093.0	2,371.0
Brezno	2,241.0	2,892.3	2,836.9	3,217.4
Liesek	1,562.0	2,011.1	2,267.5	2,601.7
Lučenec – airport, Boľkovce	2,608.9	3,409.2	3,190.7	3,400.4
Poprad – airport	1,814.0	2,537.9	2,227.5	2,374.9
Ratková	2,417.6	3,218.7	3,001.3	3,221.3
Rimavská Sobota	2,833.2	3,415.8	3,195.3	3,417.6
Rožňava	2,381.3	3,211.7	2,999.9	3,234.9
Švedlár	1,968.5	2,896.9	2,616.4	2,878.4
Štós	1,939.6	2,903.8	2,599.9	2,845.7
Zlatá Idka	2,567.9	3,373.3	3,171.3	3,402.5
Spišské Vlachy	2,191.8	2,978.0	2,707.5	2,903.3
Podolínec	1,761.4	2,478.9	2,298.8	2,515.7
Červený Kláštor – Pieninský národný park	1,899.2	2,702.2	2,496.3	2,746.0
Gánovce – Filice	1,746.0	2,453.4	2,166.8	2,307.6
Revúca	2,356.1	3,120.2	2,882.0	3,067.6
Prešov – Nižná Šebastová	2,260.0	3,039.0	2,907.8	3,176.2
Stará Lesná	1,533.2	1,875.8	1,993.0	2,160.7
Plaveč	1,915.0	2,663.1	2,532.5	2,816.9
Bardejov	2,231.3	2,963.8	2,851.7	3,124.8

Source: Author

Based on the results of our climate indicator $Ts \geq 10$ °C, which defines the beginning and end of the main growing season (HVO) of plants, we can say with certainty that this period will be extended, because the results of our work show an increase in the value of $Ts \geq 10$ °C in the forecast from now until 2100 to 800 °C (Figure 10). Similar results regarding the extension of HVO can be found e.g. in the work (Ďörď, Ložek, Hronský, 2010), where their results show for the years 2005–2008 the extension of HVO vineyards by an average of 12 days (earlier onset, later termination), due to increasing the amount of active temperatures. Furthermore, for example, in the report by VÚPOP-Climate change and its possible impacts on the soil of Slovakia for 2005 (Sobocká, Šurina, Torma, Dodok, 2005), there are mentioned predictions for an increase in the amount of $Ts \geq 10$ °C in 2075 in southern areas by 1,111 °C, to north by 802 °C, our assumptions are lower, but we will agree that these values will increase Sar, Avcı, Avci (2019). They evaluated the vegetation period according to climate change scenarios (RCP 4.5 and RCP 8.5) in the Inner Western Anatolia sub-area. The growing season in this locality can increase by 15–20 days and 40 days, respectively. According to Olszewski and Żmudzka

(2000), the length of the growing season is extended by 1 to 3 days per decade. According to the Walthall et al. (2012), temperature changes varied by season as well as by region. The cooling of the south-eastern country has slowed down in recent decades. In most of the United States, the century-old linear trend is dominated by autumn warming in the 1930s and 1940s, and therefore, long-term trends remain small, with the southwest exception. This total warming is reflected in the extension of the growing season in the northern hemisphere by approximately 4 to 16 days since 1970 (i.e. 1 to 4 days per decade).

Conclusions

In Slovakia, climate change will have an impact on the production of some crops, either negatively or in some cases positively. Value of climatic indicator $Ts > 10$ will increase by 800 °C in sum to the year 2100. Based on the results, we can state that the duration of the main vegetation period in Slovakia will be extended. The data and findings in this paper can be used in further research into the effects of climate change.

Figure 10 Prognosis *Ts* >10 °C for years 2020 (a) and 2100 (b), divided into categories
Source: Author

References

Climateactiontracker.org (1. 12. 2020). Temperatures-Adressing global warming. https://climateactiontracker.org/global/temperatures/

Crippa, M., Oreggioni, G., Guizzardi, D., Muntean, M., Schaaf, E., Lo Vullo, E. et al. (2019). Fossil CO_2 and GHG emissions of all world countries – 2019. *Report JRC Publications Repository*. https://publications.jrc.ec.europa.eu/repository/handle/JRC117610

Ďörď, L., Ložek, O., Hronský, Š. (2010). *Vplyv klimatických faktorov na kvalitu hrozna a vína v Modrokamenskom vinohradníckom rajóne.* (Vedecká monografia). Nitra: SPU.

Enviroportal.sk (2016). Zmena klímy – projekcie skleníkových plynov. *Správa o stave životného prostredia Slovenskej republiky v roku 2016.* https://www.enviroportal.sk/uploads/report/7043.pdf

Enviroportal.sk (2020). Emisie skleníkových plynov z poľnohospodárstva. https://www.enviroportal.sk/indicator/detail/?&id=704&print=yes

Kleger, L., Válek P. (2014). *Top of form bottom of form oxid uhličitý.* Arnika.org, https://arnika.org/oxid-uhlicity

Kriegler, E., Auer, C., Baumstark L., Volkholz, J., Krey V., Kok K. et al. (2020). *What are Climate Change Scenarios?* Climatescenarios.org https://climatescenarios.org/primer

Lapin, M. (22. 9. 2014). *Úvod do problematiky klimatických zmien.* eStranky.sk https://milanlapin.estranky.sk/clanky/klimaticke-zmeny-strucne/

Leman, J. (25. 9. 2020). *What Is Methane, Anyway?* Popularmechanics.com https://www.popularmechanics.com/science/environment/a28858699/what-is-methane/

Luna-anapa.ru (2019). *Zdroje skleníkových plynov v atmosfére. Skleníkový plyn. Zdroje skleníkových plynov.* https://kraskivam.ru/sk/rossiya/istochniki-parnikovyh-gazov-v-atmosfere-parnikovyi-gaz/

Metelka, L., Tolasz, R. (2009). *Klimatické změny: fakta bez mýtů.* web.archive.org, http://web.archive.org/web/20120111082610/http://www.czp.cuni.cz/Knihovna/publikace/klimaticke-zmeny-web.pdf

Midriak, R., Zaušková, Ľ. (2014). Krajina Slovenska a jej využívanie vo vzťahu ku klimatickej zmene. In Kobza, J. (ed.) *Klimatická změna – zmierňujúce a adaptačné opatrenia v sektore pôdohospodárstva.* Slovenská akadémia pôdohospodárskych vied. Zborník 74, Nitra: Národné poľnohospodárske centrum a potravinárske centrum (pp. 64–72).

Olszewski, K., Žmudzka, E. (2000). Variability of the Vegetative Period in Poland. *Miscellanea Geographica, 9,* 59–70. DOI: 10.2478/mgrsd-2000-090108

Polák, J. (24. 4. 2018). *Klimatická zmena a jej možný vplyv na poľnohospodárstvo Slovenska.* Fapz.uniag.sk, https://fapz.uniag.sk/sk/aktualne-informacie-reader/klimatick%C3%A1-zmena-a-jej-mo%C5%BEn%C3%BD-vplyv-na-po%C4%BEnohospod%C3%A1rstvo-slovenska/

Sar, T., Avcı, S., Avci, M. (2019). Evaluation of the vegetation period according to climate change scenarios: a case study in the inner west anatolia subregion of Turkey. *Journal of Geography, 39,* 29–39. DOI: 10.26650/JGEOG2019-0018

Sobocká, J., Šurina, B., Torma, S., Dodok, R. (2005). *Klimatická zmena a jej charakteristika. Klimatická zmena a jej možné dopady na pôdny fond Slovenska.* Bratislava: Výskumný ústav pôdoznalectva a ochrany pôdy (46 p.).

Takáč, J., Zuzula, I. (2000). Adaptácia pôdohospodárstva v Slovenskej republike na klimatickú zmenu. *Národný klimatický program SR.* NKP 9/00. Bratislava: MŽP SR a SHMÚ (pp. 74–86).

Walthall, C. L. J., Hatfield, P., Backlund, L., Lengnick, E., Marshall, M., Walsh, S. et al. (2012). *Climate Change and Agriculture in the United States: Effects and Adaptation.* usda.gov. https://www.usda.gov/sites/default/files/documents/CC%20and%20Agriculture%20Report%20(02-04-2013)b.pdf

A REVIEW OF IMAGING AND SENSING TECHNOLOGIES FOR FIELD PHENOTYPING

Lenka BOTYANSZKA

Institute of Hydrology, Slovak Academy of Sciences, Bratislava, Slovak Republic

Over the past few decades, food production has been sufficient. However, climate change has already affected crop yields around the world. With climate change and population growth, threats to future food production come. Among the solutions to this crisis, breeding is deemed one of the most effective ways. However, traditional phenotyping in breeding is time-consuming as it requires thousands and thousands of individuals. Mechanisms and structures of stress tolerance have a great variability. Today, bigger emphasis is placed on the selection of crops based on genotype information and this still requires phenotypic data. Their use is limited by insufficient phenotypic data, including the information on stress photosynthetic responses. The latest research seeks to bring rapid, non-destructive imaging and sensing technology to agriculture, in order to greatly accelerate the in-field measurements of phenotypes and increase the phenotypic data. This paper presents a review of the imaging and sensing technologies for the field phenotyping to describe its development in the last few years.

Keywords: field phenotyping, imaging technologies, phenotyping platform, remote sensing

Feeding the world's growing population is a challenge, even compounded, since climate change has a considerable impact on crop yields and food supplies (Godfray et al., 2010). By 2050, nearly 10 billion people will be there on Earth. Thus, it will be necessary to ensure that the crop production is sufficient to meet the needs of the human population (Bruinsma, 2009). FAO estimates that the world food production will have to rise by 60% to keep pace with a demographic change (FAO, 2009). This goal is challenging, primarily because climate change will impact the plant productivity. Moreover, it also presents the challenges of drought, extreme weather events and rising temperatures all over the world (Godfray et al., 2010).

Parfitt, Barthel, Macnaughton (2010) report that for every degree Celsius that the global thermostat rises by, there will be a 5 to 15% decrease in the overall crop production. The most important food crops are more prone to abiotic stresses because of the high yield and quality losses (Wang, Frei, 2011). The issue of the ongoing climate change needs to be addressed from a perspective of plant physiology by knowing the laws of physiological processes in the plant (Becklin et al., 2016). Various molecular mechanisms and morphological and anatomical structures have been developed in plants to overcome different stress factors. Cognition of these processes will allow their subsequent application and use in the cultivation practice and breeding of plants (Hasanuzzaman, Nahar, Alam, Roychowdhury, Fujita, 2013; Morales et al., 2020).

There are two main (non-GMO) ways to get higher increases in the crop yields through breeding – either by increasing the total biomass production (increasing photosynthesis) or by decreasing the crop variability (increasing tolerance to abiotic stress) (Long, Zhu, Naidu, Ort, 2006; Araus, Slafer, Reynolds, Royo, 2002). However, they both are polygenic in their nature, so provision of thousands and thousands of individuals is needed. Just alone the mechanisms and structures of stress tolerance have a great variability. Thus, it functions as an important determination and subsequent breeding for the specific resistance (Khan, Sovero, Gemenet, 2016; Sallam, Alqudah, Dawood, Baenziger, Börner, 2019).

Phenotyping is therefore essential to accelerate and facilitate development in conventional, molecular, and transgenic breeding. By connecting the analysis of the genotype-phenotype-environment with high yielding, stress-tolerant plants can be selected far more rapidly and efficiently than is currently possible (Rahaman, Chen, Gillani, Klukas, Chen, 2015). Phenotyping research and knowledge are required to understand the emerging and unknown threats to the global food security.

Traditional plant phenotyping tools, which rely on the selection of traits from a small sample of plants, have very limited throughput (Ubbens, Stavness, 2017). Non-invasive and rapid techniques (Figure 1) have great potential to increase the scale vastly, together with the throughput of the plant phenotyping activities. Among such techniques, we can include new imaging technologies, robotic and phenotyping platform and ground-based and aerial imaging platforms. The technique of the plants phenotyping has expanded dramatically in the last 5 years (Yang et al., 2020).

Contact address: Lenka Botyanszka, Institute of Hydrology, Slovak Academy of Sciences, Bratislava, Slovak Republic;
e-mail: botyanszka@uh.savba.sk

RGB   fluorescence imaging   thermal imaging   mulrispectral   hyperspectral   high-throughput phenotyping
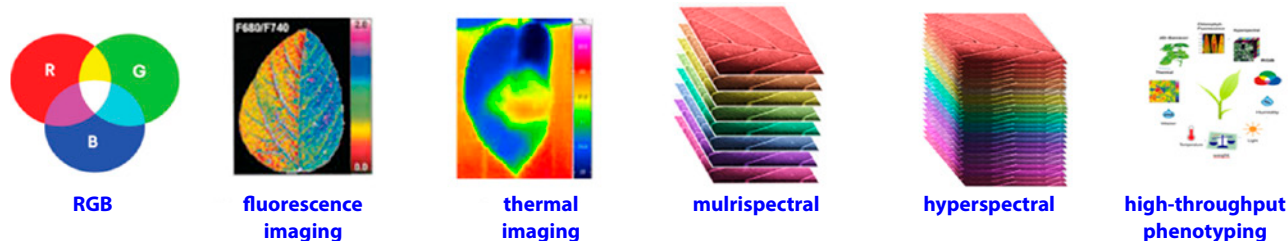
Figure 1 An overview of different imaging techniques in the plant phenotype application used for the automated detection and identification of environment – the plant interactions. These sensors are implemented in breeding, forest and agriculture applications, together with plant phenotyping on different scales, from single cells through single plants to entire ecosystems
Source: Oerke, Mahlein, Steiner, 2014

Field phenotyping imaging technologies

Visible spectral range imaging (RGB)

The essence of digital image recording is to imitate human perception and thus, to tell information about the state of an object or environment. The cameras used are sensitive in the visible spectral range. Raw data is obtained in grey or RGB (Red – Green – Blue) colour images. RGB images are 'classical' photographs. Conventional RGB cameras, which often work in phenotyping, provide higher quality and fast recording at a very reasonable price (Li, Zhang, Huang, 2014). RGB images distinguish plants from the surrounding background. However, the segmentation of plants and background is complicated by numerous factors, such as
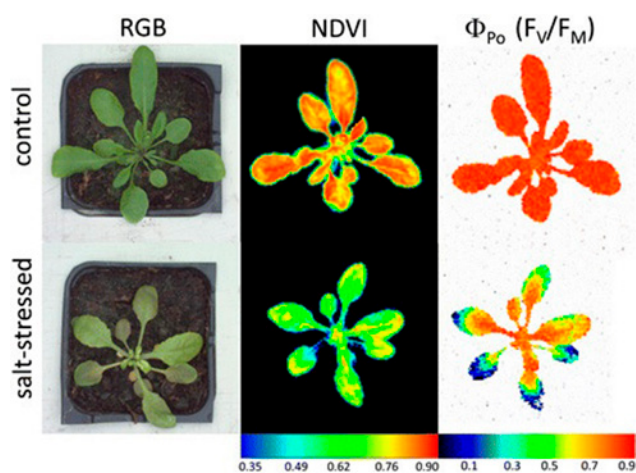
Figure 2 An illustrative figure showing the result of simultaneous analysis of control and salt-stressed Arabidopsis plants by RGB, hyperspectral and Chl fluorescence imaging
Source: Humplík, Lazár, Husičková, Spíchal, 2015

soil, shadows and miscellaneous objects. Therefore, various robust algorithms are created to eliminate such variations (Fernandez-Gallego et al., 2019).

Digital cameras are easy to handle and are a simple source of RGB (red, green, and blue) that enable measurements of the shoot area and detect mass, plant height and width, canopy density, other morphometric data, leaf colour and senescence. By measuring dimensions of the visible plant tissue over time, we can monitor growth of plants. Changes in growth are very sensitive indicators of plant stress. Morphology and colour distribution can serve as indicators of developmental processes and stress responses (Figure 2).

Colour band properties obtained from red, green, and blue (RGB) data may not adequately assess the biophysical properties of the interesting vegetation objects (Putra, Soni, Marhaenanto, Harsono, Fountas, 2020). It is generally preferred to use a combination of RGB and other phenotyping techniques; for example, 3D-based remote sensing is more effective. Several studies have shown the applicability of RGB to obtain relevant information about plants status, e.g. to evaluate growth and flowering dynamics (Ge, Bai, Stoerger, Schnable, 2016; Guo, Fukatsu, Ninomiya, 2015), growth of plant shoots (Golzarian et al., 2011), and yield traits (Fernandez-Gallego et al., 2019), to count seedlings in a field (Liuet al., 2016), predict plant density (Ranđelović et al., 2020), plant stress (Enders et al., 2019; Briglia et al., 2019; Li et al., 2018) and more. Description of the typical devices and software used in plant phenotyping measurement are listed in Table 1.

Fluorescence imaging

Chlorophyll fluorescence (ChlF) analysis is a non-destructive technique that has been used for plant phenotyping for several years and is one of the most popular techniques used in photosynthesis research (Buschmann, Langsdorf, Lichtenthaler, 2008). As ChlF imaging is non-destructive,

Table 1 Description of the typical devices and software used in plant phenotyping measurement

Type	Sensor	Sensor Model	Manufacturer	Examples
Colour digital camera	Nikon, Canon	Nikon 5200, Canon EOS 60D	Tokyo, Japan	Kleefeld, Gypser, Herppich, Bader, Veste (2018)
	Sony	Sony NEX-5N	Tokyo, Japan	Sugiura et al. (2016).
Type	software			
RGB	PlantCV	LemnaGrid (LemnaTec GmbH, Aachen, Germany)		ImageJ

it can be easily combined with other methods (e.g. gas exchange, thermal imaging, UV imaging) and can follow changes in photosynthesis, too (Rolfe, Scholes, 2010).

The principle of measurement excitation of ChlFscence is accomplished by illuminating samples with visible or UV light lasers (light-emitting diode) and capturing image of fluorescence by device cameras (CCD). Fluorescence imaging permits the simultaneous capture of fluorescence emission from four spectral bands – blue (F440), green (F520), red (F690), and far-red (F740) (Kalaji et al., 2016). Another broadly-used approach for measuring ChlF is to measure through the principle of using light induction kinetics (known as Kautsky effect). These methods allow the measurement of photochemical and non-photochemical processes involved in the fluorescence quenching occurring in the presence of actinic light.

From the measurements of fluorescence, parameters can be calculated. These are the minimum (F0) and maximum (Fm) fluorescence yield, steady-state value of fluorescence yield (Fs), photochemical quenching (qP), non-photochemical quenching (NPQ), or the effective quantum yield of energy conversion in PSII (φPSII).

Other chlorophyll fluorescence imaging systems with different measurement protocols or with different combinations of measurement techniques are being developed, for example, integrating into a high-throughput phenotypic analysis.

However, implementation of the large plant populations screening in a field environment is difficult, because most often, they use hand-held fluorimeters, which are more cumbersome and time-consuming.

There are many examples of successful application of ChlF for studying reactions to different environmental stresses, such as temperature (Hou et al., 2016), drought (Bürling et al., 2013; Banks, 2018), salinity (Hniličková, Hnilička, Martinková, Kraus, 2017), and nutrient deficiency (Simkó, Gáspár, Kiss, Makleit, Veres, 2020; Aleksandrov, 2019). This technique can also be used to screen multiple plants, for example in agriculture (Betemps et al., 2012; Baluja, Diago, Goovaerts, Tardaguila, 2012; Van Iersel et al., 2016; Miao et al., 2018; Sytar, Bruckova, Plotnitskaya, Zivcak, Brestic, 2019), forestry (Hernández-Clemente, North, Hornero, Zarco-Tejada, 2017; Sonti, Hallett, Griffin, Trammell, Sullivan, 2020), climate change studies (He et al., 2019; Luus et al., 2017), and plant breeding programmes (Watanabe, Fekih, Kasajima, 2019; Kalaji, Guo, 2008). In addition, the

chlorophyll fluorescence imaging technique can easily be used at different scales – from the whole plant (Eguchi, Konishi, Hosoi, Omasa, 2008; Miao et al., 2018) through the leaf (Montero et al., 2016; Leipner, Oxborough, Baker, 2001) to the cellular resolution (Noble et al., 2017). Several typical sensors that were implemented in the fluorescence imaging technique and representative products are listed in Table 2.

Thermal imaging

Thermal imaging is a technique that allows visualization of infrared radiation of an object, indicating as temperature. The surface temperature of any object can be mapped in a high resolution in two dimensions.

Thermal imaging is now an established technology for study of plant water relations and specifically for stomatal responses and for the phenotyping of plants. Methods of the remote sensing of the leaf temperature can be a way to detect changes in the physiological status of plants and plant responses to biotic or abiotic stresses.

In agriculture, thermal imaging can be used to monitor the plant stress responses, such as water stress (Egea, Padilla-Díaz, Martinez-Guanter, Fernández, Pérez-Ruiz, 2017; Khorsandi, Hemmat, Mireei, Amirfattahi, Ehsanzadeh, 2018; Xu et al., 2016), temperature stress (Poirier-Pocovi, Volder, Bailey, 2020; Park et al., 2017), nutrient stress (Christensen et al., 2005) and be used further in irrigation scheduling (Zovko, Boras, Švaić, 2018; Parihar, Praveen, Padgaonkar, Giri, 2020), crop protection (Lenthe, Oerke, Dehne, 2007; Mahlein et al., 2019; Wang, Poque, Valkonen, 2019), and breeding programmes (Sirault, James, Furbank, 2009; Pushpavalli, Kanatti, Govindaraj, 2020).

Remote sensing has been used by ecologists in larger-scale studies such as landscape ecology (Hwang, Chandler, Shaw, 2020; Nowakowski, Frishkoff, Agha, Todd, Scheffers, 2018), forestry (Chen, Yu, Yan, Wang, 2019; Song et al., 2017), and species diversity (Leuzinger, Körner, 2007).

Thermal imaging has been used by many researchers in agro-food industries, horticultural products, detection of bruises in fruits (Zeng, Miao, Ubaid, Gao, Zhuang, 2020; Kuzy, Jiang, Li, 2018), detection of spoilage by a microbial activity (Chelladurai, Jayas, White, 2010; ElMasry et al., 2020), content volatile compounds (Ding, Dong, Jiao, Zheng, 2017; Dong, Jiao, Li, Zhao, 2019), and food quality evaluation (Ghosh, Rana, Nayak, Pradhan, 2016; Sanchez, Hashim, Shamsudin, Nor, 2020). Several typical sensors are listed in Table 3.

Table 2   Description of the typical devices and software used in plant phenotyping measurement

Type	Sensor	Sensor Model	Manufacturer	Examples
Fluorescence sensor	Open FluorCam	Open FluorCam FC 800-O	Photon Systems Instruments, Brno, Czech Republic	Pérez-Bueno, Pineda, Cabeza, Barón (2016); Kleefeld et al. (2018)
	Z200	Z200 Open- FluorCam	Qubit Systems Inc, Kingston, ON, Canada	Singh, Jones, Shukla, Saxena (2017)
	Multiplex ®	Multiplex 3	Force-A, Orsay, France	Bürling et al. (2013)
Type	software			
Fluorescence imaging	PlantScreenTM Analyser (Photon Systems Instruments, Brno, Czech Republic)		ImagingWin (Heinz Walz GmbH, Effeltrich, Germany)	QUBIT Systems (Kingston, ON, Canada)

Table 3　　　Description of the typical devices and software used in plant phenotyping measurement

Type	Sensor	Sensor Model	Manufacturer	Examples
Thermal sensors	FLIR	Flir SC660, FLIR I7	FLIR systems, Wilsonville, OR, USA	García-Tejero et al. (2018); Santesteban et al. (2017)
	thermoMap	thermoMap	senseFly, Cheseaux-sur-Lausanne, Switzerland	Sagan et al. (2019); Raeva, Šedina, Dlesk (2019)
	Fluke	Fluke Ti32	Fluke Corporation, Everett, WA, USA	Elsayed et al. (2017); Omran (2017)
Type	software			
Thermal imaging	ENVI (Exelis Visual Information Solutions, Boulder, CO, USA)	ERDAS-IMAGINE (Intergraph Corporation Part of Hexagon, Huntsville, AL, USA)		FLIR Tools (FLIR Systems, Wilsonville, OR, USA)
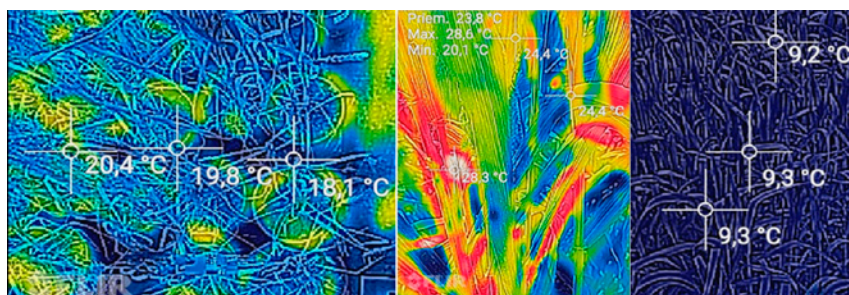
Figure 3　　Sample images of thermal imaging of wheat plants. Obtained from cheap Smartphone Cat S60 with an integrated thermal imaging camera FLIR®
Source: Wilsonville, OR, USA

Due to the progress in the detector technology and image processing, cheap thermal cameras with very high thermal sensitivity have become available in recent years (Figure 3). These cameras are used alone or in combination with other phenotyping sensors.

However, there are also limiting factors of the method. Changes in ambient conditions lead to changes in plant temperature, making the comparison through time difficult. Therefore, its calibration is often required. Furthermore, it is also difficult to separate soil temperature from plant temperature in sparse canopies. These shortcomings should be eliminated in the future by combining thermal imaging with imaging at other spectral wavelengths.

Multispectral imagery

Multispectral imagery enables to see RGB, infrared, ultraviolet and reflected EM radiation. Multispectral imaging is very similar to hyperspectral imaging in the aspect of obtaining UV and VIS-IR spectra for all pixels in the image of a test sample. Multispectral imaging concentrates on several wavebands that are preselected, based on the application. Depending on the application, the multispectral imaging generally refers from 3 to 10 bands. Each band has a descriptive title (UV, NIR, and IR) and there is no continuum between the bands. The vegetation index is the result of the measurements, which quantify biomass or plants. Vegetation indices are algebraic combinations of several spectral bands, designed for quantitative and qualitative evaluations of the vegetation cover. They are used in spectral remote sensing for hyperspectral imagery and multispectral imagery.

Multispectral sensors provide an effective and a low-cost solution, when it comes to acquiring data for various applications. Several sensors are listed in Table 4. Measured data are widely used for analysing the crop biophysical and biochemical parameters and for plant monitoring and protection (Stagakis, Markos, Sykioti, Kyparissis, 2010). The potential of multispectral imaging techniques for agriculture has been demonstrated several times, such as monitoring the effects of water stress (Ballester, Brinkhoff, Quayle, Hornbuckle, 2019; Zhang, Zhang, Niu, Han, 2019), water use efficiency (Zúñiga, Khot, Jacoby, Sankaran, 2016; Thorp, Thompson,

Table 4　　　Description of the typical devices and software used in plant phenotyping measurement

Type	Sensor	Sensor model	Manufacturer	Examples
Multispectral sensors	RedEdge™	RedEdge™ MultiSpectral camera	MicaSense Inc., Seattle, WA, USA	Ballester et al. (2019); Zhang et al. (2020)
	Parrot	Parrot® Sequoia™	Parrot Drones S.A.S, Paris, France	Thorp et al. (2018)
	Tetracam	Tetracam mini-MCA-6	Tetracam, Inc., CA, USA	Torres-Sánchez et al. (2013); De Castro et al. (2015)
Type	software			
Multispectral imaging	Esri (Redlands, CA,USA)	Tetracam (Tetracam Inc., Chatsworth, CA, USA)		Pix4Dmapper (Pix4D SA, Switzerland),

Harders, French, Ward, 2018), detection of diseases (De Castro, Ehsani, Ploetz, Crane, Abdulridha, 2015; Veys, Hibbert, Davis, Grieve, 2017; Zhang et al., 2018), weed management (Torres-Sánchez, Peña-Barragán, Gómez-Candón, De Castro, López-Granados. 2013; Huang, Reddy, Fletcher, Pennington, 2018), also in breeding programmes (Potgieter et al., 2017; Delgado Fajardo, 2018; Barnhart, 2020) or forestry (Awad, 2018; Franklin, 2018; Stoyanova, Kandilarov, Koutev, Nitcheva, Dobreva, 2018; Aleshko, Bogdanov, Shoshina, Ilintsev, 2020).

Hyperspectral analysis

Hyperspectral imaging, like other spectral imaging, collects and processes information from across the electromagnetic spectrum. Solar radiation is measured in wavelengths in the interaction with the surface of the objects. In the case of vegetation, the reflectance signal is in the visible spectral range (400–700 nm). Chlorophyll pigments a and b selectively absorb blue (400–500 nm) and red (600–700 nm) wavelengths for photosynthesis (Ashraf, Maah, Yusoff, 2011; Hallik et al., 2017). With light passing from the visible zone to the near-infrared part of the spectrum (NIR, 700–1,200 nm), a sharp increase in reflectance can occur (Medina et al., 2018). Further increase in wavelengths then leads to a gradual decrease in reflectance, because of the absorption of infrared radiation by water and other leaf components. Spectral reflectance is measured up to 2,500 nm (Knipling 1970; Boegh, Soegaard, Thomsen, 2002). Spectral reflectance curves indicate the reflectance of the objects. Such curves can give us information about the condition of the plant as well as of the whole vegetation.

The measurement is recorded as a reflectance curves graph. The most common applications of this method in phenotyping include the use of reflectance (hyperspectral) indices for field phenotyping to determine biomass growth, greenery, nitrogen content and photosynthesis status (Mistele, Schmidhalter, 2008; Fu, Meacham-Hensold, Guan, Bernacchi, 2019). Non-invasiveness, reliability and good specificity of the individual indices in the cases where the user has been verified and confirmed, are all the advantages of this method. However, their application to new crops or other traits requires a thorough verification and selection of the appropriate indices. The method is highly suitable for the field applications, including air vehicles but also ground carriers. A large amount of generated data and currently still too high cost of the equipment, especially the hyperspectral cameras (Li, Zhang, Huang, 2014), are the disadvantages of this method.

Measured spectral data are used to calculate the vegetation indices (ratios or differences among values on certain wavelengths), such as normalised differential vegetation indices (NDVI and his variations), enhanced vegetation index (EVI), wide dynamic range vegetation index (WDRVI), and many more. These indices usually correlate with some characteristics of the aboveground biomass, such as pigment content, biomass size, LAI, greenness or water content, and also, they are used as predictors of total biomass or crop yields (Prabhakara, Hively, McCarty, 2015; Cabrera-Bosquet et al., 2011).

Hyperspectral remote sensing is used in a wide array of fields as ecology, food processing, mineralogy, surveillance, astronomy, agriculture and many more. The applications of spectral indices in the phenotyping of tolerance to the biotic factors such as pests (Huang, Wang, Liu, Fu, Zhu, 2014) and diseases are also highly interesting (Ritchie, Holzinger, Li, Pendergrass, Kim, 2015).

The estimation of water content in leaves, using the indices based on the reflectance measurements, is relatively a frequented area (Yi, Bao, Wang, Zhao, 2013; De Bei, Fuentes, Wirthensohn, Cozzolino, Tyerman, 2017; Kovar et al., 2018, 2019). Such data can be used to identify the onset and intensity of the plant drought stress. Among the other favourite areas belong, for example, the detection of nitrogen status (Zhao, Reddy, Kakani, Reddy, 2005; Feng, Yao, Zhu, Tian, Cao, 2008), salt stress (Sytar et al., 2017; Moghimi, Yang, Miller, Kianian, Marchetto, 2018), heavy metal (Liu, Liu, Ding, Wu, 2011) and any more. Several sensors, which were implemented in hyperspectral imaging and representative products, are listed in Table 5.

Sensor carriers – phenotyping platforms

Automation and robotics, new sensors, and imaging technologies have led to the advent of a new field, the high-throughput phenotyping. This has been applied to various combinations of sensing technologies (multispectral imaging) and different sensor carriers (phenotyping platforms). Multispectral sensing technologies can usually provide data from a large number of instruments (hyperspectral cameras, thermal imaging cameras, chlorophyll fluorescence cameras, and RGB-3D cameras,

Table 5   Description of the typical devices and software used in plant phenotyping measurement

Type	Sensor	Sensor Model	Manufacturer	Examples
Hyperspectral sensors	PIKA	PIKA II	Resonon, Inc., Bozeman, MT 59715, USA	Moghimi et al. (2018); Moghimi, Yang, Anderson, Reynolds (2019)
	FieldSpec	FieldSpec 3 Field Spec Pro	Analytical Spectral Devices, Boulder, America	De Bei et al. (2017); Zheng et al. (2016)
	Hyperspec	Micro-Hyperspec®	Headwall Photonics, Fitchburg, MA, USA	Camino et al. (2018); Kalisperakis, Stentoumis, Grammatikopoulos, Karantzalos (2015)
Type	software			
Hyperspectral imaging	hyperspectral scanning and image rendering software (Headwall Photonics Inc., Fitchburg, USA).	Hyperspec® III (Headwall Photonics, Fitchburg, MA, USA)		spectral view software (Headwall Photonics Inc., Fitchburg, MA)

Figure 4   Examples of the devices used in plant phenotyping (plant phenotyping platform Photon Systems Instruments, Brno, Czech Republic; phenoMobile® Lite APPF, Australia; drone DJI P4 multispectral Delair-Tech, Delair, Toulouse, France)

etc.). In fact, sensors with different spectral bands enjoy different advantages – they can simultaneously measure several parameters (chlorophyll content, chlorophyll fluorescence, water content, etc.) and also they are non-destructive, easy for use and fast (Agati, Traversi, Cerovic, 2008).

Phenotyping sensor carriers are called phenotyping platforms. They can be either fixed platforms, flying platforms or mobile platforms (Figure 4).

Controlled environment-based phenotyping platforms are being developed in the public domain and are also being sold commercially. They have been deployed in growth chambers or greenhouses (Lemna Tec, Plantscreen, WIWAM, GrowScreen, etc.). These platforms are specifically designed for research and large-scale phenotyping, but for a limited range of plant species. The advantage is that the controlled environments offer cultivation conditions that can be set to the experimental needs (from humidity through temperature to irrigation) and can be repeatedly applied to reproducibility of observations or to a different plant material. The disadvantage is that they cannot be used for field measurements.

Ground-based phenotyping platforms include handcarts, agricultural machinery and mobile robots, which are often referred to as 'phenomobiles'. Equipped with different sensing payloads, fully-mobile platforms can perform observations of the multiple parcels in a field.

Different field monitoring systems have been developed within the last few years, for example, field phenotyping for various plants such as maize (Qiu et al., 2019; García-Santillán, Montalvo, Guerrero, Pajares, 2017), wheat (Sadeghi-Tehran, Virlet, Sabermanesh, Hawkesford, 2017), soybean (Kirchgessner et al., 2017), sugar beet (Benet et al., 2018) and sorghum (Young, Kayacan, Peschel, 2019).

Aerial-based phenotyping platforms are being increasingly considered an alternative option to ground-based phenotyping platforms. Airships, helicopters and drones could serve as flying platforms. The potential advantages of airborne phenotyping approaches are indeed higher than that of ground-based approaches, and for several reasons: from the air a wider viewing angle is possible, together with higher speed of travelling, also physical contact is absent and hence, no mechanical damage of the growing crops (non-destructive phenotyping) is reached and independence of wet soil conditions that prevent traffic on the ground is ensured. Satellite imaging is a great method for growing, devoted to the viewing satellite image data from around the world. Satellite imagery is in the quality of high-resolution and is used in agriculture, forestry, natural disasters (flood), geomorphology and water management. Using an airship or aerostat is suitable for flying over large areas, which we are not allowed to enter because of the vegetation density, or where ultra-quiet propulsion systems are needed, such as protected forests, rainforests and

Table 6   Description of the phenotyping platforms

Phenotyping platform	Type	Institution
Controlled environment-based phenotyping platforms	colour digital camera, hyperspectral camera, multispectral sensor, thermography, fluorescence sensor, CO_2 sensor, radiometer, humidity sensor, etc.	Photon Systems Instruments, Brno, Czech Republic
		LemnaTec GmbH, Würselen, Germany
		Phenospex BV, Heerlen, The Netherlands
		Keygene, Wageningen, The Netherlands
Ground-based phenotyping platforms	Field Scanalyzer	Würselen, Germany
	phenoMobile® Lite	APPF, Australia
	PlantScreenTM Field Systems	Photon Systems Instruments, Brno, Czech Republic
Aerial-based phenotyping platforms	DJI P4 multispectral	Delair-Tech, Delair, Toulouse, France
	phenoAIR™ pod	APPF, Australia
	senseFlyeBee	senseFly, Lausanne, Switzerland
	Draganfly X4-P	Draganfly Innovations Inc., Saskatoon, SK, Canada

national parks (Dorrington, 2005). Unmanned aerial vehicles (UAV) and drones have been used for a wide variety of applications in agriculture, forestry, plant ecology, including mapping of the vegetation over small- up to medium-sized regions. By observing experiments with high temporal frequency, the full plant growth phase can be tracked and analysed. High-resolution maps of the current stage can be generated to support the precision management strategy. There is currently a large number of experiments using the UAV in plant ecology (Nowak, Dziób, Bogawski, 2019; Cruzan et al., 2016), forestry (Klosterman, Richardson, 2017; Weil, Lensky, Resheff, Levin, 2017), and agriculture (Burkart, Hecht, Kraska, Rascher, 2018; Yue et al., 2017). Examples of several chosen platforms that were generally implemented to different aspects of plant phenotyping, are described in Table 6.

Way Forward

In the rapid development of the genotyping methods, not the same attention was paid to the phenotyping methods. Development of the phenotyping methods can help to link the already identified gene sequences with the structure of plants by their morphology, growth and development characteristics, but also by their performance in a certain environment. However, without good phenotypic data, genotyping data cannot be used effectively to improve the plant properties. For this reason, efforts are underway to develop rapid and high-throughput plant phenotyping methods and to keep pace with revolutionary advances in genotyping techniques.

Phenotyping techniques have developed very fast, but the automaticity in collecting data to screen large-scale plant populations under field conditions is required to be more promoted. Phenotyping focused on the use of the non-destructive methods is based on various measurement principles, few of them are mentioned above. Their summary comparison is given in Table 7. Phenotyping methods are currently widely used in agriculture. UAVs, which give farmers/scientists information about the complete field, have the greatest potential. Handheld applications are useful concerning the individual plants as they determine some parameters, which are useful for agriculture to remove some limiting factors (e.g., a nitrogen deficit). When it comes to breeding programmes, it is more difficult to perform measurements, control and data processing, so the labour and financial costs increase. It is questionable, whether the value of the data obtained exceeds the costs incurred. New phenotyping imaging and non-destructive methods are technically manageable and their investment intensity is acceptable, in some cases, even the costs are relatively low. Data acquired from the phenotyping imaging have a great scientific value and can reflect the real situation in the field conditions very well, as presented in this article.

Despite the great interest and intensive research, a number of questions remains unanswered, so the scope for innovation and new knowledge in this area is still very large. Availability of appropriate and novel sensors is a key to implement urgent technological development needs. Optimising and innovating the algorithms is

Table 7   A summary comparison of different imaging techniques

Imaging techniques	RGB	Fluorescence imaging	Thermal imaging	Multispectral imaging	Hyperspectral imaging
Sensor	cameras sensitive to the visible spectral range	fluorescence cameras and setups	near-infrared cameras	multispectral line scanning cameras	hyperspectral cameras
Sensing method	remote sensing	remote sensing	remote sensing	remote sensing	remote sensing
Range of the provided information	growth dynamics; morphology; yield traits; flowering; weed and disease detection	photosynthetic status, state of PSII photochemistry (size of antennas, state of reaction centres, electron transport, etc.)	leaf temperature, stomata openness, insect infestation	leaf pigments, water status, photosynthetic activity, coverage density, panicle health status	leaf pigments, water status, photosynthetic activity, coverage density, panicle health status
Non-destructive measurement	yes	yes	yes	yes	yes
Size of the measurement area	whole plants, part of the field	whole plants, part of a plant,	whole plants, part of the field	whole plants, part of the field	whole plants, part of the field
Possibility of image information	yes	yes	yes	yes	yes
Technical limitations (deceleration)	non	non (*dark adaptation)	frequented calibration	frequented calibration	frequented calibration
Environmental limitations	shadows, overexposure automatically processing image	sensitive to changes in temperature and light intensity	sensitive to temperature changes, necessary direct sunlight	cloudless weather, adequate sun above the horizon	cloudless weather, adequate sun above the horizon

important, especially to increase the data management and computational efficiency. Parameters such as soil nutrient, temperature, humidity and solar radiation should be recorded to build a corresponding database for analysing the relationship between phenotyping and genotyping of plants. Monitoring the environment of plants is also necessary.

The crop productivity limits are a major challenge for agricultural and biological research to overcome the global limiting factors. Plant phenotyping is one of the potential solutions to the crop improvement through breeding.

References

Agati, G., Traversi, M. L., Cerovic, Z. G. (2008). Chlorophyll fluorescence imaging for the non-invasive assessment of anthocyanins in whole grape (*Vitis vinifera* L.) bunches. *Photochem. Photobiol., 84*(6), 1431–1434.

Aleksandrov, V. (2019). Identification of nutrient deficiency in bean plants by prompt chlorophyll fluorescence measurements and Artificial Neural Networks. https://doi.org/10.1101/664235

Aleshko, R., Bogdanov, A., Shoshina, K., Ilintsev, A. (2020). Development of methods for automated determination of forest resource parameters using multispectral survey data from unmanned aerial vehicles. IOP Conference Series: *Earth and Environmental*. IOP Publishing. Science (pp. 012002).

Araus, J. L., Slafer, G. A., Reynolds, M. P., Royo, C. (2002). Plant breeding and drought in C3 cereals: what should we breed for? *Annals of botany, 89*(7), 925–940.

Ashraf, M. A., Maah, M. J., Yusoff, I. (2011). Introduction to remote sensing of biomass. *Biomass and remote sensing of biomass*. IntechOpen (pp. 129–170).

Awad, M. M. (2018). Forest mapping: A comparison between hyperspectral and multispectral images and technologies. *Journal of Forestry Research, 29*(5), 1395–1405.

Ballester, C., Brinkhoff, J., Quayle, W. C., Hornbuckle, J. (2019). Monitoring the effects of water stress in cotton using the green red vegetation index and red edge rRatio. *Remote Sensing, 11*(7), 873.

Baluja, J., Diago, M. P., Goovaerts, P., Tardaguila, J. (2012). Assessment of the spatial variability of anthocyanins in grapes using a fluorescence sensor: relationships with vine vigour and yield. *Precision Agriculture, 13*(4), 457.

Banks, J. M. (2018). Chlorophyll fluorescence as a tool to identify drought stress in Acer genotypes. *Environmental and experimental botany*, 155, 118–127.

Barnhart, I. (2020). *High-resolution UAS multispectral imaging for cultivar selection in grain sorghum breeding trials* (Doctoral dissertation).

Becklin, K. M., Anderson, J. T., Gerhart, L. M., Wadgymar, S. M., Wessinger, C. A., Ward, J. K. (2016). Examining plant physiological responses to climate change through an evolutionary lens. *Plant physiology, 172*(2), 635–649.

Benet, B., Dubos, C., Maupas, F., Malatesta, G., Lenain, R. (2018). Development of autonomous robotic platforms for sugar beet crop phenotyping using artificial vision. *AGENG Conference*, July 2018, Wageningen, NLD.

Betemps, D. L., Fachinello, J. C., Galarça, S. P., Portela, N. M., Remorini, D., Massai, R., Agati, G. (2012). Non-destructive evaluation of ripening and quality traits in apples using a multiparametric fluorescence sensor. *Journal of the Science of Food and Agriculture, 92*(9), 1855–1864.

Boegh, E., Soegaard, H., Thomsen, A. (2002). Evaluating evapotranspiration rates and surface conditions using Landsat TM to estimate atmospheric resistance and surface resistance. *Remote Sensing of Environment, 79*(2–3), 329–343.

Briglia, N., Montanaro, G., Petrozza, A., Summerer, S., Cellini, F., Nuzzo, V. (2019). Drought phenotyping in *Vitis vinifera* using RGB and NIR imaging. *Scientia Horticulturae, 256*, 108555.

Bruinsma, J. (2009). The resource outlook to 2050: by how much do land, water and crop yields need to increase by 2050. *Expert meeting on how to feed the world in, 2050*, 24–26.

Burkart, A., Hecht, V. L., Kraska, T., Rascher, U. (2018). Phenological analysis of unmanned aerial vehicle based time series of barley imagery with high temporal resolution. *Precision agriculture, 19*(1), 134–146.

Buschmann, C., Langsdorf, G., Lichtenthaler, H. K. (2008). Blue, green, red, and far-red fluorescence signatures of plant tissues, their multicolor fluorescence imaging, and application for agrofood assessment. *Optical monitoring of fresh and processed agricultural crops* (pp. 272).

Bürling, K., Cerovic, Z. G., Cornic, G., Ducruet, J. M., Noga, G., Hunsche, M. (2013). Fluorescence-based sensing of drought-induced stress in the vegetative phase of four contrasting wheat genotypes. *Environmental and Experimental Botany, 89*, 51–59.

Cabrera-Bosquet, L., Molero, G., Stellacci, A., Bort, J., Nogues, S., Araus, J. (2011). NDVI as a potential tool for predicting biomass, plant nitrogen content and growth in wheat genotypes subjected to different water and nitrogen conditions. *Cereal Research Communications, 39* (1), 147–159.

Camino, C., González-Dugo, V., Hernández, P., Sillero, J. C., Zarco-Tejada, P. J. (2018). Improved nitrogen retrievals with airborne-derived fluorescence and plant traits quantified from VNIR-SWIR hyperspectral imagery in the context of precision agriculture. *International journal of applied earth observation and geoinformation, 70*, 105–117.

Chelladurai, V., Jayas, D. S., White, N. D. G. (2010). Thermal imaging for detecting fungal infection in stored wheat. *Journal of stored products research, 46*(3), 174–179.

Chen, Z., Yu, G., Yan, J., Wang, H. (2019). Contrasting temperature and precipitation patterns of trees in different seasons and responses of infrared canopy temperature in two asian subtropical forests. *Forests, 10*(10), 902.

Christensen, L. K., Rodriguez, D., Belford, R., Sadras, V., Rampant, P., Fisher, P. (2005). Temporal prediction of nitrogen status in wheat under the influence of water deficiency using spectral and thermal information. *Precision Agriculture, 5*, 209–215.

Cruzan, M. B., Weinstein, B. G., Grasty, M. R., Kohrn, B. F., Hendrickson, E. C., Arredondo, T. M., Thompson, P. G. (2016). Small unmanned aerial vehicles (micro-UAVs, drones) in plant ecology. *Applications in plant sciences*, 4(9), 1600041.

De Castro, A. I., Ehsani, R., Ploetz, R., Crane, J. H., Abdulridha, J. (2015). Optimum spectral and geometric parameters for early detection of laurel wilt disease in avocado. *Remote Sensing of Environment, 171*, 33–44.

De Bei, R., Fuentes, S., Wirthensohn, M. G., Cozzolino, D., Tyerman, S. D. (2017). Feasibility study on the use of Near Infrared spectroscopy to measure water status of almond trees. *VII International Symposium on Almonds and Pistachios, 1219* (pp. 79–84).

Delgado Fajardo, C. C. (2018). *Multispectral image quality assessment to enhance classification rates of rice hojablanca virus (RHBV) in rice breeding programs* (Doctoral dissertation).

Ding, L., Dong, D., Jiao, L., Zheng, W. (2017). Potential using of infrared thermal imaging to detect volatile compounds released from decayed grapes. *PloS one, 12*(6), 0180649.

Dong, D., Jiao, L., Li, C., Zhao, C. (2019). Rapid and real-time analysis of volatile compounds released from food using infrared and laser spectroscopy. *TrAC Trends in Analytical Chemistry*, 110, 410–416.

Dorrington, G. E. 2005. Development of an airship for tropical rain forest canopy exploration. *Aeronautical Journal*, *109*(1098), 361–372.

Egea, G., Padilla-Díaz, C. M., Martinez-Guanter, J., Fernández, J. E., Pérez-Ruiz, M. (2017). Assessing a crop water stress index derived from aerial thermal imaging and infrared thermometry in super-high density olive orchards. *Agricultural Water Management*, *187*, 210–221.

Eguchi, A., Konishi, A., Hosoi, F., Omasa, K. (2008). Three-dimensional chlorophyll fluorescence imaging for detecting effects of herbicide on a whole plant. *Photosynthesis. Energy from the Sun*. Springer, Dordrecht, 2008. pp. 577–580.

ElMasry, G., Elgamal, R., Mandour, N., Gou, P., Al-Rejaie, S., Belin, E., Rousseau, D. (2020). Emerging thermal imaging techniques for seed quality evaluation: Principles and applications. *Food Research International*, *131*, 109025.

Elsayed, S., Elhoweity, M., Ibrahim, H. H., Dewir, Y. H., Migdadi, H. M., Schmidhalter, U. (2017). Thermal imaging and passive reflectance sensing to estimate the water status and grain yield of wheat under different irrigation regimes. *Agricultural Water Management*, *189*, 98–110.

Enders, T. A., St. Dennis, S., Oakland, J., Callen, S. T., Gehan, M. A., Miller, N. D., Spalding, E. P., Springer, N. M., Hirsch, C. D. (2019). Classifying cold-stress responses of inbred maize seedlings using RGB imaging. *Plant direct*, *3*(1), 00104.

FAO. (2009). *How to Feed the World in 2050*. Rome, Italy: Food and Agriculture Organization.

Feng, W., Yao, X., Zhu, Y., Tian, Y. C., Cao, W. X. (2008). Monitoring leaf nitrogen status with hyperspectral reflectance in wheat. *European Journal of Agronomy*, *28*(3), 394–404.

Fernandez-Gallego, J. A., Kefauver, S. C., Vatter, T., Gutiérrez, N. A., Nieto-Taladriz, M. T., Araus, J. L. (2019). Low-cost assessment of grain yield in durum wheat using RGB images. *European Journal of Agronomy*, *105*, 146–156.

Franklin, S. E. (2018). Pixel-and object-based multispectral classification of forest tree species from small unmanned aerial vehicles. *Journal of Unmanned Vehicle Systems*, *6*(4), 195–211.

Fu, P., Meacham-Hensold, K., Guan, K., Bernacchi, C. J. (2019). Hyperspectral leaf reflectance as proxy for photosynthetic capacities: An ensemble approach based on multiple machine learning algorithms. *Frontiers in Plant Science*, *10*, 730.

García-Santillán, I. D., Montalvo, M., Guerrero, J. M., Pajares, G. (2017). Automatic detection of curved and straight crop rows from images in maize fields. *Biosystems Engineering*, *156*, 61–79.

García-Tejero, I. F., Rubio, A. E., Viñuela, I., Hernández, A., Gutiérrez-Gordillo, S., Rodríguez-Pleguezuelo, C. R., Durán-Zuazo, V. H. (2018). Thermal imaging at plant level to assess the crop-water status in almond trees (cv. Guara) under deficit irrigation strategies. *Agricultural Water Management*, *208*, 176–186.

Ge, Y., Bai, G., Stoerger, V., Schnable, J. C. (2016). Temporal dynamics of maize plant growth, water use, and leaf water content using automated high throughput RGB and hyperspectral imaging. *Computers and Electronics in Agriculture*, *127*, 625–632.

Ghosh, P., Rana, S. S., Nayak, A., Pradhan, R. C. (2016). Quality evaluation of food by thermal imaging. Internat. *J. Proc. & Post Harvest Technol.*, *7*(1), 126–133.

Godfray, H. C. J., Beddington, J. R., Crute, I. R., Haddad, L., Lawrence, D., Muir, J. F., Pretty, J., Robinson, S., Thomas, S. M., Toulmin, C. (2010). Food security: the challenge of feeding 9 billion people. *Science*, *327*(5967), 812–818.

Golzarian, M. R., Frick, R. A., Rajendran, K., Berger, B., Roy, S., Tester, M., Lun, D. S. (2011). Accurate inference of shoot biomass from high-throughput images of cereal plants. *Plant methods*, *7*(1), 2.

Guo, W., Fukatsu, T., Ninomiya, S. (2015). Automated characterization of flowering dynamics in rice using field-acquired time-series RGB images. *Plant methods*, *11*(1), 7.

Hallik, L., Kazantsev, T., Kuusk, A., Galmés, J., Tomás, M., Niinemets, Ü. (2017). Generality of relationships between leaf pigment contents and spectral vegetation indices in Mallorca (Spain). *Regional Environmental Change*, *17*(7), 2097–2109.

Hasanuzzaman, M., Nahar, K., Alam, M., Roychowdhury, R., Fujita, M. (2013). Physiological, biochemical, and molecular mechanisms of heat stress tolerance in plants. *International journal of molecular sciences*, 14(5), 9643–9684.

He, L., Chen, J. M., Liu, J., Zheng, T., Wang, R., Joiner, J., Chou, S., Chen, B., Liu, Y., Liu, R., Rogers, C. (2019). Diverse photosynthetic capacity of global ecosystems mapped by satellite chlorophyll fluorescence measurements. *Remote Sensing of Environment*, *232*, 111344.

Hernández-Clemente, R., North, P. R., Hornero, A., Zarco-Tejada, P. J. (2017). Assessing the effects of forest health on sun-induced chlorophyll fluorescence using the FluorFLIGHT 3-D radiative transfer model to account for forest structure. *Remote Sensing of Environment*, *193*, 165–179.

Hniličková, H., Hnilička, F., Martinková, J., Kraus, K. (2017). Effects of salt stress on water status, photosynthesis and chlorophyll fluorescence of rocket. *Plant, Soil and Environment*, *63*(8), 362–367.

Hou, W., Sun, A. H., Chen, H. L., Yang, F. S., Pan, J. L., Guan, M. Y. (2016). Effects of chilling and high temperatures on photosynthesis and chlorophyll fluorescence in leaves of watermelon seedlings. *Biologiaplantarum*, *60*(1), 148–154.

Huang, S., Wang, L., Liu, L., Fu, Q., Zhu, D. (2014). Nonchemical pest control in China rice: a review. *Agronomy for sustainable development*, *34*(2), 275–291.

Huang, Y., Reddy, K. N., Fletcher, R. S., Pennington, D. (2018). UAV low-altitude remote sensing for precision weed management. *Weed technology*, *32*(1), 2–6.

Humplík, J. F., Lazár, D., Husičková, A., Spíchal, L. (2015). Automated phenotyping of plant shoots using imaging methods for analysis of plant stress responses – a review. *Plant methods*, *11*(1), 29.

Hwang, K., Chandler, D. G., Shaw, S. B. (2020). Patch scale evapotranspiration of wetland plant species by ground-based infrared thermometry. *Agricultural and Forest Meteorology*, *287*, 107948.

Kalaji, M. H., Guo, P. (2008). Chlorophyll fluorescence: a useful tool in barley plant breeding programs. *Photochemistry research progress*, *29*, 439–463.

Kalaji, H. M., Jajoo, A., Oukarroum, A., Brestic, M., Zivcak, M., Samborska, I. A., Cetner, M. D., Łukasik, I., Goltsev, V., Ladle, R. J. (2016). Chlorophyll a fluorescence as a tool to monitor physiological status of plants under abiotic stress conditions. *Actaphysiologiaeplantarum*, *38*(4), 102.

Kalisperakis, I., Stentoumis, C., Grammatikopoulos, L., Karantzalos, K. (2015). Leaf area index estimation in vineyards from UAV hyperspectral data, 2D image mosaics and 3D canopy surface models. *The International Archives of Photogrammetry, Remote Sensing and Spatial Information Sciences*, *40*(1), 299.

Khan, A., Sovero, V., Gemenet, D. (2016). Genome-assisted breeding for drought resistance. *Current Genomics*, *17*(4), 330–342.

Khorsandi, A., Hemmat, A., Mireei, S. A., Amirfattahi, R., Ehsanzadeh, P. (2018). Plant temperature-based indices using infrared thermography for detecting water status in sesame under greenhouse conditions. *Agricultural Water Management*, *204*, 222–233.

Kirchgessner, N., Liebisch, F., Yu, K., Pfeifer, J., Friedli, M., Hund, A., Walter, A. (2017). The ETH field phenotyping platform FIP: a cable-suspended multi-sensor system. *Functional Plant Biology*, *44*(1), 154–168.

Kleefeld, A., Gypser, S., Herppich, W. B., Bader, G., Veste, M. (2018). Identification of spatial pattern of photosynthesis hotspots in moss-and lichen-dominated biological soil crusts by combining chlorophyll fluorescence imaging and multispectral BNDVI images. *Pedobiologia*, *68*, 1–11.

Klosterman, S., Richardson, A. D. (2017). Observing spring and fall phenology in a deciduous forest with aerial drone imagery. *Sensors*, *17*(12), 2852.

Knipling, E. B. (1970). Physical and physiological basis for the reflectance of visible and near-infrared radiation from vegetation. *Remote sensing of environment*, *1*(3), 155–159.

Kovar, M., Brestic, M., Zivcak, M., Olsovska, K., Sytar, O., Botyanszka, L., Chovancek, E., Bárek, V. (2018). Hyperspectral imaging-tool for non-destructive evaluation of water content in plant (Conference poster). *Vlivabiotických a Biotických stresorů na vlastnosti rostlin, 5*, 135–138.

Kovar, M., Brestic, M., Sytar, O., Barek, V., Hauptvogel, P., Zivcak, M. (2019). Evaluation of hyperspectral reflectance parameters to assess the leaf water content in soybean. *Water*, *11*(3), 443.

Kuzy, J., Jiang, Y., Li, C. (2018). Blueberry bruise detection by pulsed thermographic imaging. *Postharvest Biology and Technology*, *136*, 166–177.

Leipner, J., Oxborough, K., Baker, N. R. (2001). Primary sites of ozone-induced perturbations of photosynthesis in leaves: identification and characterization in *Phaseolus vulgaris* using high resolution chlorophyll fluorescence imaging. *Journal of Experimental Botany*, *52*(361), 1689-1696.

Lenthe, J. H., Oerke, E. C., Dehne, H. W. (2007). Digital infrared thermography for monitoring canopy health of wheat. *Precision Agriculture*, *8*(1–2), 15–26.

Leuzinger, S., Körner, C. (2007). Tree species diversity affects canopy leaf temperatures in a mature temperate forest. *Agricultural and forest meteorology*, *146*(1–2), 29–37.

Li, L., Zhang, Q., Huang, D. (2014). A review of imaging techniques for plant phenotyping. *Sensors*, *14*(11), 20078–20111.

Li, H., Malik, M. H., Gao, Y., Qiu, R., Miao, Y., Zhang, M. (2018). Maize plant water stress detection based on RGB image and thermal infrared image. *2018 ASABE Annual International Meeting*. American Society of Agricultural and Biological Engineers (pp. 1).

Liu, M., Liu, X., Ding, W., Wu, L. (2011). Monitoring stress levels on rice with heavy metal pollution from hyperspectral reflectance data using wavelet-fractal analysis. *International Journal of Applied Earth Observation and Geoinformation*, *13*(2), 246–255.

Liu, T., Wu, W., Chen, W., Sun, C., Zhu, X., Guo, W. (2016). Automated image-processing for counting seedlings in a wheat field. *Precision agriculture*, *17*(4), 392–406.

Long, S. P., Zhu, X. G., Naidu, S. L., Ort, D. R. (2006). Can improvement in photosynthesis increase crop yields? *Plant, cell & environment*, *29*(3), 315–330.

Luus, K. A., Commane, R., Parazoo, N. C., Benmergui, J., Euskirchen, E. S., Frankenberg, C., Zona, D., Joiner, J., Lindaas, J., Miller, C. E., Oechel, W. C., Wofsy, S., Lin, J. C. (2017). Tundra photosynthesis captured by satellite-observed solar-induced chlorophyll fluorescence. *Geophysical Research Letters*, *44*(3), 1564–1573.

Mahlein, A. K., Alisaac, E., Al Masri, A., Behmann, J., Dehne, H. W., Oerke, E. C. (2019). Comparison and combination of thermal, fluorescence, and hyperspectral imaging for monitoring fusarium head blight of wheat on spikelet scale. *Sensors*, *19*(10), 2281.

Medina, I., Newton, E., Kearney, M. R., Mulder, R. A., Porter, W. P. – Stuart-Fox, D. (2018). Reflection of near-infrared light confers thermal protection in birds. *Nature communications*, *9*(1), 1–7.

Miao, G., Guan, K., Yang, X., Bernacchi, C. J., Berry, J. A., Delucia, E. H., Wu, J., Moore, C. E., Meacham, K., Cai, Y., Kimm, H., Masters, M. D. Peng, B. (2018). Sun-induced chlorophyll fluorescence, photosynthesis, and light use efficiency of a soybean field from seasonally continuous measurements. *Journal of Geophysical Research: Biogeosciences*, *123*(2), 610–623.

Mistele, B., Schmidhalter, U. (2008). Estimating the nitrogen nutrition index using spectral canopy reflectance measurements. *European Journal of Agronomy*, *29*(4), 184–190.

Moghimi, A., Yang, C., Miller, M. E., Kianian, S. F., Marchetto, P. M. (2018). A novel approach to assess salt stress tolerance in wheat using hyperspectral imaging. *Frontiers in plant science*, *9*, 1182.

Moghimi, A., Yang, C., Anderson, J. A., Reynolds, S. K. (2019). Selecting informative spectral bands using machine learning techniques to detect *Fusarium* head blight in wheat. *2019 ASABE Annual International Meeting* (pp. 1).

Montero, R., Pérez-Bueno, M. L., Barón, M., Florez-Sarasa, I., Tohge, T., Fernie, A. R.,, El AouOuad, H., Flexas, J., Bota, J. (2016). Alterations in primary and secondary metabolism in Vitis vinifera 'Malvasía de Banyalbufar'upon infection with Grapevine leafroll-associated virus 3. *Physiologiaplantarum*, *157*(4), 442–452.

Morales, F., Ancín, M., Fakhet, D., González-Torralba, J., Gámez, A. L., Seminario, A., Soba, D., Ben Mariem, S., Garriga, M., Aranjuelo, I. (2020). Photosynthetic Metabolism under Stressful Growth Conditions as a Bases for Crop Breeding and Yield Improvement. *Plants*, *9*(1), 88.

Noble, E., Kumar, S., Görlitz, F. G., Stain, C., Dunsby, C., French, P. M. (2017). In vivo label-free mapping of the effect of a photosystem II inhibiting herbicide in plants using chlorophyll fluorescence lifetime. *Plant methods*, *13*(1), 48.

Nowak, M. M., Dziób, K., Bogawski, P. (2019). Unmanned Aerial Vehicles (UAVs) in environmental biology: a review. *European Journal of Ecology*, *4*(2), 56–74.

Nowakowski, A. J., Frishkoff, L. O., Agha, M., Todd, B. D., Scheffers, B. R. (2018). Changing thermal landscapes: merging climate science and landscape ecology through thermal biology. *Current Landscape Ecology Reports*, *3*(4), 57–72.

Oerke, E. C., Mahlein, A. K., Steiner, U. (2014). Proximal sensing of plant diseases. *Detection and Diagnostics of Plant Pathogens*. Dordrecht: Springer (pp. 55–68).

Omran, E. S. E. (2017). Early sensing of peanut leaf spot using spectroscopy and thermal imaging. *Archives of Agronomy and Soil Science*, *63*(7), 883–896.

Parfitt, J., Barthel, M., Macnaughton, S. (2010). Food waste within food supply chains: quantification and potential for change to 2050. *Philosophical transactions of the royal society B: biological sciences*, *365*(1554), 3065–3081.

Parihar, G., Praveen, S., Padgaonkar, R., Giri, L. I. (2020). Infrared thermography based smart irrigation scheduling for horticulture plants. *Thermosense: Thermal Infrared Applications XLII International Society for Optics and Photonics*, *11409*, 1140908.

Park, E., Hong, S. J., Lee, A. Y., Park, J., Cho, B. K., Kim, G. (2017). Phenotyping of low-temperature stressed pepper seedlings using infrared thermography. *Journal of Biosystems Engineering*, *42*(3), 163–169.

Pérez-Bueno, M. L., Pineda, M., Cabeza, F. M., Barón, M. (2016). Multicolor fluorescence imaging as a candidate for disease detection in plant phenotyping. *Frontiers in plant science*, *7*, 1790.

Poirier-Pocovi, M., Volder, A., Bailey, B. N. (2020). Modeling of reference temperatures for calculating crop water stress indices from infrared thermography. *Agricultural Water Management*, *233*, 106070.

Potgieter, A. B., George-Jaeggli, B., Chapman, S. C., Laws, K., Suárez Cadavid, L. A., Wixted, J., Watson, J., Eldridge, M., Jordan, D. R., Hammer, G. L. (2017). Multi-spectral imaging from an unmanned aerial vehicle enables the assessment of seasonal leaf area dynamics of sorghum breeding lines. *Frontiers in Plant Science*, *8*, 1532.

Prabhakara, K., Hively, W. D., McCarty, G. W. (2015). Evaluating the relationship between biomass, percent groundcover and remote sensing indices across six winter cover crop fields in Maryland, United States. *International journal of applied earth observation and geoinformation*, *39*, 88–102.

Pushpavalli, R., Kanatti, A., Govindaraj, M. (2020). Use of infrared thermography imaging for assessing heat tolerance in high and low iron pearl millet lines. *Electronic Journal of Plant Breeding*, *11*(2), 626–632.

Putra, B. T. W., Soni, P., Marhaenanto, B., Harsono, S. S., Fountas, S. (2020). Using information from images for plantation monitoring: A review of solutions for smallholders. *Information Processing in Agriculture*, *7*(1), 109–119

Qiu, Q., Sun, N., Bai, H., Wang, N., Fan, Z., Wang, Y., Fan, Z., Wang, Y., Meng1, Z., Li1, B.- Cong, Y. (2019). Field-based high-throughput phenotyping for Maize plant using 3D LiDAR point cloud generated with a "Phenomobile". *Frontiers in plant science*, *10*(219), 554.

Rahaman, M., Chen, D., Gillani, Z., Klukas, C., Chen, M. (2015). Advanced phenotyping and phenotype data analysis for the study of plant growth and development. *Frontiers in plant science*, *6*, 619.

Ranđelović, P., Đorđević, V., Milić, S., Balešević-Tubić, S., Petrović, K., Miladinović, J., Đukić, V. (2020). Prediction of soybean plant density using a machine learning model and vegetation indices extracted from RGB images taken with a UAV. *Agronomy*, *10*(8), 1108.

Raeva, P. L., Šedina, J., Dlesk, A. (2019). Monitoring of crop fields using multispectral and thermal imagery from UAV. *European Journal of Remote Sensing*, *52*, 192–201.

Ritchie, M. D., Holzinger, E. R., Li, R., Pendergrass, S. A., Kim, D. (2015). Methods of integrating data to uncover genotype-phenotype interactions. *Nature Reviews Genetics*, *16*(2), 85–97.

Rolfe, S. A., Scholes, J. D. (2010). Chlorophyll fluorescence imaging of plant-pathogen interactions. *Protoplasma*, *247*(3–4), 163–175.

Sadeghi-Tehran, P., Virlet, N., Sabermanesh, K., Hawkesford, M. J. (2017). Multi-feature machine learning model for automatic segmentation of green fractional vegetation cover for high-throughput field phenotyping. *Plant methods*, *13*(1), 103.

Sagan, V., Maimaitijiang, M., Sidike, P., Eblimit, K., Peterson, K. T., Hartling, S., Esposito, F., Khanal, K., Newcomb, M., Pauli, D., Fritschi, F., Shakoor, N., Mockler, T., Ward, R. (2019). UAV-based high resolution thermal imaging for vegetation monitoring, and plant phenotyping using ICI 8640 P, FLIR Vue Pro R 640, and thermomap cameras. *Remote Sensing*, *11*(3), 330.

Sallam, A., Alqudah, A. M., Dawood, M. F., Baenziger, P. S., Börner, A. (2019). Drought stress tolerance in wheat and barley: advances in physiology, breeding and genetics research. *International journal of molecular sciences*, *20*(13), 3137.

Sanchez, P. D. C., Hashim, N., Shamsudin, R., Nor, M. Z. M. (2020). Applications of imaging and spectroscopy techniques for non-destructive quality evaluation of potatoes and sweet potatoes: A review. *Trends in Food Science & Technology*, *96*, 208–221.

Santesteban, L. G., Di Gennaro, S. F., Herrero-Langreo, A., Miranda, C., Royo, J. B., Matese, A. (2017). High-resolution UAV-based thermal imaging to estimate the instantaneous and seasonal variability of plant water status within a vineyard. *Agricultural Water Management*, *183*, 49–59

Singh, A. S., Jones, A. M. P., Shukla, M. R., Saxena, P. K. (2017). High light intensity stress as the limiting factor in micropropagation of sugar maple (*Acer saccharum* Marsh.). *Plant Cell, Tissue and Organ Culture*, *129*(2), 209–221.

Simkó, A., Gáspár, G. S., Kiss, L., Makleit, P., Veres, S. (2020). Evaluation of nitrogen nutrition in diminishing water deficiency at different growth stages of maize by chlorophyll fluorescence parameters. *Plants*, *9*(6), 676.

Sirault, X. R., James, R. A., Furbank, R. T. (2009). A new screening method for osmotic component of salinity tolerance in cereals using infrared thermography. *Functional Plant Biology*, *36*(11), 970–977.

Song, Q. H., Deng, Y., Zhang, Y. P., Deng, X. B., Lin, Y. X., Zhou, L. G., Fei, X., Sha, L., Liu, Y., Zhou, W., Gao, J. B. (2017). Comparison of infrared canopy temperature in a rubber plantation and tropical rain forest. *International journal of biometeorology*, *61*(10), 1885–1892.

Sonti, N. F., Hallett, R. A., Griffin, K. L., Trammell, T. L., Sullivan, J. H. (2020). Chlorophyll fluorescence parameters, leaf traits, and foliar chemistry of white oak and red maple trees in urban forest patches. *Tree Physiology*.

Stagakis, S., Markos, N., Sykioti, O., Kyparissis, A. (2010). Monitoring canopy biophysical and biochemical parameters in ecosystem scale using satellite hyperspectral imagery: An application on a Phlomisfruticosa Mediterranean ecosystem using multiangular CHRIS/PROBA observations. *Remote Sensing of Environment*, *114*(5), 977–994.

Stoyanova, M., Kandilarov, A., Koutev, V., Nitcheva, O., Dobreva, P. (2018). Potential of multispectral imaging technology for assessment coniferous forests bitten by a bark beetle in Central Bulgaria. *MATEC Web of Conferences*. EDP Sciences (pp. 01005).

Sugiura, R., Tsuda, S., Tamiya, S., Itoh, A., Nishiwaki, K., Murakami, N., Shibuyaa, Y., Hirafujiab, M., Nuske, S. (2016). Field phenotyping system for the assessment of potato late blight resistance using RGB imagery from an unmanned aerial vehicle. *Biosystems engineering*, *148*, 1–10.

Sytar, O., Brestic, M., Zivcak, M., Olsovska, K., Kovar, M., Shao, H.- He, X. (2017). Applying hyperspectral imaging to explore natural plant diversity towards improving salt stress tolerance. *Science of the Total Environment*, *578*, 90–99.

Sytar, O., Bruckova, K., Plotnitskaya, A., Zivcak, M., Brestic, M. (2019). Non-destructive methodology in comparative physiology of buckwheat genotypes within the different origin. *Fagopyrum*, *36*(1), 11–21.

Thorp, K. R., Thompson, A. L., Harders, S. J., French, A. N., Ward, R. W. (2018). High-throughput phenotyping of crop water use efficiency via multispectral drone imagery and a daily soil water balance model. *Remote Sensing*, *10*(11), 1682.

Torres-Sánchez, J., Peña-Barragán, J. M., Gómez-Candón, D., De Castro, A. I., López-Granados, F. (2013). Imagery from unmanned aerial vehicles for early site specific weed management. *Precision agriculture '13*. Wageningen: Wageningen Academic Publishers (pp. 193–199).

Ubbens, J. R., Stavness, I. (2017). Deep plant phenomics: a deep learning platform for complex plant phenotyping tasks. *Frontiers in plant science*, *8*, 1190.

Van Iersel, M. W., Mattos, E., Weaver, G., Ferrarezi, R. S., Martin, M. T., Haidekker, M. (2016). Using chlorophyll fluorescence to control lighting in controlled environment agriculture. *VIII International Symposium on Light in Horticulture* (pp. 427–434).

Veys, C., Hibbert, J., Davis, P., Grieve, B. (2017). An ultra-low-cost active multispectral crop diagnostics device. *IEEE SENSORS*, 1–3.

Wang, Y., Frei, M. (2011). Stressed food–The impact of abiotic environmental stresses on crop quality. *Agriculture, Ecosystems & Environment*, *141*(3–4), 271–286.

Wang, L., Poque, S., Valkonen, J. P. (2019). Phenotyping viral infection in sweetpotato using a high-throughput chlorophyll fluorescence and thermal imaging platform. *Plant methods*, *15*(1), pp. 116.

Watanabe, E., Fekih, R., Kasajima, I. (2019). Advances in Chlorophyll Fluorescence Theories: Close Investigation into Oxidative Stress and Potential Use for Plant Breeding. *Redox Homeostasis in Plants*. Springer, Cham (pp. 137–154).

Weil, G., Lensky, I. M., Resheff, Y. S., Levin, N. (2017). Optimizing the timing of unmanned aerial vehicle image acquisition for applied mapping of woody vegetation species using feature selection. *Remote Sensing*, *9*(1)1, 1130.

Xu, J., Lv, Y., Liu, X., Dalson, T., Yang, S., Wu, J. (2016). Diagnosing crop water stress of rice using infra-red thermal imager under water deficit condition. *Int. J. Agric. Biol*, *18*, 565–572.

Yang, W., Feng, H., Zhang, X., Zhang, J., Doonan, J. H., Batchelor, W. D., Xiong, L., Yan, J. (2020). Crop phenomics and high-throughput phenotyping: past decades, current challenges, and future perspectives. *Molecular Plant*, *13*(2), 187–214.

Yi, Q. X., Bao, A. M., Wang, Q., Zhao, J. (2013). Estimation of leaf water content in cotton by means of hyperspectral indices. *Computers and electronics in agriculture*, *90*, 144–151

Young, S. N., Kayacan, E., Peschel, J. M. (2019). Design and field evaluation of a ground robot for high-throughput phenotyping of energy sorghum. *Precision Agriculture*, *20*(4), 697–722.

Yue, J., Yang, G., Li, C., Li, Z., Wang, Y., Feng, H., Xu, B. (2017). Estimation of winter wheat above-ground biomass using unmanned aerial vehicle-based snapshot hyperspectral sensor and crop height improved models. *Remote Sensing*, *9*(7), 708.

Zeng, X., Miao, Y., Ubaid, S., Gao, X., Zhuang, S. (2020). Detection and classification of bruises of pears based on thermal images. *Postharvest Biology and Technology*, *161*, 111090.

Zhang, D., Zhou, X., Zhang, J., Lan, Y., Xu, C., Liang, D. (2018). Detection of rice sheath blight using an unmanned aerial system with high-resolution color and multispectral imaging. *PloS one*, *13*(5), 0187470.

Zhang, J., Wang, C., Yang, C., Xie, T., Jiang, Z., Hu, T., Luo, Z., Zhou, G., Xie, J. (2020). Assessing the Effect of Real Spatial Resolution of In Situ UAV Multispectral Images on Seedling Rapeseed Growth Monitoring. *Remote Sensing*, *12*(7), 1207.

Zhang, L., Zhang, H., Niu, Y., Han, W. (2019). Mapping maize water stress based on UAV multispectral remote sensing. *Remote Sensing*. *11*(6), 605.

Zhao, D., Reddy, K. R., Kakani, V. G., Reddy, V. R. (2005). Nitrogen deficiency effects on plant growth, leaf photosynthesis, and hyperspectral reflectance properties of sorghum. *European journal of agronomy*, *22*(4), 391–403.

Zheng, H., Zhou, X., Cheng, T., Yao, X., Tian, Y., Cao, W., Zhu, Y. (2016). Evaluation of a UAV-based hyperspectral frame camera for monitoring the leaf nitrogen concentration in rice. *In 2016 IEEE International Geoscience and Remote Sensing Symposium IEEE* (pp. 7350–7353).

Zovko, M., Boras, I., Švaić, S. (2018). Assessing plant water status from infrared thermography for irrigation management. *Proc. 14*th *Quantitative Infrared Thermography Conference*.

Zúñiga, C. E., Khot, L. R., Jacoby, P., Sankaran, S. (2016). Remote sensing based water-use efficiency evaluation in sub-surface irrigated wine grape vines. *Autonomous Air and Ground Sensing Systems for Agricultural Optimization and Phenotyping. International Society for Optics and Photonics*, 9866 (pp. 98660).

ECOSYSTEMS AND GLOBAL CHANGES

Viliam NOVÁK

Institute of Hydrology, Slovak Academy of Sciences, Bratislava, Slovakia

Increasing population has led to the increasing demand for food, raw materials, and energy. Continuing land use changes, intensification of its exploitation, deforestation, fossil fuel combustion, and related carbon dioxide production have been contributing to change of water and energy balance of the globe, thus changing conditions for life. Other reasons for changing conditions on the Earth are natural changes in interactions between the Earth and outer space. Actual climate change is a part of other global changes resulting in both natural and anthropogenic changes. It is mostly felt as a change of global temperature and increase of precipitation intensities and totals. Flood periods are followed by long periods without precipitations. Increasing population as well as increasing consumption of resources lead to the increasing imbalance between our planet production and consumption. To preserve good conditions for population of the Earth, it is necessary to decrease consumption of energy, raw materials, and food to reach equilibrium between Earth´s ecosystem production and consumption of the ecosystem products.

Keywords: ecosystem, global changes, climate change

Planet Earth is one of the smaller planets of the Solar system, its surface is 520×10^6 km^2, where dry land comprises less than one third of our planet surface (149×10^6 km^2). Area of arable land comprises 12% of dry land only (19.8×10^6 km^2), thus creating ecosystem of crops, which is the basic source of food for mankind. Animals as well as fish and plants are important parts of food supply. It could be a surprise, that the area of deserts of the Earth is approximately the same as the area of arable land. Forests cover a major part of dry land (60×10^6 km^2), which represents 38% of Earth`s surface. The dry land glaciers are covering the area 15.7×10^6 km^2, which is a little bit less than is the area of arable land. The rest of dry land is covered by steppes, savannas, non-vegetated surfaces in the Antarctic zone, and residential zones, industrial areas, and non-permeable surfaces like roads and water surfaces.

Earth is populated approximately by 1.5×10^6 of animal species, and about 1.0×10^6 of them are insects, therefore our planet is often called the "planet of insects". The existence of individual animal species is dependent on other animal or plant species. It means that elimination of one of species can lead to extinction of another. Any animal or plant species is an important element in food chain link of animals and human beings. During the period 1,600–1,975, about 136 species of birds and 68 species of mammals went extinct, but in 20th century, 85 mammals' species disappeared from the planet Earth for good.

According to the Food and Agricultural Organisation (FAO) (2012), rate of natural ecosystems degradation is increasing. In 1937, 66% of worlds ecosystems were in natural (intact) state, but in 2020, natural ecosystems comprised only about 35% of the dry land area. In the European Union, only 17% of biotopes preserved by European legislative are in favourable state.

In Slovakia, there are only 14.68% of natural ecosystems in natural state, which is an exceptionally low value. The rest of ecosystems are highly modified (Izakovičová, Špulerová, 2018), and 75.1% of mammals were living in unfavourable conditions in 2017, according to the Ministry of Environment of the Slovak Republic (MŽP SR) (2018).

Therefore, protection and preservation of all the assortment of existing animal and plant species is so important for mankind.

The only anomaly among living species of Earth is human beings. It is the only living species, which can adapt to changing conditions, and to change environment in such a way, that it not only preserves, but increases its population in an uncontrolled way. As it was mentioned before, people are changing the biosphere of the planet and thus endangers mankind as well as the rest of living organisms (Kutílek, Landgráfová, Navrátilová, 2013). Some philosophers assume existence of human beings on the Earth as anomaly, and danger for a functional planet (Münz, 2019).

An example of ecosystem devastation is the story of Mesopotamia. The fertile soils of this area gave yields much higher than in previous sites, but soil salinization due to irrigation by mineralized water dropped yields significantly to only 10 to 20% of the former yields. In the final stage of soil degradation, the state system collapsed, and inhabitants moved to other, more favourable sites. In the Northern Hemisphere, "movement of nations" was accompanied by

Contact address: Viliam Novák, Institute of Hydrology, Slovak Academy of Sciences, Dúbravská cesta 9, 84104 Bratislava, Slovakia; ☏ +421 91 02 596 79; e-mail: viliamnovak42@gmail.com

the cooling effect of the climate (Kutilek, Nielsen, 2010) and probably by the degradation of soils by the exhaustion of natural fertilizers. Today's organization of the world does not allow for massive transfer of people to other, more favourable sites for living and lead to intense, spontaneous immigration to Europe and the USA.

Human beings as biological species live in an environment called biosphere, it is a thin layer of Earth's surface, with favourable conditions for life. The thickness of this layer is about 10 kilometres. Let the Earth be represented by a geoid 3 meter in diameter, then the thickness of biosphere (ecosystem) will be 1 mm only. It is a thin, very vulnerable area, characterized mostly by influx of photosynthetic active radiation, suitable biosphere temperature, specific properties of the atmosphere, and other properties needed for photosynthesis.

Plants (their seeds) and men (if there is enough sources of energy) can survive in all the temperature intervals present on Earth (-88 to +58 °C). Biomass is the first element in nutrition chain of animals and is a product of photosynthesis, which can occur in the air temperature interval 0 to +40 °C, but the optimum air temperature is about 30 °C. Therefore, the existence of human beings on Earth is limited by environmental (ecosystem) properties, suitable to produce biomass, which is the source of energy for all living organisms on Earth.

The share of arable land is approximately 12% of the dry land surface of Earth (with possible increasing to up to 14%). It is clear that Earth's biomass production is limited and can supply only a limited number of population. The same is valid for supply by energy and especially for non- renewable resources like oil, raw materials, gas, etc.

Global changes

Global changes refer to planetary scale changes in Earth system. Global changes comprise of changes in environment, human society and economy. In principle, any activity in the ecosphere is influencing the Earth globally, but it is assumed that "global change" is such a change which can be clearly identified at the global scale. Global change interactions are those among Earth, the Sun and planets, and also changes in quantity and quality of Earth's surfaces, increase in carbon dioxide concentration in the atmosphere, and changes in plants and animals quantity and quality. All those changes can contribute to the well known effect called "climate change" which is only one of many particular global changes, and could contribute to creation of new conditions for life.

Risks for the ecosystems on the Earth

Natural (non-anthropogenic) risks

Continuous decrease of Solar radiation rate

The time interval during which solar energy income of Earth will cover the necessary rate needed to preserve actual state of life is limited. Calculations show that the Sun has the fuel for the next 4×10^{12} years. Todays´ average rate of solar radiation income to the upper limit of the Earth's atmosphere can be expressed by the so called Solar constant, 1,360 W.m^{-2}. It is expected that the Sun radiation rate will be

decreasing, depending on the quantity of remaining fuel, and the conditions for preserving existing state of life can cease long before the total burn out of the Sun. There is not expected a significant decrease of solar radiation in the next million of years.

Collision of Earth with a space object

Collision of this type is not excluded, it can have a fatal consequence on the life on Earth.

Anthropogenic risks

Increasing population

In 2019, 7.75 billion of people lived on Earth. It is assumed that in 2050, the number will increase to about 10 billion. Two thousand years ago, at 0 A.D. it was estimated, there were about 180 million people inhabiting Earth. In 1820, there were about one billion people, and about 110 years later (in 1930) there were approximately two billion people. During the last 90 years there was a gain by 5 billion people. Approximately 6 billion of people live in Asia and Africa. Even now, population explosion in Africa is generating a population gain higher than 50 million per year i.e. higher than 3%. It is expected that in the sub-Saharan Africa and in Asia there will live about three quarters of the Earth's population by 2050. The sub-Saharan Africa and some Asian countries are economically known as developing countries with low GDP values. This trend in population generates pressure on increase of food production, as well as on production of raw materials and energy. In those countries, there is a lack of arable land, food, water, and fertilizers. The shortage of arable land, fresh water and energy, and lack of resources to intensify agriculture in countries with the highest population increase are the main reasons for increasing emigration, mostly to Europe. International aid from the developed countries can help, but the existing and future problems cannot be fully solved this way.

Food

The lack of food itself is not the threat for ecosystems, but it generates the pressure on them. Intensification of agriculture and overfertilizing as well as massive application of herbicides and pesticides contribute to soil degradation. The change of former forests to arable land, especially rainforests clearing and their transformation to arable land, is changing the structure of mass and energy flow. Increasing number of cattle and other domesticated animals has led to overgrazing and degradation of soils. Extensive fishing can lead to the critical decrease in their populations. The lack of food in developing and most populated countries can lead to non-equilibrium states, to riots and war, and to extensive emigration within countries and to relatively more economically developed countries. According to FAO (2012), about 800 million of people suffer by the lack of basic food, more than two billion is without balanced food and suffer from the lack of vitamins and minerals, which can lead to malnutrition and to unfavourable state of population health. According to the data of the UNO, the food production have to be doubled by 2050 (Rosen and Ritchie, 2013). Proportional increase of arable land area is constrained, food production increase has to be done by

intensification of agriculture; by introduction of new, more productive crops species, by irrigation, drainage, fertilizing, and application of herbicides and pesticides. This process has its downside, as it was mentioned before. Approximately 20% of irrigated fields produce up to 40% of all agricultural products; such soils are located mostly in the developed countries, which possess enough funds to built and run such intensive agriculture.

Water

Water quantity on the Earth (in the part of the environment called hydrosphere) is approximately the same as it was in the past. Water we are drinking is the same which was drunk by dinosaurs millions of years ago. The freshness and redistribution of water is kept by the process, known as water (hydrological) cycle. Water is fresh, thanks to the process of evapotranspiration. The process of evapotranspiration (evaporation from wet surfaces plus evaporation from plants – transpiration) is energetically the most demanding process on Earth. Hydrological cycle starts by the evapotranspiration of water from water surfaces, plants and other wet surfaces on Earth. Water vapour in the atmosphere is turn into water drops in the process of condensation when ambient temperature decreases. Water vapour creates clouds; and if the diameter of water drops reaches about 0.1 mm, then they fall as precipitation. Water falling on the Earth's surface partially evaporates, partially accumulates in the soil as a soil water and groundwater, and part of it outflows by rivers to the sea or accumulates in lakes and wetlands.

All the water on Earth can cover the layer of 2,800 m thick; as a part of it, the thickness of fresh water layer would be about 70 m. Technically, all the water on Earth can be treated by known technologies to fresh water; but it needs complicated and expensive technology.

Water cycle is important in order to preserve life on Earth. Approximately 90% of incoming energy from the Sun is used to change liquid or solid state of water to water vapour by evaporation from seas or rain forests. Evapotranspiration of the dry land is usually less intensive, because water content of soil is sometimes limiting evapotranspiration rate. In general, more than 50% of solar energy reaching the Earth`s dryland surface is consumed by the process of evapotranspiration.

Without consumption of solar energy by evapotranspiration, temperature of biosphere would increase to the level not compatible with life on Earth. As it will be shown later, anthropogenic changes of dry land surfaces can significantly contribute to modification of water and energy balance equation structure and thus strongly influence climate of Earth. Consumption of energy by evapotranspiration from surface of the globe (latent heat of evaporation) is equivalent to 2×10^4 of all energy, transformed by the Earth's power plant stations. Therefore, evapotranspiration is the main consumer of energy on Earth and is creating favourable conditions for life (Novák, 2012).

Another basic feature of the water cycle of the Earth is permanent cleaning (distillation) of water by evaporation. Natural water cycle works as a gigantic distillation system powered by solar energy. Its first phase is evapotranspiration. The result of its function is clean, distilled water, permanently

returning to the Earth surface by precipitation. To do so, it is necessary to keep atmosphere clean, because precipitation during the fall to the surface is dissolving substances in the atmosphere. The most dangerous kind of precipitation has been the so called "acid rain" water dissolving sulphur in the air as a product of coal burning, so the result is a low concentration of sulfur acid. Such rain is devastating plants and small animals. Thus, one of the main conditions of good water quality preservation is clean atmosphere. Water infiltrating the soil, groundwater and rivers is dissolving minerals contained in the surface soil layers. Water with concentration of minerals less than 500 mg.l^{-1} which meets additional 82 criteria according to Slovak standards (The Government Regulation no 354/2006 Coll.), can be used as fresh water.

Is there enough fresh water for all of us?

Assuming "business as usual", i.e. discharge of rivers will not change, and 10^{10} people by 2050, then for one person and one day there will be approximately 10,000 litres of fresh water in rivers. WHO recommends a minimum consumption of 70 litres of water per person per day (l.person^{-1}.day^{-1}). The discharge of one of the rivers (the Amazon) can deliver 1,300 l.person^{-1}.day^{-1}, which represents about 16 times of minimum consumption quantity per person and day. Why are we dealing with rivers only? The rest of precipitation (about two thirds of total precipitation falling to the dry land) evaporates, mostly as a transpiration, and participating in biomass production. Therefore, rivers discharge represents real resources of mankind consumption.

In conclusion, there is enough fresh water for everybody even in the future. But freshwater resources are not distributed evenly over the globe and are not available everywhere. Correction in uneven geographic distribution of water e.g. by desalinisation of salty water – can be conducted by the richest countries only. On the other hand, a lack of fresh water can lead to existential problems (lack of water for irrigation), to health problems, and generate pressure on emigration.

Water and Slovakia

Average river discharge from the Slovak territory is approximately 400 m^3.s^{-1}, or 6,400 l.person^{-1}.day^{-1}. The average discharge of the Danube itself is 2,000 m^3.s^{-1}, which represents about five times volume of all the Slovak rivers. Of course, the Danube as an international river body cannot be exploited without limits according to international agreements. Water from the Danube is continuously recharging groundwater, mainly in the upper part of Žitný ostrov, the area that is the most important reservoir of groundwater in Slovakia to supply population by fresh water. Therefore, the upper part of Žitný ostrov was declared a protected area (Chránená vodohospodárska oblasť); it is one of ten protected areas in Slovakia. According to the Slovak Hydrometeorological Institute (SHMÚ) and Slovak Agency of Environment Protection (SAŽ (Kollár, 2001)), the estimated capacity of fresh water resources of Slovakia is 146.7 m^3.s^{-1}, and as a part of it the estimated capacity of groundwater resources is 79 m^3.s^{-1}. Žitný ostrov resources of groundwater is 25 m^3.s^{-1}. The estimated capacity of existing resources of water in Slovakia (surface and groundwater

resources) is 32,800 l.s^{-1}, which covers about three times of contemporary fresh water consumption, 12,800 l.s^{-1}. Actual public freshwater consumption in Slovakia is approximately 80 l.person^{-1}.day^{-1}, just above the minimum consumption limit recommended by the WHO. This is the result of economic stimulation of freshwater consumption because the price of fresh water is relatively high. Groundwater resources of freshwater cover 80% of fresh water consumed in Slovakia. The quality of fresh water depends on its protection against pollution. The main risks of Žitný ostrov groundwater pollution are overfertilizing, intensive application of herbicides and pesticides as well as illegal waste dumping.

Raw materials and energy

Raw materials and energy are special entities needed to preserve human beings on the Earth. This term represents basic, unprocessed materials needed as inputs into the production process. They can be divided to basic and others raw materials. Raw materials are non-renewable, and their resources are limited. Their intensive consumption means threat for the mankind. The sustainable source of energy for processes on Earth is solar energy. It drives all the processes of mass and energy as global water and energy cycles, and part of its spectrum – photosynthetically active radiation (PAR) is active in biomass production. Fossil fuels deposits are results of biomass production in the distant past. The role of solar energy is extremely important in order to keep conditions suitable for life on Earth.

Basic renewable materials (water, air)

Renewable materials are prerequisites for life on Earth. Their quantity is constant, and they cover the need of population. The problem is to maintain their cleanliness because existing technologies of fossil fuels burning and deposits of waste are danger to both water and air. The problem of fresh water is its uneven distribution in time and space, there are areas chronically wet while others are chronically dry.

Raw materials

Raw materials such as oil, gas, raw mineral materials, coal, building materials, salt, etc. are non – renewable, and their mining rate is increasing. Biomass (wood, natural fibres, crops, animals) represents the renewable ones. The annual world production of raw minerals in 2017 was 17.2×10^9 t.year^{-1}; it has increased by 50% during the last 17 years (World Mining Data, 2019). Production of oil is 4.31×10^9 t.year^{-1} (largest producer is USA, 5.71×10^8 t.year^{-1}, and Saudi Arabia with production 5.61×10^8 t.year^{-1}). Production of gas in 1917 was 3.77×10^9 t.year^{-1} (largest producer is the USA, 7.72×10^8 t.year^{-1}, then Russia 6.91×10^8 t.year^{-1}). The major producer of raw materials is China (4×10^9 t.year^{-1}), and the USA with production 2×10^9 t.year^{-1}. China is producing more than a half of the world production of coal (2.62×10^9 t.year^{-1}) and more than a half of the world production of aluminium (33.3×10^6 t.year^{-1}). Burning of coal produces great amounts of carbon dioxide, which is an important greenhouse gas and therefore its mining ought to be limited. In Europe, coal is mined in Poland and the Czech republic only. Specific raw-materials are rare elements (comprising 17 metals, like neodymium, praseodymium, lanthanum,

europium, yttrium, etc), that are used in IT hardware. The title "rare earth" is characterized by its low content in surface layers of Earth. Up to 90% of rare metals is produced by China. The biggest deposits of rare metals are in Venezuela (17.8% of world`s deposits), 40% of cooper is mined in Chile, the largest producer of iron ore is Australia, representing about one third of world production (5.48×10^8 t.year^{-1}).

Raw materials are non-renewable resources, and their deposits are limited. If their mining will run at the same rate as until now, the maximum mining rate is expected around 2030. The estimated stores of coal would last approximately 150 years, gas deposits about 50 years, oil deposits could last 30 to 80 years depending on the rate of extraction (according to the British Petroleum). Phosphorus, used to produce fertilizers, could last 50–100 years. In Europe, basic deposits of raw materials were exploited; their exploitation runs mainly in Africa, Asia, Australia and South America. It is expected that the yield of those deposits will decrease in next decades. Recycling of materials can improve the situation, but it cannot replace expected raw materials deficits in the future.

Above estimations are approximate, because it is expected that new deposits of the above-mentioned raw materials could be found. Across the globe, there are huge deposits with relatively low content of minerals and their extraction is not economical yet, but in the future, the lack of raw materials can change economical criteria, and even those deposits would become interesting, because the price of products using them will be increasing. Waste collection and their recycling will be an important part of economy. Products using recycled materials will be much cheaper than products from raw materials. Deposits of raw materials in Slovakia were mined out in previous centuries, and at present are minimal, therefore import of raw materials or products will be necessary.

Energy

Population at any stage of its development is transforming (consuming) some quantity of energy. In the past, there were used renewable sources of energy (wood, wind) or the energy of animals, including human beings. In the past (around 1,600 AD) the estimated consumption of energy was 20 kWh.d^{-1}.person^{-1}, which is equivalent to energy gained by burning 4 kg of wood. The total consumption of energy was about 8 GW. Actual (2010) estimations are 125 kWh.d^{-1}.person^{-1} (MacKay, 2015). Modern civilisation is consuming approximately 15 TW energy, mostly from burning fossil fuels (oil, gas, coal). It means that actual energy consumption is more than three order higher than in the Middle Ages. Renewable resources of energy cover relatively a small part of civilisation needs (approximately 20%), the substantial part of it is energy of water, other resources of energy (solar energy, energy of wind) are contributing only about 3%. Water energy use is close to its maximum, but solar and wind energy are increasing their share, because their price is continuously decreasing.

At the global scale, the most important source of energy is oil (37%), then coal (27%), gas (23%), and nuclear energy (6%) (Makarieva, Gorskhkov, Li, 2008). Those resources are also producers of carbon dioxide (with exception of nuclear energy), which is a significant greenhouse gas. The share of

renewable sources of energy is about 13% only. About 87% of Earth`s energy input is related to procedures generating greenhouse gases. As it can be seen from the structure of energy sources, the highest consumption of energy is related to transportation. Specific feature of renewable sources of energy is their instability because they depend on the rate and duration of the sun radiation, wind velocity, generally, on weather conditions. Potential renewable sources of energy depend on their geographical position. The hope is a nuclear synthesis, but realisation of this idea cannot be expected in the near future.

The income of solar energy at the upper boundary of the atmosphere is 1.7×10^5 TW. The consumption of the contemporary population is about 15 TW, which is only 0.0001 part of income of solar energy at the upper boundary of the atmosphere. The Earth`s surface income is $8 \times 10^4$ TW, but about $2 \times 10^4$ TW is radiating back to the atmosphere. Atmosphere is partially intercepting this energy and radiating it to all directions, even back, to Earth. This radiation of the atmosphere back to the Earth`s surface is increased by the presence of carbon dioxide as a result of fossil fuel burning. The basic part of energy available at soil surface (net radiation) is consumed by evaporation and transpiration. Therefore, transpiration, which is even a part of the biomass production process is also a basic process of Earth`s temperature stabilisation, needed to keep temperature of the ecosystem in the comfort zone.

Under conditions of environmental stability, it was estimated (Makarieva, Gorskhkov, Li, 2008), that renewable sources of energy (energy of water, solar and wind energy, energy of tide) could cover about one tenth of modern civilisation needs. It is necessary to decrease consumption of energy to the level which can be covered by renewable sources of energy, because its deficit can endanger existence of civilisation.

Energy and Slovakia

Slovakia is a country without significant sources of energy. Resources of oil, gas and coal are small, and energy or raw materials for its production are imported. As renewable sources of energy there can be used water, and eventually biomass. Conditions to use solar or wind energy are limited, because of orography and limited rate and duration of solar radiation.

In 2016, nuclear power plants in Slovakia generated 59.6% of all energy used, hydro plants 16.8%, power plants combusting coal and oil 12.9%, biomass 4.2%, and photovoltaic and wind powerplants 7.3%. In Slovakia, about 28.3% of the generated energy was from renewable resources, which is a remarkable result. Development of nuclear power plants seems to be reasonable in Slovakia. Slovak economy should be oriented on production with minimum inputs of raw materials and energy (Lubyová, Filčák, 2016).

Climate change

The climate is a generalized characteristic of weather, typical for a particular area; it can be characterized by meteorological characteristics, such an air temperature, wind velocity, and precipitation. There are no doubts that the climate of Earth has been changing. During the last century, the average temperature of Earth increased by about 1 °C. Climate changes are not homogeneous across the globe; they are more intensive in southernmost and northernmost parts of Earth. As an example of temperature increase, there can be mentioned the meteorological station Hurbanovo, where the average air temperature increased by about 2 °C since 1908 (Pekárová, Miklánek, Pekár, 2017). It is approximately the difference of average annual air temperature between Bratislava and Banská Bystrica.

During pre-industrial era (approximately up to the half of the nineteenth century), the climate changed mostly by the natural reasons, like interaction among Earth, the Sun, and planets. The volcanic activity proved important; eruption of huge quantity of volcanic material changed optical properties of atmosphere and thus impacted energy flow among Earth and outer space.

The present state of society is characterized by increasing population and by the proportional demand for fresh water, energy, food, and raw materials. This demand provokes increasing exploitation of raw materials, industrial and food production. This process is related to building of industry, extensification and intensification of agriculture, and new sources of energy. There is pressure on enlarging areas of arable land, production of chemicals used in agriculture and the need to increase quantities of water for irrigation and thus change of land use and land surface properties.

Anthropogenic activity significantly changed the properties of our planet´s surface. Natural plants canopy is strongly modified. Instead of natural, green surfaces there are fields, buildings, and communications. Approximately 60% of dry land surface is significantly changed by human activity and thus, it is changing the structure of water and energy balance of Earth and its climate.

The reasons of climate change

The reasons of climate change can be divided to natural and anthropogenic ones.

Natural reasons of climate change

Natural reasons of climate change are due to the changes of interrelations between Earth and the Sun, resulting in the rate of solar energy delivery change. Among those reasons, there are irregularities of Earth`s orbiting, the changes of the Earth axis angle in relation to the ecliptic and wobbling of the Earth`s axis during its orbiting. Even the Sun periodically changes its radiation rate (Kutílek, Nielsen, 2010). Those phenomena were changing climate in pre-industrial age (up to 19th century). The ice age ended about 10 thousand years ago, a medieval warm period and little ice age (14th–19th century) were the results of natural (non-anthropogenic) change of climate (Figure 1.).

Anthropogenic reasons of climate change

These are changes of ecosystems by anthropogenic activities, during the last two centuries, and they are becoming more intensive (Kutílek, 2008). The most important reason of the anthropogenic climate change is related to land use changes. The production of carbon dioxide by fossil fuels burning is contributing to the climate change, too.
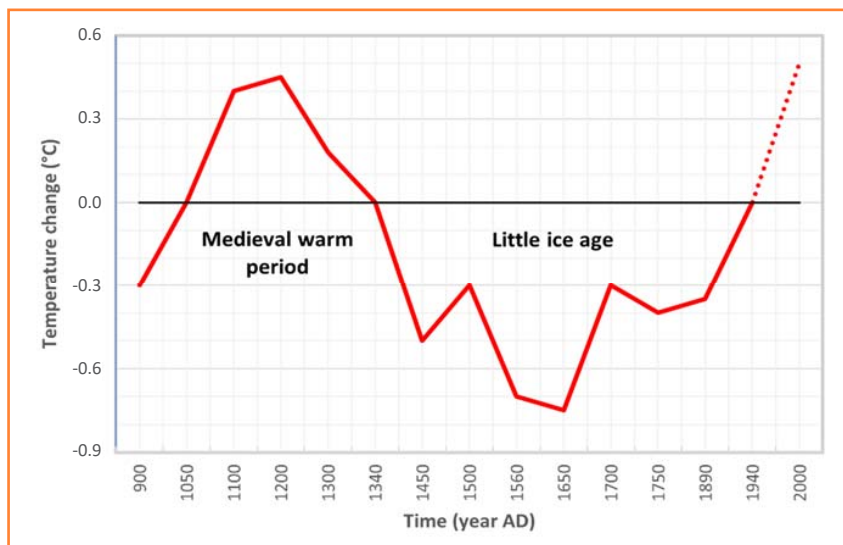
Figure 1 Temperature change in the last millennium according to IPCC, 1990
Source: Houghton et al., 1990

Land use changes

Probably the most important contribution of human activities to the climate change is the continuous change of land use by increasing population. The most important activities are deforestation of rain forests (Brazil, Africa, South Asia), elimination of wetlands, increasing area of arable land, overgrazing, monoculture agriculture, increasing urban and industrial areas as well as transport facilities (highways) (Kutílek, 2008). Those activities completely change natural vegetation and structure of water and energy balance of territories. The obvious result is the decrease of evapotranspiration totals. Solar energy not used to water phase change heats biosphere and thus contributes to global warming. Tropical rain forests are characteristic by high precipitation totals (more than 3,000 mm of water layer per year), and by high income of solar energy (average income is 350 $W.m^{-2}$; for comparison, on the territory of Slovakia this income is 125 $W.m^{-2}$). High income of water and energy is resulting in annual evapotranspiration totals of more than 2,500 mm of water per year (in Slovakia, there is approximately 500 mm water layer) (Shuttleworth, 1988; Novák, 2012). What does it mean for water and energy balance of Earth?

Intensive deforestation of rain forest and its change to agricultural land, buildings, and transport infrastructure is changing properties of evaporating surface. According to the Food and Agricultural Organisation (FAO) (2012), about 100,000 km^2 of rain forests are eliminated per year (more than the area of two Slovak territories). If it goes this way, to the end of this century, all the tropical forests will be changed into agricultural land. The most important is that evapotranspiration rate will decrease significantly because the increased part of precipitation will run off. It is estimated that evapotranspiration flow will decrease approximately to one half of the previous state. Therefore, about a half of the solar energy reaching soil surface at the constant rate will not be used as latent heat of evapotranspiration but will be heating biosphere and thus increasing its temperature. This is the primary reason of warming with adjective "global", because it is contributing to temperature increase around the globe.

The most important "glasshouse" gas is water vapour, because it disperses long wave radiation of Earth in all the spectrum range more effectively than carbon dioxide, with its relatively narrow range of dispersion. The concentration of water vapour is proportional to air temperature and increasing temperature of atmosphere increases equilibrium water vapour concentration and thus increase the "greenhouse" effect of the atmosphere. Carbon dioxide concentration is changing. From 318 ppm in 1960 (ppm means parts of

CO_2 molecules, per million of all air particles), to 420 ppm in 2020. But water vapour concentration depends on air temperature and ranges from 6,000 ppm (at 0 °C) to 20,000 at 20 °C. Nevertheless, absorption spectrum of water vapour is much broader than this spectrum for carbon dioxide.

Existence of the atmosphere (and water vapour and carbon dioxide as its components) is increasing biosphere temperature to about 33 °C. Without this function of the atmosphere there will be average air temperature of -18 °C, instead of the current 15 °C. The problem we are dealing with is the actual increase of this effect, so we should try to eliminate the anthropogenic effects on air temperature. Until now (2020), this additional increase of the greenhouse effect on average air temperature is about 1 °C. The biosphere is a very sensitive area and increase of the greenhouse effect can dramatically change the conditions of life on Earth.

Fossil fuels burning

Fossil fuels (oil, gas, coal), as well as renewable sources (biomass) burning produces the greenhouse gas carbon dioxide (CO_2). This gas, as a part of the atmosphere, disperses energy of long-wave radiation of Earth to all directions and thus increases the temperature of the biosphere. The production of CO_2 in Europe has significantly decreased, but the world production has still been continuously increasing.

Climate change consequences

Increased dynamics of water and energy in biosphere

Biosphere temperature increase means additional available energy, which can be used to transport mass and energy. Because about 70% of the Earth's surface is covered by oceans and other water surfaces, evaporation from those surfaces will increase proportionally. Higher amounts of evaporated (evapotranspirated) water mean higher and more intensive precipitation and increased weather extremization. It means that there could be expected more intensive precipitation and higher precipitation totals leading to "flash" floods. Weather extremes mean even longer periods without precipitation.

What can be expected in water and energy dynamic change in Slovakia?

Forests of temperate climatic zone in Slovakia are slowly increasing their area and cover more than 40% of the Slovak territory. Reduction of arable land area (14,400 km^2, i.e. 29% of Slovak territory) in the last decades is significant. Impermeable surfaces (buildings, communications, industrial objects) have grown in the last decades, which leads to local runoff increase and decrease of evaporation, followed by the temperature increase.

As a result of the climate change, there was measured air temperature increase during the last century of about 1 °C. This gain increases the potential evapotranspiration, i.e. maximum possible under given conditions. Global increase of evaporation, particularly from oceans and seas is resulting in precipitation totals increase around the world. Evapotranspiration in Slovakia has increased by about 10% during the past 30 years, but the potential evapotranspiration increased even more, reflecting higher temperature of the atmosphere (Pekárová, Miklánek, Pekár, 2017). As a result, the runoff – especially in southern parts of Slovakia – is decreasing and recharge of groundwater, the basic resource of fresh water supply in Slovakia, is decreasing, too. Therefore, there is an urgent need to retain as much water as possible in catchments. The effective methods of water retention increase are relatively large water reservoirs (with volumes of several million cubic meters) and managed aquifer recharge (MAR).

The arrangement of small water reservoirs is not a good solution. In reservoirs with a small retention volume, water quickly increases its temperature, followed by eutrophication and overgrowing. Water in such reservoirs cannot be used for irrigation and communal consumption, and they are not worth investment. A suitable method to increase retention of water is artificial infiltration of water from channels or rivers to recharge groundwater. Utilisations of infiltration basins with permeable bottom to recharge groundwater are often used in some countries (managed aquifer recharge (MAR)).

Another frequent myth is the idea of increasing retention of water in the landscape by forestation. Forestation of land is a good idea, because green woody surfaces with relatively high rate of transpiration consume solar energy and thus decrease ambient temperature, as well as incorporate carbon dioxide in the process of photosynthesis, and they are important anti-erosion elements, but they do not accumulate water.

On the contrary, water retention by forests is small, and forests intensify water circulation. About one third of annual precipitation in coniferous forests is intercepted and evaporated (in deciduous forests it is about one fifth of annual precipitation); this part of precipitation even does not reach soil surface. This phenomenon is not felt negatively, because forests are usually located in mountains with high precipitation totals. But this phenomenon significantly decreases the runoff.

Climate change is accompanied with increasing risks of local floods. Forests´ interception capacity up to 6 mm water layer cannot prevent floods, because rain intensity is often higher than 10 mm per hour and such precipitation event total is often higher than 100 mm. If the soil is fully saturated with water from previous precipitation events, practically all the precipitation can outflow and the result is "flash flood" (Pekárová, Svoboda, Novák, Miklánek, 2011). Such floods were observed in small, forested catchments in last years.

The idea of the "green landscape" is a good solution. Green canopies consume energy to transpire, absorbing carbon dioxide in photosynthesis; they are important anti – erosion elements and, what is most important for people, they produce biomass as the basic element of food chain of all living organisms.

Desertification and soil degradation

Desertification

Desertification is the process of soil degradation of agricultural land to the areas unsuitable for agricultural activity such as steppes, savannas, and deserts. Such territories are becoming dry, due natural or anthropogenic activity, or by combination of both. These processes were running even in the past, but their intensities were different. Today`s degradation and desertification process is intensified by global warming and by intensified land use. Degradation of soils and eventual desertification is actual mostly in arid zones of Earth. Arid zones of Earth cover about 38% of dry land area (57×10^6 km^2), where live about 2.7 billion people. Up to 90% of the arid area is located in developing countries with high natality rates (Dregne, 1977).

Approximately one eighth of dry land (12.5%, i.e. 19.8×10^6 km^2) are deserts, and the rate of their expansion (desertification) is approximately 120,000 km^2 annually, which is more than the two territories of Slovakia. The Sahara Desert is the most extensive desert of the planet (its area is about 9×10^6 km^2), and it is expanding according to the satellites measurements by about 60,000 km^2 annually. Since 1900, the Sahara Desert moved its boundary to the south by 250 km, the additional desert area is about 1.5×10^6 km^2, and this process accelerates. The process of desertification is actual even in South America, Australia and in Asia, but its intensity is smaller.

What are the main reasons of desertification?

They can be divided to natural (contribution of extra-terrestrial interactions on the climate change) and anthropogenic due to mankind activities. Main land use changes (anthropogenic activities) leading to soil degradation are the following: unsuitable agrotechnics, forests clearing (mostly rain forests), and overgrazing.

Land use changes and desertification

Natural surfaces of dry land were mostly forests, savannas, steppes, and deserts. Arable land area and impermeable surfaces (buildings, roads) areas are so small they cannot influence the climate. During the last two centuries, the natural structure of land`s surfaces significantly changed as a result of the increasing number of populations with their claims, on food, energy, and water. As it was mentioned previously, during the last 100 years the number of Earth population increased four times, from 2 billion in 1927 to 7.6 billion in 2019. Increasing of arable land area and intensification of agriculture by application of chemicals (fertilizers, herbicides, and pesticides), and using heavy

machinery is the result of increased population needs. Correspondingly, it led to the decrease of forest and meadow areas and increase of impermeable surfaces like roofs, roads, etc., which significantly influence water and energy regimen of territory. Even in Slovakia, there is a surprisingly high ratio of industrial buildings and stores built on the best agricultural soils. This means loss of production capacity of agriculture and increasing ratio of impermeable surfaces, less consumption of energy on evaporation and thus additional increase of air temperature. By the extensive building activities in Slovakia, the portion of impermeable surfaces is close to 5% of the Slovak territory. This increase can significantly influence water and temperature regimen of area and its microclimate.

Unsuitable agrotechnics

Unsuitable agrotechnics is the reason of soil degradation, too. Unprotected and disturbed soil surface is sensitive to wind (and water) erosion especially in desert and semi-desert areas. Agricultural land is not protected (especially after the season) against the wind and high temperatures, which can be the reason of soil surface destruction and its transport by wind or occasional rain. Remember the transport of Sahara fine sand (May 2020) to Slovakia, which was visible on cars surfaces. This is one of the ways how deserts expand. Bulk density of subsoil increasing, and its hydraulic conductivity decrease by heavy machinery prevents water infiltration to soil and to groundwater.

Overgrazing

Increasing number of cattle is the reaction to the increasing demand for food. Cattle is grazing sparse vegetation in savannas and steppes, mostly in Africa. This way of pasture is usually leading to vegetation canopy damage and to destruction of soil surface by cattle hooves. The result is increased sensitivity to wind (and water) erosion and to desertification of territory.

Deforestation

This problem was partially discussed previously, in the part of rain forests clearing and its influence on climate. Existence of rain forests is basic for climate stability not in a particular site, but across the planet. Its significance is given by extremely high rates of water and energy fluxes between rain forests and the environment. High rates of evapotranspiration are expressed in water layer thickness (2,500 mm.m^{-2}.year^{-1}) and related extremely high energy consumption by evapotranspiration (6.25×10^9 J.m^{-2}.year^{-1}). This huge consumption of energy to evaporate water from rain forests basically influences water and energy fluxes in the planet scale. To evaporate water from wet surfaces in the area between tropics, about 90% of all solar energy reaching the Earth`s surface is needed (Shuttleworth, 1988). It is estimated that after clearing of rain forests, evaporation will decrease by about a half, and the rest of energy is used to heat the biosphere and thus contribute to global warming. Rain forests also incorporate great amount of atmospheric carbon dioxide in their mass by photosynthesis and thus decreasing its concentration in the atmosphere. This effect is important, because rain forests produce about one third of dry land biomass production.

Quite a different situation is in our temperate climate zone. Annual average evapotranspiration total in the southern part of Slovakia is approximately 500 mm water layer, 5 times less than annual evapotranspiration total of rain forests, and consumption of energy to evaporate in our climate zone is correspondingly lower. But the good state of green evaporating surfaces is important to preserve local climate and, of course, contributes to the global climate, too. Therefore, the preservation of the good state of green surfaces in Slovakia is important. Good state of forest ecosystems is important not only to produce organic material (wood); it is important as anti-erosion measure, and irreplaceable element of ecosystem stability together with all the spectrum of plants and living organisms.

Soil degradation

Desertification in Slovakia is not an actual problem, because precipitation totals are high enough, and are even increasing. But, intensification of agriculture leads to worsening of soil properties, and to soil degradation.

The term soil degradation is understood as worsening of production properties of soil, erosion of ploughing soil layer, decrease of the organic matter content of the soil, which can lead to the negative soil structural changes and finally to the unfavourable hydrophysical properties of the soil (decrease of hydraulic conductivity, water retention capacity, reduction of infiltration capacity and surface runoff increase).

Soil erosion

Soil erosion across Slovakia is often observed particularly on arable land, but even in forest ecosystems, and is a part of soil degradation. Potential rate of erosion is expected to rise, proportionally to the expected heavy rain occurrence. Heavy machinery used in agriculture is increasing subsoil bulk density, thus decreasing its hydraulic conductivity. As a result, infiltration rate decreases and water starts to accumulate in the soil surface, then evaporates, and eventually contributes to the surface runoff formation. Therefore, less water from precipitation and from water courses can recharge groundwater. Sensitive to water erosion are mainly soils on the slopes because erosion intensity is proportional to the rain intensity and inversely proportional to hydraulic conductivity of the soil. Erosion of forest soils and meadows occurs usually in areas damaged by human activity, such as forest roads and cleared areas.

Rise of sea and ocean level

Sea level changes are usually results of climate change. Increased temperature of the atmosphere is responsible for two important effects: glaciers and icebergs melting, and water expansion with increasing water temperature.

The sea level has risen by about 0.20 m since the beginning of 20th century, and during the last 20 years it was 0.05 m, in the time interval 1992–2019, sea level rose in average by about 0.074 m (Vinas, Rasmussen, 2015).

Figure 2 presents the smoothed cumulative sea level rise during the past century. It is in accordance with the above-mentioned results. The rise of sea level is not so smooth as it is shown in Figure 2, but its rise is sensitive to short term fluctuations of weather. There are even short time intervals
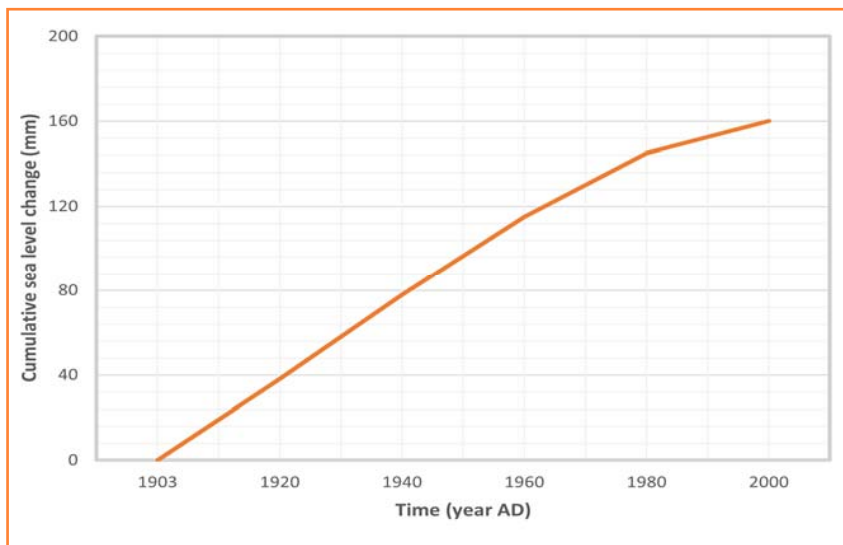
Figure 2   The smoothed rise of the sea level during the past century
             Source: according to Holgate (2007)

of sea level decrease, but in general, the tendency is as it can be seen in Figure 2. The potential rise of sea level due to Greenland glaciers melting $(1.7 \times 10^6$ km$^2)$ is 6 m, melting of the Antarctic continental glacier $(14 \times 10^6$ km$^2)$, could cause sea level rise up to 58 metres. Complete melting of those glaciers is not expected in near future. Real values of sea level rise are about 5 mm per year; during this century, it is expected to rise by about 50 cm.

The coefficient of thermal expansion of water is about 1×10^{-4} m.K^{-1} (its value depends slightly on temperature too). It means the sea level will rise 0.0001 of water layer thickness when temperature of water will rise about 1 °C. The average sea depth is approximately 2800 meters, then the increase of water temperature about 1 °C can rise sea level due to thermal expansion of water about 28 cm. This is not expected. There is one secondary effect of sea level rise. Usually, with a sea level rise, there is increased the area of inundated land. The positive feature of this phenomenon is increase of evaporation from this additional inundation and related consumption of energy as latent heat, which can lead to air temperature decrease. In general, increase of water areas due to ice lands melting can contribute to decrease of ecosystem temperature. This is one of the ecosystem autocorrection factors.

Ecosystems stability and climate change

There is no doubt; current global changes (climate change, land use change, fossil fuels burning, interactions of Earth and outer space) strongly influence biosphere (ecosystem) and its components: plants and living organisms.

Climate is the most important phenomenon responsible for distribution of vegetation and living organisms across Earth. Flow of water and energy are determined by the input of energy from the Sun. Global warming in the range 1 °C to 4 °C increases temperature of the ecosystems and changes their properties. In principle, those phenomena are initiating shift of plant and animal species to the poles. Plant species (including crops) were changing their territories, depending on global changes even in the past, but the speed of global change (and climate as its part) which is higher now suggests that such changes can be realised relatively fast, up to ten times faster, than it was previously, following warming after the last glacial maximum. It is not clear if plant communities (and animals as well) would be able to follow the relatively rapid shift of climate zones. It is expected that some plant species will not be able to follow climate change speed and will die out, because they will not be able to adapt to such climate change. The "filtration" effect will be proportional to the speed of such changes. It is expected that the

areas with natural conditions suitable to alpine and arctic plant and animal species will be smaller, fragmented and isolated in the future, so it is expected that some of them die out (Malcolm and Pitelka, 2000). Displacement of the so-called invasive plants observed in the last decades even in Slovakia is probably amplified by the effect of climate zones shift to northern direction.

Conclusions

Global changes refer to the planet scale changes of the environment, human society, and economy. The climate change is a part of the global changes, one of many global changes. Reasons of such changes are natural and anthropogenic. Natural reasons for the climate change depend on interactions among Earth and the outer space.

Since nineteenth century, increasing population has caused pressure to increase consumption of food, raw material and energy, and therefore, the so-called industrial revolution started, inducing great scale of land use change, replacing natural surfaces by artificial ones. This activity changed the structure of mass and energy fluxes in the ecosystem. It was estimated that about 60% of the dry land on the Earth`s surfaces are anthropogenically modified. Clearing of forests, especially rain forests, also decreased carbon dioxide sequestration and thus secondarily contributes to global temperature increase. Those anthropogenic changes of land surface quality and quantity also led to the decreasing evapotranspiration and a part of solar energy previously spent as latent heat of evaporation contributed to the global Earth`s temperature increase.

By combustion of fossil fuel, carbon dioxide is produced, and its concentration in the atmosphere has been increasing. It is followed by increasing dissipation of Earth`s long–wave radiation by carbon dioxide molecules, and thus increasing the ecosystem temperature.

Increasing demand on food, raw materials, and energy creates pressure on their production. Deposits of raw materials are limited and would be exhausted in the next century. Arable land areas, needed to produce biomass

as a basic source of food are limited as well as areas suitable for cattle breeding. Results of analysis have shown that renewable resources of energy can cover about ten per cent of the expected demand at the end of this century.

To preserve environment of the planet sustainably suitable for life, it is necessary to achieve equilibrium between production of the ecosystem and its consumption by living organisms. Until now, civilisation is consuming much more than sustainable productivity of Earth`s ecosystem can bear.

Acknowledgement

References

Dregne, H. E. (1977). Desertification of arid lands. *Economic Geography*, *53*(4), 322–331.

Food and Agriculture Organisation (FAO). (2012). *World Agriculture towards 2030/2050*: The 2012 revision, ESA Working Paper 12–03. Rome, Italy: FAO.

Holgate, S. J. (2007). On the decadal rate of sea level change during the 20th century. *Geophysical Research Letters, 34,* 1–4. 10.1029/2006GL028492.

Houghton, J. T., Jenkins, G. J., Ephraumus, J. J. (Eds.). (1990). *Climate change*. The IPCC Scientific Assesment. Cambridge, UK & NY: Cambridge University Press.

Izakovičová, Z., Špulerová, J. (2018). *Dopad globálnych megatrendov na krajinu a jej ekosystémy*. Bratislava: Ústav krajinnej ekológie Slovenskej akadémie vied.

Kollár, A. (2001). Vodné zdroje, ich využívanie a ochrana. *Životné prostredie*, *35*(3), 160–162.

Kutílek, M. (2008). *Racionálne o globálním oteplování*. Praha: Vyd. Dokořán.

Kutílek, M., Nielsen, D. R. (2010). *Facts about global warming*. Reiskirchen, Germany: Catena Verl. Gmbh.

Kutílek, M., Landgráfová, R., Navrátilová, H. (2013). *Homo adaptabilis* (Lidé jsou přizpůsobiví). Praha: Vyd. Dokořán.

Lubyová, M., Filčák, R. (Eds.). (2016). *Globálne megatrendy. Hodnotenie a výzvy MGT z pohľadu Slovenskej republiky*. Bratislava: Centrum spoločenských a psychologických vied, SAV.

Makarieva, A. M., Gorskhkov, V. G., Li, B.L. (2008). Energy budget of the biosphere and civilisation: Rethinking environmental security of global renewable and non – renewable resources. *Biological Complexity*, *5*, 281–288.

Malcolm, J. R., Pitelka, L. F. (2000). *Ecosystem and global climate changes*. Arlington, Virginia. Pew Center on Global Climate Changes. https://www.c2es.org/document/ecosystems-and-global-climate-change/

MacKay, D. J. C. (2015). *Obnoviteľné zdroje energie s chladnou hlavou* (4th ed.). Bratislava: Slovenská inovačná a energetická agentúra.

Münz, T. (2019). *Odchádzame*? Bratislava: Petrus.

Ministerstvo životného prostredia (MŽP SR) (2018). *The state of an environment in Slovak republic in 2017*. Annual Report, Ministry of Environment, Slovak republic. Bratislava: SAŽP SR (in Slovak).

Nariadenie vlády SR číslo 354/2006 Z. z. (2006).

Novák, V. (2012). *Evapotranspiration in the Soil – Plant – Atmosphere System*. Doordrecht: Springer Science + Business Media.

Pekárová, P., Miklánek, P., Pekár, J. (2017). *Zmena prvkov hydrologickej bilancie na Slovensku*. In: 24th Int. Poster Day Transport of water, chemicals and energy in the SPAC, Bratislava: ÚH – SAV (pp. 204–210).

Pekárová, P., Svoboda, A., Novák, V., Miklánek, P. (2011). Historická hydrológia a integrovaný manažment povodí a krajiny. *Vodohosp. spravodajca,* (1–2), 4–7.

Rosen, M., Ritchie, H. (2013). *Food supply*. Our world data. https://www.ourworldindata.org./food-supply).

Shuttleworth, W. J. (1988). Evaporation from the Amazonian rainforest. *Proc. Roy. Soc.*, B233, 321–346.

Vinas, M. J., Rasmussen, C. (2015). Warming seas and melting ice sheets. *Features*, 25.

World Minig Data (2019). https://www.world-mining-data.info

STATISTICAL ANALYSIS AND TREND DETECTION OF THE HYDROLOGICAL EXTREMES IN THE VÁH RIVER AT LIPTOVSKÝ MIKULÁŠ

Veronika BAČOVÁ MITKOVÁ*, Dana HALMOVÁ

Institute of Hydrology, Slovak Academy of Sciences, Bratislava, Slovakia

Natural climate fluctuation, as well as expected climate change, brings additional water regimes in the flow of a number of serious issues and uncertainties. The upper parts of the river basins are suitable for studying the effect of potential climate change or increased air temperature on drainage conditions in the basin. The Váh River is the biggest left-side Danube River tributary and the second biggest river in Slovakia. Gauging station Váh – Liptovský Mikuláš is the final profile above the water reservoir Liptovská Mara, one of the largest reservoirs in Slovakia. The contribution deals with the trend analysis of the extreme flows regime and the waves volume belongs to the annual maximum flow at gauging station Váh – Liptovský Mikuláš in a selected time period (1931–2015). Consequently, the trend analyses of precipitation depth and air temperature have been made at three selected meteorological stations located in the upper part of the Váh River basin. We have used the Mann-Kendall nonparametric test, which is one of the most widely used nonparametric tests to detect significant trends in a time series.

Keywords: trend analysis, MANN-KENDALL, annual maximum flow, volume of the wave, the Váh River

We are facing the information about climate change and the longer and more extremes of the hydrological or meteorological events and their catastrophic consequences more and more frequently. Climate variability impacts on the hydrological system on the regional scale have received a great deal of attention over the past years. The river flow is one of the main driving factors of the hydrological system and can change temporally as a result of the climate variability like change in precipitation, temperature and evaporation or human activities like land use change and urbanisation. Therefore, the first aim of hydrologists should be to verify these hypotheses and identify sources of the mentioned changes. Analyses of trends in river flows or volume of flow waves can predict its development and minimise its negative impacts on society and the environment. It is important to note that the extreme flow is one of the characteristics that can define hydrological regime. To answer these questions, it is necessary to statistically analyse a long and high quality time series of hydrological observations from the river basins, which are little affected by anthropogenic activities. Effects on the environment, which we live in, have escalated because of the increasing population, industrialisation, chemical substances used in agriculture, nonpoint pollutions, changes dependent on time, global climate change (warming or cooling), greenhouse gases, depletion of the ozone layer, and various other reasons since the mid-twentieth century, according to the Intergovernmental Panel on Climate Change (IPCC Climate Change, 2007). According to IPCC, statistical cases (mean, median, variance, autocorrelation, skewness or almost any other aspect of data) of meteorological, hydrological and climatological

data parameters show variability in time. This variability may be cyclical with the seasons, steady (a trend), include sudden jumps or some other established variations. From the year 1970 onwards, considerable literature concerning the trend detection techniques is available in the environmental and the hydrological field. Some of those studies are: Sen's nonparametric slope estimator (Sen, 1968), a least squares linear regression for the detection of trends in a time series of the hydrological variables (Haan, 1977), and work concerning the Spearman rank correlation test and the seasonal Mann-Kendall test (Hirsch, Slack, Smith, 1982; Hirsch, Slack, 1984; Lettenmaier, Wood, Wallis, 1994; Yue, Pilon, Cavadias, 2002). A number of studies were attempted on the basin, regional and country level for the trend detection, such as Burn, Hag Elnur (2002); Xiong, Shenglian (2004); Zhang, Harvey, Hogg, Yuzyk (2001). The Bayesian, time series and nonparametric methods with resampling approaches were mostly used in the trend detection studies for different hydrologic and climatic variables. Specific examples of the trends analyses in rainfall-runoff time series can be found in several works of the authors as Pekárová (2003); Falarz (2004); Fu, Chen, Liu, Shepard (2004); Franke, Goldberg, Eichelmann, Freydank, Bernhofer (2004); Schoner, Auer, Bohm (2009); Onoz, Bayazit (2003); Helsel, Frans (2006); Sonali and Nagesh Kumar (2013); etc.).

The hydrological research in the Tatra Mountains has a long history. In the '70s, an extensive hydrological research – organized by the Slovak Hydrometeorological Institute – took place in the representative pristine mountainous Belá River basin up to the town Liptovský Hrádok (Hlubocký, Dulovič, Matuška, Turčan, 1980; Pacl,

Contact address: Veronika Bačová Mitková, Institute of Hydrology Slovak Academy of Sciences, Račianska 75, 831 02 Bratislava, Slovak Republic; ☎ +421(2)32 29 35 02; e-mail: mitkova@uh.savba.sk

1973). Climatic conditions in the Tatra Mountains were analysed in the monograph of Konček (1974). Many authors (Hladný, Pacl, 1974; Molnár, Pacl, 1999; Molnár, Miklánek, Trizna, 1991; Pacl, 1994; Parajka, 2000) have dealt with the Tatra Mountain hydrology. Niedźwiedź et al. (2014) studied the variability of high rainfalls and related synoptic situations causing heavy floods at the northern foothills of the Tatra Mountains. Pribullová, Chmelík, Pecho (2011) analysed monthly temperatures and annual air temperature (climate changes from normal and linear trends and periodicity) at eight climate stations in the Tatra Mountains for the period 1961–2007. Hydrological balance of six catchments of the Western and High Tatra Mountains was elaborated by Holko, Parajka, Majerčaková, Faško (2001) and Holko, Kostka (2006) for the time period 1989–1998. Its results have shown that the use of all existing data and advanced computational methods does not give a satisfactory answer to the doubts which arise when determining the essential elements of the hydrological balance in different mountain watersheds. The hydrological balance of mountain river basins still remains an unexplained problem.

The aim of the study is to detect, whether significant trends occurred in the time series of annual maximum flows in the Váh River at Liptovský Mikuláš during the period of 1931–2015. With regard to more frequent information about increasing extremities or durations of the hydrological events due to the climate changes, we also deal with the trend analysis of total volumes and durations of the wave that belongs to the annual maximum flows. Consequently, the air temperature and precipitation depth trends have been detected at three selected meteorological stations (Podbanské, Liptovský Hrádok and Kasprowy Wierch) located into the upper Váh River basin.

Material and method

Study field and data

The Váh River is the biggest left-side Danube River tributary and the longest river in Slovakia. It rises in the Tatra Mountains by the confluence of the White Váh and the Black Váh (Figure 1). The Váh River flows over northern and western Slovakia and finally flows into the Danube near town of Komárno. The Váh River basin accounts for about 37% of water bearing of Slovakia. The Váh has a large number of tributaries, many of which are mountain streams from the Tatra Mountains and the Carpathians (e.g. Belá, Orava, Kysuca, Rajčianka, Turiec, Malý Dunaj, etc.). The long-term daily flows of the Váh River during the period of 1931–2015 reached value of about 20.4 $m^3.s^{-1}$ at Liptovský Mikuláš gauge (basin drainage depth is 582.4 mm) and the maximum flow reached value 540 $m^3.s^{-1}$ (29th June 1958). The gauging station Váh – Liptovský Mikuláš is the final profile above the water reservoir Liptovská Mara, one of the largest reservoirs in Slovakia and the basin area is 1,107.21 km^2. For this reason, it is useful to know the hydrological changes in the flow profiles (Figure 1). Some extreme floods occurred in 1934, 1948, 1958 and 1997 and a relatively longer wet period occurred between the years 1973–1981 (Figure 1).

Mann-Kendal nonparametric test

The Mann-Kendall nonparametric test (M-K test) is one of the most widely used nonparametric tests for significant trends detection in a time series. Nonparametric tests are more suitable for detection of the trends in the hydrological time series, which are usually irregular with many extremes (Hamed, 2008; Yue, Pilon, Phinney, 2003; Gilbert, 1987). The study performs two types of statistical analyses: 1) the presence of a monotonic increasing or decreasing trend and 2) the slope of a linear trend is estimated with the nonparametric Sen's method, which uses a linear model to estimate the slope of the trend, while the variance of the residuals should be constant in time. The Mann-Kendall trend test and its adaptation for auto-correlated data by Hamed, Rao (1998) were used to analyse the significance of the detected changes in flows by Jeneiová, Kohnová, Sabo (2014). By the M-K test, we want to test the null hypothesis H_0 of no trend, i.e. the observations x_i are randomly ordered in time against the alternative hypothesis H_1, where there is an increasing or decreasing monotonic trend. The data values are evaluated by an ordered time series. Each data value is compared with all subsequent data values. If a data value
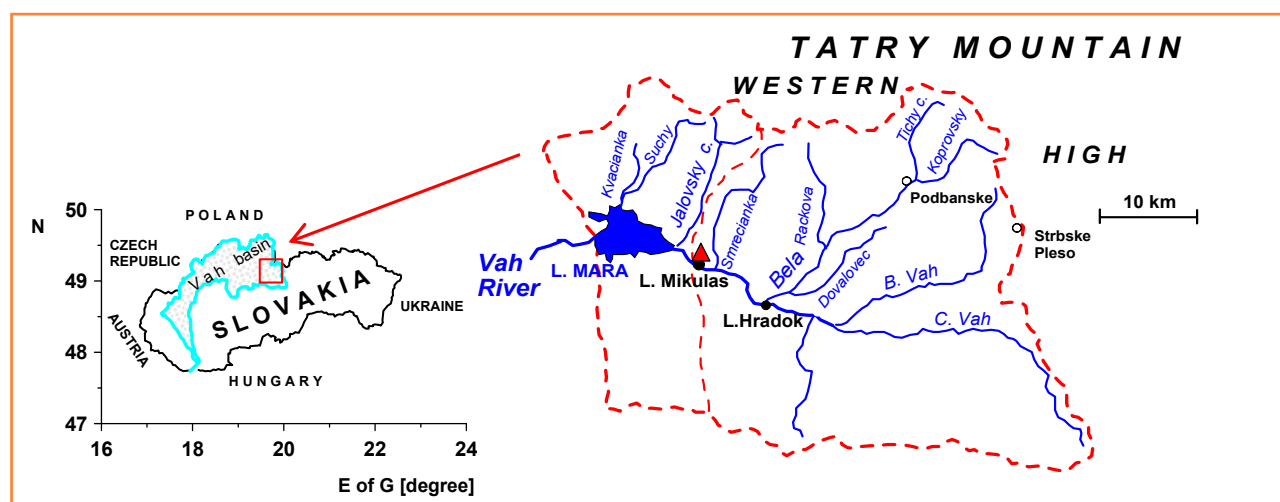
Figure 1   Map of Slovakia and the location of the selected Váh River section

from a later time period is higher than a data value from an earlier time period, the statistic *S* is incremented by 1. On the other hand, if the data value from a later time period is lower than a data value sampled earlier, S is decremented by 1. The net result of all such increments and decrements yields the final value of S (Shahid, 2011).

For *n* (a number of tested values) ≥10, the statistic *S* is approximately normally distributed with the mean and variance as follows

$$E(S) = 0 \qquad (1)$$

$$VAR(S) = \frac{1}{18}\left[n(n-1)(n-2) - \sum_{p=1}^{q} t_p(t_p-1)(2t_p+5) \right] \qquad (2)$$

where:
q – the number of tied groups
t_p – the number of data values in the *p* group

The standard test statistic *Z* is computed as follows:

$$Z = \begin{cases} \dfrac{S-1}{\sqrt{VAR(S)}} & if \quad S > 0 \\ 0 & if \quad S = 0 \\ \dfrac{S+1}{\sqrt{VAR(S)}} & if \quad S < 0 \end{cases} \qquad (3)$$

The presence of a statistically significant trend is evaluated using the *Z* value. A positive (negative) value of *Z* indicates an upward (downward) trend. The statistic Z has a normal distribution. To test either an upward or downward monotone trend (a two-tailed test) at α level of significance, hypothesis H_0 (no trend) is rejected, if the absolute value of |*Z*| is greater than $Z_{1-\alpha/2}$, where $Z_{1-\alpha/2}$ is obtained from the standard normal cumulative distribution tables. The M-K test detects trends at four levels of significance: α = 0.001, 0.01, 0.05 and α = 0.1. Significance level of 0.001 means that there is a 0.1% probability that the value of x_i is derived from a random distribution and it is likely to make a mistake, if we reject the hypothesis H_0; Significance level of 0.1 means that there is a 10% probability that we make a mistake, if we reject the hypothesis H_0. If the absolute value of *Z* is less than the level of significance, there is no trend.

For the four tested significance levels, the following symbols are used in the template:

***   if trend at α = 0.001 level of significance – H_0 seems to be impossible;

**   if trend at α = 0.01 level of significance;

*   if trend at α = 0.05 level of significance – 5% mistake, if we reject the H_0;

\+   if trend at α = 0.1 level of significance;

Blank: if the significance level is greater than 0.1, it cannot be excluded that the H_0 is true

The most significant trend is marked with three stars (***), with a gradual decrease in importance, the number of stars also decreases.

Results and discussion

Trend analysis of the annual maximum flows on the Váh River at Liptovský Mikuláš

The analysed upper part of the Váh River catchment area concerning the profile Liptovský Mikuláš has a cold climate character. The maximum number of the events with maximum annual flows occurs in May, when snow melts in the higher parts of the basin and rainfall occur in the lower parts of the basin. The second peak of the number in occurrence of the annual maximum flows is in July, which can be caused by summer rainfall. The two extreme annual maximum flows occurred in June. The Figure 2 illustrates the annual maximum flows occurrence in individual months during the period of 1931–2015.
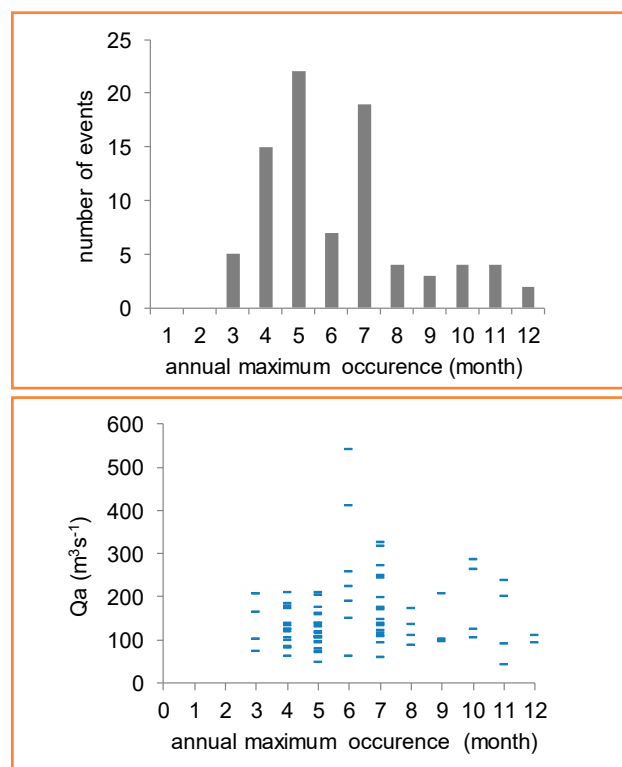
Figure 2   Monthly distribution of the annual maximum flows, the Váh River: Liptovský Mikuláš (1931–2015)

The annual maximum flows of the Váh River at Liptovský Mikuláš showed a decreasing long-term linear trend during the selected period of 1931–2015. Some extreme floods in 1934, 1948, 1958 and 1997 occurred. A relatively longer wet period occurred in the period of 1973–1981. Scenarios of the changes of the selected elements of the hydrosphere and biosphere in the Váh basin are reported in the monograph of Pekárová, Szolgay (2005) and in the work of Jeneiová, Kohnová, Sabo (2014).

The hydrological regime of the upper part of the Váh River basin is affected by the regime of its individual tributaries. The effect of the partly different flood regime is caused by the direction of the mountains and depressions of the catchment area and a different spatial distribution

Table 1   Conclusions of the Mann-Kendall trend test for the annual maximum flows ($m^3.s^{-1}$) for the period 1931–2015 and for the period II. June – November, the Váh River: Liptovský Mikuláš

Mann-Kendall trend					Sen's slope estimate		
Time series Q ($m^3.s^{-1}$)	first year	last year	*n*	test *Z*	signific.	A	B
Qa	1931	2015	85	-1.82	+	-0.530	151.37
Qa I. December – May			44	-0.48		-0.242	123.59
Qa II. June – November			41	-1.66	+	-1.707	182.24

A, B are parameters of the linear trend line $y = A * x + B$, A is a slope of the trend line

of the rainfall (Pekárová, Szolgay, 2005). Therefore, we divided the data period 1931–2015 into two time periods (seasons), based on the month of the maximum annual flow occurrence and tried to detect the trends: I. December – May and II. June – November. The annual maximum flows show a decreasing linear trend for the period II. June – November.

The Mann-Kendall nonparametric test (M-K test) was used for detection of the significance in the long-term trends in the annual maximum flows for the period 1931–2015 and for the periods I. December – May and II. June – November. The M-K nonparametric test shows a decreasing long-term trend in the annual maximum flows for the Váh River at Liptovský Mikuláš and also in the annual maximum flows in the period II. June – November and thus, we can reject the hypothesis H_0 at the significance level $\alpha = 0.1$ (Table 1). The long-term trends of the M-K test for the annual maximum flows of the Váh River at Liptovský Mikuláš (1931–2015) and for the period II. June – November are illustrated in the Figure 3.

Jeneiová, Kohnová, Sabo (2014) dealt with the trend analysis of the annual maximum flow series at different lengths of 40, 50, 60 years and in the whole observation period in the east Tatra Mountain region. These authors

also found statistically significant increasing and decreasing trends in the annual maximum flow series in different regions of the Váh River catchments. The analysis detected a significant increasing trend in the upper part of the catchment, mainly in the east Tatra Mountain region and a decreasing trend in the lower part of the upper Váh River basin.

Trend analysis of durations and volumes of the wave belonging to the annual maximum flows on the Váh River at Liptovský Mikuláš

For determination of the total duration and total volume of the wave, it was necessary to identify the beginning and end of the wave. It is quite difficult to identify the beginning and end of the flow wave, in some cases. In our analysis, the beginning and end of the wave was determined approximately at the level of the long-term average daily flow $Q_d = 21$ $m^3.s^{-1}$ (1931–2015). We also assumed that there were no other significant atmospheric events.

Figure 4 illustrates the total runoff duration and the month of the annual maximum flow occurrence. The total wave durations above 25 days occur most often in May. The longest duration ($t = 43$ days) with the Q_d level criterion was identified for the wave which occurred in April – May 2013. The maximum flow of this wave was about 133.50 $m^3.s^{-1}$. In contrast, the wave that belongs to the highest annual maximum flows (years 1948 and 1958) lasted only 25 days. The total volume and duration of the waves show a slightly increasing trend during the selected period of 1931–2015. The total runoff volumes V and total runoff duration t of the waves show a slightly increasing linear trend for the I. period: December – May and period II. June – November.
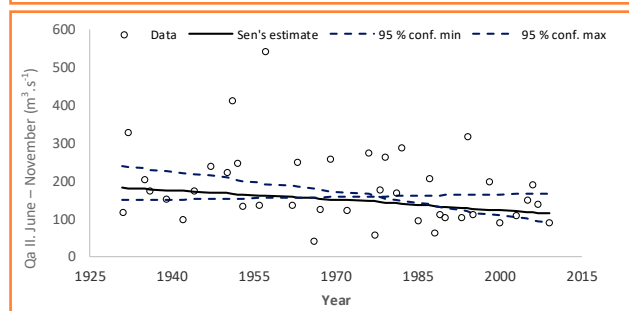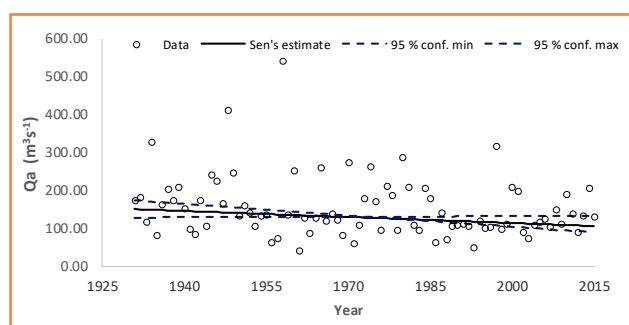
Figure 3   The long-term trend – conclusions of the Mann-Kendall trend test for the annual maximum flows for the period 1931–2015 and for the period II. June – November, the Váh River: Liptovský Mikuláš
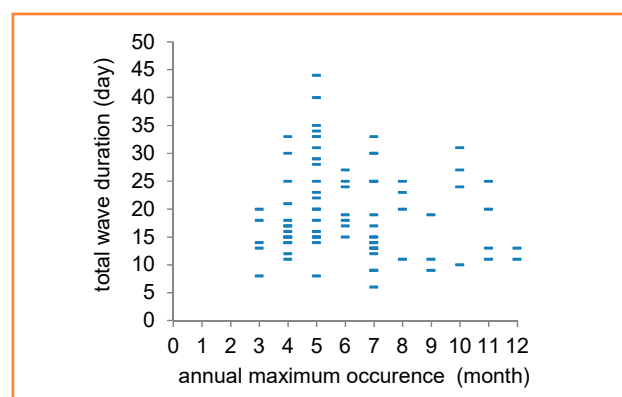
Figure 4   Monthly distribution of the total duration of the wave that belongs to the annual maximum flows, the Váh River: Liptovský Mikuláš (1931–2015)

Table 2   Conclusions of the Mann-Kendall trend test for the total wave volumes (mil.m^3) and total wave durations (day) belonging to the annual maximum flows for the period 1931–2015 and for the periods I. December-May and II. June – November, the Váh River: Liptovský Mikuláš

Mann-Kendall trend						Sen's slope estimate	
Time series V (mil.m^3)	first year	last year	n	test Z	signific.	A	B
Vatot	1931	2015	85	0.66		3.193	1,157.36
Vatot I. December – May			44	0.48		6.53	1,080.91
Vatot II. June – November			41	0.51		8.60	1,837.30
Time series t (day)	first year	last year	n	test Z	signific.	A	B
ta_{tot}	1931	2015	85	0.85		0.023	17
ta_{tot} I. December – May			44	0.59		0.043	17
ta_{tot} II. June – November			41	0.59		0.045	17.19

Table 3   Conclusions of the Mann-Kendall trend test of the total annual precipitation depth (mm) at Podbanské, Liptovský Hrádok and Kasprowy Wierch stations

Mann-Kendall trend						Sen's slope estimate	
Time series P (mm)	first year	last year	n	test Z	signific.	A	B
P Podbanské	1961	2014	54	0.91		1.148	898.7
P Liptovský Hrádok	1951	2014	64	2.51	*	1.748	623.26
P Kasprowy Wierch	1946	2014	69	0.57		1.321	1,676.75

The Mann-Kendall nonparametric test (M-K test) was used for detection of the significance in the long-term trends of the total wave volumes and total wave durations that belong to the annual maximum flows of the Váh River at Liptovský Mikuláš for the period 1931–2015 and for the period I. December – May and II. June – November. The M-K trend test did not show any significant long-term trends in the total wave volumes and total wave durations belonging to the annual maximum flows of the Váh River at Liptovský Mikuláš for the period 1931–2015 and for the period of I. December – May and II. June – November. Table 2 lists conclusions of the M-K trend test for the total wave volumes and total wave durations belonging to the annual maximum flows for the period 1931–2015 and for two shorter time periods of the data set for the Váh River at Liptovský Mikuláš.

Based on the results of the trend analysis of the annual maximum flows, we also analysed the trends and their significance in air temperatures and rainfall totals. Three meteorological stations located in the upper Váh River basin were selected for the trend analysis: Podbanské P (1951–2014 and T (1931–2014), Liptovský Hrádok (1951–2014) and Kasprowy Wierch (1946–2014). We analysed monthly and annual total precipitation depth and mean annual and monthly air temperature using the nonparametric M-K test.

Trend analysis of the precipitation depth at the selected stations located in the upper Váh River basin

The M-K nonparametric test shows an increasing long-term trend in the annual precipitation depth at Liptovský Hrádok station and thus, we can reject the hypothesis H_0 at the significance level $\alpha = 0.05$ (Table 3 and Figure 5). Due to the fact that the maximum annual flows for the period
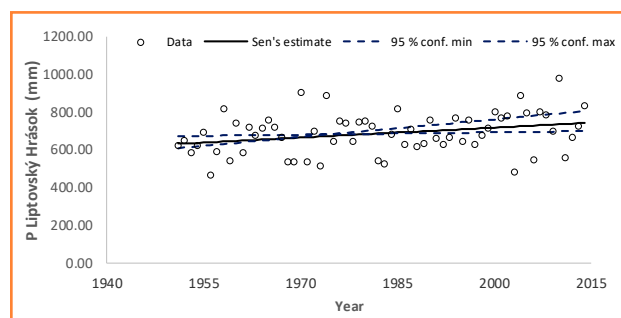
Figure 5   The long-term trend – conclusions of the Mann-Kendall trend test for the annual precipitation depth at Liptovský Hrádok station (1951–2014)

II. June – November showed a decreasing trend, we analysed changes in the monthly precipitation depth, especially in the months included in this period. At Podbanské station, no long-term significant trends in monthly precipitation in the individual months of June – November were detected. The M-K nonparametric test shows a decreasing long-term trend of monthly precipitation for Liptovský Hrádok station in June and thus, we can reject the hypothesis H_0 at the significance level $\alpha = 0.1$ (Table 4 and Figure 6). The M-K test shows an increasing trend in long-term monthly precipitation for Kasprowy Wierch station in September and thus, we can reject the hypothesis H_0 at the significance level $\alpha = 0.05$ (Table 4 and Figure 6).

Trend analysis of the air temperature at the selected stations located in the upper Váh River basin

The M-K nonparametric test shows an increasing trend in the long-term mean annual air temperature during the

Table 4　　Conclusions of the Mann-Kendall trend test of the monthly precipitation depth (mm) at Liptovský Hrádok and Kasprowy Wierch stations

Mann-Kendall trend						Sen's slope estimate	
Time series P (mm)	first year	last year	*n*	test *Z*	signific.	A	B
Liptovský Hrádok							
P June	1951	2014	64	-1.66	+	-0.371	105.98
P July	1951	2014	64	1.26		0.411	73.58
P August	1951	2014	64	0.49		0.110	69.89
P September	1951	2014	64	0.21		0.045	50.08
P October	1951	2014	64	1.14		0.267	35.88
P November	1951	2014	64	1.11		0.219	36.20
P sum	1951	2014	64	1.26		0.827	396.19
P average	1951	2014	64	1.26		0.138	66.03
Kasprowy Wierch							
P June	1946	2014	69	-0.97		-0.550	237.65
P July	1946	2014	69	0.60		0.316	171.62
P August	1946	2014	69	0.31		0.158	175.06
P September	1946	2014	69	2.41	*	1.036	84.32
P October	1946	2014	69	1.21		0.423	92.15
P November	1946	2014	69	-0.05		-0.018	114.47
P sum	1946	2014	69	1.10		1.408	894.35
P average	1946	2014	69	1.10		0.235	149.06
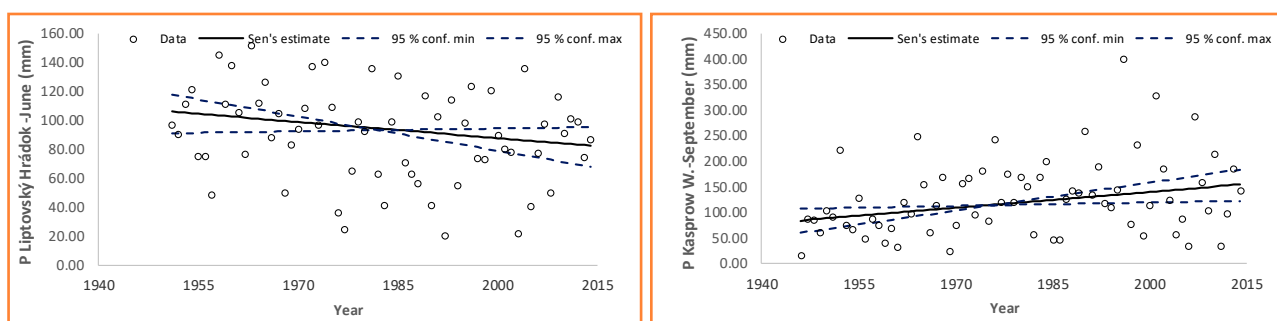
Figure 6　　The long-term trend – conclusions of the Mann-Kendall trend test for the monthly precipitation depth at Liptovský Hrádok station (left) (1951–2014) and Kasprowy Wierch station (right) (1946–2014)

selected periods and thus, we can reject the hypothesis H_0 at the significance levels α = 0.001 (Podbanské) and α = 0.01 (Liptovský Hrádok and Kasprovy Wierch) (Table 5). The mean annual air temperatures and their long-term trends – conclusions of the M-K test for the selected stations are illustrated in Figure 7.

Table 5　　Conclusions of the Mann-Kendall trend test of the mean annual air temperature (°C) at Podbanské, Liptovský Hrádok and Kasprowy Wierch stations

Mann-Kendall trend						Sen's slope estimate	
Time series *T* (°C)	first year	last year	*n*	test *Z*	signific.	A	B
T Podbanské	1931	2014	84	4.42	***	0.016	4.25
T Liptovský Hrádok	1951	2014	64	3.10	**	0.020	5.48
T Kasprowy Wierch	1946	2014	69	2.65	**	0.013	-1.06
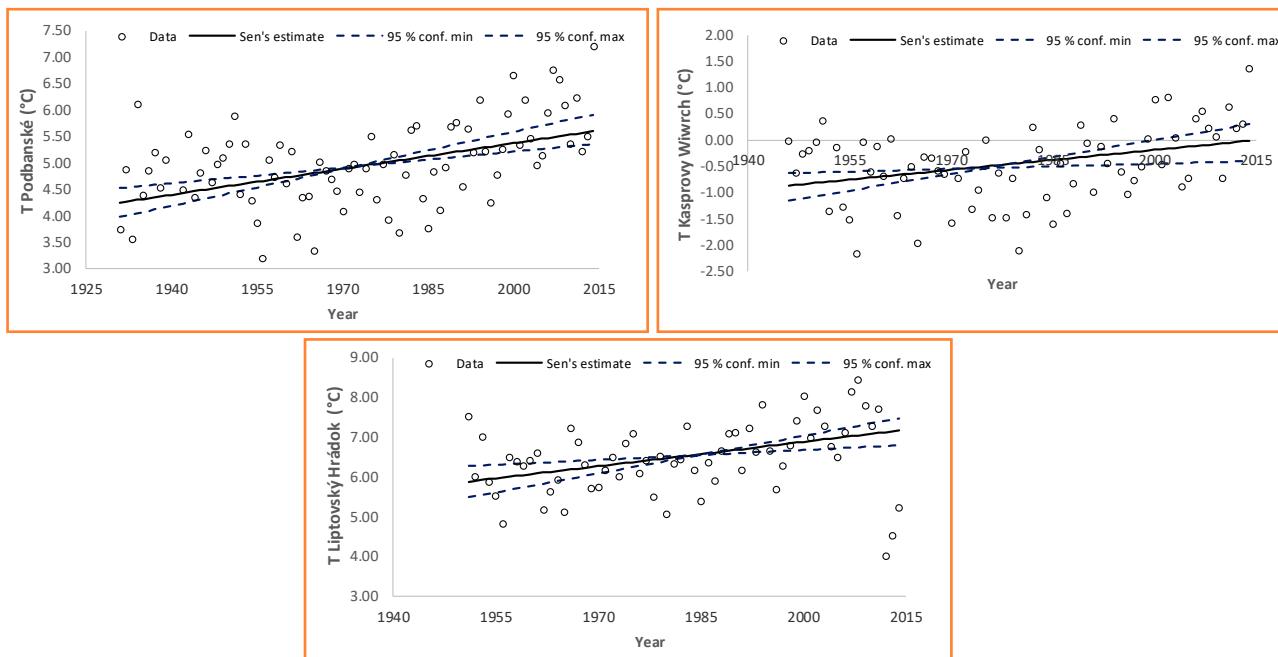
Figure 7 The long-term trend – conclusions of the Mann-Kendall trend test for the mean annual air temperature (°C) at Podbanské (1931–2014), Liptovský Hrádok (1951–2014) and Kasprowy Wierch stations (1946–2014)

The trend analysis of the mean monthly air temperature shows the most significant increasing long-term trends especially in months: April, May, June, July and August at Podbanské and Liptovský Hrádok stations and the M-K test shows that we can reject the hypothesis H_0 at the significance levels $\alpha = 0.001$ and $\alpha = 0.01$, respectively (Table 6). Figure 8 illustrates a significant long-term trend of the monthly air temperature at Podbanské and Liptovský Hrádok stations for the above mentioned spring and summer months.

Table 6 Conclusions of the Mann-Kendall trend test of the mean monthly air temperature (°C) at Podbanské, Liptovský Hrádok and Kasprowy Wierch stations (months with a significant long-term trend)

Mann-Kendall trend						Sen's slope estimate	
Time series T (°C)	first year	last year	n	test Z	signific.	A	B
Podbanské							
T April	1931	2014	84	4.11	***	0.036	2.77
T May	1931	2014	84	3.68	***	0.030	8.31
T June	1931	2014	84	3.50	***	0.023	11.82
T July	1931	2014	84	2.75	**	0.019	13.74
T August	1931	2014	84	3.03	**	0.019	13.19
Liptovský Hrádok							
T April	1951	2014	64	3.26	**	0.042	2.01
T May	1951	2014	64	4.22	***	0.038	7.70
T June	1951	2014	64	3.51	***	0.033	11.66
T July	1951	2014	64	3.79	***	0.040	12.23
T August	1951	2014	64	4.21	***	0.035	11.87
Kasprowy Wierch							
T May	1946	2014	69	1.70	+	0.018	1.73
T July	1946	2014	69	2.30	*	0.025	6.84
T August	1946	2014	69	3.02	**	0.026	6.78
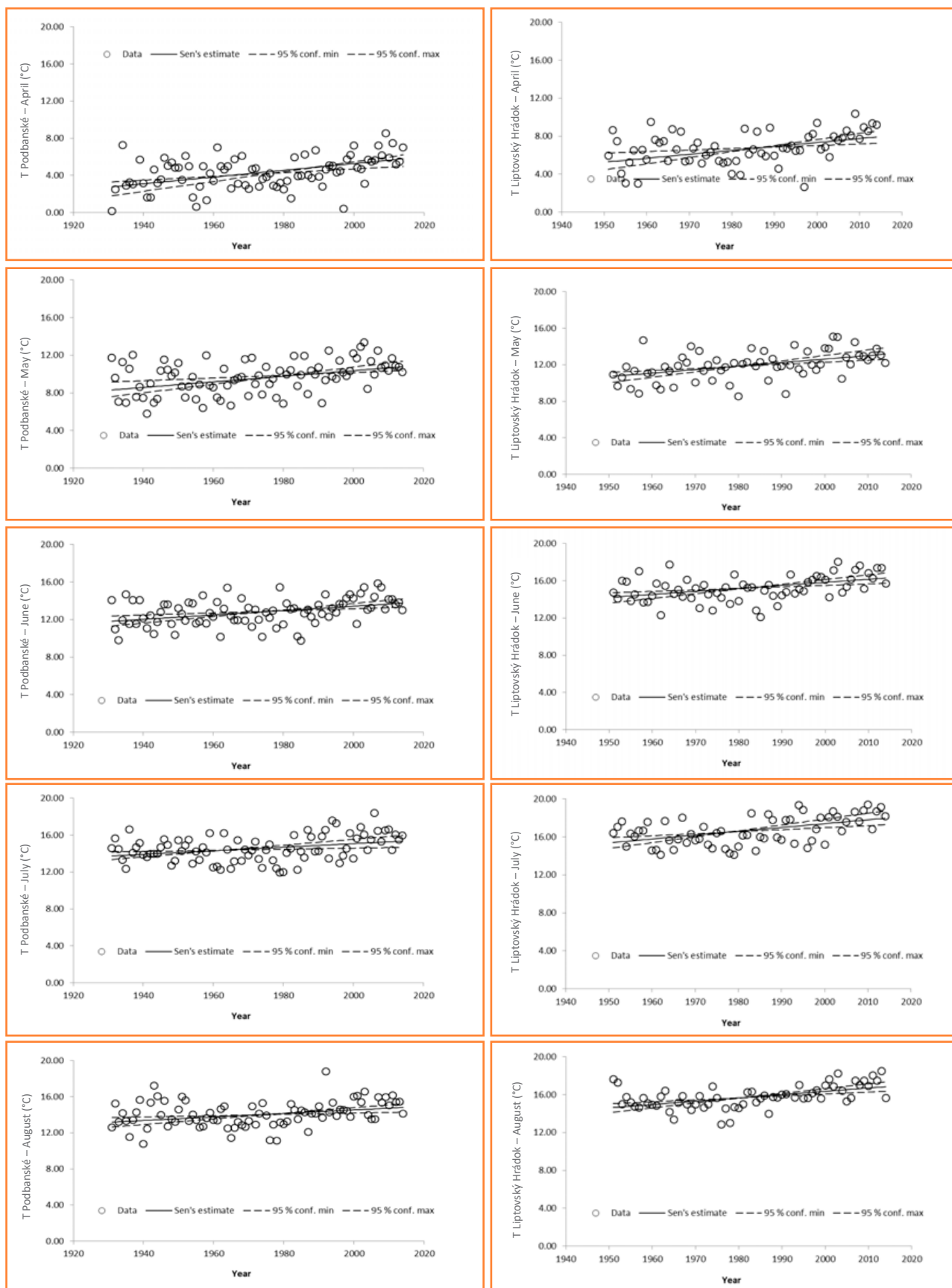
Figure 8 The long-term trend – conclusions of the Mann-Kendall trend test for the mean monthly air temperature (°C) at Podbanské (1931–2014, left) and at Liptovský Hrádok stations (1951–2014, right)

Conclusions

The study presents a statistical analysis and a trend detection of the hydrological extremes in the upper part the Váh River. The upper part of the Váh River basin is particularly suitable for studying the effect of potential climate change or increased air temperature on drainage conditions in the basin (Majerčáková, Škoda, Danáčová, 2007; Demeterová, Škoda, 2009). Our analysis showed that in terms of the analysed period 1931–2015, the annual maximum flows have a decreasing trend. The hydrological regime of the upper part of the Váh River basin is affected by the regime of its individual tributaries, direction of the mountains and depressions of the catchment, different spatial distribution of the rainfall and temperature variability. Therefore, we analysed also the trends in two time periods (seasons): I. December – May (snowmelt or a combination of snowmelt and rainfall) and II. June – November (rainfall). Analysis of the divided period into two time periods according to the occurrence of the annual maximum flows and seasonality (I. December – May and II. June – November) showed a significant decreasing trend in the annual maximum flows for the period II. The analysis of the total wave length and the total volumes of wave belonging to the annual maximum flow showed no significant trend in terms of all analysed cases.

The trend analysis of the precipitation depth and air temperature at three selected meteorological stations (Podbanské, Liptovský Hrádok and Kasprowy Wierch) showed some significant trends at various significance levels of α. The analysis of the annual precipitation depth at the selected stations showed an increasing trend in general, but only at Liptovský Hrádok station, it is significant at $\alpha = 0.1$. The analysis of the monthly precipitation depths of the period June – November showed a decreasing long-term trend in June ($\alpha = 0.1$, Liptovský Hrádok) and an increasing trend in September ($\alpha = 0.05$, Kasprowy Wierch).

The M-K test showed a significant increasing long-term trend in the mean annual air temperature for all three stations. The trend analysis of the mean monthly air temperature showed a significant long-term trend especially in months from April to August. The M-K test confirms significantly an increasing long-term trend in the mean monthly air temperature at the significance levels $\alpha = 0.001$ and $\alpha = 0.01$ at the lower stations in Podbanské and Liptovský Hrádok. Results of the trend analysis of the hydrological and meteorological data from the upper part of the Váh River basin show that the potential and even the actual evapotranspiration reaches possible increase. In a complex view on the studied river basin, we can state that the hydrological elements are changing, but it is important to time their increase or decrease in space and time. Some studies reported not so univocal trends in the runoff and precipitation in the Tatra Mountains area, while the trends in air temperature are increasing in the last decades (Bičárová, Holko, 2013; Pribullová, Chmelík, Pecho, 2013; Łupikasza, Niedźwiedź, Pinskwar, Ruiz-Villanueva, Kundzewicz, 2016; Holko, Sleziak, Danko, Bičárová, Pociask-Karteczka, 2020). The frequency analysis in the work of Pekárová, Pekár, Miklánek (2019) showed changes in the distribution curves of air temperatures also at the station Hurbanovo in southern Slovakia, which is ranked among the best meteorological

stations in Central Europe providing sufficiently long, high quality and homogenous observations.

The results are useful in the water planning and flood protection and can help mapping the flood-risk areas and developing river basin management plans in the Váh River basin.

Acknowledgements

References

Bičárová, S., Holko, L. (2013). Changes of characteristics of daily precipitation and runoff in the High Tatra Mountains, Slovakia over the last fifty years. *Contributions to Geophysics and Geodesy, 43*(2), 157–177.

Burn, D. H., Hag Elmur, M. A. (2002). Detection of hydrologic trends and variability. *J. of Hydrology, 255,* 107–122.

Demeterová, B., Škoda, P. (2009). Low flow in selected streams of Slovakia. *J. Hydrol. Hydromech.,* 57(1), 55–69.

Falarz, M. (2004). Variability and trends in duration and depth of snow cover in Poland in the 20th century. *International Journal of Climatology*, *24*, 1713–1727.

Franke, J., Goldberg, V., Eichelmann, U., Freydank, E., Bernhofer, C. (2004). Statistical analysis of regional climate trends in Saxony, Germany. *Climate Research, 27*, 145–150.

Fu, G., Chen, S., Liu, C., Shepard, D. (2004). Hydro-climatic trends of the Yellow River basin for the last 50 years. *Climatic Change, 65*, 149–178.

Gilbert, R.O. (1987). *Statistical Methods for Environmental Pollution Monitoring*. New York: John Wiley & Sons, Inc.

Haan, C.T. (1977). *Statistical Methods in Hydrology*. The Iowa State University Press (378). www.scribd.com/doc/265472254/Statistical-Methods-in-Hydrology-Charles-T-HAAN

Hamed, K. H. (2008). Trend detection in hydrologic data: The Mann-Kendall trend test under the scaling hypothesis. *Journal of Hydrology, 349*(3–4), 350–363.

Hamed, K. H., Rao, A.R. (1998). A Modified Mann-Kendall Trend Test for Autocorrelated Data. *Journal of Hydrology*, *204*(1), 182–196. DOI: 10.1016/S0022-1694(97)00125-X

Helsel, D.R., Frans, L.M. (2006). Regional Kendall Test for Trend. *Environmental Science and Technology*, *40*, 13.

Hirsch, R.M., Slack, J.R. (1984). A nonparametric trend test for seasonal data with serial dependence. *Water Resour. Res.*, *20*(6), 727–732.

Hirsch, R.M., Slack, J.R., Smith, R.A. (1982). Techniques of trend analysis for monthly water quality data. *Water Resour. Res., 18*(1), 107–121.

Hladný, J., Pacl, J. (1974). Analysis of the precipitation-runoff relationships in mountain watersheds. *J. Hydrol. Hydromech.*, *22*(4), 346–356.

Hlubocký, B., Dulovič, L., Matuška, M., Turčan, J. (1980). *Hydrological regime of Bela representative basin*. Final report No. 2231. Bratislava: SHMI (97 p.) (in Slovak).

Holko, L., Kostka, Z. (2006). Hydrological research in a high-mountain catchment of the Jalovecky creek. *J. Hydrol. Hydromech.*, *54*(2), 192–206.

Holko, L., Parajka, J., Majerčaková, O., Faško, P. (2001). Hydrological balance of selected catchments in the Tatra Mountains region

in hydrological years 1989 – 1998. *J. Hydrol. Hydromech.*, *49*(3–4), 200–222.

Holko, L., Sleziak, P., Danko, M., Bičárová, S., Pociask-Karteczka, J. (2020). Analysis of changes in hydrological cycle of a pristine mountain catchment. 1. Water balance components and snow cover. *Journal of Hydrology and Hydromechanics, 68*(2), 180–191.

IPCC Climate Change (2007). *The Physical Science Basis.* Contribution of Working Group I to the Fourth Assessment Report of the Intergovernmental Panel on Climate Change Cambridge. Cambridge, New York: University Press (996 p.).

Jeneiová, K., Kohnová, S., Sabo, M. (2014). Detecting Trends in the Annual Maximum Discharges in the Vah River Basin, Slovakia. *Acta Silv. Lign. Hung., 10*(2), 133–144. DOI: 10.2478/aslh-2014-0010.

Konček, M. (1974). *Klíma Tatier (*855 p) Bratislava: Veda (in Slovak).

Lettenmaier, D. P, Wood, E. F., Wallis, J. R. (1994). Hydro-climatological trends in the continental United States, 1948–1988. *J. of Climate, 7*, 586–607.

Łupikasza, E., Niedźwiedź, T., Pinskwar, I., Ruiz-Villanueva, V., Kundzewicz, Z. W. (2016). Observed Changes in Air Temperature and Precipitation and Relationship between them, in the Upper Vistula Basin. In Z.W. Kundzewicz, M. Stoffel, T. Niedźwiedź, B. Wyżga (eds.). *The Upper Flood Risk in the Upper Vistula Basin, GeoPlanet: Earth and Planetary Sciences*, Springer (pp. 155–188).

Majerčáková, O., Škoda, P., Danáčová, Z. (2007). Development of selected hydrological and rainfall characteristics for the periods 1961–2000 and 2001–2006 in the High Tatras. *Meteorological journal*, *10*(4), 205–210.

Molnár, L., Miklánek, P., Trizna, M. (1991). Experimental research of water balance components in the mountainous watershed. *J. Hydrol. Hydromech.*, *39*(5–6), 448–456.

Molnár, L., Pacl, J. (1999). The hydrological characteristics of the High Tatra region. *Workshop on Hydrology of Mountainous areas.* IH SAS (28 p.).

Niedźwiedź, T., Łupikasza, E., Pińskwar, I., Kundzewicz, Z. W., Stoffel, M., Małarzewski, Ł. (2014). Variability of high rainfalls and related synoptic situations causing heavy floods at the northern foothills of the Tatra Mountains. *Theor Appl. Climatology.* DOI: 10.1007/s00704-014-1108-0

Onoz, B., Bayazit, M. (2003). The power of statistical tests for trend detection. *Turkish J. Eng. Environ. Sci.*, *27*, 247–251. <http://journals.tubitak.gov.tr/engineering/issues/muh-03-27-4/muh-27-4-5-0206-6.pdf>

Pacl, J. (1973). Hydrology of the Tatra National Park. *Proc. of the works of the Tatra National Park, 15*, 181–238.

Pacl, J. (1994). *Tatra National Park – Water*. Tatranska Lomnica: Publ. TANAP? (pp. 66–78).

Parajka, J. (2000). Estimation of the average basin precipitation for mountain basins in the Western Tatra mountains. *ERB2000-Monitoring and modelling catchment water quantity and quality*, Belgium: Ghent (pp. 27–29).

Pekarová, P. (2003). Identification of long-term trends and fluctuations of hydrological time series (Part II, Results). *Journal of Hydrology and Hydromechanics*, *51*(2), 97–108.

Pekárová, P., Szolgay, J. (eds.). 2005. Scenarios of changes in selected hydrosphere and biosphere components in the Hrona and Vah catchment areas due to climate change. Bratislava: Veda (496 p.) (in Slovak).

Pekárová, P., Pekár, J., Miklánek, P. (2019). Effect of water on bimodality of air temperature distribution functions and changes in T-year air temperature values in Hurbanovo. *Acta Hydrologica Slovaca*, *20*(1), 53–62.

Pribullová, A., Chmelík, M., Pecho, J. (2011). Long-term changes in air temperature in Tatras mountains. *The Environment, revue for theory and care of the environment*, *45*(2), 71–77 (in Slovak).

Pribullová A., Chmelík M., Pecho J. (2013). Air Temperature Variability in the High Tatra Mountains. In J. Kozak, K. Ostapowicz, A. Bytnerowicz, B. Wyżga (eds.). *The Carpathians: Integrating Nature and Society Towards Sustainability, Environmental Science and Engineering, Environmental Science*, Berlin–Heidelberg: Springer-Verlag (pp. 111–130).

Schoner, W., Auer, I., Bohm, R. (2009). Long term trends of snow depth at Sonnblick (Austrian Alps) and its relation to climate change. *Hydrological Processes*, *23*, 1052–1063.

Sen, P. K. (1968). Estimates of the regression coefficient based on Kendall's tau. J. *Am. Stat. Assoc., 63*, 1379–1389.

Shahid, S. (2011). Trends in extreme rainfall events of Bangladesh. *Theoretical and Applied Climatology*, *104*, 489–499.

Sonali, P., Nagesh Kumar, D. (2013). Review of trend detection methods and their application to detect temperature changes in India. *Journal of Hydrology 476*, 212–227.

Xiong, L., Shenglian, G. (2004). Trend test and change-point detection for the annual discharge series of the Yangtze River at the Yichang hydrological station. *Hydrol. Sci. J., 49*(1), 99–112.

Yue, S., Pilon, P., Cavadias, G. (2002). Power of Mann-Kendall and Spearman's rho tests for detecting monotonic trends in hydrological series. *J. of Hydrology*, *259*, 254–271.

Yue, S., Pilon, P., Phinney, B. (2003). Canadian streamflow trend detection: impacts of serial and cross-correlation. *Hydrol. Sci. J., 48*(1), 51–64.

Zhang, X., Harvey, K. D., Hogg, W. D., Yuzyk, T. R. (2001). Trends in Canadian streamflow. *Water Resour. Res., 37*(4), 987–998.

CLIMATE CHANGE, ITS IMPACTS AND POSSIBLE MEASURES IN SLOVAKIA

Milan Lapin

Comenius University in Bratislava, Faculty of Mathematics, Physics and Informatics, Slovakia

Total climate changes are a combination of climate changes due to human activities and climate changes of natural origin. Further development of climate change can be predicted, if we know the future development of GHG emission into the atmosphere and other human interventions with the world climate system. The future development in natural climate changes cannot be reliably predicted. It is very probable that climate change caused by humans will be much more significant than the natural climate changes, already from 2020. It is almost certain that the concentration of GHG in the Earth's atmosphere will rise further for at least 100 years. The climate change scenarios can be prepared, according to the outputs of General Earth's atmospheric circulation physical models (GCM). Adapting and mitigation measures projection to utilise or slow down the impact of the expected climate change are the next steps of the climate change issues solving.

Keywords: climate change, impacts, adaptation and mitigation, natural climate changes

Material and methods

In the entire history of the Earth (except for the last few centuries), the Earth's climate evolution had been in progress and the Earth's climate system (ECS) had been functioning essentially without a conscious human activity, more or less based on the natural climate-forming processes and factors. Before the year 1,500 AD, less than 500 million people lived on the Earth and before the Common Era, less than 150 million people. The man began to emit greenhouse gases (GHG) into the atmosphere above the natural level only after 1750 AD, very significantly only after 1950 AD (IPCC, 2014; Peixoto, Oort, 1992).

In the 1950s of the 20th century, a serious increase in the concentration of carbon dioxide (CO_2) in the Earth's atmosphere was found by measurements at Mauna Loa Observatory (NOAA, 2020), since 1958 (Figure 1) and the theoretical assessments of a possible relation of global warming and increase in the atmospheric greenhouse effect were confirmed (mentioned for the first time by Svante Arrhenius (1896), increase by about 4 °C at $2 \times CO_2$). Meanwhile, it was found that climate change (including global warming) is influenced by a number of factors definitely related to the human activities (emissions of other GHG and aerosols into the atmosphere, changes in land use...), more in IPCC (2014).

The following effects on ECS by man are presently considered as the most serious:

1. stratospheric ozone layer reduction (freons and halons);
2. enhancement of the overall greenhouse effect of the atmosphere (from the natural about 33 °C before the year 1750, to about 36 °C in the year 2075 (currently around 34 °C), mainly by the emission of the active radiation, so called greenhouse gases (GHG);
3. change of the energy balance of the Earth's surface (urbanisation (cities), reduction of glaciers and snow albedo, agricultural fields, land use change, drainage and irrigation...);
4. thermal pollution of the atmosphere, hydrosphere and lithosphere, other types of pollution of the atmosphere (e. g. aerosols), land, water and oceans...
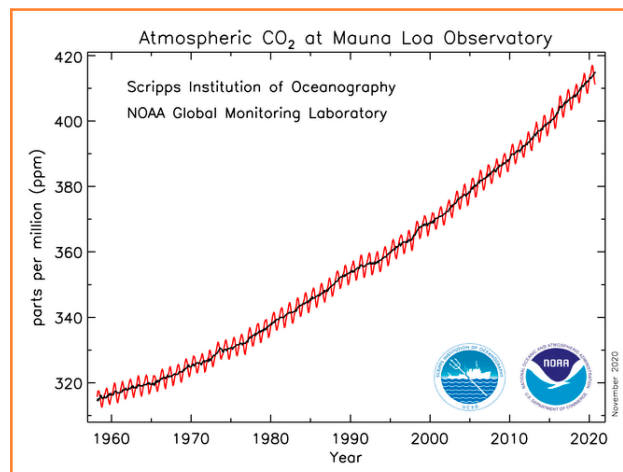
Figure 1 Annual course and a long-term development of a CO_2 concentration in the atmosphere as measured by NOAA (2020) (USA) at Mauna Loa Observatory (Hawaiian Islands) at an altitude of 3,400 m above sea level (before the year 1750, a level of about 280 parts per million (ppm) was measured)
Source:
NOAA data, https://www.esrl.noaa.gov/gmd/ccgg/trends/

Contact address: Milan Lapin, Comenius University in Bratislava, Faculty of Mathematics, Physics and Informatics, Mlynská dolina, F-1, 842 48 Bratislava, Slovakia

The threat of climate change does not arise suddenly, such as pollution of the ground atmospheric layer and the destruction of the ozone layer, but has a long time horizon. Currently, global warming is around 0.2 to 0.3 °C in 10 years – on average, during the last 50 years, Figure 2, for the year 2020 a preliminary estimate is provided (HadCRUT4, 2020).

The rising trend of air temperature at a global scale is overlapped by non-periodic climate changes and even greater climate variability, which becomes more evident at a regional scale, such as in Slovakia (Figure 3), where deviations of annual average air temperatures (as an average from 3 stations) and a percentage of the long-term average annual precipitation

totals (as a double-weighted average from 203 stations) are listed.

Results and discussion

It is almost certain that the concentration of GHG in the Earth's atmosphere will rise further for at least 100 years (IPCC, 2014). The Earth's population will grow in the same way and likewise, growth in the global gross domestic product is expected. The increasing activity of the humanity will demand more consumed energy, raw materials and goods, but also more emissions (GHG and other unnatural substances released into the atmosphere and hydrosphere, as well as harmful substances into the lithosphere). People will interfere with the Earth's climate system (ECS) more and more and this will apparently cause further climate warming. The question how long it will last for our environment to return to its original state, if we take radical mitigation measures, remains. For the main GHG, it would probably last decades or centuries and for some even millennia. The most important GHG (besides water vapour) is carbon dioxide; its mean lifetime in the atmosphere is 50 to 200 years and only then, its concentration declines by natural mechanisms, mainly through photosynthesis and subsequent storage of biomass carbon into fossils. For some freons and halons, the average lifetime period in the atmosphere is more than a thousand years and this also holds true for the substituents of freons, which are permitted under the Montreal Protocol and its amendments. We cannot do anything directly with a water vapour in the atmosphere, it will change according to the temperature of the atmosphere and the sea surface (an increase in temperature by 1 °C will raise the amount of water vapour in the atmosphere by about 6%, which will also cause enhancement of the greenhouse effect) (Peixoto, Oort, 1992; IPCC, 2014).

The ECS is affected by altered energy balance of the Earth's atmosphere and surface mainly due to the so-called "radiative forcing", meaning that the enhanced greenhouse effect works as if the radiation balance was rising, thus, there is more energy for the
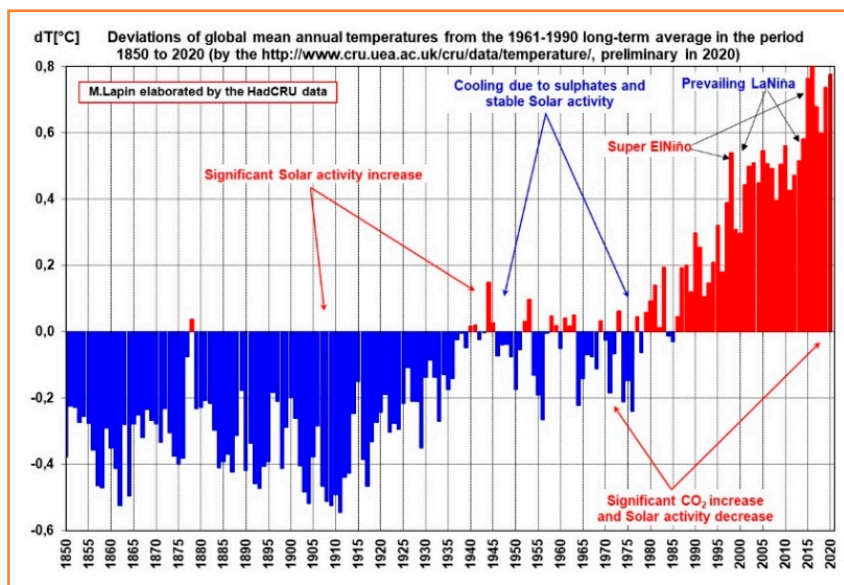
Figure 2   Deviations of the annual global average air temperature from the long-term average of the period 1961–1990, according to the processing in the Climatic Research Unit and Hadley centres (the United Kingdom)
Soure: CRU data, https://crudata.uea.ac.uk/cru/data/temperature/
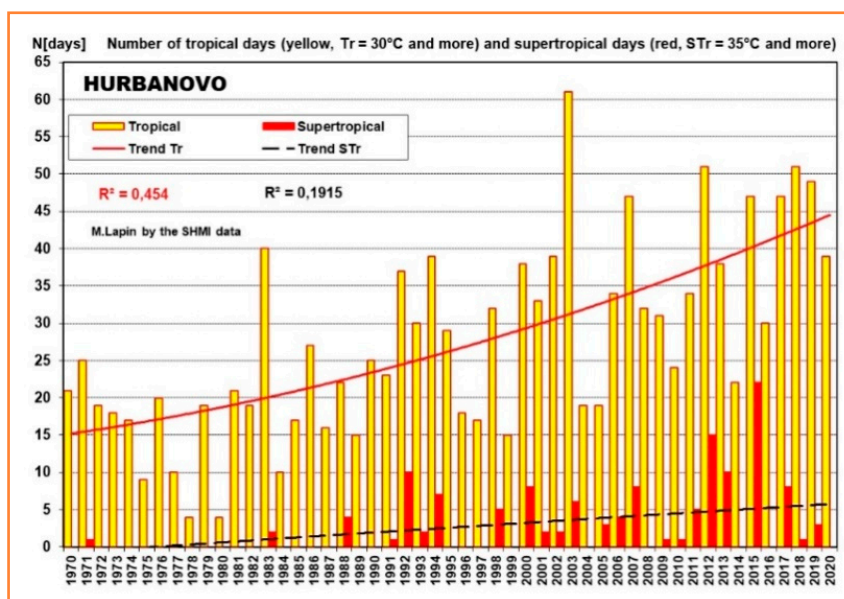
Figure 3   Deviations of the annual mean air temperatures in Slovakia from the long-term average of the period 1961–1990 and a percentage of the long-term average annual precipitation totals in Slovakia, compared to the long-term average of the period 1901–1990
Source: Slovak Hydrometeorological Institute (SHMI) data, preliminary in 2020

meteorological processes and the climate is warming. This growth represents currently more than 2.5 W.m^{-2}, which is around 10 times more than the fluctuation in the average radiation balance of the entire Earth's surface, only as a result of changes in solar activity in 11-year moving averages. In addition, the Earth surface's radiation balance is changing also due to the changes in land use. The destruction of tropical rainforests and other changes in the country have been causing additional emission of carbon (as CO_2) into the atmosphere in the amount of more than 1 billion tons per year. Use of fossil fuels and cement production represent about 10 billion tons of fossil carbon annually. Although nearly half of the emitted fossil CO_2 is absorbed by a global ocean, the rest remains in the atmosphere and a rising CO_2 concentration in the atmosphere contributes by about 55% to the enhancement of the atmospheric greenhouse effect (the rest falls into other GHG, dust and black carbons on snow and glaciers). A variety of aerosols (especially sulphates) causes the opposite effect – the weakening of the atmospheric greenhouse effect, but it compensates only about a third of the GHG emissions (IPCC, 2014).

In addition to the warming of the Earth's atmosphere and oceans, the enhancement of the atmospheric greenhouse effect also causes changes in the atmospheric circulation. The scheme of a general atmospheric circulation is besides the Earth's rotation (which is stable on the long-term basis) influenced also by a difference between the temperature of atmosphere and surface in different parts of the Earth, especially between the tropical and polar latitudes. As it is expected that the polar latitudes will be getting warmer 3 times faster than the tropics, and continents will be getting warmer 2 times faster than the ocean surface, substantial changes of the position of the determining air pressure systems in the atmospheric circulation system can be expected. A polar high-altitude cyclone will probably be

weakened and zonal atmospheric currents in mid-latitudes will slow down, while the polar frontal zone will probably shift to the higher latitude (towards the poles). This will probably result in the change of precipitation patterns as well as in the occurrence of extreme weather events due to the weakening impact of oceans on continents on one hand and due to an increase in water vapour amount in the atmosphere on the other. The shift of the frontal zone to the north of Europe will result in the increasing precipitation during winter in the northern half of Europe, but a reduction in precipitation in the southern half of Europe is expected, which will bring lower rainfall during summer also in southern Slovakia. Furthermore, the rainfall will follow the pattern that short periods with intense convective rainfall in the warm season of the year will be followed by long periods with low rainfall and high temperatures. This will undoubtedly cause more droughts, heat waves and increased forest fire (wildfire) risk than before (details are in IPCC, 2014).

The climate change scenarios for Slovakia were prepared according to the outputs of General Earth's atmospheric circulation physical models (GCM) with adjusted parameters due to the enhancement of the atmospheric greenhouse effect. There are several such models and scenarios because it is not possible to definitely estimate the future development of the GHG emissions and human interference with the ECS. The trend of the so-called positive and negative feedbacks in the ECS is uncertain as well. Table 1 shows several alternative changes of the monthly averages of air temperature, water vapour pressure and monthly precipitation totals for the Sliač weather station, the centre of Slovakia. The increase of precipitation will be probably lower in the south of Slovakia and higher in the north of the country, especially in the cold half of the year, while during summer in the south of Slovakia, the precipitation totals will be probably even lower. At this point, it should be noted

Table 1 Deviations of the monthly air temperature averages (dT in °C), quotients of the monthly water vapour pressure averages (qe) and quotients of the monthly precipitation totals (qR) in the time period until 2075 (the average for the period 2051–2100) compared with the average for the period 1951–1980 according to the scenarios CGCM3.1-B1, CGCM3.1-A2, KNMI-A1B and MPI-A1B for the weather station Sliač – airport (B1, A2 and A1B are the so-called SRES emission scenarios under IPCC, a quotient of 1.30 represents an increase by 30%). Previous scenarios are presented in Lapin, Melo (2004) and Lapin et al. (2012)

Model-Scenario	Element	I	II	III	IV	V	VI	VII	VIII	IX	X	XI	XII
CGCM3.1-B1	dT(°C)	3.45	3.66	3.51	3.08	2.66	2.02	0.94	1.57	2.39	2.53	2.23	2.34
CGCM3.1-B1	qe	1.30	1.30	1.35	1.26	1.16	1.14	1.12	1.11	1.17	1.16	1.18	1.22
CGCM3.1-B1	qR	1.36	0.99	1.38	1.42	1.14	1.16	1.12	1.04	1.02	0.88	1.42	1.15
CGCM3.1-A2	dT(°C)	4.56	4.75	5.06	4.82	3.67	2.87	2.07	3.38	3.76	3.58	3.73	3.14
CGCM3.1-A2	qe	1.43	1.43	1.51	1.41	1.23	1.20	1.18	1.21	1.22	1.22	1.32	1.29
CGCM3.1-A2	qR	1.39	1.10	1.34	1.50	1.21	1.15	0.94	0.87	0.86	1.06	1.34	1.32
KNMI-A1B	dT(°C)	2.81	2.75	2.70	2.17	2.41	3.16	3.17	3.10	2.88	3.06	2.05	2.48
KNMI-A1B	qe	1.25	1.24	1.22	1.15	1.13	1.17	1.13	1.16	1.17	1.21	1.14	1.21
KNMI-A1B	qR	1.24	1.27	1.32	1.16	0.93	0.81	0.65	0.94	1.07	1.04	1.23	1.21
MPI-A1B	dT(°C)	3.11	2.69	2.38	1.90	1.54	2.50	2.37	3.36	3.40	3.34	2.31	2.95
MPI-A1B	qe	1.23	1.21	1.18	1.17	1.14	1.16	1.15	1.17	1.19	1.21	1.15	1.20
MPI-A1B	qR	1.20	1.37	1.24	1.25	0.93	0.92	0.72	0.83	1.16	1.22	1.17	1.31

Source: SHMI, GCM and RCM data, modified by the Lapin et al. (2012) method
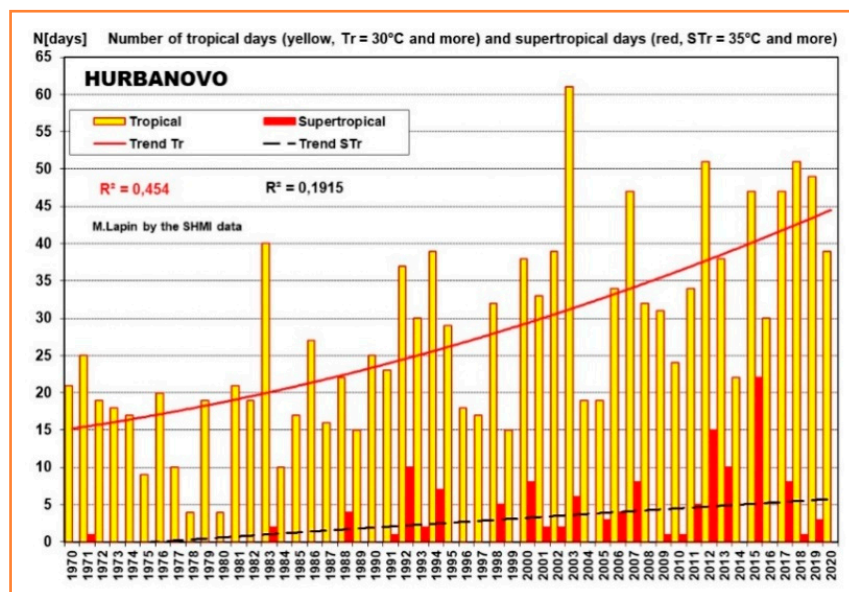
Figure 4　The number of tropical days (yellow, with a maximum temperature $T \geq 30$ °C) and supertropical days (red, with a maximum temperature $T \geq 35$ °C) at Hurbanovo for the period 1970–2020 (according to the data by the Slovak Hydrometeorological Institute – SHMI). The R^2 (the coefficient of determination) indicates that this trend is significant (more in Table 2 and in Lapin et al., 2016)
Source: SHMI data

that a normal temperature difference between Hurbanovo (115 m a.s.l) and Poprad (695 m a.s.l.) is approximately 4 °C. Further information can be found in Lapin, Melo (2004), Lapin et al. (2012); Lapin, Damborská, Gera, Hrvoľ, Melo (2015) and Gera, Damborská, Lapin, Melo (2018).

Such development can be seen also after the year 1990. The air temperature averages have increased, when compared to the period 1951–1990 and the precipitation pattern has changed, too. The number of tropical and supertropical days increased significantly (with a maximum temperature of 30 °C and more and 35 °C and more, Figure 4, Table 2). An increased occurrence of dry periods is also affected by rising temperature and high potential evapotranspiration, which causes a very deep decrease of the soil moisture, too (Hlavčová, Szolgay, Čunderlík, Parajka, Lapin, 1999; NCCC, 1995–2017; Lapin et al., 2015 and Lapin, Šťastný, Turňa, Čepčeková (2016)).

Such changes have also been observed by laymen and unconcerned experts. When in the past, the temperature during summer climbed to 30–35 °C within a period of two to four days, we were quite happy. It was bearable, as buildings did not overheat and we could sleep well. But after 1990, such heat waves lasted sometimes for two or three weeks, or even four months with short pauses, as it was in 2003. People in the Mediterranean region, in the south of the U.S.A. or in the tropics have adapted to such conditions, they adjusted their housing and life accordingly, but for us in the temperate zone, it is not so

easy to adapt to it. Our region in the lowlands is set to the average summer temperature of around 20 °C. The long-term average for the 20th century at Hurbanovo during summer (June 1 to August 31) is just 19.4 °C. In the northern Slovakia, the average at an altitude of 700 m is lower by 4 °C. People and natural ecosystems have adapted to such conditions. The temperature fluctuated also in the past, but only by a few tenths of a degree Celsius, if we consider it average for 30 years. Today, it is significantly more, for example the last two decades were warmer by 2 °C, when compared to the entire 20th century. It is a normal difference between the cities of Komárno and Žilina in Slovakia, showing how much the climate has shifted in Slovakia already. Of course, this has a number of negative consequences. New plants and animals have been coming from the south to us, while our original biological species are forced to move northwards and to the higher altitudes. Sometimes, they have nowhere to move, so several species must become extinct.

Someone may say that it is actually good news, as we will save on heating. However, greater heat also produces increased potential evaporation, the land is drying and there is an increased need for irrigation, or to import more food instead of irrigation. Moreover, it would be necessary to equip houses and vehicles with air conditioning. In the U.S.A., more energy is spent on air conditioning than on heating already today. By the end of the century, it will be probably warmer by further 2 to 4 °C. This can be compared to the possible climate shift – as if the climate of Podunajská nížina (Danubian Lowland, about 120 m a.s.l.) shifts to the area of Poprad or northern Orava (700 m a.s.l.). It seems that in the summer, there will be less rainfall or it will appear in a form of short intense showers. We need to

Table 2　Mean April – September air temperature and number of characteristic days at Hurbanovo in three periods, according to the evaluation of the daily maximum air temperature in two m heights and time from 21st to 21st h of MLT and % of days in 1991–2020, compared to 1951–1990

	Description	1901–1950	1951–1990	1991–2020	dT (°C) (%)
Mean temperature	April – September (°C)	16.4	16.7	18,1	+1.4 °C
Supertropical days	$T_{max} \geq 35$ °C	N	0.6	4.0	666.7%
Tropical days	$T_{max} \geq 30$ °C	14.8	19.0	33.8	178.3%
Summer days	$T_{max} \geq 25$ °C	67.8	75.3	91.9	122.0%

Source: SHMI data

take into consideration that our country will be affected by severe drought episodes lasting for several weeks almost every year. We experienced such episodes also in 2000–2020 in the large part of Central Europe. The precipitation totals will not be perhaps much lower even in the summer, the rain will fall also in the future, but in the warmer and drier climate. Such tendency can be identified that the rainfall in the warm period of the year occurs mainly in the form of showers and thundery downpours. Such showers are falling so fast that most of them just drain away and do not manage to soak into the soil.

The need for changes and the likely direction of the problem in the future

Already in 1992 at the global UNCED summit in Rio de Janeiro, in relation to the presentation of the FCCC (the United Nations Framework Convention on Climate Change), it was stated that measures, which will slow down the human-induced climate change to the speed corresponding to the adaptation capacities of the Earth's natural ecosystems, while not compromising the economic development and global food safety, have to be adopted. Later, it was particularized that global warming by less than 2 °C per century is concerned, in this case until the year 2100. At the beginning, there was an idea that the industrialized countries will stabilize and gradually reduce the GHG emissions into the atmosphere by modernization and new technologies (Annex 1 to the FCCC) and that the OECD countries shall provide effective aid to the developing countries, so that they do not use outdated technology with high GHG emissions, relative to the produced GDP. It turned out that such an appeal was completely ineffective, therefore, a quantitative solution of the GHG emission reduction through the Kyoto Protocol was sought (December 1997). Then, the commitments to reduce the GHG emissions in developed countries by 5.2% until 2010 were adopted (average of 2008–2012), together with the mechanism of trading with the emission quotas. A massive shift of the problematic industrial production to the countries, where the Kyoto Protocol was not applied, as well as the corruption in the emission quotas trading, were the results. Global emissions of the fossil CO_2 were rising, later even faster than in the period before 1997, while the U.S.A. and several other important countries did not implement the Kyoto Protocol at all. Since 2010, no interesting progress was achieved on the climate summits, as the politicians of different countries were defending interests of their own countries and not taking into account opinions of the climate change experts (not only climatologists but also the representatives of all concerned sectors). The above mentioned experts dissociated themselves from the climate summits over time mainly publicly and labelled them as a costly political theatre at taxpayers' expense, which cannot produce a desirable outcome. However, it is obvious that without the political agreement, no global commitments can be adopted (more in UNFCCC (1992) and IPCC (2014)).

Differences between the adaptation to climate change and measures to mitigate the climate change

The necessity of adaptation to ongoing and upcoming climate changes is being emphasized nowadays, because such solution is politically more convenient and inhabitants of developed countries accept it better than the reduction of the GHG emissions to the atmosphere. The principle of the adaptation measures is quite easy, in fact:

1. we need to estimate the potential future development of climate in individual regions in at least two variants (better is middle upper, middle lower and total average scenarios);
2. based on such scenarios, impact studies with a quantification of the possible impacts of climate changes in various social-economic sectors and in ecosystems will be prepared (negative as well as positive impacts);
3. requirements for the adaptation measures will arise from the economic assessment (cost-benefit), so that the potential negative impacts will be reduced and the positive ones utilised;
4. the adaptation measures can be applied by individual countries, sectors, regions, cities, enterprises, as well as individuals independently;
5. the adaptation measures may be evaluated continuously from the economic point of view, while the final contribution can be calculated only after some decades (at least 50 years).

Mitigation measures are focused on slowing down the global climate change and therefore, it is obvious that they must be executed under global coordination. Individual proposals (as those performed by the EU already for years) are good promotion, but have only a small global effect. The mitigation measures make sense, only if they influence the reduction of the GHG concentration in the Earth's atmosphere and in the improvement of land use in the whole world in average. It is necessary to emphasise that the CO_2 concentration in the atmosphere is already 49% higher and CH_4 is higher by 165% as before 1,750, while the whole increase is of anthropogenic origin. Irretrievable destruction of forests and tropical rainforests still continues as fast as approximately 100 thousand km^2 per year. Due to the fact that the individual countries bear various historical responsibilities for their interventions with the ECS (in calculation per one inhabitant), it is obvious that the mitigation measures will also be different for the individual countries. Countries such as the U.S.A., the EU, Japan, Russia, Canada, Australia and some others should provide the greatest contribution to the reduction of the GHG emission to the atmosphere. Countries such as China, India, Indonesia, Philippines and many others should try to use modern technologies with low emission of GHG per GDP unit in their fast growing economies and should also try to take vigorous measures in the required management of the country. The poorest developing countries should receive help from the developed ones, regarding the adaptation measures, as well as the GHG emission reduction in case of industry development. We ought to pay more attention to woodlands on the whole Earth and to a particular country management, as well as to the ecological waste management. The mitigation measures need to be coordinated globally under the auspices of the UN, obviously. The national and international coordination of the adaptation and mitigation measures, which should not stand in mutual contradiction, should be the essential outcomes of this process. A global treaty under the UN is necessary for this coordination, too.

Possible solutions for Slovakia

In 1991, the Federal Ministry of Environment established the National Climate Programme (NKP, more than 50 institutions and other entities in Slovakia participated), which was divided into Slovak and Czech NKP, in 1993. In 1995, 1997, 2001, 2005, 2009, 2013 and 2017, the National Communications of the Slovak Republic on Climate Change (NCCC) in Slovak and English language (under the coordination of Ministry of Environment of the Slovak Republic) including the proposal for the adaptation and mitigation measures were developed. The NCCC were prepared by the experts from SHMI, NKP and other concerned institutions. These Communications were discussed by the Government of the Slovak Republic and assigned particular tasks to the individual ministries. English version of the NCCC has been sent to the respective UN-Commission (NCCC, 1995–2017).

In the NCCC, the most attention is paid to the inventory of the GHG emission in Slovakia, based on the individual sectors and to the measure proposals to reduce the GHG emission in the upcoming years and decades. Various possible consequences arising from the GHG emission reduction were also analysed. The social-economic development after 1989 caused the natural reduction of the GHG emission in Slovakia, especially due to the fact that some industrial segments limited their production drastically and new enterprises were projected on the basis of more economical energy use. This caused rapid decrease of the GHG emission in 1994 (by more than 40% in comparison to 1989) and then, there was only moderate increase of the GHG emission, even though the GDP exceeded the value from the period before 1990 already until 2005. Thus, in 2014, the aggregate GHG emission (calculated for the CO_2 effect) was lower by more than 30% in comparison to 1990 (the GHG emission increase was recorded only in automotive transport). Transport, as well as other segments contributed to the GHG reduction, a lot of costs was saved also in heat delivery to residential and non-residential premises, especially due to the extensive insulation of buildings and other modernisation.

The section dealing with the potential impacts of climate changes, scenarios of climate change and proposals of the adaptation measures for climate change were the important parts of the NCCC. In all NCCC, the main focus was put on agriculture, forestry and water management, where the most negative impacts are expected and where the adaptation to climate change will be inevitable. In the last NCCC, from 2013 and 2017, the possible impacts in other concerned segments, including the natural ecosystems were analysed. When speaking about the most interesting results, it is necessary to emphasise the expected negative impacts on the hydrological cycle and water management that will be visible in other segments, too. Climate warming, increase of potential evapotranspiration or the changes in the precipitation regime will change the annual operation of the hydrological regime of Slovak rivers and soil in such a manner that the available volumes of water in flows, as well as soil humidity will decrease. This is the most important in spring, in the first vegetation period. In winter months in the altitudes of up to 1,000 m (almost over 95% of the Slovak territory), there will be irregular snow cover that can disappear anytime in winter, after 2030. This will change the regime of winter and spring runoff and therefore, the soil humidity will be reduced

too early, in February to April. At the same principle, the periods of hot weather will come earlier with unfavourable impacts on natural, agricultural and other ecosystems. Irregular runoff from the individual river basins will continue as a result of more frequent long drought periods and short periods with substantial rainfall, even in summer months. Potential evapotranspiration will rise in comparison to the period 1951–1980 by at least 15% already in 2025, while no significant increase of summer rainfall in the Slovak lowlands is being expected. More frequent drought and lowering of the soil moisture imply the need for more irrigation in agriculture, approximately for more than 500 thousand ha (in Slovakia, irrigation systems were built before 1990 for more than 300 thousand ha, but the systems for hardly 100 thousand ha are still functional). Vulnerability and impact assessments due to climate change in Slovakia can be found also in Hlavčová et al. (1999), Gaál, Beranová, Hlavčová, Kyselý (2014), NCCC (1995–2017) and Fendeková, Poórová, Slivová (Eds.) (2018).

Regarding other impacts, it is important to mention the changes in forest ecosystems, where the conditions for spruce vegetation will get worse significantly, especially below 1,000 m a.s.l. This means more xerophyte wood species and plants from the southern territories in all Slovak regions, especially on the south, while these plants will force the original species out and thus, intensify the instability of ecosystems. The conditions for thermophilic plants and wood species will worsen due to the prolonged vegetation period up to spring months (sometimes even by more than 40 days), while the risk of damage by spring frosts, which will appear episodically also in the future, will be higher (spring frosts depend especially on night duration, which is longer at the beginning of March as in April, by more than one hour and approximately by 2 hours in the middle of May, therefore, deeper decline of the land surface air temperature is possible). Heat waves, namely the episodes with high temperature or high air humidity lasting few days are ones of the interesting consequences of climate warming. In Central Europe, a heat wave is usually considered a period of at least 5 days with the highest air temperature of 30 °C and more and maximum pressure of water vapour above 18.7 hPa. Until 1990, such episodes were rare, but from 1992, they appear almost every year, in 2015, these episodes lasted for 38 days (in 22 days, the highest daily temperature in Hurbanovo achieved 35 °C or more), after 2030, they may last almost continuously whole summer (Lapin et al., 2016)). Necessity of air conditioning in residential and non-residential premises, including the means of transport and work premises, is also connected with such phenomena. In the U.S.A. as well as in other countries with warmer weather belonging to subtropical zone, the air conditioning is running at each place, where the air temperature exceeds 27 °C for more than few days. In the U.S.A., more energy is spent on air conditioning than on heating in cold seasons of the year.

There will be some more interesting impacts of climate change on Slovak conditions. Some of them will affect us even if they do not appear directly at our territory. This concerns especially the so called environmental or climate migrants. People have always migrated due to changing conditions, especially because it got more difficult to grow agricultural crops, the availability of fresh water got more complicated, volume of game decreased or conditions for

fishing got inconvenient. When climate was changing slowly (a few tenths of °C per century), the migration of population was slow too and sometimes, nobody even realized it. Worse climate conditions and migration of population were usually related to ethnic, religious and military conflicts. However, in the past, climate changes were not the only reason of migration. This is true for the present as well. However, the difference is that while at the beginning of our age, approximately 150 million people lived in the world, now this number is 7,800 million, namely 52 times more. Moreover, native inhabitants and the migrating people carry more effective guns and technical devices. Migration of endangered inhabitants can be thus seen from a completely different perspective than in the past. It is also true that the climate is currently changing and in the next decades, it will be probably changing more than 5 times faster than any time in the last 2000 years. Climate change means the situation, when 30-year long-term average air temperatures, precipitation totals or other climate elements, one following another, change significantly.

Conclusions

Climate change is evoked by human activities in global extent, especially by the emission of GHG with unecological utilisation of a country. This creates global increase of the average air temperature (more in the polar areas than in the tropical ones and rather on continents than on the ocean) and many other changes in climate, hydrological and environmental elements. Eventually, climate change is combined with climate changes of natural origin and as a result, irregular increase of the global and regional temperature for the individual years in average occurs. Another development of climate change can be predicted, if we know the future development of the GHG emission into the atmosphere and other human interventions with the world's climate system. The development of the natural climate changes cannot be reliably predicted, even if we know the oscillation of solar activity and influence range of the oceanic oscillations (especially El Niño and La Niña phenomena). It is very probable that the climate change caused by humans will be much more significant than the natural ones from 2020 already.

Global mankind, individual countries, cities, institutions, companies and individuals can react in three following ways to ongoing and expected climate change: 1) they can behave as if it was only natural climate change and pay no attention to it; 2) accept the fact that the climate changes are real and will change in the extent of scenarios for climate change and thus, they prepare adaptation measures at least for middle size scenarios, and in important areas, for the biggest size scenarios of climate change on national, enterprise and local level; 3) understand that it is necessary to take the mitigation measures to slow down the climate change by the reduction of the GHG emission and improvement of the country management, while such measures have to be based on the treaties on global level; in coordination with the mitigation measures, also the adaptation measures to reduce the negative impacts and utilise the positive impacts of climate change need to be prepared. It is obvious that the highest priority belongs to the measures connected with more frequent appearance of drought and storm rainfall than in the past. Slovakia still belongs to the countries with low

efficiency of energy use and small share of renewable energy resources on the total energetic mixture, while this brings another possibility to reduce the human interventions with the world's climate system.

References

Fendeková, M., Poórová, J. Slivová, V. (Eds.). (2018). *Hydrological drought in Slovakia and its forecast*. Bratislava: Univerzita Komenského (300 p.) (in Slovak).

Gaál, L., Beranová, R., Hlavčová, K., Kyselý, J. (2014). Climate change scenarios of precipitation extremes in the Carpathian Region based on an ensemble of regional climate models. *Advances in Meteorology*, *2014*, 14. http://dx.doi.org/10.1155/2014/943487

Gera, M., Damborská, I., Lapin, M., Melo, M. (2019). Climate Changes in Slovakia: Analysis of Past and Present Observations and Scenarios of Future Developments. In Negm, Abdelazim, M., Zeleňáková, M. (eds). *Water Resources in Slovakia: Part 2: Climate Change, Drought and Floods*. Cham: Springer International Publishing AG (pp. 21–47).

HadCRUT4 (2020). *Temperature*. https://crudata.uea.ac.uk/cru/data/temperature/

Hlavčová, K., Szolgay, J., Čunderlík, J., Parajka, J., Lapin, M. (1999). Impact of climate change on the hydrological regime of rivers in Slovakia. *Publication of the Slovak Committee for Hydrology no. 3*. Bratislava: NCH UNESCO, SUT (101 p.).

IPCC (2014). *Climate change 2013*. The physical science basis. Cambridge University Press (1552 p.). https://www.ipcc.ch/report/ar5/wg1/

Lapin, M., Melo, M. (2004). Methods of climate change scenarios projection in Slovakia and selected results. *Journal of Hydrology and Hydromechanics*, *52*(4), 224–238.

Lapin, M., Bašták, I., Gera, M., Hrvoľ, J., Kremler, M., Melo, M. (2012). New climate change scenarios for Slovakia based on global and regional general circulation models. *Acta Meteorologica Universitatis Comenianae*, *37*, 25–73.

Lapin, M., Damborská, I., Gera, M., Hrvoľ, J., Melo, M. (2015). Trends of evapotranspiration in Slovakia, including scenarios up to 2100. *International Bioclimatological Conference: Toward Climatic Services*, Nitra: Slovak Bioclimatological Society SAS (5 p.).

Lapin, M., Šťastný, P., Turňa, M., Čepčeková, E. (2016). High temperatures and heat waves in Slovakia. *Slovak Meteorological Journal, 19*(1), 3–10.

NCCC (1995, 1997, 2001, 2006, 2009, 2014, 2017). *National Communications on Climate Change*. Bratislava: Slovak Ministry of the Environment and Slovak Hydrometeorological Institute (vol. 1–7). http://ghg-inventory.shmu.sk/documents.php

NOAA (2020). *Trend in Atmospheric Carbon Dioxide*. https://www.esrl.noaa.gov/gmd/ccgg/trends/

Peixoto, J. P. and Oort, A. H. (1992). *Physics of Climate*. New York: American Inst. of Physics (520 p.).

UNFCC (1992). *UN Convention on Climate Change*. https://unfccc.int/resource/docs/convkp/conveng.pdf

EVALUATION OF DROUGHT – REVIEW OF DROUGHT INDICES AND THEIR APPLICATION IN THE RECENT STUDIES FROM SLOVAKIA

Slavomír Hološ[1,2]*, Peter Šurda[2]

[1]Slovak University of Agriculture in Nitra, Slovakia
[2]Institute of Hydrology, Slovak Academy of Sciences, Bratislava, Slovakia

Drought has recently become an important topic in Europe but also in Slovakia. Observed results from various studies suggest that this drought phenomenon has a serious impact on hydrology, agriculture and social and economic sectors. The first part of the paper was devoted to the study of literature from the field of existing drought indices, which serve to identify all types of drought such as meteorological, agricultural and socio-economic drought. The second part of the paper dealt with selected scientific studies on drought assessment and the use of drought indices in Central Europe and Slovakia.

Keywords: drought, drought index, meteorological drought, agricultural drought, socio-economic drought

Definition and concept of drought

Climate change has led to an increasing trend of drought in the recent decades, and models predict that the global drought risk will intensify further in the 21st century (Dai, 2013). While mean precipitation will increase, precipitation in the subtropical latitudes tends to decrease, particularly in the Mediterranean. Precipitation changes become statistically significant only when the temperature rises by at least 1.4 °C, and in many regions, the projected changes during the 21st century lie within the range of the late 20th century natural variability (Mahlstein, Portmann, Daniel, Solomon, Knutti. 2012).

The research on drought has attracted the attention of scholars, government departments and the public. The development of drought is relatively slow, but its effects are very devastating. Drought is easily reflected in agriculture in reduced yields, but it is also associated with soil degradation and intense erosion. It could also result in the extinction of certain species of animals in the affected areas. In some areas of the Earth, drought can result in malnutrition, hunger and diseases that can lead to reduction of population. Dried soil and vegetation pose a fire hazard (Mouillot, Rambal, Joffre, 2002).

Drought is a complex phenomenon and there is no clear physical quantity or definition by which drought can be measured. The lack of precipitation, relative to the climatic average of the area, is the main cause of drought. The increased rate of evapotranspiration, which is increased especially by higher air temperature, low relative humidity, low clouds, more intense sunlight or faster air flow, contributes to a significant intensification of drought. In certain cases, drought may result from the anomaly of other variables, such as temperature or evapotranspiration (Cook, Smerdon, Seager, Coats, 2014; Livneh, Hoerling, 2016; Luo et al., 2017). Moreover, drought may not be a purely natural hazard; human activities such as land use changes and reservoir operation may alter the hydrologic processes and affect drought development (Van Loonet al., 2016a). Overall, the development of drought results from the complicated interactions among the meteorological anomalies, land surface processes and human activities (Mishra, Singh, 2010).

Material and methods

Drought types and characterization

Traditionally, drought can be classified into meteorological, agricultural, hydrological and socioeconomic drought, based on both physical and socioeconomic factors (Wilhite, Glantz, 1985). According to Dracup, Lee and Paulson (1980), meteorological drought is determined by the meteorological characteristics such as air temperature, total precipitation and duration of sunshine. Hydrological drought is defined as the lack of water in rivers due to normal flow, lack of groundwater and the lack of water supply in natural or artificial reservoirs. If there is lack of water in soil for animals and plants, we are talking about physiological or agricultural drought. Socio-economic drought is characterised by lack of water for normal social and economic human activities (Pedro-Monzonís, Solera, Ferrer, Estrela, Paredes-Arquiola, 2015).

According to Svoboda and Fuchs (2016), it is essential to define drought indices and indicators. Indicators are parameters used to describe drought conditions (e.g. precipitation, temperature, streamflow, groundwater and reservoir levels, soil moisture and snowpack). Indices are

Contact address: Slavomír Hološ, Slovak University of Agriculture, Faculty of Horticulture and Landscape Engineering, Department of Biometeorology, 949 76 Nitra, Slovakia

typically computed numerical representations of drought severity, assessed using hydrometeorological inputs.

More than 100 drought indices have been proposed so far (Heim, 2002; Liu et al., 2018; Vicente-Serrano et al., 2012; Zargar, Sadiq, Naser, Khan, 2011). These indices correspond to different types of drought, including meteorological, agricultural and hydrological drought.

With the help of drought indices, we can provide information to the decision-makers in business, government and many stakeholders. These tools can be used to provide an early drought warning system (Lohani, Loganthan, 1997) to calculate the probability of a drought ending (Karl, Quinlan, Ezell, 1987), determine drought relief (Wilhite, Rosenberg, Glantz, 1986), assess the risk of forest fires (Wheaton, 1994), predict crop yield (Sakamoto, 1978; Kumar, Panu, 1997) and examine spatial and temporal characteristics of drought, drought severity and comparison between different regions (Alley, 1985; Soule, 1992; Nkemdirim, Weber, 1999).

Meteorological drought

The meteorological drought (or precipitation deficit) is generally caused by persistent anomalies in the large-scale atmospheric circulation patterns due to anomalous sea surface temperatures (SSTs) or other remote conditions (Dai, 2011). Globally and also in the conditions of the Slovak Republic, in the recent years, there has been a noticeable increase in the annual average air temperatures, which is closely related to a significant decrease in relative humidity (SHMÚ, 2015). The dry period can only be evaluated on the basis of total precipitation, which also takes into account the duration of precipitation-free days and the time distribution of precipitation. The meteorological drought does not result from a single cause but from a combination of multiple causes (e.g. reduced soil moisture and increased temperature), which may also contribute to the atmospheric anomaly (Dai, 2013; Kam, Sheffield, Wood, 2014). The commonly used meteorological drought indices are listed below.

Standardized precipitation index

The Standardized Precipitation Index (SPI) (Figure 1A a) is a widely used index to characterise the meteorological drought in a range of timescales. McKee, Doesken, Kleist (1995) used the probability of the precipitation occurrence for 3, 6, 12, 24, 48 months, and the output values ranged from -2.0 to +2.0. It was found that the Gamma distribution fits the precipitation time series very well. The Gamma distribution is defined by its frequency or probability density function as:

$$g(x) = \frac{1}{\beta^{\alpha}\Gamma(\alpha)} x^{\alpha-1} e^{\frac{-x}{\beta}} \ (x > 0) \tag{1}$$
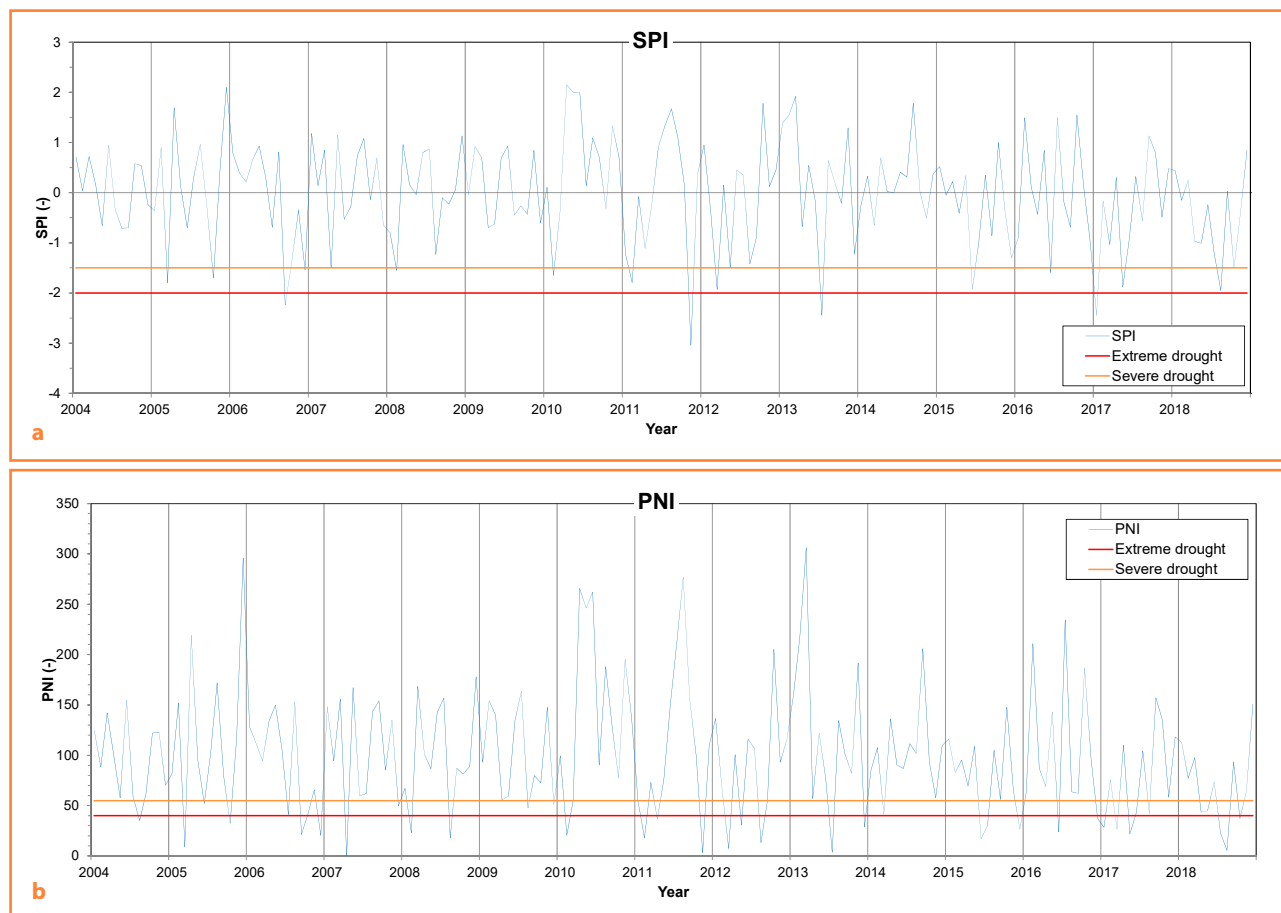
Figure 1A Values of SPI (a), PNI (b) index for the Malanta site, during the period 2004–2018; limit for severe (orange line) and extreme (red line) drought
Source: Šurda, Vitková, Rončák, 2020

where:
$\Gamma\,(\alpha)$ – for gamma function
x – (mm) for precipitation amount (x >0)
α – for shape parameter (α >0)
β – for scale parameter (β >0)

Percent of normal index

Index PNI (Figure 1A b) was described by Willeke, Hosking, Wallis (1994) as a percentage of normal precipitation. It can be calculated for different time scales (monthly, seasonally and yearly). PNI (Percent of Normal Index) has been found to

be rather effective for describing drought for a single region or/and for a single season (Hayes, 2006).
PNI is calculated as following:

$$PNI = \frac{P_i}{P} \times 100 \qquad (2)$$

where:
P_i – for the precipitation in time increment (mm)
P – for the normal precipitation for the study period (mm)
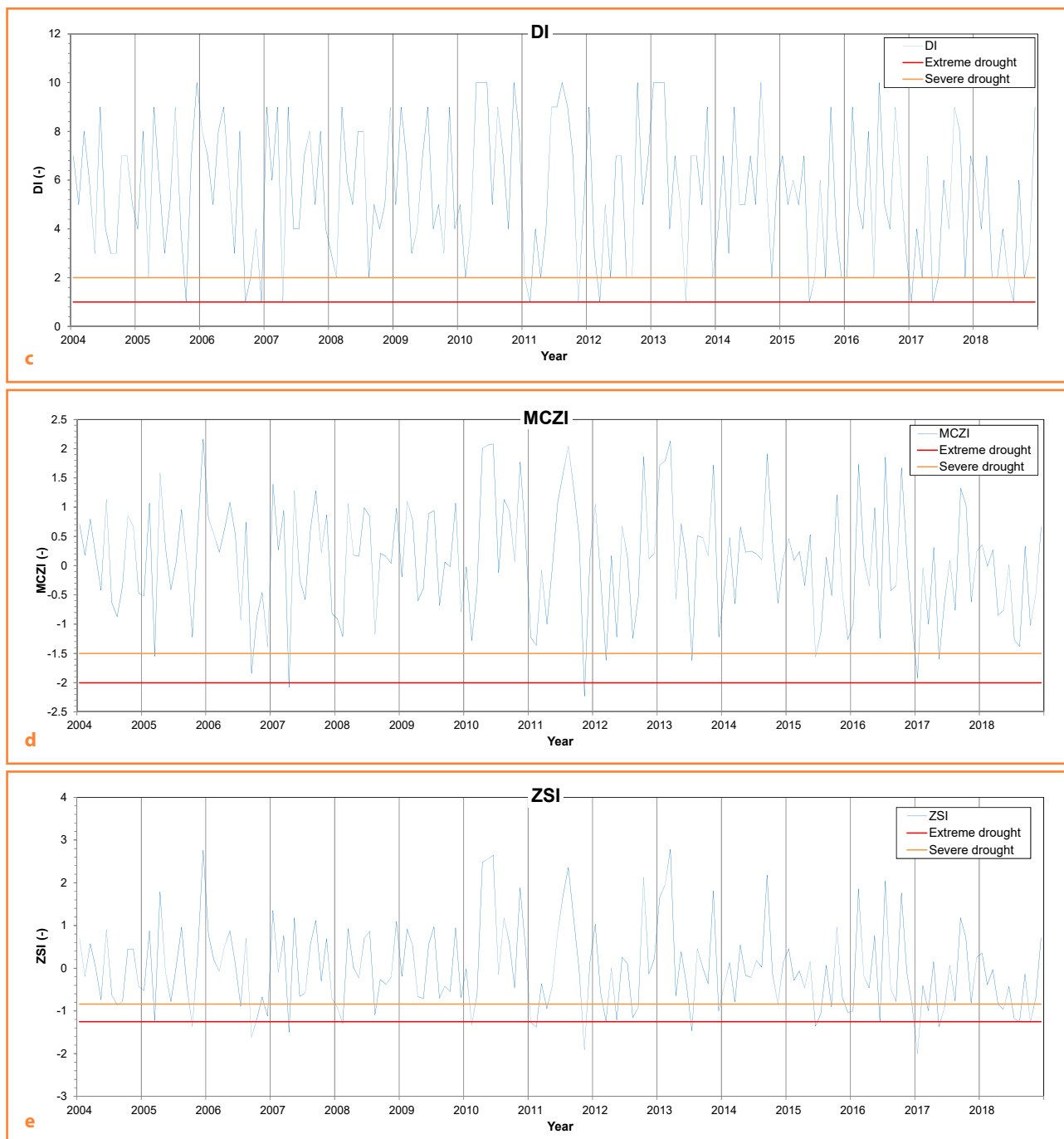
Figure 1B Values of DI (c), MCZI(d), ZSI(e) index for the Malanta site, during the period 2004–2018; limit for severe (orange line) and extreme (red line) drought
Source: Šurda, Vitková, Rončák, 2020

DI (deciles)

The DI index (Figure 1A c) was defined as a classification of precipitation totals during a time period over the whole monitoring period (Gibbs, Maher, 1967). In particular, monthly precipitation totals data are sorted from the lowest to the highest and are divided into ten equal categories or deciles. Thus, precipitation in a given month can be placed in a historical context by deciles.

MCZI (modified z-index)

The National Climate Centre in China developed CZI (Figure 1A d) in 1995 as an alternative to the SPI index (Ju, Yang, Chen, 1997). Assuming that the average precipitation totals have a III. Pearson distribution, the CZI is calculated as:

$$CZI_{ij} = \frac{6}{C_{si}} \left(\frac{C_{si}}{2} \times \varphi_{tj} + 1 \right)^{\frac{1}{3}} - \frac{6}{C_{si}} + \frac{C_{si}}{6} \qquad (3)$$

where:
i – for the observed time span and j is for the current month
CZI_{ij} – for the sum of the CZI values in the current month (j) during the period i
C_{si} – for the skew coefficient
φ_{tj} – for a standardized variation

　　The MCZI is calculated using the above formula and the median prtecipitation total is replaced by the arithmetic mean value.

ZSI (z-sum)

The ZSI index (Figure 1A e) is sometimes confused with the SPI index. This drought index is an analogue to the CZI, but does not work with gamma or Pearson's distribution of precipitation total data. The ZSI index can be calculated according to the following formula:

$$ZSI = \frac{P_i - \overline{P}}{SD} \qquad (4)$$

where:
$\overline{P}$ – for the average monthly precipitation total (mm)
P_i – for the precipitation total in a particular month (mm)
SD – for the standard deviation of the precipitation totals over the monitoring time interval (mm)

Standardized precipitation-evapotranspiration index (SPEI)

The SPEI index is based on the SPI index, but the SPEI index also includes the temperature component. This component allows the index to take into account the effect of temperature on drought. The SPI index is calculated using monthly (or weekly) precipitation as the input data. The SPEI index uses the monthly (or weekly) difference between precipitation and PET. This represents simple climatic water balance (Thornthwaite, 1948) that is calculated on different time scales to obtain SPEI.

Reconnaissance drought index (RDI)

The RDI index includes potential evapotranspiration and precipitation based on a simplified water balance equation, and the index also contains three outputs: a standardized value, normalized value and an initial value. If the standardized RDI value has a similar character as the SPI index, then it can be directly compared with it. RDI is more representative than SPI, because it uses complete water balance instead of precipitation itself. The parameters that enter the RDI index are: monthly precipitation temperatures and temperatures (Svoboda, Fuchs, 2016).

Effective precipitation concept (DEP)

Byun and Wilhite (1999) used the term of Effective Precipitation to describe the summed value of daily precipitation with a time-dependent reduction function, representing the daily depletion of water resources. The choice of the best reduction function (equation) remains an unsolved problem, because many parameters, like topography, soil characteristics, ability to keep water in reservoirs, air temperature, humidity, and wind speed, must be considered together precisely to represent the depletion of water resources in nature by runoff and evapotranspiration (Akhtari, Morid, Mahdian, Smakhtinm, 2009; Kalamaras, Michalopoulou, Byun, 2010; Kim, Byun, 2009; Kim, Byun, Choi, 2009; Morid, Smakhtin, Moghaddasi, 2006; Roudier, Mahe, 2010).

　　The EPI index is calculated in a daily time step to overcome the big limitation of other indices – the long-time unit of assessment (most of the current drought indices use a monthly or longer time period as a unit).The EP index is based on the calculation of the effective precipitation during the selected time period. For the purposes of this work, 365-day effective precipitation (EP$_{365}$) and a linear reduction function were selected, representing uniform loss of water resources throughout the year.

$$EP_i = \sum_{n=1}^{i} \left[\left(\sum_{m=1}^{n} H_{zm} \right) / n \right] \qquad (5)$$

where:
i – number of days whose total precipitation is included in the EP calculation
H_{zm} – total precipitation m-days before the first day included in the EP calculation (mm)

　　For the needs of the complex drought diagnosis, it is necessary to supplement the EP index with other derived values. The first is the value of the long-term EP average for each day of the calendar year (MEP). In this work, the average value of the effective precipitation was calculated from the 14-year series EP$_{365}$ (period 2004–2018) (Figure 2). Long-term EP (MEP$_n$) for a normal (slightly humid) period was computed for the years 2005–2012 and long-term EP (MEP$_d$) for a long-term dry period for the years 2012–2018, in this work. This time periods were selected according to the DEP index (Figure 3). With respect to the long-term average, the surplus or scarcity of water resources (DEP) for each day of the analysed period can be evaluated, according to the equation:

$$DEP = EP_{365} - MEP \qquad (6)$$
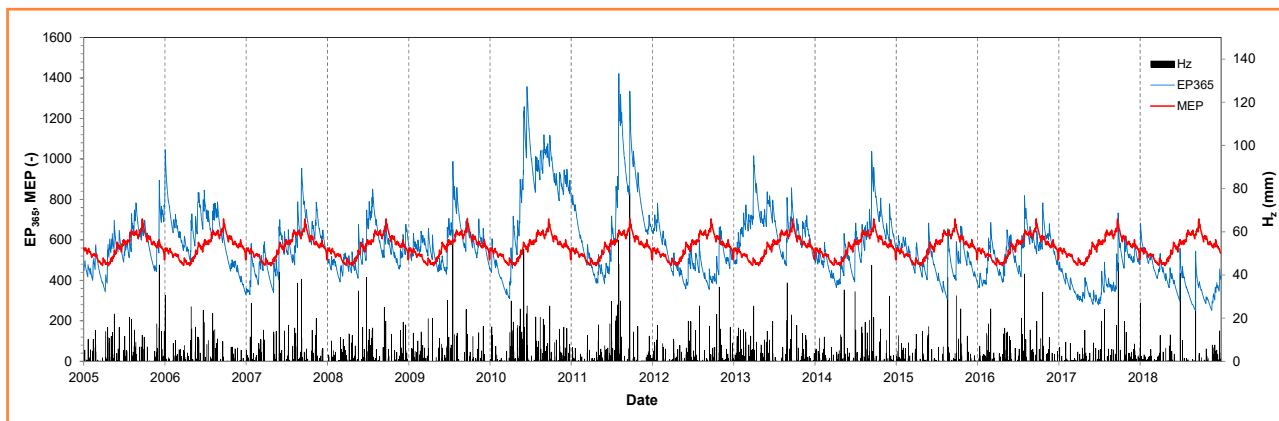
Figure 2   Daily values of *Hz*, MEP and EP$_{365}$ for the meteorological station of Nitra, for the period 2005–2018
Source: Šurda, Rončák, Vitková, Tárnik, 2019
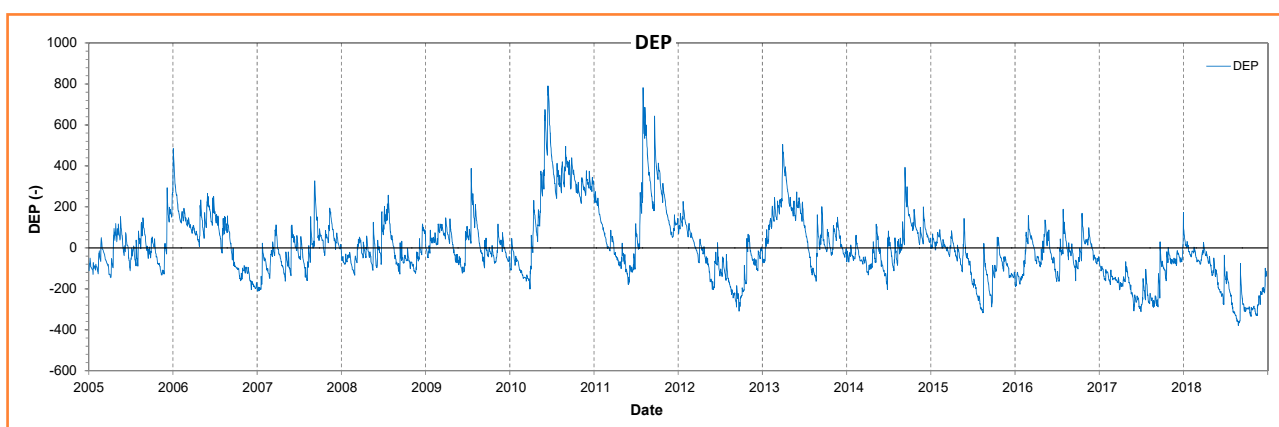
Figure 3   Daily values of the DEP index for the meteorological station of Nitra, for the period 2005–2018
Source: Šurda, Rončák, Vitková, Tárnik, 2019

Agricultural drought

Agricultural drought is commonly related to the deficit in soil moisture, which affects plant production and crop yield. This occurs mainly because the soil moisture availability governs the physiological processes in plants, and any paucity of water content in the crop root-zone can impede productivity (Wang, Lettenmaier, Sheeld, 2011; Mannocchi, Todisco, Vergni, 2004). A drought index using soil moisture would be directly related to the crop growth potential and could provide a decision supporting tool. The commonly used agricultural drought indicators according to Ajaz, Taghvaeian, Khand, Gowda, Moorhead (2019), are listed below.

Palmer drought severity index (PDSI)

This index was developed by Palmer (1965) as one of the first attempts to identify droughts using more than just precipitation data. Monthly precipitation and temperature along with the latitude and the available water capacity of the soil are the input data. PDSI has been used to identify droughts affecting agriculture, and also for identifying and monitoring droughts associated with other types of impacts. It takes into account received moisture (precipitation) as well as moisture stored in the soil, accounting for the potential loss of moisture due to the temperature influences (Svoboda, Fuchs, 2016; Wells, Goddard, Hayes, 2004).

Palmer's Z-Index

Palmer's Z-Index (Z-Index) is a derivative of PDSI, and the *Z* values are s part of the PDSI output. It is sometimes referred to as the 'Moisture Anomaly Index', and the derived values provide comparable measure of the relative anomalies of a region for both dryness and wetness when compared to the entire record for that location. The moisture loss is multiplied with empirically derived climatic characteristics, and the monthly moisture anomaly index known as Z-Index is estimated (Karl, 1986). Z Index responds to short-term conditions better than PDSI and is typically calculated for much shorter timescales, enabling it to identify rapidly developing drought conditions (Svoboda, Fuchs, 2016).

Soil waterdeficit index

The SWDI was developed by Martínez-Fernández, González-Zamora, Sánchez, Gumuzzio (2015) and was estimated as:

$$SWDI = \left(\frac{\theta - \theta_{FC}}{\theta_{AWC}} \right) \times 10 \qquad (7)$$

where:
θ   – for the aggregated volumetric water content (VWC) of soil profile
θ$_{FC}$ – for the VWC at field capacity (*FC*)

θ_{AWC} – for the available water content estimated as the difference between VWC at *FC* and wilting point (WP) (all in m^3.m^{-3})

Water deficit index

This index was developed by Cammalleri, Micale, Vogt (2016):

$$d = \frac{1}{1+\left(\dfrac{\theta}{\theta_{50}}\right)^n} \qquad (8)$$

where:
n – for an empirical exponent (unitless)
θ_{50} – estimated by averaging VWC between the soil moisture thresholds as described by Cammalleri et al. (2016)
θ – aggregated for the soil profile based on depth

Normalized soil moisture

The NSM was proposed by Dutra, Viterbo, Miranda (2008) as:

$$NSM_{m,y} = \frac{\theta_{m,y} - \overline{\theta_m}}{\sigma_m} \qquad (9)$$

where:
$\theta_{m,y}$ – for VWC for the month *m* and the year y (m^3.m^{-3})
$\overline{\theta_m}$ – for mean monthly VWC (m^3.m^{-3})
σ_m – for the standard deviation for all studied years

Finally, remote sensing-based indicators such as the Normalized-Difference Vegetation Index (NDVI) or the fraction of the Absorbed Photosynthetically Active Radiation (*f*APAR) are used to monitor drought impacts on the vegetation cover.

The normalized difference vegetation index (NDVI)

NDVI is defined as:

$$NDVI = \frac{(\alpha_{nir} - \alpha_{vis})}{(\alpha_{nir} + \alpha_{vis})} \qquad (10)$$

where:
α_{nir} and α_{vis} represent surface reflectance averaged over ranges of wavelengths in the visible (λ ~0.6 µm, "red") and near infrared, IR (λ ~0.8 µm) regions of the spectrum, respectively

It is clear from its definition that NDVI (like most other remotely sensed vegetation indices) is not an intrinsic physical quantity, although it is indeed correlated with certain physical properties of the vegetation canopy: leaf area index (LAI), fractional vegetation cover, vegetation condition and biomass.

Fraction of absorbed photosynthetically active radiation (fAPAR)

The quantity *f*APAR is defined as the fraction of incident photosynthetically active radiation (PAR) that is absorbed by a canopy, which usually includes the overstory and sometimes the understory and ground cover (e.g. moss). *f*APAR is calculated using:

$$f\,APAR = \frac{\left[(PAR_{\downarrow AC} - PAR_{\uparrow AC}) - (PAR_{\downarrow BC} - PAR_{\uparrow BC})\right]}{PAR_{\downarrow AC}} \qquad (11)$$

where:
$PAR_{\downarrow AC}$ and $PAR_{\uparrow AC}$ – incident (downward) and reflected (upward) PAR above the canopy, respectively
$PAR_{\downarrow BC}$ and $PAR_{\uparrow BC}$ – the corresponding terms for the below of the canopy

Hydrological drought

Hydrological drought is associated with deficiency in the bulk water supply, which may include water levels in streams, lakes, reservoirs and aquifers. Since it is directly linked to the drought impacts, it is argued that more attention is needed to study the hydrological drought (Cloke, Hannah, 2011; Mishra, Singh, 2010; Pozzi et al., 2013). From the major drought forms, the hydrological drought may be the slowest to develop (Soule, 1992). For example, a shortage of snowfall may not manifest itself as depressed runoff until half a year later. It is possible to minimise the negative impacts of the hydrological drought on the environment and society through the analysis of the minimum flows. These minimum flows are one of the characteristics that can define hydrological drought.

The commonly used hydrologic drought indicators include Palmer hydrologic Drought Severity Index (PHDI), Standardized Runoff index (SRI), or reservoir level (Hayes, Svoboda, Wall, Widhalm, 2011).

Total water deficit

Total water deficit is a traditional assessment of the hydrological drought, synonymous with the drought severity *S*. This severity is the product of the duration *D*, during which flows are consistently below a truncation level (e.g., the hydro-climatic mean), and the magnitude M, which is the average departure of streamflow from the truncation level, during the drought period (Dracup et al., 1980). After the drought ends, the total water deficit resets to 0.

Cumulative streamflow anomaly

A cumulative departure of streamflow from mean conditions can show long-term tendencies in the water availability.

Palmer hydrological drought severity index

The Palmer Hydrological Drought Severity Index (PHDI) is very similar to PDSI, using the identical water balance assessment. Specifically, PDSI considers drought finished when the moisture conditions start an uninterrupted rise that ultimately erases the water deficit, whereas PHDI considers drought ended when the moisture deficit actually vanishes (Heim, 2000, 2002). This retardation is appropriate for the assessment of the hydrological drought, which is slower in developing than the meteorological drought.

Surface water supply index

The Surface Water Supply Index (SWSI) explicitly accounts for snowpack and its delayed runoff (Garen, 1993; Doesken, McKee, Kleist, 1991). SWSI is a suitable measure of the

hydrological drought for regions, such as the mountainous catchments, where snow contributes significantly to the annual streamflow. Computations require measurements for snowpack, precipitation, streamflow and reservoir storage.

Standardized runoff index (SRI)

Shukla and Wood (2008) applied the concept for SPI in defining a standardized runoff index (SRI) as the standard normal deviation unit associated with the percentile of hydrologic runoff accumulated over specific duration. Different duration (e.g., 1-month, 9-month) and different spatial aggregations of the index can be calculated, depending on the source data resolution and desired application.

Socioeconomic drought

The socioeconomic drought incorporates features or impacts of three other types of drought. Drought impacts span a wide range of societal (e.g., health), economic (e.g., water supply, agricultural production and recreation), and environmental (e.g., forest productivity and wildfires) systems. The subject of the socio-hydrology, firstly conceived by Sivapalan, Savenije, Blöschl (2012), seeks to understand the 'dynamics and co-evolution of coupled human-water systems', including the impacts and dynamics of the changing social norms and values, system behaviours such as tipping points and feedback mechanisms, some of which may be emergent (unexpected), caused by non-linear interactions among processes occurring on different spatiotemporal scales. According to Van Loon et al. (2016b), human activities influence water input and output, and storage, and therefore modify the propagation of drought and can even be the cause of drought in the absence of natural drivers of drought. The drought typology based on natural processes should therefore be complemented with drought types based on human processes. According to Pedro-Monzonís et al. (2015), socio-economic drought is associated with the impact of water scarcity on people and the economic activity causing socio-economic, social and environmental impacts. To assess water scarcity, the water resource vulnerability index (Raskin, Gleick, Kirshen, Pontius, Strzepek, 1997), water stress index (Falkenmark, Lundqvist, Widstrand, 1989), critical ratio (Alcamo, Henrichs, Rösch, 2000), the water poverty index (Sullivan, 2002) and water footprint (Hoekstra, 2012) are the most commonly used approaches.

Water resource vulnerability index considers scarcity to be the total annual withdrawals, and a percent of the available water resources. It is focused on the assessment of use for being more objective than demanding.

Water stress index

Countries may be classified according to the renewable water resources per capita per year. It is easily understood and data are generally available. In contrast, average values may hide scarcity problems on smaller scales. It does not take into consideration the infrastructures that modify the water availability or the variations in demands among different countries.

Critical ratio considers scarcity to be the ratio of water withdrawals for human use to the total renewable water

resources. The difficulty of distinguishing the amount of water that could be available for human use considering evapotranspiration, return flows, environmental requirements, or the possibility of the society to adapt to water scarcity, belong among its limitations.

Water poverty index represents the weighted average of its five dimensions: access to water; water quantity, quality and variability; water use; water management capacity; and environmental aspects. The input data are huge and expert judgments are required.

Water footprint is defined as the total volume used to produce goods and services. It can be divided into three types: blue water footprint, green water footprint and grey water footprint.

Results and discussion

Drought quantification studies for the region of Slovakia over the last decade

Despite some controversy over global drought trends (Dai, 2012; Sheffield, Wood, Roderick, 2012), climate models project increases in mean temperature in the most of the land and ocean regions, hot extremes in the most inhabited regions, heavy precipitation in several regions, and the probability of drought and precipitation deficits in some regions (IPCC, 2018). Between 1990 and 2015, drought in the European Union affected more than 37% of its territory, representing 800.000 km^2 and affecting 100 million people. Over a 30-year period (1985–2015), drought has cost the European Union more than € 100 billion (Andreu, Solera, Paredes-Arquiola, Haro-Monteagudo, van Lanen (Eds.), 2015). Therefore, drought has become an important research topic for scientists in the region of Central Europe and also in Slovakia.

Meteorological drought studies

Janacova, Labudova, Labuda (2018) assessed the occurrence of the meteorological drought in the regions of the Záhorská, Danubian (Podunajská) and the Eastern Slovakian (Východoslovenská) lowlands and the Southern Slovakian (Juhoslovenská) and the Košická basins in the period 1981–2010. The analysis of the meteorological drought was evaluated on the basis of the monthly data of SPI. Areas which are the most threatened with the meteorological drought in different seasons were identified. There is greater hazard of drought for the Danubian lowland in spring and summer. On the contrary, the eastern part of Slovakia is threatened during the winter season.

Nagy, Zelenaková, Kapostasová, Hlavatá, Simonová (2020) evaluated dry and wet periods at six climatic stations in eastern Slovakia using the following indices: standardized precipitation index (SPI), streamflow drought index (SDI), drought reconnaissance index (RDI) and standardized evapotranspiration index (SPEI) in a 12-month step over the period 1960–2015. The evaluation of the results showed an alternation of wet and dry periods and proved that the dry periods also occurred in the north of eastern Slovakia.

Vido, Nalevanková, Valach, Šustek, Tadesse (2019) focused on the characterisation of the historical drought occurrences in the Horné Požitavie region, in Slovakia, over

the period 1966–2013 using the Standardized Precipitation-Evapotranspiration Index (SPEI). The results showed that drought occurred in the region regularly (recurrent climate feature), while the trend analysis indicated the trend towards more arid climatic conditions. Analyses of the SPEI trends in the individual months showed a decreasing trend of drought occurrences during the cold months of the year (i.e., October to March), while an increasing trend was indicated from April to August.

Vido, Nalevanková (2020) analysed drought occurrence and trends using the SPI and the SPEI index in the upper Hron region within the 1984–2014 period. They found that:
1. drought incidence decreased with an increasing altitude;
2. increasing air temperature increased also the difference in the drought trends between lowlands and mountains during the studied period;
3. abrupt changes in the time series of drought indices, which could indicate some signals of the changing atmospheric circulation patterns, were not revealed.

Trnka et al. (2016) used the index SPI, PDSI, Z-index and SPEI, in their work. The time series of the drought indices were calculated for 411 climatological stations across Austria (excluding the Alps), the Czech Republic and Slovakia. Up to 45% of the evaluated stations (depending on the index) became significantly drier during the 1961–2014 period. An increase in the evaporative demand of the atmosphere, driven by higher temperatures and global radiation with limited changes in the precipitation totals, was the main driver behind this development.

The study by Vido et al. (2015) focused on how drought occurs at higher altitudes of the Tatra National Park, which is a significant biological reserve of the Central European fauna and flora. Authors used the time series of SPI from 1961 to 2010 and standard GIS methods. The results showed that the frequency of drought occurrence has a cyclic pattern with approximately a 30-year period. The spatial analyses showed that the precipitation shadow of mountains influences the risk of drought occurrence.

Zelenáková et al. (2018) evaluated the trend analysis applied to the precipitation and temperature monthly data for the period from 1962 to 2014 at sixteen climatic stations in eastern Slovakia. All climatic stations in eastern Slovakia show a positive trend in temperature during the year. Trends in precipitation are also mostly positive during winter and spring. An abrupt shift in precipitation at the highest climatic station, Lomnický peak, began around 1985 (+). Abrupt shifts in temperature began around 1970 (+) at the presented climatic stations. The extremity of climate is confirmed by an analysis of the trends in wet and dry spells. Trends showed increasing tendencies in medium- and long-term wet spells.

Zelenáková et al. (2017) analysed the temporal and spatial trends in the annual and seasonal precipitation in Slovakia, in their work, utilising 487 gauging station data collected state-wide in the period from 1981 to 2013. In general, the precipitation data in the studied area have not changed during the last 33 years, and there are no big gaps. However, predominantly increasing trends in the precipitation time series were found at most of the gauging stations in Slovakia. There is also evidence of different rain distribution from the monthly point of view. Decreasing trends were detected in December in the northern part of Slovakia, while the central and southern parts revealed increasing trends. Most of the stations showed increasing summer precipitation trends, especially in July.

Nikolová, Nejedlik, Lapin (2016) analysed drought in lowlands of Slovakia on the basis of SPI and SPEI for the period 1961–2011. The results show that temperature has an important role for occurrence of moderate and severe drought at monthly level and precipitation is the main factor for occurrence of extreme drought. There are an increasing number of cases with severe or extreme drought in summer. Future projection of drought shows a general tendency to the increasing frequency of severe dry events in 2001–2050 and 2051–2100, while there will be a little decreasing of the extremely dry months in comparison to 1961–2010.

Lapin, Gera, Hrvol, Melo, Tomlain (2009) claimed that regimes of evapotranspiration, soil moisture and runoff have changed mainly in southern Slovakia. A physical model for the estimation of the energy balance equation components has been developed. Input data was gained from 31 meteorological stations in Slovakia since 1951. The 20-year period of 1988–2007 was by 0.9 °C warmer than the normal period mean. Annual precipitation totals have not changed significantly, but the substantial changes have been found in the precipitation regime. The scenarios show significant changes in the hydrological cycle not only at river basins balance but also in case of soil water balance, mainly in southern Slovakia.

Hydrological drought studies

Fendeková, Fendek (2012) analysed groundwater drought indices, which could be derived for different groundwater parameters, among them for base flow, groundwater head stage, spring yield, or groundwater recharge. Base flow drought assessment methods were proposed in the paper. The base flow drought severity index was applied, calculated as the value of the base flow drought deficit volume divided by the drought duration. After that, the standardized base flow drought severity index was proposed as the ratio of the base flow drought index and the average long-term annual base flow. Proposed methods were applied in the Nitra River basin. Base flow drought occurrence was characterised also from the seasonality point of view.

Fendeková et al. (2018) used SPI and SPEI for assessment of the meteorological drought occurrence. The research was established on a discharge time series representing twelve river basins in Slovakia, within the period 1981–2015. Results showed that the drought parameters in the evaluated river basins of Slovakia differed in respective years, most of the basins suffered more by 2003 and 2012 drought than by the 2015 one. Water balance components analysis for the entire period 1931–2016 showed that because of the continuously increasing air temperature and evapotranspiration balance, there is a decrease of runoff in the Slovak territory.

Zelenáková et al. (2014) identified statistically significant trends in the stream flow characteristics of the low water content in eastern Slovakia, in their work, which are used in the evaluation of the hydrological drought. This analysis was carried out due to the statistical data from 63 river stations,

lying in the eastern part of Slovakia. Mann-Kendall statistical test identifies the frequency of minimal stream flow trends. Obtained results from the statistically significant trends in the stream flows are in a role of a basement for the regionalisation of the eastern Slovakia territory from the point of the hydrological drought risk.

Hanel et al. (2014) used global climate models to develop climate change scenarios for four small catchments in the Czech and Slovak Republic. This method applies a nonlinear transformation to precipitation in order to match projected changes in the precipitation variability. Similarly, temperature is transformed considering the changes in mean and variability. The results show an increase in the number of minor droughts and an increase in the most severe droughts. There are clear differences in the changes of drought characteristics related to the dominant runoff regime in a catchment.

Blahušiaková et al. (2020) investigated changes in the seasonal runoff and low flows related to the changes in snow and climate variables in the mountainous catchments in Central Europe. The results showed an increase in air temperature, decrease in snowfall fraction and snow depth, and changes in precipitation. Most of the hydrological droughts were connected either to low air temperatures and precipitation during winter or high winter air temperatures, which caused below-average snow storages. Findings show that besides precipitation and air temperature, snow plays an important role in summer streamflow and drought occurrence in the selected mountainous catchments.

Agricultural (physiological) drought studies

Labudová, Labuda, Takáč (2016) focused on the assessment of drought intensity impact on crop yields on the Danubian and the Eastern Slovakian Lowland. Limited yield data resulted in the limited length of the assessed period (1996–2013). The standardised yields of ten crops (winter wheat, spring wheat, winter barley, spring barley, rye, maize, potatoes, oilseed rape, sunflower and sugar beet) were correlated with monthly, 2-, and 3-monthly SPI and SPEI. The highest correlation was between maize and the 3-monthly SPEI. Crop yields in the Eastern Slovakian Lowland do not seem to be influenced by wet/dry periods, identified using SPI and SPEI, as their correlation with both indices is quite low and insignificant.

Čistý, Jarabicová and Minarič (2016) evaluated a spatial indicator of the threat of droughts, namely the available water capacity of soil. Data from a soil survey and data measured in a laboratory were used for the development of the pedotransfer functions with the help of the Random Forest algorithm. On the basis of the pedotransfer function, the available water capacity was spatially evaluated by geostatistical methods in the investigated area, i.e., in the Záhorská Lowland, in Slovakia.

Vido et al. (2016) analysed the physiological response of tree species in central Slovakia to the driest months of 2012.

Lukasová et al. (2020) focused on the onset of leaf colouring-LCO-((BBCH)92) of the European beech (*Fagus sylvatica*, L.). The limiting climate conditions for LCO were defined by the meteorological drought indices: climatic water balance (CWB), standardized precipitation index (SPI), standardized precipitation-evapotranspiration index

(SPEI), dry period index (DPI), and heat waves (HW). During 23-year period (1996–2018) of ground-based phenological observations, the timing of LCO was significantly delayed at the middle to high altitudes. Over the last decade, LCO at the middle altitudes started at comparable to low altitudes. This resulted mainly from the significant negative effect of drought prior to this phenological phase. The ongoing warming trend of summer months suggests further intensification of drought spreading from the continual increase of evapotranspiration over the next decades.

Bernáth et al. (2020) evaluated the drought impact on the quality parameters of grapes in the locality of the Cultivar Testing Station, Dolné Plachtince. Interanual variability of the drought impact on the grape quality was evaluated according to PDSI. The 1990–2014 period was used as a basis for the evaluation. The PDSI values as well as the sugar and acid contents were correlated to find the strength of relation between them. Short drought periods did not influence the grape quality significantly, while long drought periods caused a decrease of the acid content and an increase of the sugar content.

Tuzinsky, Gregor, Tuzinsky, Homolak (2018) analysed the balance of soil water in the spruce stand mountain conditions in the Upper Orava region. The long-term research (1991–2014) shows that the predominant moisture interval in the vegetation period is semi-uvidic soil interval with good or sufficient supply of usable water. Ongoing climatic conditions with a gradual reduction of precipitation and increase of air temperature pose danger, associated with the development of dry periods, to the spruce. Under such conditions, the spruce is threatened with drought, and physiological weakness, reduced evapotranspiration, increased fall of the assimilation organs, reduced increment, degradation of physical and hydrological properties of soil, and reduction of transport of mineral and organic substances are all its responses.

Takac, Moravek, Klikusovska, Skalsky (2014) assessed drought severity in the agricultural regions of Slovakia in the years 2011–2013. Standardized index based on the daily available soil water content was used for drought severity classification. The results of the analysis confirmed the occurrence of the meteorological drought in the years 2011 and 2012 and the occurrence of the agronomic drought in the years 2011–2013. Greater areal extension of the impact of drought on crop production was observed only in the years 2012 and 2013.

Šiška, Takáč (2009) estimated the climatic index of drought and evapotranspiration deficits for the agricultural regions of the Slovak Republic. Climate change conditions were generated by general circulation model CCCM for emission scenario SIZES B2. Five categories of drought conditions were recognized in the reference period 1961–1990, and additional two very dry categories can be recognized in the agricultural regions of Slovakia, according to both estimated climatic indices.

Šustek, Vido, Škvareninová, Škvarenina, Šurda (2017) documented the impact of the 2012 dry season on the decline in the beetle species (*Carabids*) in the High Tatras. The Standardized Precipitation Evapotranspiration Index was shown, using the cross-correlation of SPEI and number of individuals and species of *Carabids* as a suitable means

to explain and predict such changes for the period of 1–2 years.

Brezianská, Vitková, Šurda (2018) analysed the occurrence of drought and reduced soil water storage in the Záhoská Lowland, in 1961–2010.

Conclusions

1. Drought is a consequence of climate anomalies, as well as of (wrong) human water use practices. This paper has reviewed the literature concerning the existing drought indices. Thus, they serve to identify and quantify all types of drought (meteorological, agricultural, hydrological or socio-economic). The paper has presented a vast number of indices demands by collecting information related to a huge variety of disciplines and representing a complex challenge.

2. The second part of paper has been devoted to an overview of the selected scientific studies about the use of various drought indices (and indicators) and drought assessment in the conditions of Slovakia and Central Europe. Most of the studies are focused on meteorological, less on hydrological or agricultural drought and on the impacts of the increased incidence of drought on flora (alternatively fauna).

Major conclusions from the reviewed studies:
- an increase in air temperature, changes in precipitation patterns, a decrease in snowfall fraction and snow depth
- a trend towards more dry (arid) climatic conditions
- catchments are becoming drier and runoff is decreasing – an increase in the evaporative demand of the atmosphere, driven by higher temperatures and global radiation with limited changes in precipitation totals are the main drivers behind this development
- an important role of snow in summer streamflow and drought occurrence in the mountainous catchments
- an increasing number of severe drought events during summer in lowlands
- a cyclic pattern of drought events in the High Tatras
- delayed phenological phases and lower quality of grapes, caused by drought at some localities.

Acknowledgments

References

Ajaz, A., Taghvaeian, S., Khand, K., Gowda, P.H., Moorhead, J.E. (2019). Development and evaluation of an agricultural drought index by harnessing soil moisture and weather data. *Water, 11*, 1375.

Akhtari, R., Morid, S., Mahdian, M.H., Smakhtinm, V. (2009). Assessment of areal interpolation methods for spatial analysis of SPI and EDI drought indices. *Int. J. Climatol.*, *29*(1), 135–145. https://doi.org/10.1002/joc.1691

Alcamo, J., Henrichs, T., Rösch, T. (2000). World water in 2025 – global modeling and scenario analysis for the world commission on water for the 21st century. In: *Report A0002, Center for Environmental Systems Research*. Kassel, Germany: University of Kassel, Kurt Wolters Strasse 3.

Alley, W.M. (1985). The Palmer Drought Severity Index as a measure of hydrologic drought. *Water Resour. Bull.*, *21*(1), 105–114.

Andreu, J., Solera, A., Paredes-Arquiola, J., Haro-Monteagudo, D., van Lanen, H. (Eds.). (2015). *Drought: Research and Science-Policy Interfacing*. London: CRC Press. https://doi.org/10.1201/b18077

Bernáth, S., Šiška, B., Paulen, O., Zuzulová, V., Pintér, E., Žilinský, M., Tóth, F. (2020). Grape Quality Parameters in Western Carpathian Region under Changing Climatic Conditions as Influenced by Drought. *Journal of Ecological Engineering*, *21*(4), 39-45. https://doi.org/10.12911/22998993/119796

Blahušiaková, A., Matoušková, M., Jenicek, M., Ledvinka, O., Kliment, Z., Podolinská, J., Snopková, Z. (2020). Snow and climate trends and their impact on seasonal runoff and hydrological drought types in selected mountain catchments in Central Europe. *Hydrological Sciences Journal*, *65*(12), 2083–2096. https://doi.org/10.1080/02626667.2020.1784900

Brezianská, K., Vitková, J., Šurda, P. (2018). Drought analysis and the impact of climate change on soil water supply in the Záhorská lowland. In *Aktuálne problémy zóny aerácie pôdy v podmienkach prebiehajúcej klimatickej zmeny, Veda* (pp. 307–335) (in Slovak).

Byun, H.R. and Wilhite, D.A. (1999). Objective quantification of drought severity and duration. *Int. J. Climatol.*, *12*(9), 2747–2756.

Cammalleri, C., Micale, F., Vogt, J. (2016). A novel soil moisture-based drought severity index (DSI) combining water deficit magnitude and frequency. *Hydrol. Process.*, *30*, 289–301.

Čistý, M., Jarabicová, M., Minarič, P. (2016). Spatial Assessment of Soil Water Storage as an Identifer of Areas Threatened by Drought. *Procedia Engineering*, *161*, 1738–1744. https://doi.org/10.1016/j.proeng.2016.08.768

Cloke, H.L., Hannah, D.M. (2011). Large-scale hydrology: Advances in understanding processes, dynamics and models from beyond river basin to global scale. *Hydrological Processes*, *25*, 991–995. https://doi.org/10.1002/hyp.8059

Cook, B. I., Smerdon, J. E., Seager, R., Coats, S. (2014). Global warming and 21st century drying. *Climate Dynamics*, *43*(9–10), 2607–2627. https://doi.org/10.1007/s00382-014-2075-y

Dai, A. (2011). Drought under global warming: A review. *Wiley Interdisciplinary Reviews: Climate Change*, *2*, 45–65.

Dai, A. (2012). Increasing drought under global warming in observations and models. *Nat. Clim. Change*, *3*, 52–8.

Dai, A. (2013). Increasing drought under global warming in observations and models. *Nature Clim Change*, *3*, 52–58. https://doi.org/10.1038/nclimate1633

Doesken, N.J., McKee, T.B., Kleist, J. (1991). Development of a Surface Water Supply Index for the western United States. *Climatology Rep. 91–93,* Colorado Climate Center, Dept. of Atmospheric Science, Colorado State University, Fort Collins, CO (76 p.).

Dracup, J.A., Lee, K.S., Paulson, E.G.J. (1980). On the definition of drought. *Water Resour. Res.*, *16*(2), 297–302.

Dutra, E., Viterbo, P., Miranda, P.M.A. (2008). ERA-40 reanalysis hydrological applications in the characterization of regional drought. *Geophys. Res. Lett.*, *35*, 2–6.

Falkenmark, M., Lundqvist, J., Widstrand, C. (1989). Macro-scale water scarcity requires micro-scale approaches. *Nat. Res. Forum*, *13*, 258–267.

Fendeková, M., Fendek, M. (2012). Groundwater drought in the Nitra River Basin – identification and classification. *J. Hydrol. Hydromecha*nics, *60*, 185–193. https://doi.org/10.2478/v10098-012-0016-1

Fendeková M., Gauster T., Labudová L., Vrabliková D., Danáčová Z., Fendek M., Pekárová P. (2018). Analysing 21st century meteorological and hydrological drought events in Slovakia. *J. Hydrol. Hydromech.*, *66*(4), 393–403.

Garen, D.C. (1993). Revised Surface-Water Supply Index for western United States. *Water Resour. Plan. Manage.*, *119*, 437-454.

Gibbs, W., Maher, J. (1967). *Rainfall Deciles as Drought Indicators*. Melbourne: Bureau of Meteorology (117 p.).

Hanel, M., Vizina, A., Martínková, M., Horáček, S., Porubská, D., Fendek, M., Fendeková, M. (2014). Changes of drought characteristics in small Czech and Slovakian catchments projected by the CMIP5 GCM ensemble. In: *Hydrology in a changing world: environmental and human dimensions*, IAHS (pp. 78–83).

Hayes, M.J. (2006). Drought Indices. *Van Nostrand's Scientific Encyclopedia*. Hoboken: John Wiley & Sons, Inc.

Hayes, M., Svoboda, M., Wall, N., Widhalm, M. (2011). The Lincoln declaration on drought indices: Universal meteorological drought index recommended. *Bulletin of the American Meteorological Society*, *92*, 485–488. https://doi.org/10.1175/2010BAMS3103.1

Heim, R.R. (2000). *Drought indices: A review*. Drought: A Global Assessment, D. A. Wilhite, Ed., Routledge (pp. 159–167).

Heim, R.R. (2002). A Review of Twentieth-Century Drought Indices Used in the United States. *Bull. Amer. Meteor. Soc.*, *83*, 1149–1166. https://doi.org/10.1175/1520-0477-83.8.1149

Hoekstra, A.Y. (2012). Water footprint accounting. In: Godfrey, J.M., Chalmers, K. (Eds.). *Water Accounting. International Approaches to Policy and Decisionmaking*. Edward Elgar Publishing Limited, Cheltenham, UK – Northampton, MA, USA (pp. 58–75).

IPCC (2018). Summary for Policymakers. *Global Warming of 1.5 °C*. Geneva, Switzerland: World Meteorological Organization (32 p.).

Janáčová, T., Labudová, L., Labuda, M. (2018). Meteorological drought in the parts of Slovakia with lowland features in 1981–2010. *Geographia Cassoviensis, 12*(1), 53–64.

Ju, X.S., Yang, X.W., Chen, L.J. (1997). Research on determination of station indexes and division of regional flood/drought grades in China. *Quarterly Journal of Applied Meteorology*, *8*(1), 26–33.

Kalamaras, N., Michalopoulou, H., Byun, H.R. (2010). Detection of drought events in Greece using daily precipitation. *Hydrol. Res.*, *41*(2), 126–133. https://doi.org/10.2166/nh.2010.001

Kam, J., Sheffield, J., Wood, E.F. (2014). A multiscale analysis of drought and pluvial mechanisms for the southeastern United States. *Journal of Geophysical Research: Atmospheres*, *119*, 7348–7367. https://doi.org/10.1002/2014JD021453

Karl, T.R. (1986). The sensitivity of the Palmer Drought Severity Index and Palmer's Z-Index to their calibration coefcients including potential evapotranspiration. *J. Clim. Appl. Meteorol.*, *25*, 77–86.

Karl, T., Quinlan, F., Ezell, D.S. (1987). Drought termination and amelioration: its climatological probability. *J. Climate Appl. Meteor.*, *26*, 1198–1209.

Kim, D.W. and Byun, H.R. (2009). Future pattern of Asian drought under global warming scenario. *Theor. Appl. Climatol.*, *98*(1–2), 137–150. https://doi.org/10.1007/s00704-008-0100-y

Kim, D.W., Byun, H.R., Choi, K.S. (2009). Evaluation, modification, and application of the effective drought index to 200 – year drought climatology of Seoul Korea. *J. Hydrol.*, *378*(1–2), 1–12. https://doi.org/10.1016/j.jhydrol.2009.08.021

Kumar, V., Panu, U. (1997). Predictive assessment of severity of agricultural droughts based on agro-climatic factors. *J. Am. Water Resour. Assoc.*, *33*(6), 1255–1264.

Labudová, L., Labuda, M., Takáč, J. (2016). Comparison of SPI and SPEI applicability for drought impact assessment on crop production in the Danubian lowland and the east Slovakian lowland. *Theor. Appl. Climatol.*, *128*, 491–506.

Lapin, M., Gera, M., Hrvol, J., Melo, M., Tomlain, J. (2009). Possible impacts of climate change on hydrologic cycle in Slovakia and results of observations in 1951–2007. *Biologia*, *64*, 454–459.

Livneh, B., Hoerling, M. P. (2016). The physics of drought in the U.S. Central Great Plains. *Journal of Climate*, *29*(18), 6783–6804. https://doi.org/10.1175/JCLI-D-15-0697.1

Liu, X., Zhu, X., Pan, Y. Bai, J. Li, S. (2018)Performance of different drought indices for agriculture drought in the North China Plain. *J. Arid Land, 10*, 507–516. https://doi.org/10.1007/s40333-018-0005-2

Lohani, V.K., Loganathan, G.V. (1997). An early warning system for drought management using the Palmer Drought Index. *J. Am. Water Resour. Assoc.*, *33*(6), 1375–1386.

Lukasová, V., Vido, J., Škvareninová, J., Bičárová, S., Hlavatá, H., Borsányi, P., Škvarenina, J. (2020). Autumn phenological response of european beech to summer drought and heat. *Water*, *12*(9), 2610.

Luo, L., Apps, D., Arcand, S., Xu, H., Pan, M., Hoerling, M. (2017). Contribution of temperature and precipitation anomalies to the California drought during 2012–2015. *Geophysical Research Letters*, *44*, 3184–3192. https://doi.org/10.1002/2016GL072027

Mahlstein, I., Portmann, R.W., Daniel, J.S., Solomon, S.,,Knutti, R. (2012). Perceptible changes in regional precipitation in a future climate. *Geophysical Research Letters*, *39*, L05701. doi:10.1029/2011GL050738

Mannocchi, F., Todisco, F., Vergni, L. (2004). Agricultural drought: indices, definition and analysis. *Basis Civ. Water Sci.*, *286*, 246–254. http://hydrologie.org/redbooks/a286/iahs_286_0246.pdf

Martínez-Fernández, J., González-Zamora, A., Sánchez, N., Gumuzzio, A. (2015). A soil water-based index as a suitable agricultural drought indicator. *J. Hydrol.*, *522*, 265–273.

McKee, T.B., Doesken, N.J., Kleist, J. (1995). Drought monitoring with Multiple Time scales. *Proceeding of the 9th Conference on Applied Climatology*. Dallas, TX: American Meteorological Society (pp. 233–236).

Mishra, A.K., Singh, V.P. (2010). A review of drought concepts. *J. Hydrol.*, *391*(1–2), 202–216. https://doi.org/10.1016/j.jhydrol.2010.07.012

Morid, S., Smakhtin, V., Moghaddasi, M. (2006). Comparison of seven meteorological indices for drought monitoring. Iran. *Int. J. Climatol.*, *26*(7), 971–985. https://doi.org/10.1002/joc.1264

Mouillot, F., Rambal, S., Joffre, R. (2002). Simulating climate change impacts on fire frequencyand vegetation dynamics in a Mediterranean-type ecosystem. *Global Change Biology*, *8*, 423–437.

Nagy, P., Zelenaková, M., Kapostasová, D., Hlavatá, H., Simonová, D. (2020). Identification of dry and wet years in eastern Slovakia using indices. *Advances in Environmental Engineering: proceedings*, IOP Publishing (pp. 1–6).

Nikolová, N., Nejedlík., P., Lapin, M. (2016). Temporal variability and spatial distribution of drought events in the lowlands of Slovakia. *Geofizika*, *33*(2), 119–135.

Nkemdirim, L., Weber, L. (1999). Comparison between the droughts of the 1930s and the 1980s in the Southern Prairies of Canada. *J. Climate*, *12*, 2434–2450.

Palmer, W.C. (1965). *Meteorological Drought*. US Weather Bur. Res. Pap. no. 45, 58. https://www.ncdc.noaa.gov/temp-and-precip/drought/docs/palmer.pdf

Pedro-Monzonís, M., Solera, A., Ferrer, J., Estrela, T., Paredes-Arquiola, J. (2015). A review of water scarcity and drought indexes in water resources planning and management. *Journal of Hydrology*, *527*, 482–493. https://doi.org/10.1016/j.jhydrol.2015.05.003

Pozzi, W., Sheffield, J., Stefanski, R., Cripe, D., Pulwarty, R., Vogt, J.V. et al. (2013). Towards global drought early warning capability: Expanding international cooperation for the development of a framework for global drought monitoring and forecasting. *Bulletin of the American Meteorological Society*, *94*(6), 776–785. https://doi.org/10.1175/BAMS-D-11-00176.1

Raskin, P., Gleick, P., Kirshen, P., Pontius, G., Strzepek, K. (1997). *Water Futures: Assessment of Long-Range Patterns and Prospects*. Stockholm, Sweden: Stockholm Environment Institute.

Roudier, P., Mahe, G. (2010). Study of water stress and droughts with indicators using daily data on the Bani River (Niger basin, Mali). *Int. J. Climatol.*, *30*(11), 1689–1705. https://doi.org/10.1002/joc.2013

Sakamoto, C.M. (1978). The Z-index as a variable for crop yield estimation. *Agric. Meteor.*, *19*, 305–313.

Sheffield, J., Wood, E.F., Roderick, M.L. (2012). Little change in global drought over the past 60 years. *Nature, 491*, 435–8.

SHMÚ (2015). *Manifestations of climate change at the global level.* http://www.shmu.sk/sk/?page=1379 (in Slovak).

Shukla, S., Wood, A.W. (2008). Use of a standardized runoff index for characterizing hydrologic drought. *Geophysical Research Letters*, *35*, L02405. https://doi.org/10.1029/2007GL032487

Šiška, B., Takáč, J. (2009). Drought analyses of agricultural regions as influenced by climatic conditions in the Slovak Republic. *Idojárás*, *13*, 135–143.

Sivapalan, M., Savenije, H.H.G., Blöschl, G. (2012). Sociohydrology: A new science of people and water. *Hydrol. Process.*, *26*, 1270–1276. doi:10.1002/hyp.8426

Soule, P.T. (1992). Spatial patterns of drought frequency and duration in the contiguous USA based on multiple drought event definitions. *Int. J. Climatol.*, *12*, 11–24.

Sullivan, C.A. (2002). Calculating a water poverty index. *World Dev.*, *30*, 1195–1210.

Šurda, P., Rončák, P., Vítková, J., Tárnik, A. (2019). Regional drought assessment based on the meteorological indices for locality Nitra. *Acta Hydrologica Slovaca*, *20*(1), 63–73 (in Slovak).

Šurda, P., Vitková, J., Rončák, P. (2020). Regional Drought Assessment Based on the Meteorological Indices. *Bulletin of the Georgian National Academy of Sciences*, *14*(2), 69–84.

Šustek, Z., Vido, J., Škvareninová, J., Škvarenina J., Šurda, P. (2017). Drought impact on ground beetle assemblages (Coleoptera, Carabidae) in Norway spruce forests with different management after windstorm damage – a case study from Tatra Mts. (Slovakia). *J. Hydrol. Hydromech.*, *65*(4), 333–342.

Svoboda, M., Fuchs, B. (2016). *Integrated Drought Management Programme (IDMP)*. Handbook of Drought Indicators and Indices. Drought Mitigation Center Faculty Publications (117 p.). http://digitalcommons.unl.edu/droughtfacpub/117

Takáč, J., Morávek, A., Klikušovská, Z., Skalský, R. (2014). Drought severity in agricultural land of Slovakia in the years 2011–2013. *Mendel and Bioclimatology*, 488–506.

Thornthwaite, C.W. (1948). An approach toward a rational classification of climate. *Geogr. Rev., 38*, 55–94.

Trnka, M., Balek, J., Štěpánek, P., Zahradníček, P., Možný, M., Eitzinger, J. et al. (2016). Drought trends over part of Central Europe between 1961 and 2014. *Clim. Res.*, *70*, 143–160.

Tužinský, L., Gregor, J., Tužinský, M., Homolák, M. (2018). Pedohydrological cycles development in the spruce ecosystem under the current climatic conditions of Slovakia. *Reports of forestry research*, *63*(4), 299-310.

Van Loon, A.F., Gleeson, T., Clark, J., Van Dijk, A. I. J. M., Stahl, K., Hannaford, J. et al. (2016a). Drought in the Anthropocene. *Nature Geoscience*, *9*(2), 89–91. https://doi.org/10.1038/ngeo2646

Van Loon, A.F., Stahl, K., di Baldassarre, G., Clark, J., Rangecroft, S., Wanders, N. et al. (2016b). Drought in a human-modified world: Reframing drought definitions, understanding, and analysis approaches. *Hydrology and Earth System Sciences*, *20*(9), 3631–3650. https://doi.org/10.5194/hess-20-3631-2016

Vicente-Serrano, S.M.,Beguería, S., Lorenzo-Lacruz, J., Camarero, J. J., López-Moreno, J. I., Azorin-Molina, C. et al. (2012). Performance of Drought Indices for Ecological, Agricultural, and Hydrological Applications. *Earth Interact.*, *16*, 1–27. https://doi.org/10.1175/2012EI000434.1

Vido, J., Nalevanková, P., Valach, J., Šustek, Z., Tadesse, T. (2019). Drought Analyses of the Horné Požitavie Region (Slovakia) in the Period 1966–2013. *Adv. Meteorol.*, 1–10.

Vido, J., Nalevanková, P. (2020). Drought in the Upper Hron Region (Slovakia) between the Years 1984–2014. *Water*, *12*(10), 2887.

Vido, J., Tadesse, T., Šustek, Z., Kandrík, R., Hanzelová, M., Škvarenina, J., Škvareninová, J., Hayes, M. (2015). Drought Occurrence in Central European Mountainous Region (Tatra National Park, Slovakia) within the Period 1961–2010. *Adv. Meteorol.*, 1–8.

Vido, J., Střelcová, K., Nalevanková, P., Leštianska, A., Kandrík, R., Pástorová, A., Škvarenina, J., Tadesse, T. (2016). Identifying the relationships of climate and physiological responses of a beech forest using the Standardised Precipitation Index: a case study for Slovakia. *J. Hydrol. Hydromech.*, *64*(3), 246–251.

Wang, A., Lettenmaier, D.P., Sheeld, J. (2011). Soil moisture drought in China, 1950–2006. *J. Clim.*, *24*, 3257–3271.

Wells, N., Goddard, S., Hayes, M.J. (2004). A self-calibrating Palmer Drought Severity Index. *J. Clim.*, *17*, 2335–2351.

Wheaton, E.E. (1994). *Impacts of a variable and changing climate on the Canadian prairies' provinces: A preliminary intergration and annotated bibliography*. SRC Publication No. E-2900-7-E-93, Saskatoon, SK: Saskatchewan Research Council.

Wilhite, D. A., Glantz, M. H. (1985). Understanding: The drought phenomenon: The role of definitions. *Water International*, *10*(3), 111–120. https://doi.org/10.1080/02508068508686328

Wilhite, D.A., Rosenberg, N.J., Glantz, M.H. (1986). Improving federal reponse to drought. *J. Climate Appl. Meteor.*, *25*, 332– 342.

Willeke, G., Hosking, J. R. M., Wallis, J. R. (1994). The national drought atlas. *Institute for Water Resources Report 94-NDS-4*. Norfolk, VA: U.S Army Corp of Engineers.

Zargar, A., Sadiq, R., Naser, B., Khan, F.I. (2011). A review of drought indices. *Environ. Rev.*, i, 333–49.

Zelenáková, M., Purcz, P., Blištan, P., Vranayová, Z., Hlavatá, H., Diaconu, D.C., Portela, M.M. (2018). Trends in Precipitation and Temperatures in Eastern Slovakia (1962–2014). *Water*, *10*, 727.

Zelenáková, M., Vido, J., Portela, M.C.A.S., Purcz, P., Blištan, P., Hlavatá, H., Hluštík, P. (2017). Precipitation Trends over Slovakia in the Period 1981–2013. *Water*, *9*, 922.

Zelenáková, M., Purcz, P., Solaková, T., Simonová, D., Harbulaková, V.O. (2014). Trends in minimal stream flows at eastern Slovakia. *Environmental Engineering 2014, 9th International Conference,* selected papers, Vilnius, Lithuania: Gediminas Technical University (pp. 1–7).

DOES BIOCHAR INFLUENCE SOIL CO2 EMISSION FOUR YEARS AFTER ITS APPLICATION TO SOIL?

Tatijana KOTUŠ*, Ján HORÁK

Slovak University of Agriculture in Nitra, Slovakia

Biochar application into soil has potential as a means for reducing soil greenhouse gas emissions and climate mitigation strategy. In this study, we evaluated the impact of two doses of biochar (10 and 20 t.ha^{-1}) applied in 2014, combined with three fertilization levels (N0, N1, N2) on carbon dioxide (CO_2) in field conditions during the growing season (April – October) in 2018. The field site is located in the Nitra region of Slovakia – Malanta. The soil in the field was classified as a silt loam Haplic Luvisol. There was not found any statistically significant (P <0.05) decreasing effect of biochar with or without N-fertilizer after four years of its application on average daily and cumulative CO_2 emissions, while the CO_2 emissions increased with additional N-fertilizer. Biochar decreased (insignificantly) the daily and cumulative CO_2 emissions only in the treatments without N-fertilization and in the treatment fertilized with higher level of biochar application (20 t.ha^{-1}) and N-fertilizer (80 kg.N.ha^{-1}). According to these results it can be concluded that the biochar applied to soil is not able to reduce CO_2 emissions after four years of its application when it is combined with usual agriculture practices which include N-fertilization.

Keywords: biochar, N-fertilization, soil CO_2 emission, sustainable agriculture

Rising concentrations of carbon dioxide (CO_2) are the main concern since CO_2 emissions from the combustion of fossil fuels account for >50% of the estimated increased greenhouse effect (IPCC, 2007). Agricultural emissions account for 49% of anthropogenic methane emissions, 66% of global anthropogenic N_2O emissions (Robertson, Grace, 2004) and 15% of anthropogenic CO_2 emissions, which in some regions is the largest land-based CO_2 flux to the atmosphere (Janssens et al., 2003). Due to the increasing concentration of CO_2 in the atmosphere, CO_2 is responsible for global climate change (Melillo, Morrisseau, 2002). Soil is a dynamic component of the global C cycle and can be a source or a sink of CO_2 depending on management practices. Although fossil fuel combustion is the major cause of the increase in atmospheric CO_2 concentration, agricultural activities have also been significant contributors. Historically, soils have lost about 40 to 90 Pg C (estimated value) to the atmosphere. Conventional plowing has been regarded as a major cause of this C loss in cropping soils. Tillage-induced soil organic carbon (SOC) losses have been well documented (Lal, 2001). The rate of soil CO_2 emission is strongly related to the amount and type of organic materials present or added to soil, and the complex interaction between soil physical, chemical, and biological processes as well as environmental conditions such as temperature, precipitation, etc. (Juma, 1999; Agehara, Warncke, 2005). It was shown that more CO_2 was produced in fertilized soils compared to the non-fertilized. It was also shown that dry soils after a subsequent increase of soil moisture (after rain) release more CO_2 than soils that have never been too dry

and that more productive soils release less CO_2 as compared to less productive soils (Lee, Six, King, Van Kessel, Rolston, 2006; Pascual, Hernandez, Garcia, Ayusot, 1998). As a result of the projected increase in atmospheric CO_2 concentration, the interest of the environmentalists is rising in reducing CO_2 emissions from soils and increasing soil carbon (C) reserves (Gregorich, Greek, Anderson, Liang, 1998). As is mentioned above, most of the carbon released to the atmosphere is originated through agricultural activities. A large portion of global soil respiration is created by agricultural land utilization (Chen et al., 2010; Zahra et al., 2016). There are three sources of soil respiration. These are soil organic matter, dead vegetation residue, and organisms living in the soil. The activities of these sources change throughout the year (Atarashi-Andoh, Koarashi, Ishizuka, Hirai, 2012) and generally depend on the soil moisture and temperature (Xu, Luo, 2012). Microbial activity is also affected by soil moisture and soil temperature (Kim, Vargas, Bond-Lamberty, Turetsky, 2012). Strong relationships between soil moisture and temperature and soil CO_2 respiration rates have been identified (Rey et al., 2011; Sugihara, Funakawa, Kılasara, Kosak, 2012; Forrester, Mladenoff, Gower, Stoffe, 2012). One of the possible and at the same time innovative solutions to decrease soil CO_2 emission (increase SOC content) can be the application of biochar to the soil. Many published results suggest that biochar can play a significant role in reducing GHG emissions from upland agricultural soils (Rondon, Ramirez, Lehmann, 2005; Renner, 2007; Yanai, Toyota, Okazaki, 2007), reducing pesticide and nutrient leaching loss (Hua, Wu, Liu, McBride, Chen, 2009; Wang, Lin,

Hou, Richardson, Gan, 2010; Zhang, Lin, Wang, Gan, 2010). According to Woolf, Amonette, Street-Perrott, Lehmann, Joseph (2010), biochar application can mitigate up to 12% of the current annual anthropogenic CO_2-C equivalent emissions. Shindo (1991) in his study reported that the total CO_2 flux from a soil amended with biochar from fire burning was similar to that without biochar after 280 days of incubation, indicating that biochar decomposed very slowly. When applied to soil, biochar has the characteristics of higher stability against decomposition (Liang et al., 2006). However, some studies have also shown that biochar is not always a promoter of greenhouse gas emissions. Ge et al. (2019) found that low biochar content had a positive effect on reducing total CO_2 emissions and promoting soil organic carbon sequestration.

The objective of this study was to evaluate, whether biochar applied in 2014 is still able to reduce daily CO_2 and cumulative CO_2 emissions from the soil in 2018 (4 years after its application). In this study we also evaluated the effect of selected soil physical properties (soil temperature and soil water content) on CO_2 emissions. Specific objectives of the study were to focus on looking for answers to the following questions:

1. is biochar able to decrease CO_2 emission after four years of its application?
2. does soil temperature and soil water content have any effect on CO_2 fluxes?

The obtained results could be used by farmers or environmentalists. However only in the case that more research is conducted on different soil types at different agro-ecosystems beyond one year before this practice is fully recommended to farmers.

Material and methods

Experimental site and climatic conditions

The field experiment was established in 2014 at the Malanta experimental site – Nitra Region (Slovakia) (48° 19' N; 18° 9' W). The soil at the experimental site was classified as the silt loam Haplic Luvisol and a silty loam texture (content of sand 15.2%, silt 59.9% and clay 24.9%). It belongs to the temperate zone, with an average annual air temperature of 9.8 °C and average annual rainfall of 539 mm (30-year climatic normal, 1961–1990). Monthly average air temperatures and precipitations in 2018 as compared to the climatic normal are shown in Table 1. The gas samples (soil CO_2 emissions) collection study was conducted during the growing season (April – October) of 2018 with the annual precipitation being 367.4 mm and temperature 11.4 °C, respectively. The daily average air temperature varied from approximately -8.6 °C in February to approximately 27.6 °C in July. The experimental site was compared to the climatic normal 1960–1991.

Experiment design

The experiment consisted of two doses of biochar application (10 and 20 t.ha^{-1}) applied in 2014 combined with three fertilization levels (N0, N1, N2) (Table 2). Altogether, the field experiment included 9 treatments in three replicates. The experimental design consisted of a completely randomized block design with an area of 4×6 m for each plot (27 plots) with wide protective strips of 0.5 m between the plots (Figure 1). In 2018, for other experimental purposes, the original plots were divided into two parts (two subplots with dimensions 4×3 m (27 former plots + 18 application subplots). Biochar was again re-applied by hand in April 2018 at rates of 0, 10 and 20 t.ha^{-1} before the spring barley (*Hordeum vulgare* L. – variety of Malz) was sown (plots "B"). In our study we used results measured during the growing

Table 1 Monthly average air temperature (°C) and precipitation (%) in 2018 as compared to the climatic normal (CN) 1960–1991

Month	Average air temperature			Precipitation		
	average (°C)	deviation of normal (°C)	description	total (mm)	% of normal	description
January	2.4	4.1	very warm	30.6	98.7	normal
February	-0.7	-1.4	normal	27.8	86.9	normal
March	3.4	-1.6	cold	38.1	12.7	wet
April	15.4	5.0	extremely warm	12.2	31.3	very dry
May	18.8	3.7	extremely warm	14.6	25.2	very dry
June	20.7	2.7	very warm	97.5	147.7	wet
July	21.7	1.9	warm	12.9	24.8	extremely dry
August	22.5	3.2	extremely warm	3.0	4.9	extremely dry
September	16.4	0.8	normal	57.2	143.0	wet
October	12.3	1.9	warm	14.4	40.0	very wet
November	5.7	1.2	normal	23.8	43.3	very wet
December	-1.5	-1.6	cold	57.6	144.0	wet

Country:	Slovakia
Experimental site:	Malanta
Location:	latitude 48° 19′ 00′′
	longitude 18° 9′ 00′′
Plot size:	4 × 6 m (4 × 3 m)
Protection row:	0.5 min width
Crop:	spring barley
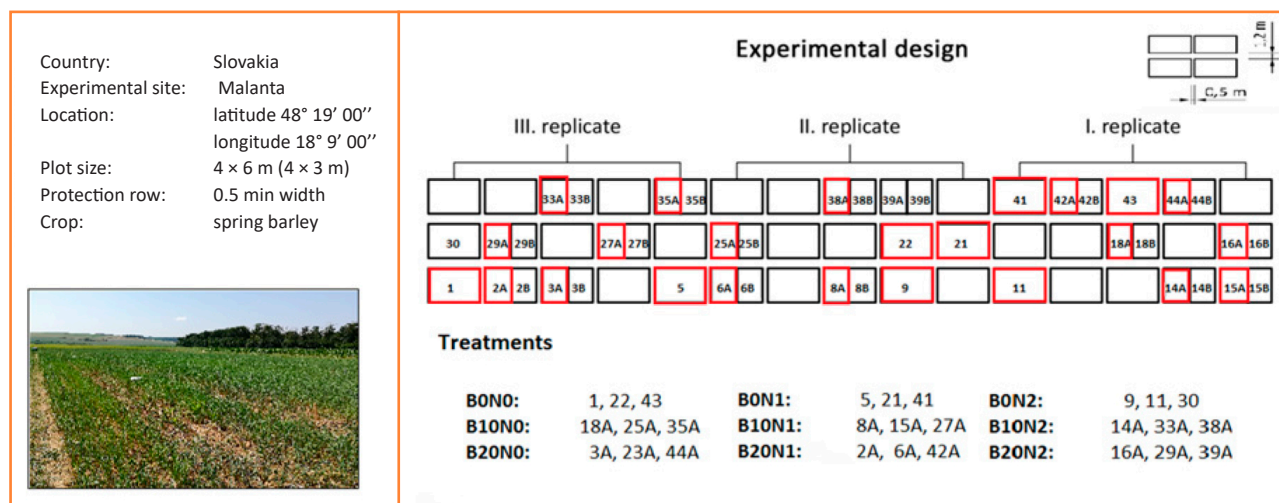
Figure 1 Schematic arrangement of the experimental field

season from April to the first part of October in 2018, only plots "A" where the biochar was applied only once in 2014 (four years after its application). The treatments are shown in the following Table 2.

The biochar used in our study was produced by pyrolyzing paper fiber sludge and grain husks (in a 1 : 1 per weight ration) at 550 °C for 30 min in a Pyreg reactor (Pyreg GmbH, Dörth, Germany). The chemical and physical parameters of the applied biochar are in Table 3. Nitrogen (LAD 27) fertilizer was applied at rates of 0, 40 and 80 kg.N.ha^{-1} (in their acronym "N0, N1 and N2"). The plots were harvested when the spring barley ripened in late July.

Gas sampling and Measurements

CO_2 emissions were measured using the closed chamber technique in every plot. In each experimental plot, one chamber consisted of a base metal collar frame (inserted 10 cm deep into the soil) and a removable top chamber was water-sealed onto bottom collars. The gas samples were collected by plastic gas – tight syringe (Hamilton) and transferred to pre-evacuated 12 mL glass vials (sealed with septum) (Labco Exetainer) at regular intervals of 0-, 30-, and 60-min. Gas was sampled every two weeks. The samples were analyzed using a gas chromatograph (GC–2010 Plus Shimadzu) with thermal conductivity detector (TCD) for CO_2 concentrations. Cumulative emissions over the monitoring period were calculated by interpolating the emissions

Table 2   Treatments of the field experiment with rates of biochar and nitrogen fertilizer

Treatments	Biochar application in 2014 (t.ha^{-1})	N fertilizer application in 2018 (kg.N.ha^{-1})
Unfertilized group (0 kg.N.ha^{-1})		
B0N0	0	0
B10N0	10	0
B20N0	20	0
Fertilized group – N1 (40 kg.N.ha^{-1})		
B0N1	0	40
B10N1	10	40
B20N1	20	40
Fertilized group – N2 (80 kg.N.ha^{-1})		
B0N2	0	80
B10N2	10	80
B20N2	20	80

Table 3   Physical and chemical parameters of applied biochar (Sonnenerde Company, Riedlingsdorf, Austria)

pH (KCl)	C (%)	N (%)	C : N	Bulk density (g.cm^{-3})	Specific surface area (m^2.g^{-1})	Ash (%)
8.8	53.1	1.4	37.9	0.21	21.7	38.3

between each sampling day and are reported in t.ha^{-1}. Before measuring CO_2 emissions in laboratory, gas chromatograph was calibrated using three standard gas mixtures (N_2O, CO_2 and N_2). At each gas sampling occasion, disturbed soil samples from the depth of 0–0.1 m were also collected to determine soil water content (gravimetric method) and the soil temperature was measured at the depth of 0.05 m (Volcraft DET3R thermometer).

Statistical analysis

The means and standard errors were calculated for the parameters. A one-way analysis of variance (ANOVA) was used to evaluate the effects of different biochar application rates on the measured parameter. And differences between the treatment means were compared using least significant difference testing (LSD). Further, regression analyses to determine the interrelationships between the CO_2 emission and selected soil physical properties (soil temperature and soil water content) were used.

Results and discussion

Soil CO_2 emissions

The Figure 2 shows the daily CO_2 emission from the soil which increased towards the summer months with increasing temperature and then decreased with decreasing temperature towards October in all treatment (with or without biochar combined with or without N-fertilizer). There was also found that during the growing season, CO_2 flux also irregularly increased and decreased. The concentration of CO_2 emission started to rise after N-fertilization addition, probably due to the stimulation of microbial activity (El-Naggar et al., 2015) or dissociation of carbonates (Bruun et al., 2011). The Figure 2 also shows that both biochar treatments without N-fertilizer (B10N0 and B20N0) had the strongest reducing effect on CO_2 emission during the summer months compared to the control treatment (B0N2). This strong reducing potential of biochar during summer was also found in one fertilized treatment B10N2 compared to B0N2. However, this effect disappeared after the end of July.
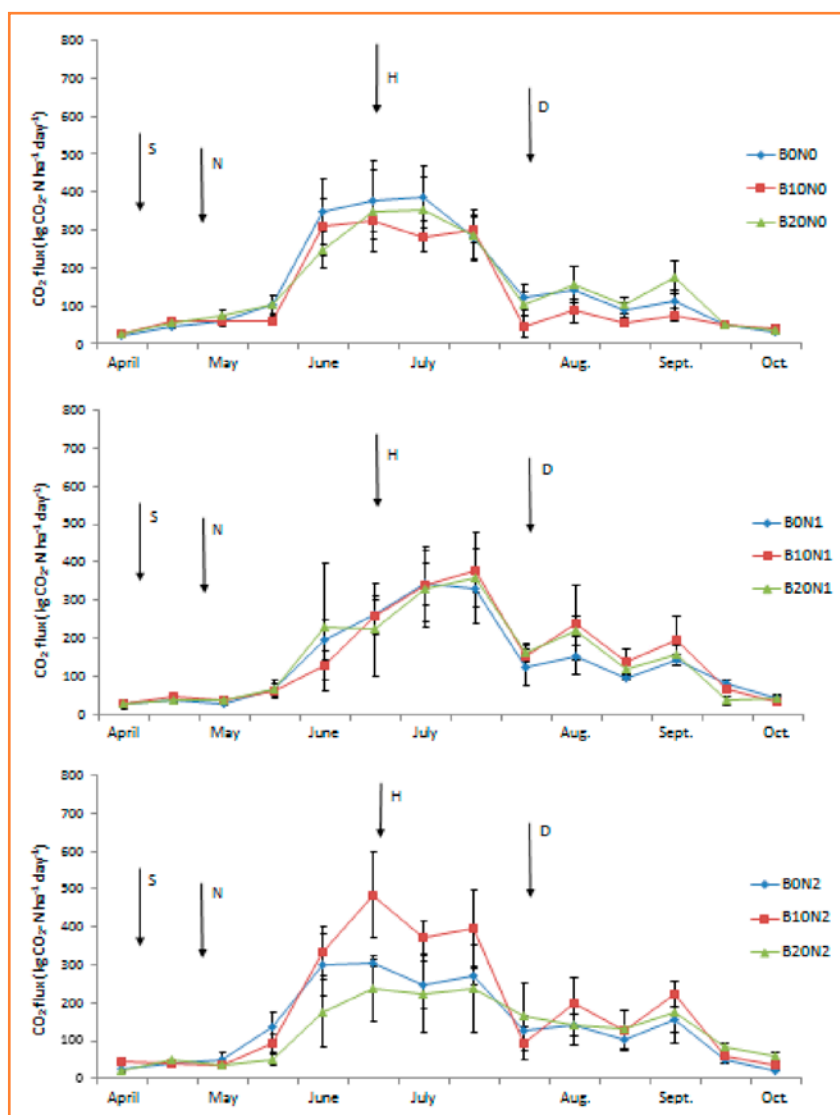
Figure 2 CO_2 flux emissions (kg.ha^{-1}.day^{-1}) of soil amendment with or without biochar and N-fertilizer
Error bars indicate standard errors of the means ($n = 3$)
S – sowing (9.4.2018); N – application of nitrogen 0, 40 and 80 kg.ha^{-1} (7. 5. 2018); H – harvesting (25. 7. 2018); D – disking (13. 9. 2018)

As Table 4 (p. 112) shows, average soil CO_2 emissions over the whole growing season from treatments with biochar (10 and 20 t.ha^{-1}) without N-fertilizer were lower (insignificantly) when compared to the control treatment (B0N0). There was also found that average soil CO_2 emissions were even lower with increasing application rate of biochar. Biochar involved a gradual reduction of CO_2 emission, which may be ascribed to the sorption of labile C onto the surface or into the pores of biochar (Lehmann et al., 2011). Our results are in line with the study of Spokas and Reicosky (2009), which found that biochar produced at

the temperature of 400–500 °C could inhibit soil CO_2 emission.

Opposite was found in biochar treatments combined with lower lever of N-fertilizer (B10N1 and B20N1) where the average soil CO_2 emissions were higher compared to the control treatment (B0N1). The same was found in B10N2 and B20N2 treatments where the average CO_2 emissions were compared to the control treatment (B0N2). No significant difference ($P < 0.05$) was found between biochar with N-fertilizer and the individual control treatments. Such results agree with the results reported by Yufang, Lixia, Hongyan, Shanchao, Shinging (2017) who found that the application

of biochar combined with N-fertilizer increased CO_2 emissions.

The Figure 3 shows the cumulative CO_2 emission. Additions of both application rates of biochar without N-fertilizer (B10N0 and B20N0) to the soil decreased cumulative CO_2 emissions by 17% and 25% for B10N0 and B20N0, respectively, as compared to the control treatment B0N0. However, no significant difference (p <0.05) was found between biochar treatments and the control treatment. On the other hand, all biochar treatments combined with both fertilization levels increased (insignificantly) the cumulative CO_2 emission compared to its individual control treatments. Biochar treatments B10N1 and B20N1 increased CO_2 cumulative emissions by 4% and 6%, respectively as compared to the control treatment B0N1. Similarly, treatment B10N2 also increased cumulative CO_2 emissions by 24% compared to the control treatment (B0N2). However, there was one exception where treatment B20N2 had lower cumulative CO_2 emissions by 19% compared to the control treatment (B0N2).

Relations between soil CO_2 emissions and selected soil physical properties (temperature of soil and soil water content)

Table 5 shows relations between soil CO_2 emissions and soil temperature and soil water content (SWC). Generally, our study showed that the temperature was the most important factor influencing soil CO_2 emission. Significant correlation was observed between soil CO_2 emission and soil temperature in all biochar treatments with or without fertilizer (0; 40; 80 kg.N.ha^{-1}) except the treatment B0N2, where significant correlation was not observed. Exploring the relationships between CO_2 emission and soil temperature, we found significant effects of temperature in treatments B0N0, B0N1, B10N1, B20N1 and B10N2 (r = 0.56–0.62; P <0.05) and treatments B10N0 and B20N0 (r = 0.62–0.63; P <0.01). The most pronounced effect between temperature and CO_2 emission was found in the treatment B20N2 (r = 0.68; P <0.001). The significant relationship between CO_2 emission and soil temperature is well known (Follett, 1997; Parkin and
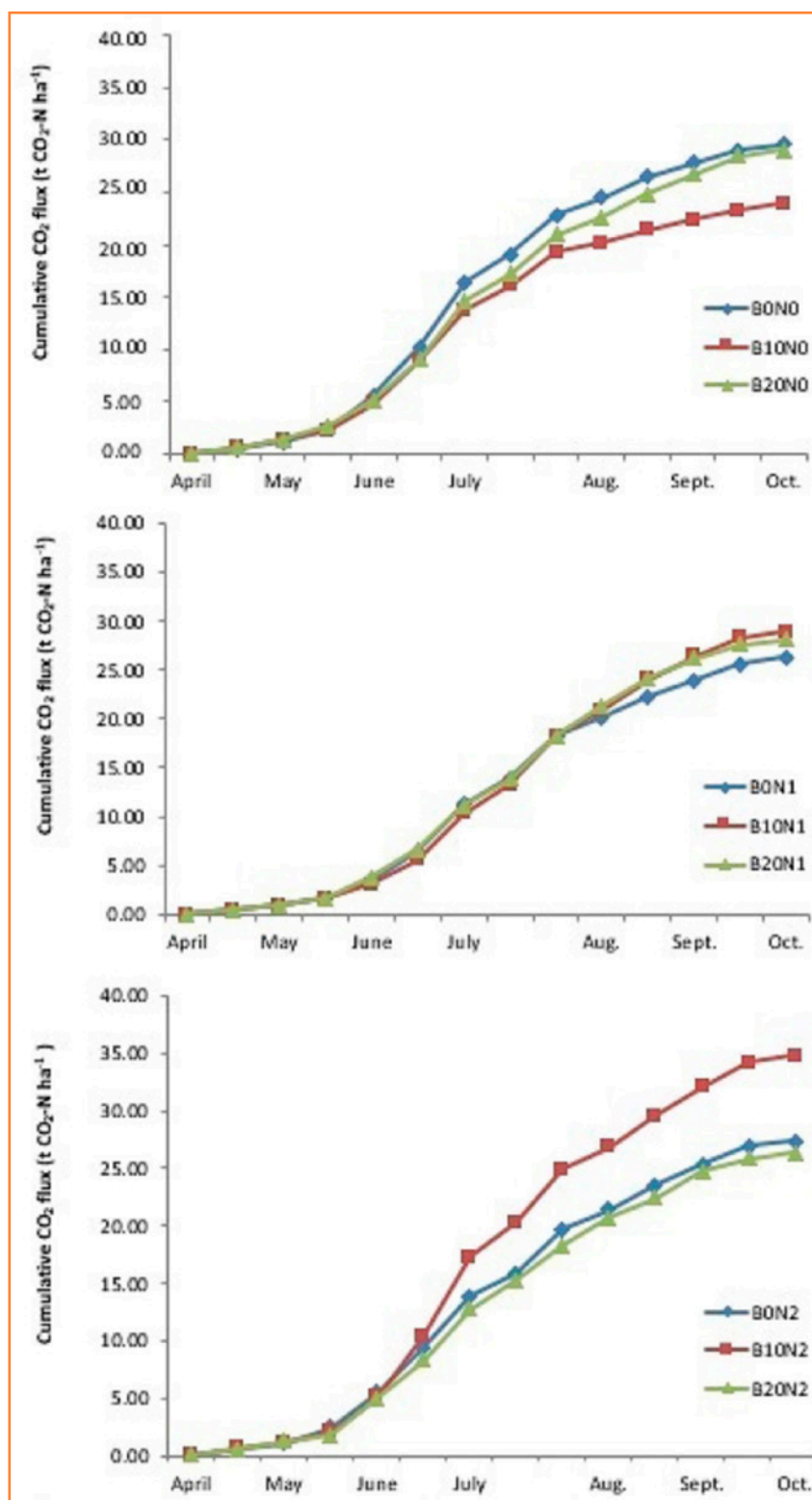
Figure 3   Cumulative CO_2 flux emissions (t CO_2 – N.ha^{-1}) of soil amendment with or without biochar and N-fertilizer

Table 4   Effect of biochar treatments on soil CO_2 emission (means ± standard error; *n* = 3) over the growing season (≥10 °C) in 2018 (April – October)

Treatments	Average CO_2 emission (kg.ha^{-1}.day^{-1})	Cumulative CO_2 emission (t.ha^{-1})
Not fertilized group (0 kg.N.ha^{-1})		
B0N0	154.88 ±1.68 a	15.40 ±0.04 a
B10N0	126.70 ±0.76 a	12.75 ±0.02 a
B20N0	113.21 ±2.23 a	11.30 ±0.04 a
Fertilized group – N1 (40 kg.N.ha^{-1})		
B0N1	138.02 ±1.85 a	12.47 ±0.03 a
B10N1	149.68 ±1.73 a	13.02 ±0.03 a
B20N1	145.34 ±2.90 a	13.18 ±0.05 a
Fertilized group – N2 (80 kg.N.ha^{-1})		
B0N2	141.41 ±4.16 a	13.79 ±0.03 a
B10N2	181.36 ±3.14 a	17.09 ±0.04 a
B20N2	147.96 ±2.60 a	11.16 ±0.05 a

Table 5   Pearson correlation coefficient between soil CO_2 emission and selected physical soil properties (t_p and SWC) for different treatments

Treatments	Soil temperature – t_p (°C)	Soil water content – SWC (% mass)
Unfertilized group (0 kg.N.ha^{-1})		
B0N0	0.62 *	0.05
B10N0	0.62 **	0.06
B20N0	0.63 **	0.29
Fertilized group – N1 (40 kg.N.ha^{-1})		
B0N1	0.56 *	0.0002
B10N1	0.58 *	0.32
B20N1	0.57 *	0.22
Fertilized group – N2 (80 kg.N.ha^{-1})		
B0N2	0.03	0.18
B10N2	0.58 *	0.09
B20N2	0.68 ***	0.17

* P <0.05; ** P <0.01; *** P <0.001

Kaspar, 2003). Our results are also in line with the study of Case, McNamara, Reay, Whitaker (2012); Shen, Zhu, Cheng, Yue, Li (2017), and Horák et al. (2020). On the other hand, the correlation between soil CO_2 emissions and soil water content was not significant (P >0.05) and showed weak relationship in all treatments. A significant correlation (p <0.05) between the CO_2 flux and soil temperature could lead to the easy conclusion that only the soil temperature was a controlling factor in all studied treatments, which probably was not our case. It was probably a synergy effect where an increase in soil water content due to precipitation events together with high soil temperature were associated with the highest CO_2 emissions and smaller CO_2 fluxes.

Conclusion

In this study we examined the carbon dioxide (CO_2) emissions from a silt loam Haplic Luvisol soil due to biochar application.

After four years of biochar addition to the soil, biochar had a statistically insignificant effect on CO_2 emissions with and without N-fertilizer. Positive effect of biochar on CO_2 reduction was found when the biochar was not combined with N-fertilizer (B10N0 and B20N0) with decrease by 17% and 25% for B10N0 and B20N0, respectively, as compared to the control treatment B0N0. There was one exception when the higher level of biochar (20 t.ha^{-1}) was combined with higher level of N-fertilizer which showed the potential to reduce CO_2 emission as well. Opposite was found in all other treatments where the biochar combined with N-fertilizer increased the cumulative CO_2 emissions. According to these results it can be concluded that the biochar applied to soil is not able to reduce CO_2 emission after four years of its application when it is combined with usual agriculture practices which include N-fertilization. Generally, our study showed that the temperature was the most important

factor influencing soil CO_2 emission in all studied treatments although soil water content did not have an effect on CO_2 emission from the soil. A significant correlation (p <0.05) between the CO_2 flux and soil temperature could lead to the easy conclusion that only the soil temperature was a controlling factor in all studied treatments, which probably was not our case. It was probably a synergy effect where increase in soil water content due to precipitation events together with high soil temperature were associated with the highest CO_2 emissions and smaller CO_2 fluxes. Based on our results we cannot suggest to farmers using biochar for reduction of CO_2, because results of our study in 2018 showed that it works only when it is not combined with N-fertilizer. Using N-fertilizer is a common practice of farmers and they would not grow the crops without adding fertilizers to decrease the CO_2 emissions from the soil.

References

Agehara, S., Warncke, D. D. (2005). Soil alternate wetting and drying pure and temperature effects on nitrogen release from organic nitrogen sources. *Soil Science Society of America Journal*, *69*, 1855.

Atarashi-Andoh, M., Koarashi, J., Ishizuka, S., Hirai, K. (2012). Seasonal patterns and control factors of CO_2 effluxes from surface litter, soil organic carbon, and root-derived carbon estimated using radiocarbon signatures. *Agricultural and Forest Meteorology*, *152*, 149–158.

Bruun, E. W., Hauggaard-Nielsen, H., Ibrahim, N., Egsgaard, H., Ambus, P., Jensen, P. A., Dam-Johansen, K. (2011). Influence of fast pyrolysis temperature on biochar labile fraction and short-term carbon loss in a loamy soil. *Biomass & Bioenergy*, *35*, 1182–1189.

Case, S. D. C., McNamara, N. P., Reay, D. S., Whitaker, J. (2012). The effect of biochar addition on N_2O and CO_2 emissions from a sandy loam soil – The role of soil aeration. *Soil Biology & Biochemistry*, *51*, 125–134.

El-Naggar, A. H., Usman, A. R. A., Al-Omran, A., Yong, S. O., Ahmad, M., Al-Wabel, M. I. (2015). Carbon mineralization and nutrient availability in calcareous sandy soils amended with woody waste biochar. *Chemosphere*, *138*, 67–73.

Follett, R. F. (1997). CRP and microbial biomass Dynamics in temperate climates. In Lal, R. (ed.). *Management of carbon sequestration in soil*. Boca Ration: CRP Press (305–322).

Forrester, J.A., Mladenoff, J.D., Gower, S.T., Stoffe. J.L. (2012). Interactions of temperature and moisture with respiration from coarse woody debris in experimental forest canopy gaps. *Forest Ecology and Management*, *265*, 124–132.

Ge, X. G., Cao, Y. H., Zhou, B., Wang, X. M., Yang, Z. Y., Li, M. H. (2019). Biochar addition increases subsurface soil microbial biomass but has limited effects on soil CO_2 emissions in subtropical moso bamboo plantations. *Applied Soil Ecology*, *142*, 155–165.

Glaser, B., Balashov, E., Haumaier, L., Guggenberger, G., Zech, W. (2000). Black carbon in density fractions of anthropogenic soils of the Brazilian Amazon region. *Organic Geochemistry*, *31*, 669–678.

Gregorich, E. G., Greek, K. J., Anderson, D. W., Liang, B. C. (1998). Carbon distribution and losses: erosion and deposition effects. *Soil and Tillage Research*, *47*(3–4), 291.

Horák, J., Šimanský, V., Aydin, E., Igaz, D., Buchkina, N., Balashov, E. (2020). Effects of biochar combined with N-fertilization on soil CO_2 emissions, crop yields and relationships with soil properties. *Polish Journal of Environmental Studies*, 29(5), 1–13; doi: 10.15244/pjoes/117656

Hua, L., Wu, W., Liu, Y., McBride, M. B., Chen, Y. (2009). Reduction of nitrogen loss and Cu and Zn mobility during sludge composting with bamboo charcoal amendment. *Environmental Science and Pollution Research*, *16*, 1–9.

Chen, S. T., Huang, Y., Zou, J. W., Shen, Q. R., Hu, Z. H., Qin, Y. M., Chen, H. S, Pan, G. X. (2010). Modeling interannual variability of global soil respiration from climate and soil properties. *Agricultural and Forest Meteorology*, *150*(4), 590–605.

Janssens, I. A., Freibauer, A., Ciais, P., Smith, P., Nabuurs, G. J., Folberth, G., Schlamadinger, B., Hutjes, R. W. A., Ceulemans, R., Schulze, E. D., Valentini, R., Dolman, H. (2003). Europe's bio-sphere absorbs 7–12% of anthrogogenic carbon emissions. *Science*, *300*, 1538–1542.

Juma, N. G. (1999). *Pedosphere and its dynamics*. Edmonton, Canada: Salman Production Ins. (335 p.).

IPCC. (2007). *Climate change: Synthesis report*. Summary for Policymakers. Intergovernmental Panel on Climate Change.

Kim, D. G., Vargas, R., Bond-Lamberty, B., Turetsky, M. (2012). Effects of soil rewetting and thawing on soil gas fluxes: a review of current literature and suggestions for future research. *Biogeosciences*, *9*(7), 2459–2483.

Lal, R. (2001). *Soil carbon sequestration and climate change*. Washington, DC: Senate Hearing, Science and Technical Sub-Committee.

Lee, J., Six, J., King, A. P., Van Kessel, C., Rolston, D. (2006). Tillage and field scale controls on greenhouse gas emission. *Journal of Environmental Quality*, *35*(1), 725.

Lehmann, J., Rilling, M. C., Thies, J., Masiello, C. A., Hockaday, W. C., Crowley, D. (2011). Biochar effects on soil biota – A review. *Soil Biology and Biochemistry*, *43*, 1812–1836.

Liang, B., Lehmann, J., Solomon, D., Kinyangi, J., Grossman, J., O'Neill, B., Skjemstad, J. O., Thies, J., Luizao, F. J., Petersen, J., Neves, E. G. (2006). Black carbon increases cation exchange capacity in soils. *Soil Science Society of America Journal*, *70*, 1719–1730.

Major, J., Steiner, C., DiTommaso, A., Falcão, N. P. S., Lenmann, J. (2005). Weed composition and cover after three years of soil fertility management in the central Brazilian Amazon: compost, fertilizer, manure and charcoal applications. *Weed Biology and Management*, *5*, 69–76.

McHenry, M. P. (2009). Agricultural bio-char production, renewable energy generation and farm carbon sequestration in Western Australia: Certainty, uncertainty and risk. *Agriculture, Ecosystem & Environment*, *129*, 1–7.

Melillo, J. M., Morrisseau, S. (2002). Soil warming and carbon – cycle feedbacks to the climate system. *Science*, *298*, 2173–2176.

Parkin, T. B., Kaspar, T. C. (2003). Temperature controls on diurnal carbon dioxide flux: Implication for estimating soil carbon loss. *Soil Science Society of America Journal*, *67*, 1763–1772.

Pascual, J. A., Hernandez, T., Garcia, C., Ayusot, M. (1998). Carbon mineralization in an arid soil amended with organic wastes of varying degrees of stability. *Communication in Soil Science and Plant Analysis*, *29,* 835.

Rey, A., Pegoraro, E., Oyonatre, C., Were, A., Escribano, P., Raimundo, J. (2011). Impact of land degradation on soil respiration in a steppe (*Stipa tenacissima* L.) semiarid ecosystem in the SE of Spain. *Soil Biology and Biochemistry*, *43*, 393–403.

Renner, R. (2007). Rethinking biochar. *Environmental Science & Technology*, *41*, 5932–5933.

Robertson, G. P., Grace, P. R. (2004). Greenhouse gas fluxes in tropical and temperate agriculture: The need for a full-cost accounting

of global warming potentials. *Environment, Development and Sustainability*, *6*, 51–63.

Rondon, M., Ramirez, J. A., Lehmann, J. (2005). Charcoal additions reduce net emissions of greenhouse gases to the atmosphere. In *Proceedings of the 3ʳᵈ. USDA Symposium on Greenhouse Gases and Carbon Sequestration*, Baltimore, USA (pp. 21–24, p. 208).

Shen, Y., Zhu, L., Cheng, H., Yue, Sh., Li, Sh. (2017). Effects of biochar application on CO_2 emissions from a cultivated soil under semiarid climate conditions in Northwest China. *Sustainability*, *9,* 1482. Doi:10.3390/su9081482

Shindo, H. (1991). Elementary compostion, humus composition and decomposition in soil of charred grassland plants. *Soil Science and Plant Nutrition*, *37*, 651–657.

Sugihara, S., Funakawa, S., Kılasara, M., Kosakı, T. (2012). Effects of land management on CO_2 flux and soil C stock in two Tanzanian croplands with contrasting soil texture. *Soil Biology and Biochemistry*, *46*, 1–9.

Spokas, K. A., Reicosky, D. C. (2009). Impacts of sixteen different biochars on soil greenhouse gas production. *Annals of Environmental Science and Toxicology*, *3,* 179–193.

Steiner, C., Teixeira, W. G., Lehmann, J., Nehls, T., De Macêdo, J. L. V., Blum, W. E. H., Zech, W. (2007). Long term effects of manure, charcoal and mineral fertilization on crop production and fertility on a highly weathered Central Amazonian upland soil. *Plant Soil, 291*, 275–290.

Wang, H., Lin, K., Hou, Z., Richardson, B., Gan, J. (2010). Sorption of the herbicide terbuthylazine in two New Zealand forest soils amended with biosolids and biochars. *Journal of Soils and Sediments*, *10,* 283–289.

Woolf, D., Amonette, J. E., Street-Perrott, F. A., Lehmann, J., Joseph, S. (2010). Sustainable biochar to mitigate global climate change. *Nature Communications*, *1*, 56. Doi:10.1038/ncomms1053

Xu, X., Luo, X. (2012). Effect of wetting intensity on soil GHG fluxes and microbial biomass under a temperate forest floor during dry season. *Geoderma*, 170, 118–126.

Yanai, Y., Toyota. K., Okazaki, M. (2007). Effects of charcoal addition on N_2O emissions from soil resulting from rewetting air-dried soil in short-term laboratory experiments. *Soil Science and Plant Nutrition*, *53*, 181–188.

Yufang, S., Lixia, Z., Hongyan, Ch., Shanchao, Y., Shinqing, L. (2017). Effects of biochar application on CO_2 emissions from cultivated soil under semiarid climate conditions in Northwest China. *Sustainability*, *9*, 1482. Doi: 10.3390/su9081482

Zahra, S. I., Abbas, F., Ishaq, W., Ibrahim, M., Hammad, H. M., Akram, B., Salik, M. R. (2016). Carbon sequestration potential of soils under maize production ın ırrigated agriculture of The Punjab province of Pakistan. *Journal of Animal and Plant Science*, *26*(3), 706–715.

Zhang, H., Lin, K., Wang, H., Gan, J. (2010). Effect of Pinus radiata derived biochars on soil sorption and desorption of phenanthrene. *Environmental Pollution*, *158*, 2821–2825.

CLIMATE CHANGE IMPACT ON METEOROLOGICAL DROUGHT AND SOIL WATER STORAGE IN THE NITRA RIVER BASIN FOR THE PERIOD 2015–2019

Vladimír KIŠŠ*, Andrej TÁRNÍK, Ján ČIMO

Slovak University of Agriculture in Nitra, Slovakia

Drought impacts are significant and widespread on a year-to-year basis, affecting many economic sectors and people at any time. Definitions of drought are clustered into four types: meteorological, hydrologic, agricultural, and socio-economic. In our paper we focus on the comparison of meteorological drought (defined as a period with no precipitation) and agricultural drought (determined as the value below the amount of water storage in the soil profile accessible to plants). The meteorological stations of the Department of Biometeorology and Hydrology of the Slovak University of Agriculture (SUA) in the Nitra River Basin (Slovakia) – Bystričany, Solčany and Palárikovo – were used for the research. Soil moisture was recorded at horizons 0–0.15 m and 0.15–0.30 m. The occurrence of meteorological as well as agricultural drought in the Bystričany locality has changed quite significantly – not only in the summer months but also in the autumn and often in the spring. Meteorological drought in the Solčany locality occurs regularly almost throughout the whole year. Agricultural drought is becoming more regular in the last monitored years. In Palárikovo (the southernmost locality) the occurrence of meteorological drought is regular and even occurs in the spring and autumn months. Agricultural drought also occurs regularly. To increase agricultural production, it is necessary to focus not only on meteorological drought, but also on agricultural drought and soil characteristics in individual localities. We analysed the drought to the depth of 0.30 m, but in the deeper layers there may be enough moisture for the crops´ root systems.

Keywords: meteorological drought, agricultural drought, drought period, basin, precipitation

Drought is a normal part of the world climate, and it can occur in any climate regime around the world, even deserts and rainforests (WMO & GWP, 2016; Lecina-Diaz et al., 2020). Drought is one of the more costly natural hazards on a year-to-year basis; its impacts are significant and widespread, affecting many economic sectors and people at any time (Zhong, Cheng, Wang, 2020; Engstrőm, Jafarzadegan, Moradkhan, 2020). Drought is one of the deadliest natural hazards, and the universal definition of the term has proven to be elusive yet (Lloyd-Hughes, 2013). According to Palmer (1965) a drought period may be defined as an interval of time, generally of the order of months or years in duration, during which the actual moisture supply at a given place rather consistently falls short of the climatically expected or climatically appropriate moisture supply. The discussion of the disciplinary perspectives of drought which follows is the result of a review of more than 150 published definitions (Coles, Eslamian, 2018). For purposes of discussion, these definitions of drought are clustered into four types: meteorological, hydrologic, agricultural, and socio-economic (Wilhite, Glantz, 1985; Dracup, Lee, Paulson Jr, 1980).

Meteorological drought refers to the abrupt absence of or deficiency in precipitation in comparison with the "normal" condition. The "normal" precipitation is represented by a long-term mean value (generally 30 years or more) of precipitation of the concerned station or region (Bhuiyan, 2017; Quiring, 2009). Hydrological drought refers to a lack of water in the hydrological system, manifesting itself in abnormally low streamflow in rivers and abnormally low levels in lakes, reservoirs, and groundwater. It is a part of the bigger drought phenomenon that denotes current natural hazard (Van Loon, 2015; Stahl et al., 2020). Agricultural drought is considered to have set in when the soil moisture availability to plants has dropped to such a level that it adversely affects the crop yield and hence agricultural profitability (Mannocchi, Todisco, Vergni, 2004; Toková, 2019). In brief, the definition of agricultural drought is concerned with the soil moisture deficiency in relation to meteorological drought and climatic factors and their impacts on agricultural production and economic profitability (Łabędzki, Bąk, 2014; Seshasai, Murhy, Chandrasekar, Mohammed, Prabir, 2016). The first three types of droughts are viewed as physical phenomena, and socioeconomic drought is associated with local water supply, which tracks water demand through socioeconomic systems. As population, industries and urbanization grow, the water demand increases, and socioeconomic drought becomes a major concern (Mehran, Mazdiyasni, AghaKouchak, 2015; Tu, Wu, Singh, Chen, Lin, Xie, 2018). Socioeconomic drought thereby refers to the condition that water supply cannot satisfy demand, leading to societal and

Contact address: Vladimír Kišš, Slovak University of Agriculture in Nitra, Faculty of Horticulture and Landscape Engineering, Department of Biometeorology and Hydrology, Hospodárska 7, 949 01 Nitra, Slovakia, ☎ +421 37 641 52 47, e-mail: vladimir.kiss@uniag.sk; ORCID: https://orcid.org/0000-0002-8527-2958

economic disruptions, and environmental impacts (Eklund, Seaquist, 2015; Guo et al., 2019).

Several common features of drought propagation have been revealed, such as droughts getting longer in duration in moving from meteorological to soil moisture to hydrological drought (Wang, Ertsen, Svoboda, Hafeez, 2016). In our paper we will focus on the comparison of meteorological and agricultural drought in the Nitra river basin, Slovakia.

Material and methods

The meteorological stations of the Department of Biometeorology and Hydrology of the SUA in the Nitra River Basin (Slovakia) were used for the research (Figure 1). This basin extends between two basins – the Váh basin from the north and west and the Hron basin from the east. The total area of the Nitra river basin is 4,501 km^2 (Mazúr, Lukniš, 1980; Borgula, 2020). At selected stations – Bystričany, Solčany and Palárikovo (Figure 1), soil moisture was recorded at horizons 0–0.15 m and 0.15–0.30 m. Total precipitation was provided from the Slovak Hydrometeorological Institute.
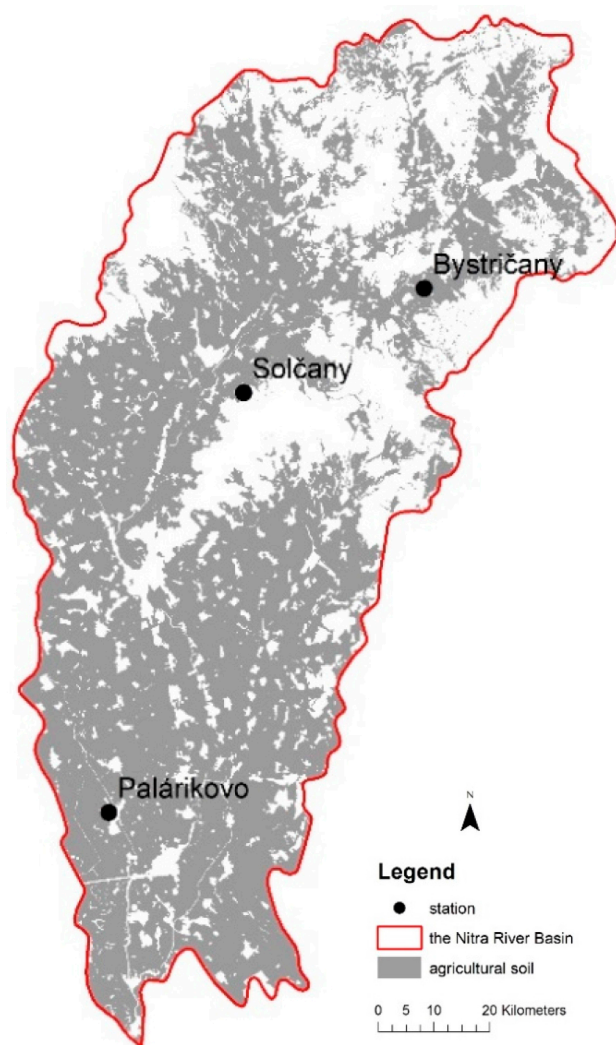
Figure 1   The Nitra river basin

Meteorological drought was defined as a period with no precipitation for purpose of this study. In this paper, the evaluation criterion is used as in Petrovič (1960). Dry periods are divided into three groups according to the number of consecutive days without precipitation:
a) 5 days and more (5–9 days);
b) 10 days or more (10–19 days);
c) 20 days or more, the day of 0.1 mm rainfall not interrupting the dry season.

Agricultural drought is not measured as a direct function of precipitation and hydrological availability of water, because soil types vary in their water uptake and holding capacity, and crops have different moisture needs (Wandel, Diaz, Warren, Hadarits, Hurlbert, Pittman, 2016; Báreková, Bárek, Kováčová, Novotná, Kišš, 2020).

To assess the available water storage in the soil for vegetation cover, the characteristic points of the moisture retention curve (characteristic states of retention-water content in the soil) are selected on the basis of a convention (Kutílek, Nielsen, 1994):
a) wilting point corresponding to pF = 4.18 (it is such soil moisture when the plant cover is permanently insufficiently supplied with water from the soil and withers);
b) a point of reduced availability corresponding to the value of pF = 3.3 (characterized by soil moisture at which the physiological processes of the plant cover are limited by the deficiency);
c) field water capacity corresponding to the value pF = 2.0 to 2.7 (characterized by soil moisture, which is maintained in the soil profile for a relatively long time, while the aeration of the soil is still sufficient for the development of plant cover (Šútor, Gomboš, Mati, 2005).

Agricultural drought was determined as the value below the amount of water storage in the soil profile accessible to plants calculated from the formula (Antal et al., 2014):

$$W_R = \sum_{i=1}^{n} (\theta - \theta_V)_i \times h_i \quad (mm) \tag{1}$$

where:
θ_i – current soil moisture of the *i*-th layer (m^3.m^{-3})
$\theta_{V,i}$ – wilting point of the *i*-th layer (m^3.m^{-3})
h_i – the thickness of the *i*-th layer of the soil profile (mm)

The water storage (W_R) was calculated as the sum of the values for the horizon 0–0.15 m and 0.15–0.30 m. The wilting point values were taken from Igaz, Štekauerová, Horák, Kalúz, Čimo (2011), where they determined the soil properties of 111 samples taken from the Nitra river basin.

We compared meteorological and agricultural drought in each year from March to November, which is the month before the beginning and the month after the end of the growing season. Due to the climate change, the length of the growing season of agricultural crops is also changing (Čimo et al., 2020; Sar, Avci, Avci, 2019; Plich, 2017). Climate anomalies that occur during these periods will have a large impact on vegetation growth (Chen, 2018).

Results and discussion

Several factors can be considered when assessing drought in a landscape. The basic indicator of drought in the landscape is the meteorological drought, which evaluates precipitation less periods. However, for the purposes of agricultural practice, it is only a secondary indicator. The soil water content and thus the assessment of soil drought is essential for growing crops.

The disadvantage of assessing drought based on precipitation is that it interrupts the meteorological drought. However, soil drought may continue. The analysis of the data shows that soil drought is often not interrupted

by rainfall with a daily total above 10 mm and even above 20 mm or is interrupted only for a very short time.

It is a long-standing fact that the distribution of precipitation is changing. Several sources (De Luis, Gonzalez-Hidalgo, Longares, Stepanek, 2008; De Luis, Cufar, Saz, Longares, Ceglar, Bogataj, 2014; Salman, Shahid, Ismail, Ahmed, Chung, Wang, 2019) report a decrease in precipitation in the spring. This potentially causes a problem for the growth of the new crop. Our measurements and analyses also confirm the recurrence of meteorological drought. Nevertheless, in the spring there is no decrease in soil moisture, the critical limit of the point of reduced availability.

Recently, however, this trend has been changing. The trend of movement of the occurrence of agricultural
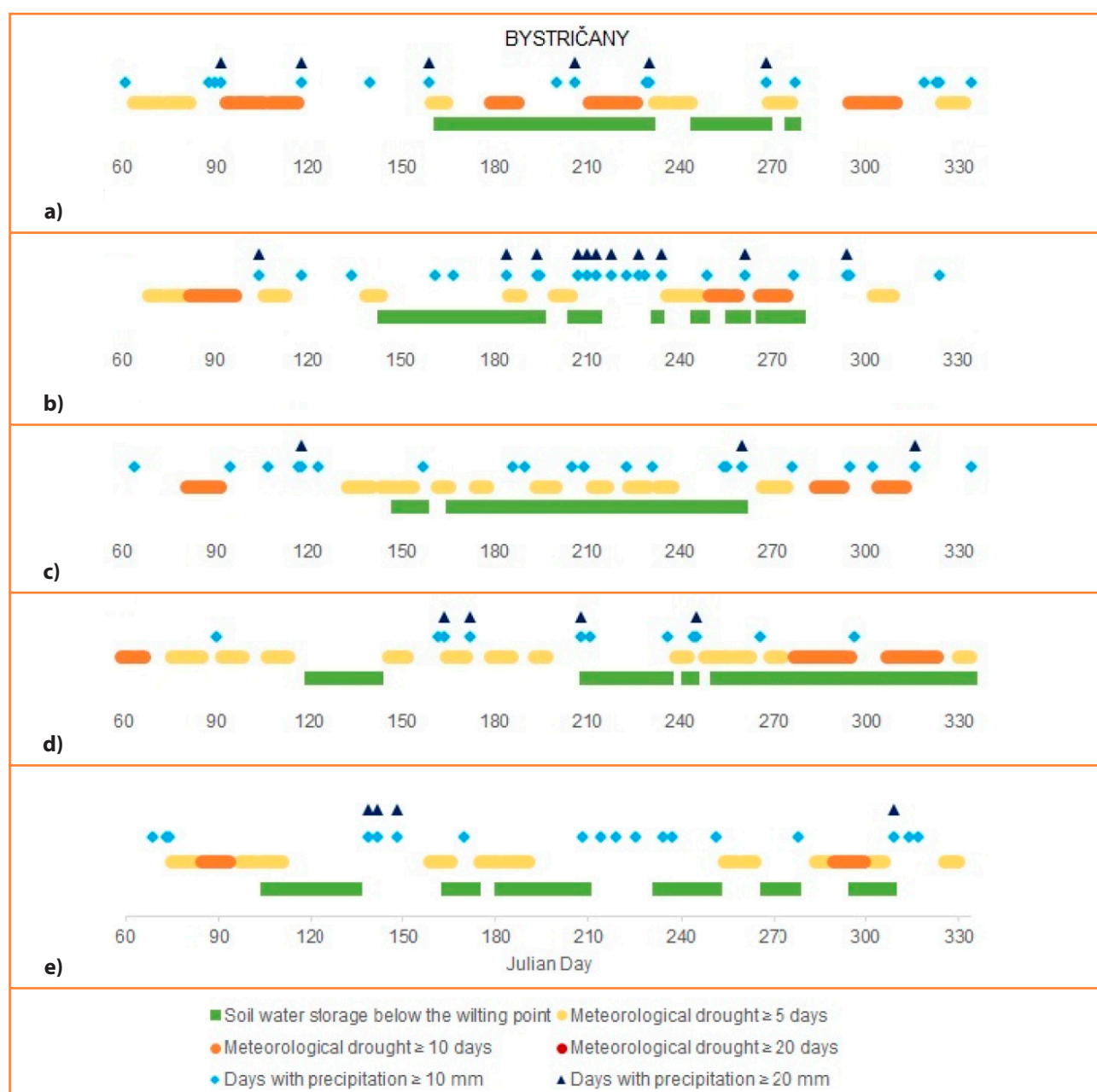
Figure 2 Comparison of meteorological and agricultural drought in the locality of Bystričany for years: (a) 2015; (b) 2016; (c) 2017; (d) 2018 a (e) 2019

drought to the spring period can be observed in the locality Bystričany and in the long term also in the locality Palárikovo. While the Palárikovo locality is the southernmost monitored locality in the middle of the lowlands, the Bystričany locality is in the northern part of the territory in a relatively undulating landscape.

Another negative trend is the prolongation of the duration and continuity of the occurrence of agricultural drought. This trend is clearly visible in the localities of Bystričany, Solčany and Palárikovo.

The occurrence of meteorological as well as agricultural drought in the Bystričany locality has changed quite significantly (Figure 2). At the beginning of the observed period, meteorological drought occurred relatively frequently, but its occurrence was not continuous (Figure

2a). In recent years, drought has occurred not only in the summer months but also in the autumn and often in the spring (Figure 2b–2e). At the same time, the individual dry seasons merge into longer periods.

Meteorological drought in the Solčany locality (Figure 3) occurs regularly almost throughout the whole year. However, agricultural drought is becoming more regular only in the recent monitored years (Figure 3c–3e). At the beginning of the research, the agricultural drought almost did not occur (Figure 3a–3b). Here we observe the adverse consequences of the climate change when the meteorological prolongation occurs, at the same time as the occurrence of agricultural drought.

Palárikovo is the southernmost monitored locality. In this location, the changes are most pronounced. The occurrence
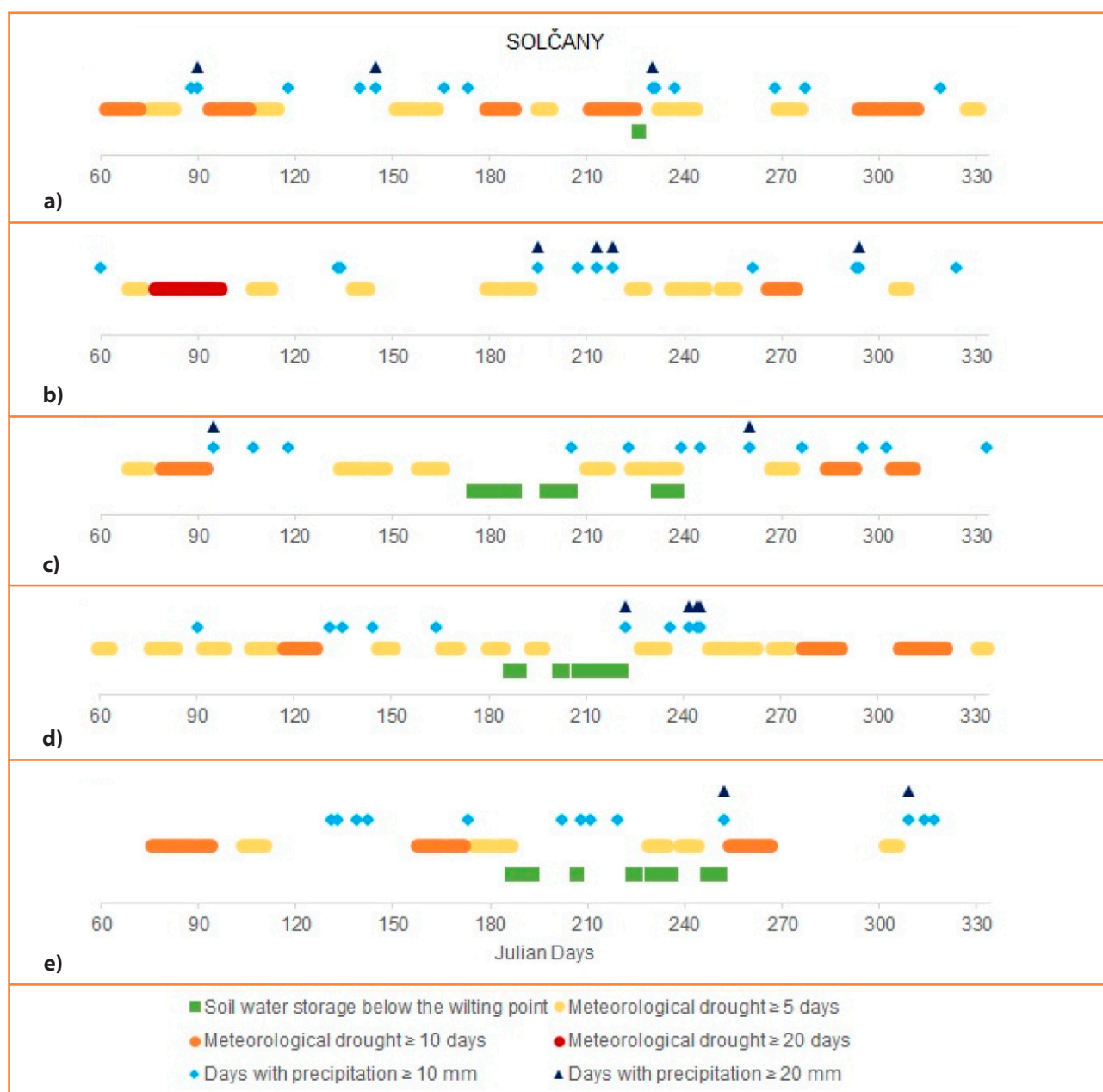
Figure 3　Comparison of meteorological and agricultural drought in the locality of Solčany for years: (a) 2015; (b) 2016; (c) 2017; (d) 2018 a (e) 2019
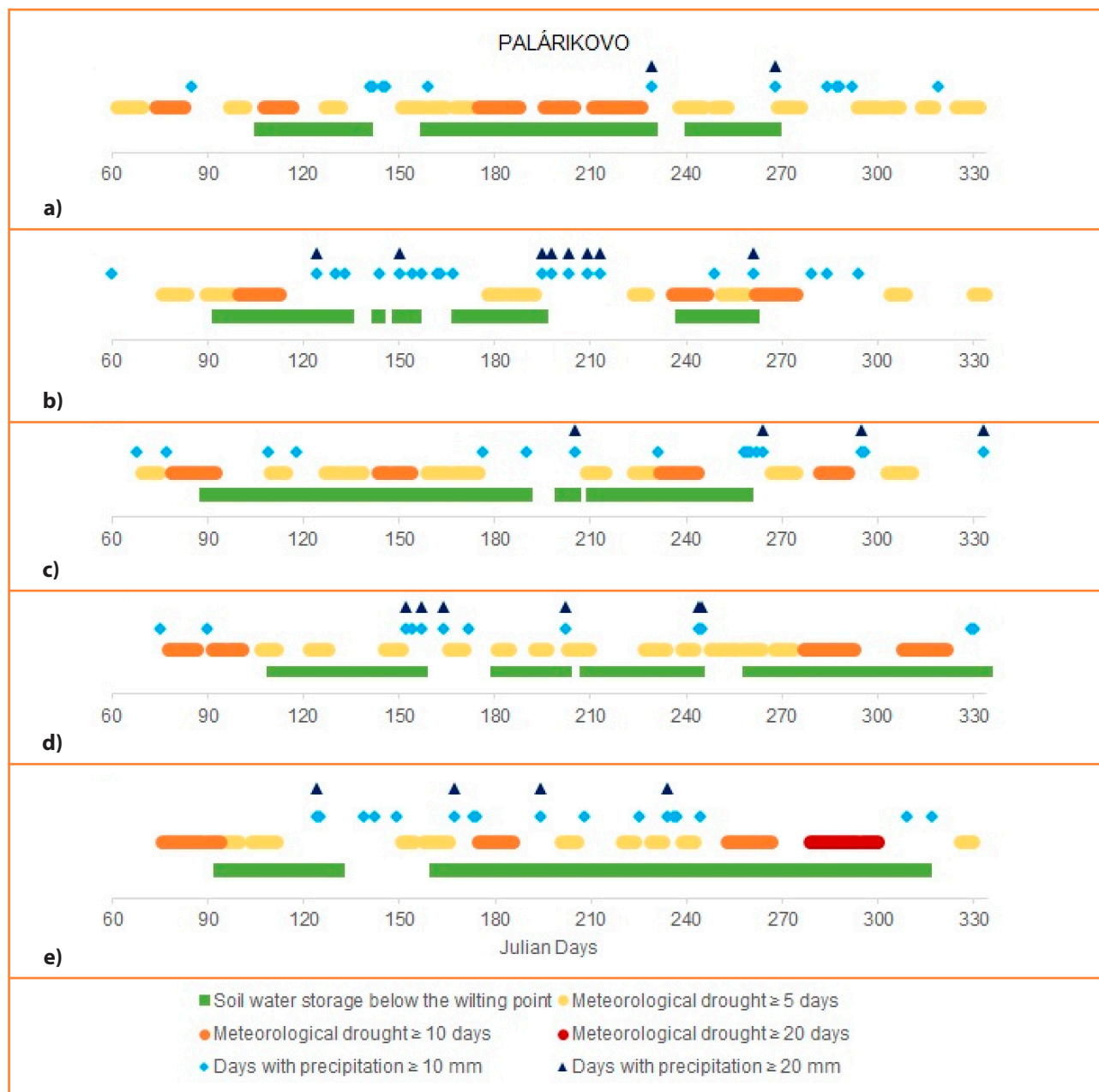
Figure 4 Comparison of meteorological and agricultural drought in the locality of Palárikovo for years: (a) 2015; (b) 2016; (c) 2017; (d) 2018 a (e) 2019

of meteorological drought is regular and even occurs in the spring and autumn months (Figure 4a-4e). The periods are both continuous and longer. Agricultural drought also occurs regularly. We also monitor its prolongation and its movement into the spring and autumn months.

Table 1 shows the number of days with the occurrence of agricultural drought in the months from March to November in the years 2015–2019 in each of the localities.

Several factors need to be considered when comparing meteorological and agricultural droughts. In this work, we considered the period without precipitation and with precipitation up to 0.1 mm as a meteorological drought. Brezianská and Vitková (2015) consider days without precipitation and days with precipitation up to 3 mm as meteorological drought. Using this methodology, the

length of meteorological drought in our selected localities would be significantly extended. In recent years, not only in Slovakia, but unevenly distributed precipitation-free periods and periods of intense precipitation have been recorded worldwide, mainly at the regional level (Zhai, Zhang, Wan, Pan, 2005; Pal and Al-Tabbaa, 2009). Several authors (Vitková, Šútur, Šurda, Stradiot, 2015; Šútor, Šurda, Štekauerová, 2011) consider soil drought below the wilting point, which we also used in our work and reflected the water supply available to plants.

However, in order to increase agricultural production, it is necessary to focus not only on meteorological drought, but also on agricultural drought and soil characteristics in individual localities. In this work, we analysed the drought to

Table 1   Number of days with agricultural drought

	III.	IV.	V.	VI.	VII.	VIII.	IX.	X.	XI.
Bystričany									
2015	0	0	0	14	31	18	23	2	0
2016	0	0	8	30	21	1	16	5	0
2017	0	0	3	21	31	31	17	0	0
2018	0	0	22	0	3	25	23	31	30
2019	0	15	15	9	28	11	14	12	4
Solčany									
2015	0	0	0	0	0	1	0	0	0
2016	0	0	0	0	0	0	0	0	0
2017	0	0	0	0	15	7	0	0	0
2018	0	0	0	0	11	9	0	0	0
2019	0	0	0	0	8	9	5	0	0
Palárikovo									
2015	0	14	20	22	31	19	25	0	0
2016	0	28	17	17	13	6	17	0	0
2017	1	30	31	30	16	31	16	0	0
2018	0	11	31	8	25	31	16	31	30
2019	0	27	11	20	31	31	27	31	11

the depth of 0.30 m, but in the deeper layers there may be enough moisture for the root system of the crops.

Conclusions

More frequent periods of drought are visible more and more often in Slovakia. In this work we compared the dependence between meteorological drought and agricultural drought, which are interesting from the agricultural point of view. In the selected localities of the Nitra river basin, we observed the occurrence of meteorological drought not only in the summer months, but also in spring and autumn. However, this drought is interrupted by precipitation and does not fully correspond to the agricultural (soil) drought, which lasts for a longer period. It is therefore necessary to focus research on the impact of these two droughts, but also on the soil characteristics in specific localities.

Acknowledgments

References

Antal, J., Bárek, V., Čimo, J., Halaj, P., Halászová, K., Horák, J. et al. (2014). Hydrology of agricultural land. Nitra: SPU (in Slovak).

Báreková, A., Bárek, V., Kováčová, M., Novotná, B., Kišš, V. (2020). Climate conditions impact on the sap flow into plants and their dendrometric changes, *Journal of Ecological Engineering*, 21(6), 224–228. DOI 10.12911/22998993/124077

Bhuiyan, Ch. (2017). Drought Vulnerability. In Eslamian, S., & Eslamian, F. A. (Ed.). Handbook of Drought and Water Scarcity: *Environmental Impacts and Analysis of Drought and Water Scarcity* Florida: CRC Press (689 p).

Borgula, A. (26.11.2020). *Nitra river around city Nitra*. http://riekanitra.szm.com (in Slovak).

Brezianská, K., Vitková, J. (2015). Analyse of periods without precipitation and their influence on soil water storage at Záhorská Lowland. *Acta Hydrologica Slovaca*, *16*(TC1), 260–266 (in Slovak).

Chen, Ch. (2018). Identifying Critical Climate Periods for Vegetation Growth in the Northern Hemisphere. *JGR Biogeosciences, 123*(8), 2541–2552. https://doi.org/10.1029/2018JG004443

Čimo, J., Aydin, E., Šinka, K., Tárník, A., Kišš, V., Halaj, P., Toková, L., Kotuš, T. (2020). Change in the Length of the Vegetation Period of Tomato (*Solanum lycopersicum* L.), White Cabbage (*Brassica oleracea* L. var. capitata) and Carrot (*Daucus carota* L.) Due to Climate Change in Slovakia. *Agronomy*, *10*(8), 1110. https://doi.org/10.3390/agronomy10081110

Coles, N. A., Eslamian, S. (2018). Definition of Drought. In: Eslamian, S., and Eslamian, F. A. (Ed.), Handbook of Drought and Water Scarcity: *Principles of Drought and Water Scarcity* Florida: CRC Press (690 p.).

De Luis, M., Gonzalez-Hidalgo, J. C., Longares, L. A., Stepanek, P. (2008). Seasonal precipitation trends in the Mediterranean Iberian

Peninsula in second half of 20th century. *International Journal of Climatology*, *29*(9), 1312–1323. https://doi.org/10.1002/joc.1778

De Luis, M., Cufar, K., Saz, M. A., Longares, L. A., Ceglar, A., Bogataj, L. K. (2014). Trends in seasonal precipitation and temperature in Slovenia during 1951–2007. *Regional Environmental Change*, *14*, 1801–1810. https://doi.org/10.1007/s10113-012-0365-7

Dracup, J. A., Lee, K. S., Paulson Jr., E. G. (1980). On the definition of droughts. *Water Resource Research*, *16*(2), 297–302. https://doi.org/10.1029/WR016i002p00297

Eklund, L., Seaquist, J. (2015). Meteorological, agricultural and socioeconomic drought in the Duhok Governorate, Iraqi Kurdistan. *Natural Hazards*, *76*, 421–441. DOI 10.1007/s11069-014-1504-x

Engstrőm, J., Jafarzadegan, K., Moradkhani, H. (2020). Drought Vulnerability in the United States: An Integrated Assessment. *Water*, *12*(7), 2033. https://doi.org/10.3390/w12072033

Guo, Y., Huang, S., Huang, Q., Wang, H., Fang, W., Yang, Y., Wang, L. (2019). Assessing socioeconomic drought based on an improved Multivariate Standardized Reliability and Resilience Index. *Journal of Hydrology*, *568*, 904–918. https://doi.org/10.1016/j.jhydrol.2018.11.055

Igaz, D., Štekauerová, V., Horák, J., Kalúz, K., Čimo, J. (2011). *The Analysis of Soils Hydrophysical Characteristics in the Nitra River Basin.* Influence of Anthropogenic Activities on Water Regime of Lowland Territory Physics of Soil Water (pp. 17–19) (in Slovak).

Kutílek, M., Nielsen D. R. (1994). How Water Flows in Soil. *Soil.* Dordrecht: Springer. https://doi.org/10.1007/978-94-017-9789-4_9

Łabędzki, L., Bąk, B. (2014). Meteorological and agricultural drought indices used in drought monitoring in Poland: a review. *Meteorology, Hydrology and Water Management*, *2*(2), 12.

Lecina-Diaz, J., Martínez-Vilalta, J., Alvarez, A., Banqué, M., Birkmann, J., Feldmeyer, D., Vayreda, J., Retana, J. (2020). Characterizing forest vulnerability and risk to climate-change hazards. *Frontiers in Ecology and the Environment*, *19*(2), 126–133. https://doi.org/10.1002/fee.2278

Lloyd-Hughes, B. (2013). The impracticality of a universal drought definition, *Theoretical and Applied Climatology*, *117*(3–4), 607–611. https://doi.org/10.1007/s00704-013-1025-7

Mannocchi, F., Todisco, F., Vergni, L. (2004). Agricultural drought: indices, definition and analysis. *Proceedings of the UNESCO/IAHS/IWIIA symposium* (pp. 246–254).

Mazúr, E., Lukniš, M. (1980). Geomorphological division. *Atlas SSR.* Bratislava: Slovenská akadémia vied, SÚGK (in Slovak).

Mehran, A., Mazdiyasni, O., AghaKouchak, A. (2015). A hybrid framework for assessing socioeconomic drought: Linking climate variability, local resilience, and demand. *Journal of Geophysical Research*, *120*(15), 7520–7533. DOI: 10.1002/2015JD023147

Pal, I., Al-Tabbaa, A. (2009). Trends in seasonal precipitation extremes – An indicator of 'climate change' in Kerala, India. *Journal of Hydrology*, *367*(1–2), 62–69. https://doi.org/10.1016/j.jhydrol.2008.12.025

Palmer, W. C. (1965). *Meteorological Drought*. Washington, D.C.: U.S. Weather Bureau.

Petrovič, Š. (1960). *Climatic Conditions of Hurbanovo*. Praha: HMÚ (pp. 138–161) (in Slovak).

Plich, J. (2017). Evaluation of the Length of the Vegetation Period of the Potato. *Plant Breeding and Seed Science*, *76*, 65–67. DOI: 10.1515/plass-2017-0023

Quiring, S. M. (2009). Monitoring Drought: An Evaluation of Meteorological Drought Indices. *Geography Compass*, *3*(1), 64–88. https://doi.org/10.1111/j.1749-8198.2008.00207.x

Salman, S. A., Shahid, S., Ismail, T., Ahmed, K., Chung, E. S., Wang, X. J. (2019). Characteristics of Annual and Seasonal Trends of Rainfall and Temperature in Iraq. *Asia-Pacific Journal of Atmospheric Sciences*, 55, 429–438. https://doi.org/10.1007/s13143-018-0073-4

Sar, T., Avci, S., Avci, M. (2019). Evaluation of the Vegetation Period According to Climate Change Scenarios: A Case Study in the Inner West Anatolia Subregion of Turkey. *Journal of Geography*, *39*, 29–39. https://doi.org/10.26650/JGEOG2019-0018

Seshasai, M. V. R., Murhy, C. S., Chandrasekar, K., Mohammed, A. J., Prabir, K. D. (2016). Agricultural drought: Assessment & monitoring. *Mausam*, *67*(1), 131–142.

Stahl, K., Vidal, J. P., Hannaford, J., Tijdeman, E., Laaha, G., Gauster, T., Tallaksen, L. M. (2020). The challenges of hydrological drought definition, quantification and communication: an interdisciplinary perspective. *Proceedings of the International Association of Hydrological Sciences*, 383, 291–295. https://doi.org/10.5194/piahs-383-291-2020

Šútor, J., Gomboš, M., Mati, R. (2005). The Quantification of Soil Drought and Its Performance. *Acta Hydrologica Slovaca*, *6*(2), 299–306 (in Slovak).

Šútor, J., Šurda, P., Štekauerová, V. (2011). Effect of the time periods without precipitation on water storage dynamics in the aeration zone of the soil. *Acta Hydrologica Slovaca*, *12*(1), 22–28 (in Slovak).

Toková, L. (2019). Using Gravimetric Method for Soil Moisture Determination. *Veda Mladých 2019 – Science of Youth 2019* (pp. 122–130).

Tu, X., Wu, H., Singh, V. P., Chen, X., Lin, K., Xie, Y. (2018). Multivariate design of socioeconomic drought and impact of water reservoirs. *Journal of Hydrology*, *566*, 192–204. https://doi.org/10.1016/j.jhydrol.2018.09.012

Van Loon, A. F. (2015). Hydrological drought explained. *Wires Water*, *2*(4), 359–392. https://doi.org/10.1002/wat2.1085

Vitková, J., Šútur, J., Šurda, P., Stradiot, P. (2015). Possibilities of interpretation of monitored values of water supplies in soil. *Acta Hydrologica Slovaca*, *16*(1), 3–12.

Wandel, J., Diaz, H., Warren, J., Hadarits, M., Hurlbert, M., Pittman, J. (2016). Drought and Vulnerability: A Conceptual Approach. In Diaz, H., Hurlbert, M., Warren, J. (Ed.). *Vulnerability and Adaptation to Drought on the Canadian Prairies.* Calgary: Univesity of Calgary Press (pp. 15–38). https://doi.org/10.2307/j.ctv6gqwv1.4

Wang, W., Ertsen, M. W., Svoboda, M. D., Hafeez, M. (2016). Propagation of Drought: From Meteorological Drought to Agricultural and Hydrological Drought. *Advances in Meteorology*, *2016*, 5. https://doi.org/10.1155/2016/6547209

Wilhite, D. A., Glantz, M.H. (1985). Understanding the Drought Phenomenon: The Role of Definitions. *Water International*, *10*(3), 111–120.

World Meteorological Organization (WMO), Global Water Partnership (GWP). (2016). Handbook of Drought Indicators and Indices. In: Svoboda, M., Fuchs, B. A. *Integrated Drought Management Programme* (IDMP). Integrated Drought Management Tools and Guidelines Series 2. Geneva.

Zhai, P., Zhang, X., Wan, H., Pan, X. (2005). Trends in Total Precipitation and Frequency of Daily Precipitation Extremes over China. *Journal of Climate*, *18*(7), 1096–1108. https://doi.org/10.1175/JCLI-3318.1

Zhong, F., Cheng, Q., Wang, P. (2020). Meteorological Drought, Hydrological Drought, and NDVI in the Heihe River Basin, Northwest China: Evolution and Propagation. *Advances in Meteorology*, *2020*, 26. https://doi.org/10.1155/2020/2409068